

A Baseline Assessment of the Ecological Resources of Jobos Bay, Puerto Rico



July 2011

Editors

David R. Whitall
Bryan M. Costa
Laurie J. Bauer
Angel Dieppa
Sarah D. Hile

NOAA Technical Memorandum NOS NCCOS 133



Citation

Whitall, D.R., B.M. Costa, L.J. Bauer, A. Dieppa, and S.D. Hile (eds.). 2011. A Baseline Assessment of the Ecological Resources of Jobos Bay, Puerto Rico. NOAA Technical Memorandum NOS NCCOS 133. Silver Spring, MD. 188 pp.

A Baseline Assessment of the Ecological Resources of Jobos Bay, Puerto Rico

Prepared by the
Coastal and Oceanographic Assessment, Status and Trends (COAST) Branch
and the Biogeography Branch (BB)
Center for Coastal Monitoring and Assessment (CCMA)
National Centers for Coastal Ocean Science (NCCOS)
National Oceanic and Atmospheric Administration National Ocean Service (NOAA)
1305 East West Highway (SSMC-IV, N/SCI-1)
Silver Spring, MD 20910
USA

July 2011

Editors

David R. Whitall
NOAA Center for Coastal Monitoring and Assessment
Coastal and Oceanographic Assessment, Status and Trends Branch

Bryan M. Costa
NOAA Center for Coastal Monitoring and Assessment, Biogeography Branch and
Consolidated Safety Services, Inc., Fairfax, VA, under NOAA Contract No. DG133C07NC0616

Laurie J. Bauer
NOAA Center for Coastal Monitoring and Assessment, Biogeography Branch and
Consolidated Safety Services, Inc., Fairfax, VA, under NOAA Contract No. DG133C07NC0616

Angel Dieppa
Jobos Bay National Estuarine Research Reserve

Sarah D. Hile
NOAA Center for Coastal Monitoring and Assessment, Biogeography Branch and
Consolidated Safety Services, Inc., Fairfax, VA, under NOAA Contract No. DG133C07NC0616

NOAA Technical Memorandum NOS NCCOS 133



United States
Department of Commerce

National Oceanic and
Atmospheric Administration

National Ocean Service

Gary Locke
Secretary

Jane Lubchenco
Administrator

David Kennedy
Assistant Administrator

About this document

This report presents an ecological characterization of the marine resources of Jobos Bay, Puerto Rico and the surrounding coral reef ecosystems. The purpose of this work, conducted by National Oceanic and Atmospheric Administration's (NOAA) Center for Coastal Monitoring and Assessment^A (CCMA), U.S. Department of Agriculture's (USDA) Agricultural Research Service (ARS) and the Jobos Bay National Estuarine Research Reserve (JBNERR), was to provide natural resource managers with a spatially comprehensive characterization of the marine ecosystem.

Funding for this project was provided by NOAA's Coral Reef Conservation Program, USDA's Conservation Effects Assessment Program and National Centers for Coastal Ocean Science.

For more information on this work and other CCMA projects, please see: <http://ccma.nos.noaa.gov/>

Direct questions or comments to:

David Whittall, Ph.D.
Center for Coastal Monitoring and Assessment
National Oceanic and Atmospheric Administration
1305 East West Highway
SSMC4, N/SCI-1
Silver Spring, MD 20910
Phone: (301) 713-3028 x138
dave.whittall@noaa.gov

Related projects include:

An Ecological Characterization of the Marine Resources of Vieques, Puerto Rico
<http://ccma.nos.noaa.gov/ecosystems/coralreef/vieques/>

Baseline Assessment of Guanica Bay, Puerto Rico in Support of Watershed Restoration
<http://ccma.nos.noaa.gov/ecosystems/coralreef/guanica.aspx>

Caribbean Coral Reef Ecosystem Monitoring Project
http://ccma.nos.noaa.gov/ecosystems/coralreef/reef_fish/

Contaminants and Coral Health in Southwest Puerto Rico
<http://ccma.nos.noaa.gov/stressors/pollution/swpr/>

All photographs provided in this document were taken by NOAA/NOS/NCCOS/Center of Monitoring Assessment around Jobos Bay, Puerto Rico unless otherwise noted.

^A The Center for Coastal Monitoring and Assessment (CCMA) is a part of National Oceanic and Atmospheric Administration (NOAA), National Ocean Service (NOS), National Centers for Coastal Ocean Science (NCCOS).

Table of Contents

Executive Summary	i
Chapter 1: Introduction and Background	1
1.1. Background	1
1.2. Objectives	1
1.3. Study Area Description	2
1.4. Site Characterization	4
1.4.1. Environmental Setting	4
1.4.2. Jobos Bay Watershed	5
Chapter 2: Shallow-water Benthic Habitats of Jobos Bay	11
<i>Bryan Costa, Laurie Bauer and Peter Mueller</i>	
2.1. Introduction	11
2.2. Benthic Habitat Classification Scheme	12
2.2.1. Comparison to Previous NOAA Habitat Classification Schemes	13
2.2.2. Geographic Zones	14
2.2.3. Geomorphological Structure Types	18
2.2.4. Biological Cover Classes	25
2.2.5. Live Coral Cover Classes	28
2.3. Benthic Habitat Creation	30
2.3.1. General Mapping Approach	30
2.4. Remotely Sensed Imagery	30
2.4.1. Acquisition and Processing of the Optical Imagery	31
2.4.2. Acquisition of the Acoustic Imagery	32
2.4.3. Processing of the Acoustic Imagery	33
2.5. Habitat Feature Identification and Delineation	36
2.5.1. Habitat Feature Identification	36
2.5.2. Habitat Feature Delineation	37
2.6. Habitat Feature Attribution (Ground Validation)	38
2.7. Expert Review	40
2.8. GIS Quality Control	40
2.9. Conclusions	40
2.9.1. Map Summary Statistics	41
2.9.2. Comparison to Previous NOAA Habitat Maps of Jobos Bay	50
Chapter 3: Baseline Characterization of Fish Communities, Associated Benthic Habitats and Marine Debris of Jobos Bay	57
<i>Laurie Bauer, Christopher F.G. Jeffrey and Kimberly Roberson</i>	
3.1. Introduction	57
3.2. Methods	58
3.2.1. Site Selection	58

3.2.2. Field methods	59
3.2.3. Data Analysis	60
3.3. Results and Discussion	62
3.3.1. Benthic habitat	62
3.3.2. Fish assemblages	72
3.4. Conclusions	104

Chapter 4: Contaminants in Sediments and Coral Tissues of Jobos Bay **111**

David R. Whitall, Anthony S. Pait, Dennis Apeti, Angel Dieppa, Sarah E. Newton, Lia Brune, Chris Caldwell, Andrew L. Mason and John Christensen

4.1. Introduction	111
4.2. Methods	111
4.2.1. Sampling Design	111
4.2.2. Field Methods	113
4.2.3. Chemical Contaminants Analyzed	114
4.2.3.1. Polycyclic aromatic hydrocarbons (PAHs)	114
4.2.3.2. Polychlorinated biphenyls (PCBs)	115
4.2.3.3. Organochlorine Pesticides	115
4.2.3.4. Butyltins	115
4.2.3.5. Major and Trace Elements	117
4.2.4. Total Organic Carbon (TOC) and Grain Size	118
4.2.5. Statistical Analyses	118
4.2.6. Providing Context for Results	118
4.3. Results – Overview of Contaminant Patterns	119
4.3.1. Environmental Parameters	119
4.3.2. Polycyclic Aromatic Hydrocarbons (PAHs)	119
4.3.3. Polychlorinated Biphenyls (PCBs)	123
4.3.4. DDT and Other Chlorinated Pesticides	124
4.3.5. Butyltins	127
4.3.6. Major and Trace Elements	128
4.3.6.1. Silver (Ag)	128
4.3.6.2. Aluminum (Al)	131
4.3.6.3. Arsenic (As)	131
4.3.6.4. Cadmium (Cd)	132
4.3.6.5. Chromium (Cr)	133
4.3.6.6. Copper (Cu)	133
4.3.6.7. Iron (Fe)	133
4.3.6.8. Mercury (Hg)	133
4.3.6.9. Manganese (Mn)	134
4.3.6.10. Nickel (Ni)	134
4.3.6.11. Lead (Pb)	135
4.3.6.12. Antimony (Sb)	136
4.3.6.13. Selenium (Se)	136
4.3.6.14. Tin (Sn)	136
4.3.6.15. Zinc (Zn)	137
4.4. Further Interpretation of Sediment Results	137
4.4.1. Inter-metal and grain size correlation	138

4.5. Conclusions	143
Chapter 5: Spatial and Temporal Variability in the Water Column Nutrients and Pesticides of Jobos Bay	151
<i>David Whitall, Angel Dieppa and Thomas L. Potter</i>	
5.1. Introduction	151
5.1.1. Nutrients	151
5.1.2. Pesticides	152
5.2. Methods	153
5.2.1. Nutrients, Pesticides and Chlorophyll a Sampling and Analysis	153
5.2.2. Nutrient and Chlorophyll a Sample Collection Methods	154
5.2.3. Diel Sampling Program of Nutrients and Chlorophyll a	155
5.2.4. Nutrient and Chlorophyll a Analysis	155
5.2.5. Pesticide Sample Collection Methods	155
5.2.6. Pesticide Sample Handling and Preparation	155
5.2.7. Statistical Analysis of Data	157
5.3. Results and Discussion	158
5.3.1. Orthophosphate	158
5.3.2. Oxidized Nitrogen	158
5.3.3. Chlorophyll a	159
5.3.4. Pesticide Results	160
5.4. Conclusions	162
Chapter 6: Conclusions	167
Appendices	171

Executive Summary

This baseline assessment of Jobos Bay and surrounding marine ecosystems consists of a two part series. The first report (Zitello *et al.*, 2008) described the characteristics of the Bay and its watershed, including modeling work related to nutrients and sediment fluxes, based on existing data. The second portion of this assessment, presented in this document, presents the results of new field studies conducted to fill data gaps identified in previous studies, to provide a more complete characterization of Jobos Bay and the surrounding coral reef ecosystems. Specifically, the objective was to establish baseline values for the distribution of habitats, nutrients, contaminants, fish, and benthic communities. This baseline assessment is the first step in evaluating the effectiveness in changes in best management practices in the watershed.

This baseline assessment is part of the Conservation Effects Assessment Project (CEAP), which is a multi-agency effort to quantify the environmental benefits of conservation practices used by agricultural producers participating in selected U.S. Department of Agriculture (USDA) conservation programs. Partners in the CEAP Jobos Bay Special Emphasis Watershed (SEW) included USDA's Agricultural Research Service (ARS) and the Natural Resources Conservation Service (NRCS), National Oceanic and Atmospheric Administration (NOAA) and the Government of Puerto Rico. The project originated from an on-going collaboration between USDA and NOAA on the U.S. Coral Reef Task Force. The Jobos Bay watershed was chosen because the predominant land use is agriculture, including agricultural lands adjacent to the Jobos Bay National Estuarine Research Reserve (JBNERR or Reserve), one of NOAA's 26 National Estuarine Research Reserves (NERR).

This report is organized into six chapters that represent a suite of interrelated studies. Chapter 1 provides a short introduction to Jobos Bay, including the land use and hydrology of the watershed. Chapter 2 is focused on benthic mapping and provides the methods and results of newly created benthic maps for Jobos Bay and the surrounding coral reef ecosystem. Chapter 3 presents the results of new surveys of fish, marine debris, and reef communities of the system. Chapter 4 is focused on the distribution of chemical contaminants in sediments within the Bay and corals outside of the Bay. Chapter 5 focuses on quantifying nutrient and pesticide concentrations in the surface waters at the Reserve's System-Wide Monitoring Program (SWMP) sites. Chapter 6 is a brief summary discussion that highlights key findings of the entire suite of studies.

The main findings of each Chapter are as follows:

CHAPTER 1: INTRODUCTION

- Jobos Bay, the second largest estuary in Puerto Rico, features diverse marine habitats, including mangroves, salt marshes, seagrasses and coral reefs.
- The Jobos Bay watershed is 137 km² in size, has a population of about 32,000 people and a variety of land uses including low density urban and industrial, with the predominant land use being agriculture.
- Precipitation patterns in the watershed are strongly seasonal with the rainiest periods occurring in the fall.
- Río Seco, in the east, is the only major river that discharges into Jobos Bay seasonally.

CHAPTER 2: BENTHIC HABITAT MAPPING

- A benthic habitat map was created for the Jobos Bay region by delineating and classifying habitat features visible in optical and acoustic remotely sensed imagery. Several improvements were made to this map (relative to the existing habitat map from 2001), including using: (1) a

smaller mapping unit (*i.e.*, 1,000 versus 4,000 m²), (2) a more detailed classification scheme, (3) more recent optical imagery (*i.e.*, from 2006 versus 1999), and (4) newly acquired acoustic imagery to supplement the optical imagery in turbid areas.

- Benthic features were classified based on five primary coral reef ecosystem attributes: 1) geographic zone, 2) geomorphological structure, 3) dominant biological cover, 4) amount of live coral cover, and 5) percent hardbottom. When linked together, 93 unique combinations of these attributes were identified and delineated.
- In total, 35.7 km² of the seafloor and 14.1 km² of the intertidal shoreline area in and around Jobos Bay were mapped. *Unconsolidated Sediment*, specifically *Mud*, constituted the majority (93%) of the mapped area, with *Coral Reef* and *Hardbottom* comprising around 7%. These substrates were colonized most commonly by *Seagrass* (31%), followed by *No Cover* (28%), *Mangroves* (21%) and *Algae* (20%). Percent live coral cover was <10% for 95% of the mapped area, while the remainder was mapped as 10% ≤ 50%.
- The thematic accuracy of this habitat map is not known as a statistically robust accuracy assessment was not conducted. However, the map was reviewed by local experts and similar products created using the same mapping protocol had high thematic accuracy levels.

CHAPTER 3: FISH COMMUNITIES, BENTHIC HABITATS AND MARINE DEBRIS

- Field surveys were conducted to characterize fish communities and associated habitats in the Jobos Bay ecosystem. Sites were selected via a stratified-random sampling design using the NOAA benthic habitat map and geographic region. A total of 45 sites were sampled (20 hardbottom, 15 unconsolidated sediments, 10 mangrove).
- On hardbottom, turf algae accounted for the highest overall mean percent cover, followed by macroalgae, hard coral, sponges, and gorgonians. Hard coral cover averaged 6.5 (±1.2)%, with higher amounts occurring on aggregate reef on the fore reef adjacent the cays. The most abundant coral was *Porites astreoides*, followed by *Siderastrea siderea*, *Montastraea cavernosa*, and the *Montastraea annularis* complex. Unconsolidated sediment and mangrove habitats were characterized by varying degrees of seagrass and algal cover.
- Fish species richness and diversity were significantly greater on hardbottom compared to mangrove and unconsolidated sediments. Hardbottom and mangroves supported higher fish densities and biomass than unconsolidated sediments.
- The fish community consisted of 34 taxonomic families and 112 species. The fish community varied by habitat type. Wrasses and damselfishes were most numerically abundant on hardbottom, whereas surgeonfishes, parrotfishes, and snappers accounted for the highest proportion of biomass. Large schools of clupeiids, which were absent on other habitats, were present at several mangrove sites. Fish abundance and biomass on unconsolidated sediments were variable but generally low compared to the other habitats. Overall, groupers (*Cephalopholis* and *Epinephelus* spp.) were infrequent across the study area and generally small in size. The majority of observed snappers were also juveniles.

CHAPTER 4: CONTAMINANTS IN SEDIMENTS AND CORAL TISSUES

- A stratified random sampling design was used to assess a suit of 154 contaminants in surficial sediments and coral (*P. astreoides*) tissues.
- Levels of contamination of sediment in the Bay were similar to what has been observed in other systems in Puerto Rico, and were generally below levels expected to be toxic to benthic organisms. No sites exceeded published sediment quality guidelines for any analyte. In general, the inner bay had significantly higher concentrations of contaminants in sediments. This is likely

driven by riverine inputs and lack of oceanic flushing in the inner bay, as well as a significantly higher percentage of fine grained sediments, which tend to accumulate more contaminants due to higher surface areas.

- Levels of contamination in coral tissues (*P. astreoides*) were similar to what has been observed in other systems in Puerto Rico. Currently, no guidelines exist for acceptable levels of contamination in corals.
- Only two out of 154 analytes measured in corals showed a difference between the inshore and offshore strata; both arsenic (As) and lead (Pb) demonstrated statistically higher values offshore.

CHAPTER 5: NUTRIENTS AND PESTICIDES IN SURFACE WATER

- In order to quantify the spatial and temporal variability of surface water nutrients and pesticides, estuarine samples were collected monthly at the previously established JBNERR SWMP sites.
- Surface water concentrations of orthophosphate were highest at site 09, which is the site closest to land. Oxidized nitrogen concentrations (nitrate plus nitrite) were lowest at site 20, which is farthest from shore. This difference in spatial patterns between nitrogen and phosphorus may reflect different flux pathways (groundwater versus surface runoff).
- Chlorophyll a concentrations were statistically unique at each site, suggesting the site specific forcing factors (e.g., nutrients, hydrology, grazing pressure) are driving water column primary productivity.
- The only current use pesticide detected in surface waters in the Bay was atrazine. The atrazine degradation product desethylatrazine (DEA) was also detected. Levels of these compounds were below levels associated with environmental toxicity.
- Time series data show that pesticide detections in the Bay occurred following herbicide applications on the farm immediately preceding a large storm event. This suggests that the dominant delivery pathway of pesticides to the Bay is surface water runoff.

CHAPTER 6: CONCLUSIONS

- The coral reef habitats outside of Jobos Bay are similar to what has been observed in other systems in the U.S. Caribbean.
- Levels of contamination in sediments and coral tissues were generally low and similar to what has been measured in other systems in Puerto Rico.
- This study serves as a baseline assessment which will allow coastal managers to assess the effectiveness of agricultural best management practices in the watershed.

REFERENCES

Zitello, A.G., D.R. Whitall, A. Dieppa, J.D. Christensen, M.E. Monaco, and S.O. Rohmann. 2008. Characterizing Jobos Bay, Puerto Rico: A Watershed Modeling Analysis and Monitoring Plan. NOAA Technical Memorandum NOS NCCOS 76. Silver Spring, MD. 81 pp.

Chapter 1



Introduction and Background

1.1. BACKGROUND

The Conservation Effects Assessment Project (CEAP) is a national, multi-agency effort to quantify the environmental benefits of best management practices used by agricultural producers participating in selected U.S. Department of Agriculture (USDA) conservation programs, including program such as the Conservation Reserve Program and the Wetlands Reserve Program. The Jobos Bay Watershed, located in south-central Puerto Rico, was selected by CEAP partners as the first tropical CEAP Special Emphasis Watershed. Special Emphasis Watersheds (SEW) are strategically located watersheds in which researchers quantify and demonstrate water quality and other environmental benefits of conservation programs. Investigations in Jobos Bay were designed to characterize terrestrial and marine ecosystems at varying spatial scales in order to evaluate the relationship between agricultural practices and the health of near-shore coral reef ecosystems.

Partners in the CEAP Jobos Bay SEW included USDA's Agricultural Research Service (ARS) and the Natural Resources Conservation Service (NRCS), National Oceanic and Atmospheric Administration (NOAA) and the Government of Puerto Rico. The project originated from an on-going collaboration between USDA and NOAA on the

U.S. Coral Reef Task Force. The Jobos Bay watershed was chosen because the predominant land use is agriculture, including agricultural lands adjacent to the Jobos Bay National Estuarine Research Reserve (JBNERR or Reserve), one of NOAA's 28 National Estuarine Research Reserves (Figure 1.1). JBNERR staff was actively involved in the planning and implementation of this study.



Figure 1.1. Mangrove inlet in southern Jobos Bay. Photo: NOAA Center for Coastal Monitoring and Assessment (CCMA).

In 2002, the U.S. Coral Reef Task Force identified the need for action at the local level to reduce key threats to coral reefs in each of the seven states and territories which possess significant coral reef resources. Local Action Strategies (LAS) were developed by Puerto Rico's local and federal agency representatives in 2003. The CEAP work in Jobos Bay directly addresses a LAS goal related to land-based sources of pollution by "reducing loss of live coral reef cover through the promotion and implementation of integrated watershed and land use management practices," such as improved water management. This effort emphasizes the interaction between upland and coastal ecosystems and involves a collaborative partnership between USDA and NOAA to address spatially complex natural resource issues.

1.2. OBJECTIVES

The primary objective of the Jobos Bay CEAP study is to determine the environmental effects that agricultural conservation practices implemented by farmers on the upland may have on coastal waters and the associated coral reef ecosystem. The first step in the process is a baseline assessment, both of the ecological condition of the marine system, including coral reef ecosystems, and the current agricultural management practices. This technical report presents the findings of the baseline assessment of the marine ecosystem.

Specific objectives of the marine component of this project were:

1. Characterize the benthic habitats of the bay and offshore waters.
2. Assess the biological condition of the bay and surrounding reef ecosystems.
3. Quantify the extent and magnitude of contamination in surficial estuarine/marine sediments and in coral tissues (*Porites astreoides*).
4. Quantify the spatial and temporal patterns in estuarine surface water nutrient and pesticide concentrations within the Reserve.

The long term plan is to re-visit this assessment after 5 or 10 years to assess the effectiveness of the management practices that had been implemented by documenting change in the marine ecosystem. This phase of the project is tentative at this point, and is funding dependent.

1.3. STUDY AREA DESCRIPTION

Jobos Bay is located on the south-central coast of Puerto Rico centered at 17° 56'N and 66° 13'W, between the municipalities of Salinas and Guayama (Figure 1.2). The second largest estuary in Puerto Rico, Jobos Bay has a total surface area of just over 25 km². Jobos Bay is classified as a coastal plain estuary that was formed by rising sea levels at the end of the last ice age. It is a natural harbor protected from offshore wind and waves by a series of mangrove islands in the southwest and Punta Pozuelo in the southeast. Jobos Bay features diverse marine habitats, including mangroves, mud flats, salt marshes, seagrasses and coral reefs (Figure 1.3).

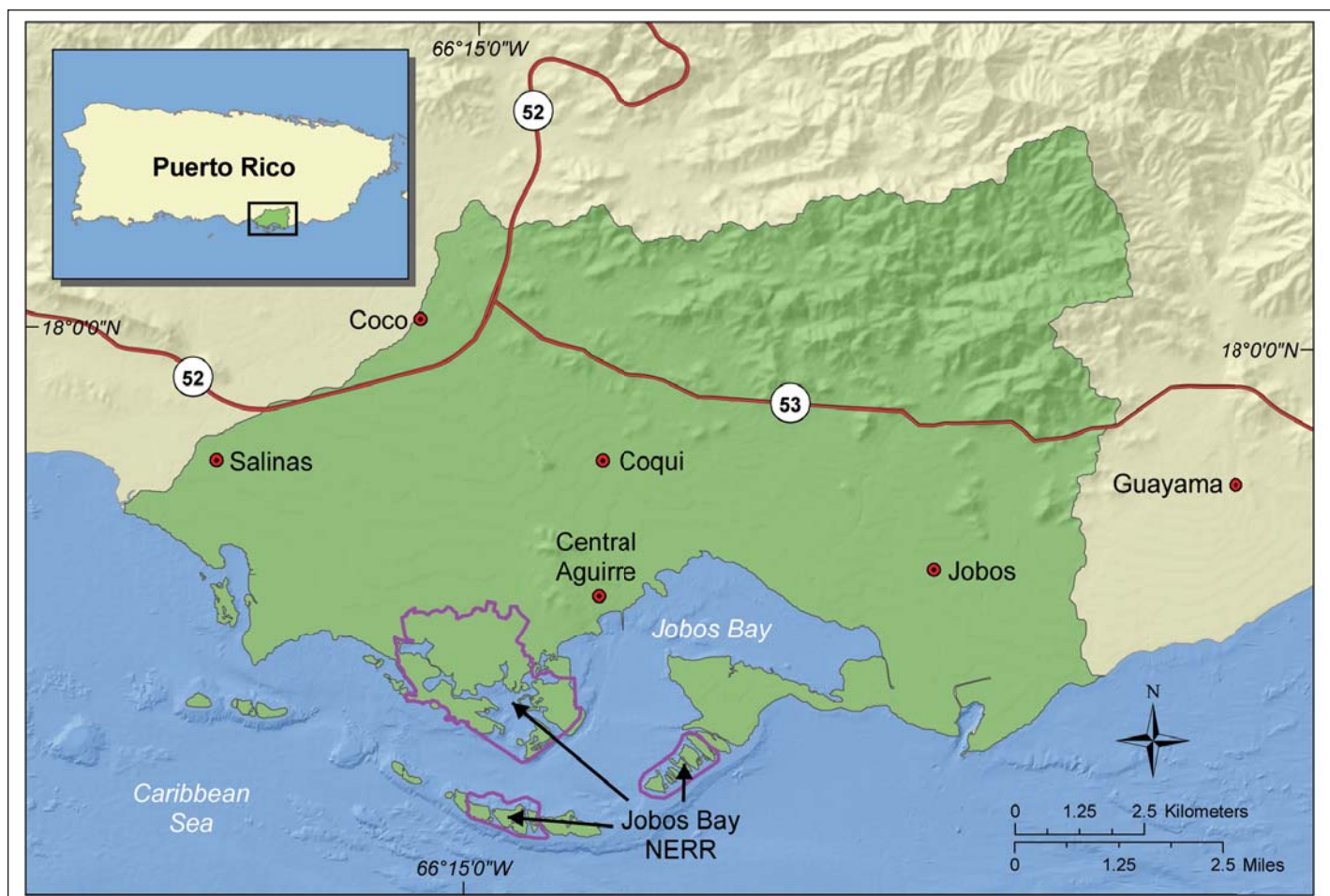


Figure 1.2. Location of Jobos Bay, its watershed and the Jobos Bay National Estuarine Research Reserve (JBNERR) in Puerto Rico.

The Jobos Bay watershed reaches as far as 11 km inland and has a total catchment area of 137 km². The watershed contains several centers of low density urban development and has an estimated total population of 32,000 people (U.S. Bureau of the Census, 2001). The predominant land use is agriculture, including diversified production of agricultural commodities such as plantains, bananas, papayas, sorghum, corn and hay, and animal operations with poultry and some beef cattle. Water quality and conservation concerns related to agricultural practices are important in the Jobos Bay watershed and may influence coral reef ecosystem health. Preliminary studies reported that pesticides and fertilizers applied in agricultural fields were being transported to the bay (DNER, 2002). Increasing industrial and commercial growth in the watershed has also been recognized as a concern to Jobos Bay's ecosystem health. There are two landfill operations within the watershed. The regional landfill, operated by BFI, is located in the middle of the watershed and is expected to broaden to twice the size of its original plans; while the other is on the eastern edge of the watershed in Guayama. Other major industries such as Chevron Phillips, Ayerst-Wyeth, IPR Pharmaceuticals, Colgate-Palmolive and ProChem maintain operations in the watershed (DNER, 2002). Two of Puerto Rico's seven power production plants operate within the Jobos Bay watershed. There are three point source dischargers with USEPA National Pollutant Discharge Elimination System (NPDES) permits in the Jobos Bay watershed: Chevron Phillips, the Aguirre power plant and Ball Metal Beverage Container (USEPA, 2010; Table 1.1; Figure 1.4).



Figure 1.3. Mud flats in JBNERR. Photo: NOAA CCMA.

Table 1.1. Facilities with NPDES discharge permits in the Jobos Bay watershed. Data from USEPA (2010). Units are displayed in pounds.

Pollutant Name	Phillips Oil Refinery ¹	Aguirre Power Plant ²	Ball Metal
Ammonia	184	--	--
Barium	15.9	--	--
BOD, 5-day, 20 deg. C	2,866	43,929	--
Chemical oxygen demand (COD)	14,166	1,817,976	--
Chlorine	197	6.13	--
Chromium	1.37	0.62	--
Chromium, Hexavalent	4.082	--	--
Copper	0.63	107	6.0036
Fluoride	1,122	--	--
Foaming agents	28.5	--	434
Iron	--	1,815	--
Lead	--	44.1	7.78
Manganese	2.17	--	--
Mercury	0.203	--	--
Oil and grease per production	0.52	--	14,031
Selenium	1.99	--	--
Solids, total suspended	2,767	278,856	--
Sulfide	4.63	--	240
Total phenols	--	187	--
Zinc	--	2,435	109

¹ Phillips Oil Refinery was cited for violations for Copper (Cu) in 2009.

² Aguirre Power Plant was cited for violations for Zinc (Zn) in 2007 and 2008, Silver (Ag) in 2009, and Iron (Fe) in 2009.



Figure 1.4. Location of point source dischargers with National Pollutant Discharge Elimination System (NPDES) permits.

1.4. SITE CHARACTERIZATION

1.4.1. Environmental Setting

The Jobos Bay watershed is primarily comprised of the low-relief South Coastal Plain of Puerto Rico, but reaches elevations of greater than 700 m at its landward boundary. Many of Jobos Bay watershed's physical characteristics are attributed to the presence of two of Puerto Rico's Central Interior Mountain Ranges to the north, La Cordillera Central and La Sierra de Cayey. These mountains serve as a barrier to the moisture-laden northeast trade winds, causing a zone of low precipitation throughout the southern coast of Puerto Rico. Mean annual rainfall between 1999 and 2008 was 996 mm at the Aguirre rain gauge station located in the watershed (NCDC, 2010). For this same time period and station, September and October were recorded as the wettest months, with an average rainfall of 167 mm, while January was the driest month, with an average rainfall of 20 mm (Figure 1.5). The Jobos Bay watershed is located in the Subtropical Dry Forest Zone, the most arid ecological life zone in Puerto Rico (Ewel and Whitmore, 1973). The vegetation is almost entirely deciduous and forms a complete ground cover on most soils. Past land uses, especially abandoned sugar cane fields, support man-modified vegetation that is characterized by a complete grass cover and sparsely distributed tall trees with flattened spreading crowns.

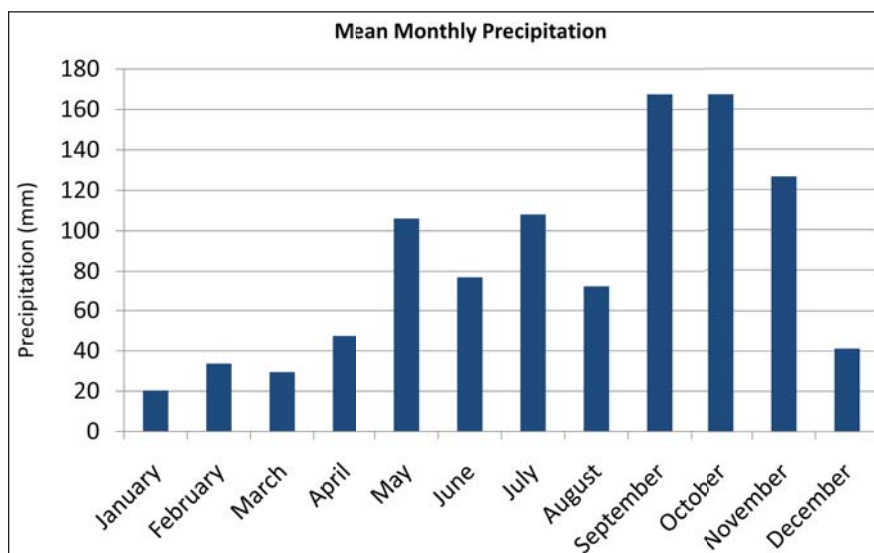


Figure 1.5. Average monthly precipitation at Aguirre weather station.

Temperatures in the Jobos Bay watershed are high throughout the year and show little seasonal fluctuation. The mean annual temperature is 26° C (78.8° F), with a maximum of 27.5° C (81.6° F) in August and a minimum of 24.3° C (75.7° F) in January (NCDC, 2010). The predominant wind comes from an easterly direction at mean speeds of 10 km/hr or less (McClymonds and Díaz, 1972). The regular daily wind pattern is for low velocity northeast winds to give way to a more brisk southeast wind as the day progresses (DNER, 2002).

Due to Jobos Bay's dry climate and relatively low seasonal rainfall, surface runoff usually only occurs during the wettest months of the year, September through November (Ewel and Whitmore, 1973). As a result, most of the watershed's natural stream beds are only intermittently flooded throughout the year. Río Seco, in the east, is the only major river that discharges into Jobos Bay seasonally. Quiñones-Aponte *et al.* (1997) described that year-round streamflow downstream is limited by where most streams meet the highly porous fan delta deposits. At that point, the streamflow infiltration becomes the most important source of groundwater recharge to the underlying aquifer. The Jobos Bay watershed is within the South Coastal Plain alluvial aquifer that extends from the bedrock hills near the watershed's northern boundary to the coast. According to Quiñones-Aponte *et al.* (1997), there are two discrete groundwater units in the coastal zone, a shallow aquifer between 3 m and 23 m thick and a deep aquifer below. The shallow aquifer is believed to supply the mangrove complex at the watershed's coastal margins, while the deep aquifer may provide freshwater to the offshore mangrove islands that form Jobos Bay's southern boundary.

1.4.2. Jobos Bay Watershed

The Jobos Bay watershed includes 137.3 km² of the South Coastal Plain of Puerto Rico and drains surface runoff directly to Jobos Bay (Figure 1.6). Jobos Bay and its associated watershed is framed by two perennial stream networks; Río Nigua to the west and Río Guamaní to the east.

The watershed's northern boundary, beginning in the foothills of the Central Interior Mountain Range, extends about 6 km to 11 km landward from the shoreline of Jobos Bay. Although Jobos Bay's shoreline represents a straight-line distance of under 20 km, the meandering Bay's mainland coast stretches a total distance of over 45 km. The Jobos Bay watershed does not contain one single river network that accumulates surface water flow throughout the basin. Instead, the watershed contains a variety of distinct pathways by which surface waters are contributed to Jobos Bay. These include perennial stream discharges, intermittent stream discharges and diffuse overland runoff to Jobos Bay. A unique composite of land cover, topography and underlying geology dictate the type of surface water contribution found in the different areas of the Jobos Bay watershed.

The Jobos Bay watershed experienced several man-made water diversion projects since the start of the 20th century. Beginning in 1914, successful agricultural operations have been achieved by transferring surface water to the Jobos Bay watershed from reservoirs outside the basin through irrigation canals. As part of the Guayama Irrigation District, two primary irrigation canals distribute water from Patillas and Carite Reservoirs, northeast of Jobos Bay, to operations throughout the watershed. Both canals flow from east to west, with Canal de Guamaní in the north and Canal de Patillas in the south. Non-irrigation drainage canals were also constructed in order to reclaim wet

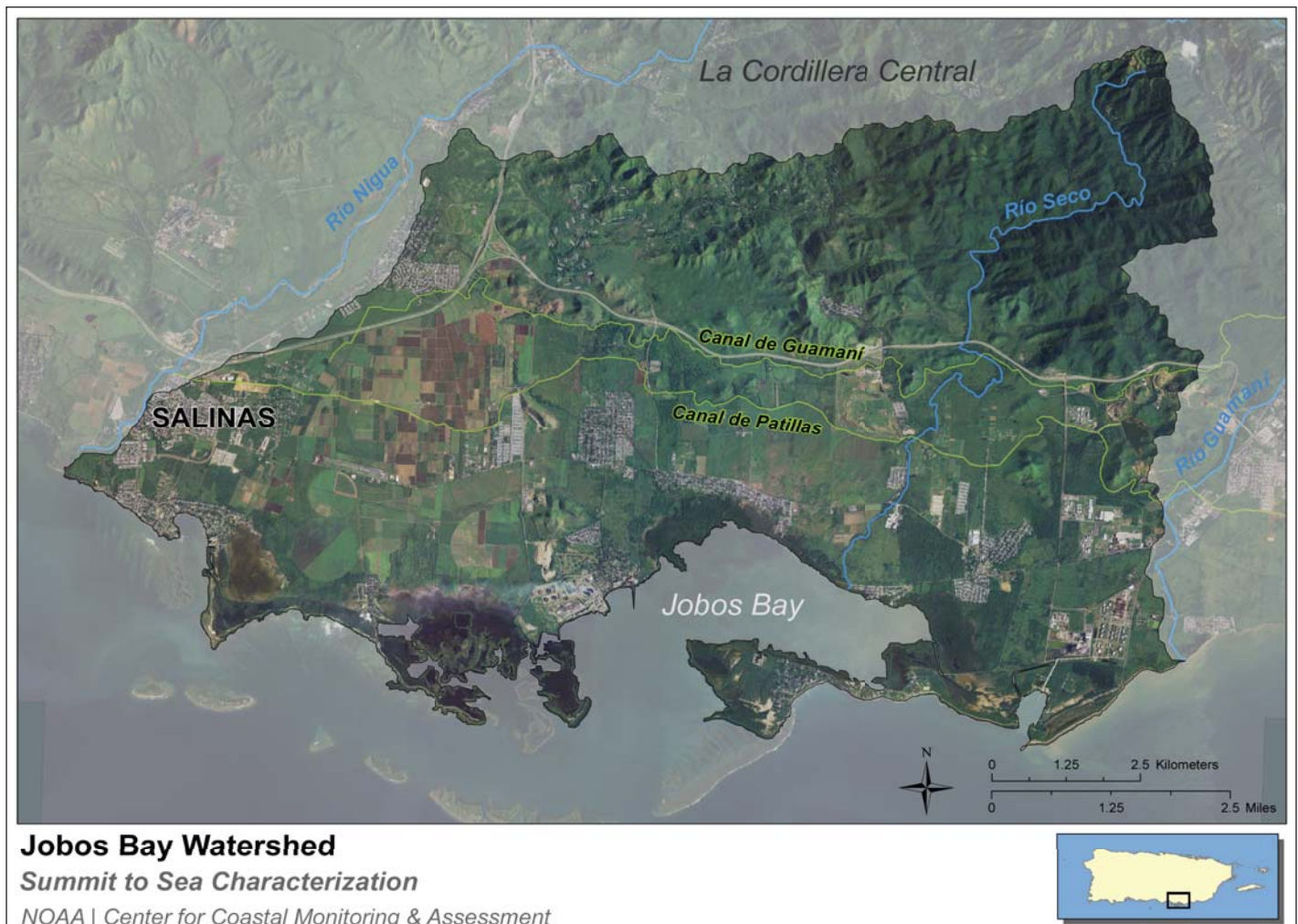


Figure 1.6. Rivers and canals in Jobos Bay watershed.

areas for agriculture and to reduce mosquito breeding in response to the risk of malaria in the 1930's (DNER, 2002).

From Spanish Colonial times up to the 1970s, the Jobos Bay watershed was primarily used for agricultural production (DNER, 2002). Almost the entire coastal plain of Jobos Bay was under sugarcane cultivation until the demise of Puerto Rico's sugarcane market during the 1960s. Over the past 35 years, sugarcane lands have been steadily converted to fruit and vegetable cultivation or entirely removed from agricultural cultivation. Today, cultivated lands in the Jobos Bay watershed only comprise 11% of the area's total land cover (Figure 1.7), which is 15 km². However, the extensive clearing of land for sugarcane cultivation of the past has had a lasting impact on the landscape of the Jobos Bay watershed.



Figure 1.7. Center pivot irrigation on silage farm adjacent to JBNERR. Photo: NOAA CCMA.

Despite the historic prevalence of agriculture in the Jobos Bay watershed, existing land cover conditions are more indicative of an ecosystem in a natural state. Vegetated lands cover 70% of the landscape with grassland, forest and scrub/shrub accounting for 42%, 15% and 13%, respectively (Figure 1.8). The large amount of vegetated lands may lead to the inaccurate conclusion that the Jobos Bay watershed is a relatively pristine system.

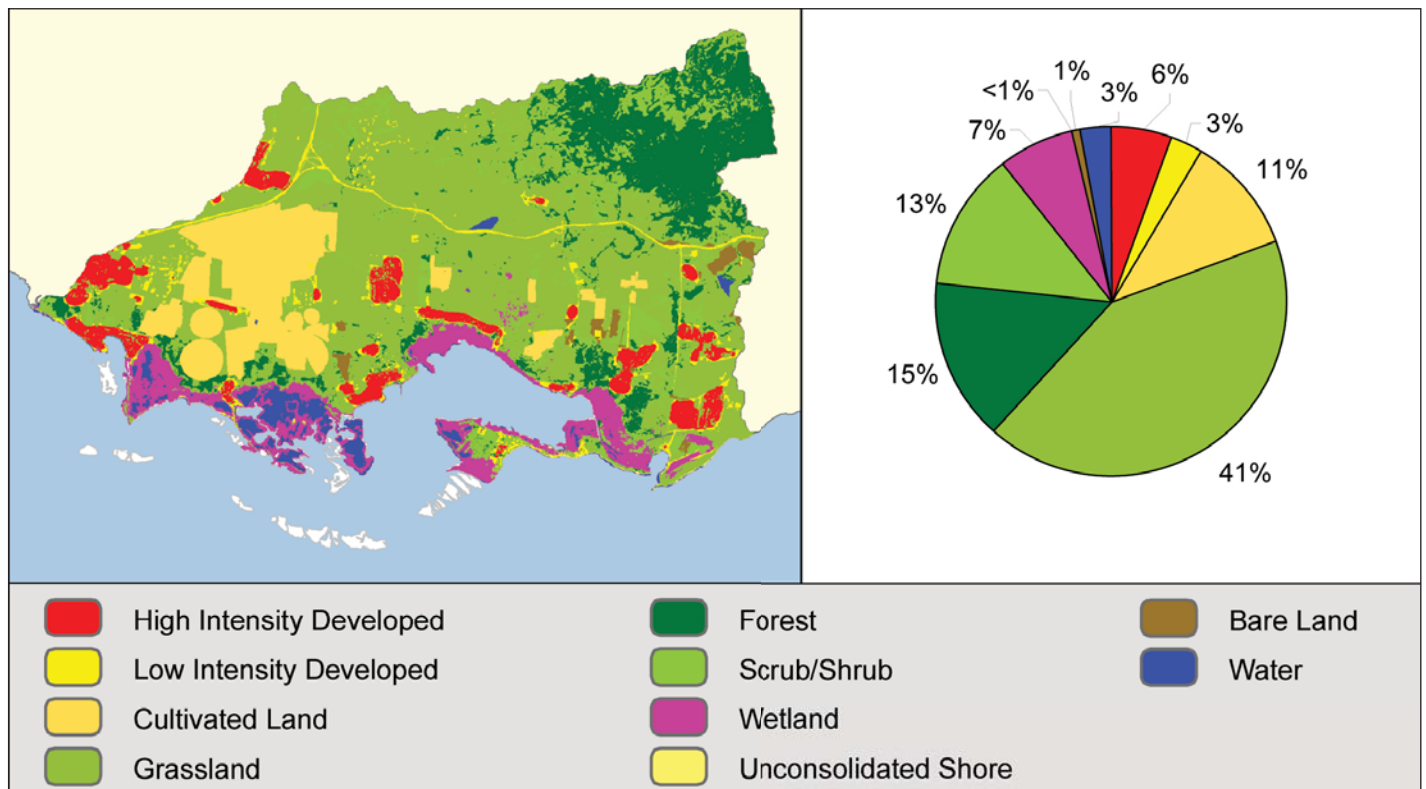


Figure 1.8. Land use/land cover in Jobos Bay watershed.

Inspection of aerial photography indicated that as much as 13.5 km² of the area classified as grassland is revegetated agriculture lands (Figure 1.9). In addition, an unspecified amount of classified grasslands are actually used for livestock pasture. If these areas were considered a separate land cover type the amount of naturally vegetated land cover would be reduced by 10% to 15%. Re-vegetated agriculture fields and pasture have a higher frequency of disturbance and serve fundamentally different ecosystem services (e.g., different types of habitat) than naturally vegetated grasslands. A majority of the disturbed grasslands exist south of the irrigation canals, while the naturally vegetated grasslands tend to lie north of the canals in the foothills of the Central Interior Mountain Range.

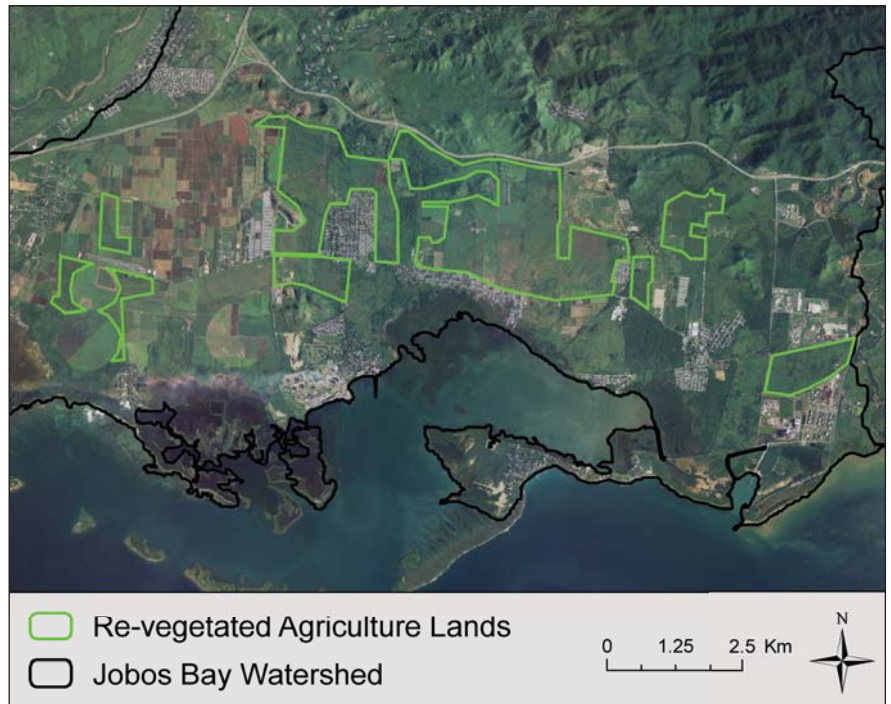


Figure 1.9. Re-vegetated lands in Jobos Bay watershed.

The 32,000 residents of the Jobos Bay watershed live in low density residential communities that are located throughout the area. Over two thirds of the population are residents of the municipality of Salinas in the western half of the watershed, while the remainder of the residents live in the municipality of Guayama in the east. The average population density in Jobos Bay is maintained at a comparatively low 234 people/km² by large areas of open space between communities. The primary transportation routes through the area are Highways 52 and 53, with Route 3 servicing local traffic. A variety of industrial activities are distributed throughout the Jobos Bay watershed. Among other industries, Jobos Bay hosts two electric power generation plants, a petroleum refinery, and several major chemical and pharmaceutical facilities, some of which discharge into the Bay (Table 1.1).

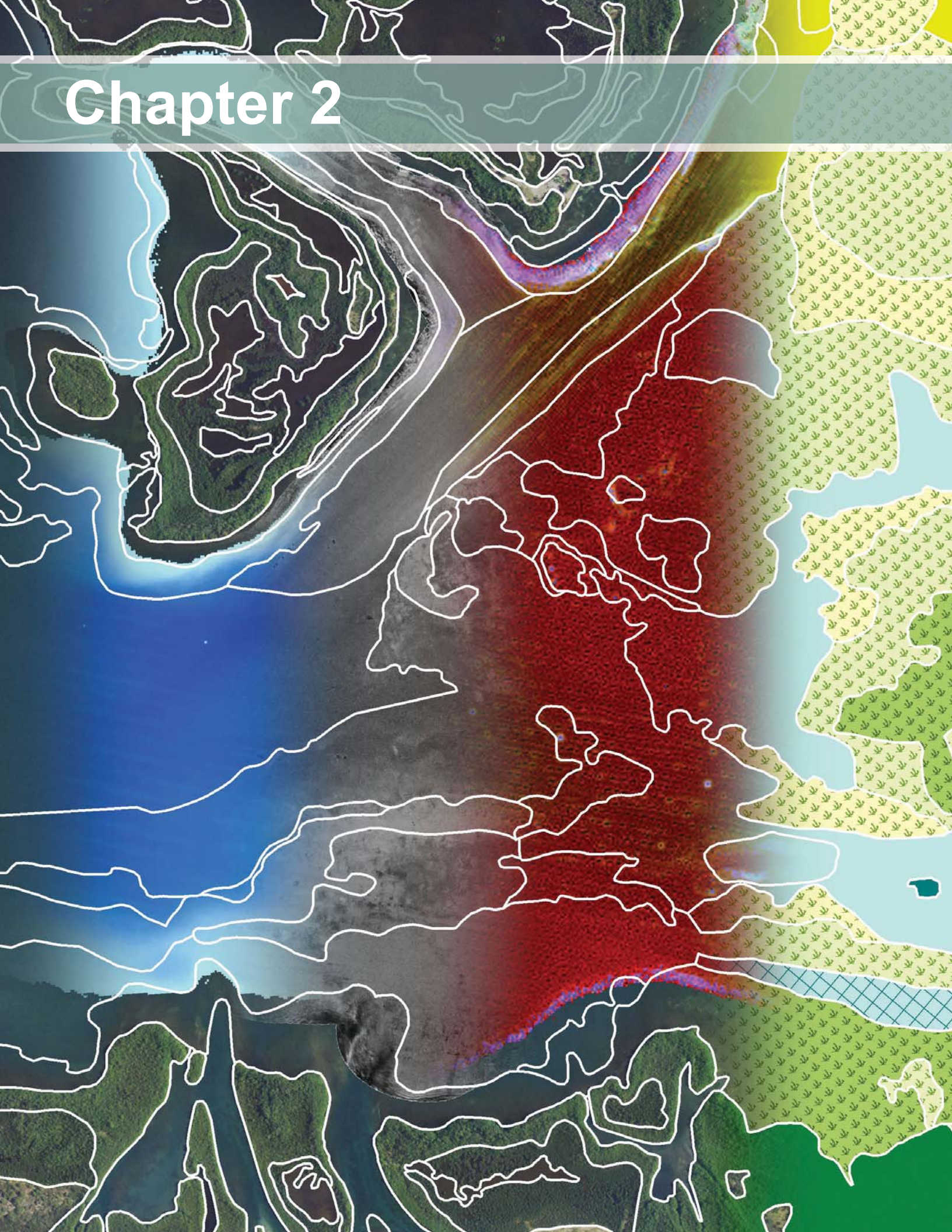
A more complete discussion of the Jobos Bay watershed and its land uses, including preliminary modeling work of sediments and pollutants can be found in Zitello *et al.* (2008).

This report is organized into six chapters that represent a suite of interrelated studies. Chapter 2 is focused on benthic mapping and provides the methods and results of newly created benthic maps for Jobos Bay and the surrounding coral reef ecosystem. Chapter 3 presents the results of new surveys of fish, marine debris, and reef communities of the system. Chapter 4 is focused on the distribution of chemical contaminants in sediments within the Bay and corals outside of the Bay. Chapter 5 focuses on quantifying nutrient and pesticide concentrations in the surface waters at the Reserve's System-Wide Monitoring Program (SWMP) sites. Chapter 6 is a brief summary discussion that highlights key findings of the entire suite of studies.

REFERENCES

- Department of Natural and Environmental Resources (DNER). 2002. Jobos Bay Estuarine Profile: A National Estuarine Research Reserve. Puerto Rico DNER and National Oceanic and Atmospheric Administration, Office of Ocean and Coastal Resource Management, Estuarine Reserve Division. 107 pp.
- Ewel, J.J. and J.L. Whitmore. 1973. The Ecological Life Zones of Puerto Rico and the U.S. Virgin Islands. U.S. Department of Agriculture (USDA) Forest Service, Institute of Tropical Forestry. Forest Service Research Paper ITF-18. 72 pp.
- McClymonds, N.E. and J.R. Díaz. 1972. Water resources of the Jobos area, Puerto Rico - A preliminary appraisal, 1962. U.S. Geological Survey Water-Resources Bulletin 13. 32 pp.
- National Climatic Data Center (NCDC). 2010. NOAA Satellite and Information Service (Online). <http://www.ncdc.noaa.gov/oa/climate/stationlocator.html> (Accessed 10 June 2011).
- Quiñones-Aponte, V., F. Gómez-Gómez, and R.A. Renken. 1997. Geohydrology and simulation of ground-water flow in the Salinas to Patillas area, Puerto Rico. U.S. Geological Survey, Water Resources Investigations Report 95-4063. 37 pp.
- U.S. Bureau of the Census. 2001. TIGER/Line Files, Redistricting Census 2000 (Online). <http://www.census.gov/geo/www/tiger> (Accessed 10 June 2011).
- U.S. Environmental Protection Agency (USEPA). 2010. Discharge Monitoring Report (DMR) Pollutant Loading Tool (Online). <http://cfpub.epa.gov/dmr/> (Accessed 10 June 2011).
- Zitello, A.G., D.R. Whitall, A. Dieppa, J.D. Christensen, M.E. Monaco, and S.O. Rohmann. 2008. Characterizing Jobos Bay, Puerto Rico: A Watershed Modeling Analysis and Monitoring Plan. NOAA Technical Memorandum NOS NCCOS 76. Silver Spring, MD. 81 pp.

Chapter 2



Shallow-water Benthic Habitats of Jobos Bay

Bryan Costa^{1,2,3}, Laurie Bauer^{1,2} and Peter Mueller^{1,2}

2.1. INTRODUCTION

The estuarine ecosystems of the Jobos Bay National Estuarine Research Reserve (JBNERR or Reserve) and the surrounding waters of southeastern Puerto Rico have been preserved because they are economically and ecologically important natural resources. The mosaic of habitats, including coral reefs, seagrasses and mangroves, are home to a diversity of marine organisms that provide valuable ecosystem services to the local community, including fishing, tourism and shoreline protection (DNER, 2002). Estuarine and coral reef ecosystems in Puerto Rico and throughout the U.S. Caribbean, however, are under increasing pressure from environmental and anthropogenic stressors that threaten these important marine communities (García-Sais *et al.*, 2008). In order to better evaluate and address these threats, a baseline understanding of the benthic communities and associated living marine resources is needed by scientists and resource managers. Habitat maps, in particular, are an integral component to this process by supporting an effective ecosystem-based approach to management (Pittman *et al.*, 2010).

Given the importance of habitat maps, NOAA's Biogeography Branch^A (BB) developed the analytical protocols used for mapping benthic habitats throughout all U.S. jurisdictions, states, and territories, including the U.S. Caribbean. These standardized protocols enable scientists and managers to quantitatively compare different estuarine and shallow-water coral reef ecosystems in tropical U.S. waters. The BB used these same protocols to generate a habitat map of the estuarine and shallow-water ecosystems surrounding JBNERR (Figure 2.1).

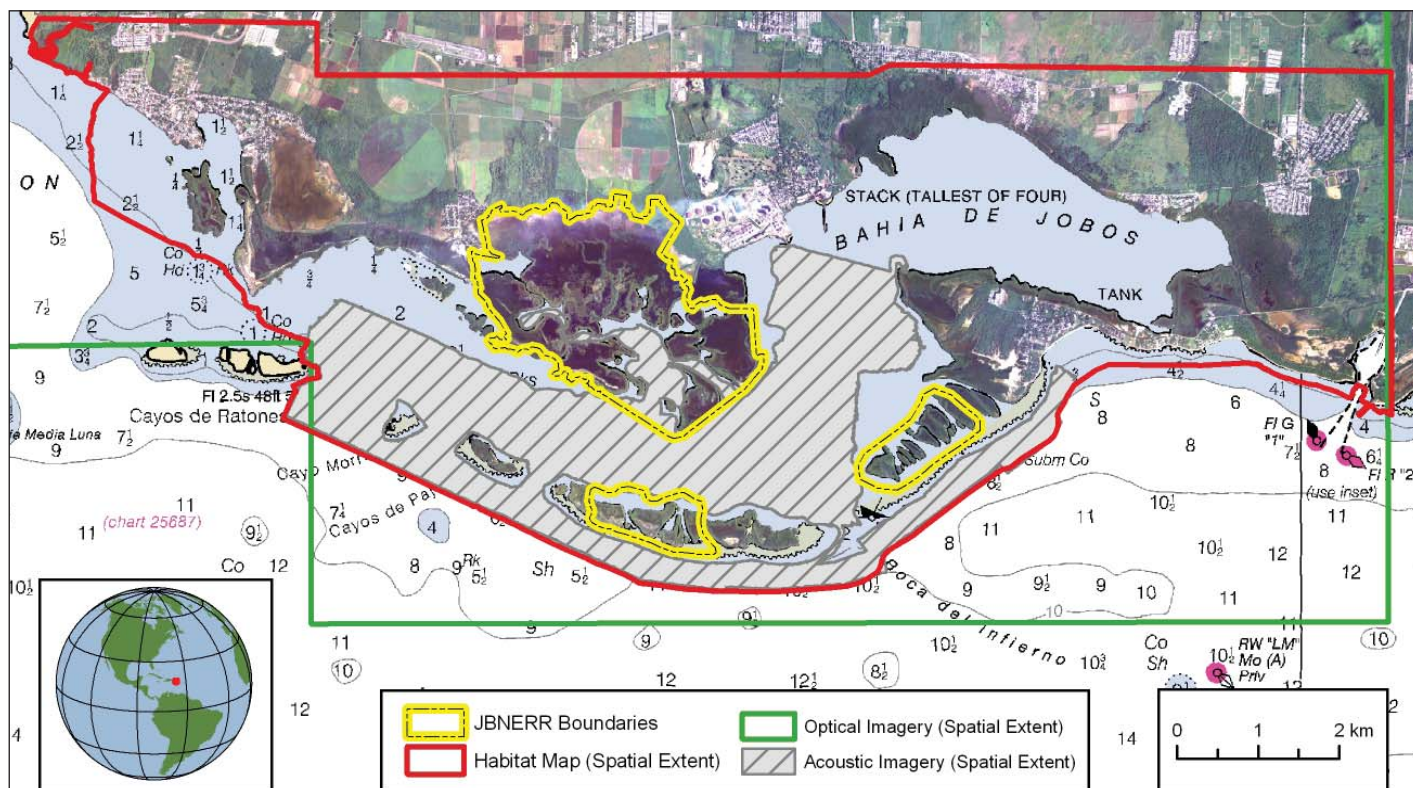


Figure 2.1. Map of Jobos Bay National Estuarine Research Reserve (JBNERR) in southeastern Puerto Rico. A benthic habitat map was created for the area in and around the Reserve using optical and acoustic imagery.

^A The Biogeography Branch is a part of National Oceanic and Atmospheric Administration (NOAA), National Ocean Service (NOS), National Centers for Coastal Ocean Science (NCCOS), Center for Coastal Monitoring and Assessment (CCMA).

¹ Center for Coastal Monitoring and Assessment, National Centers for Coastal Ocean Science, National Ocean Service, National Oceanic and Atmospheric Administration

² Consolidated Safety Services, Inc., under NOAA Contract No. DG133C07NC0616

³ Corresponding author: Bryan.Costa@noaa.gov

The objective of this chapter is to provide spatially-explicit information describing the habitat types, biological cover and live coral cover present in and around JBNERR's boundaries. The resulting fine-scale habitat map, generated by visual interpretation of optical and acoustic imagery, represents the second habitat map produced for this shallow-water (≤ 30 m) area. It is, however, the first spatially complete habitat map for Jobos Bay, as the previous mapping effort was inhibited by poor water clarity. The spatial products developed for this project will enable managers and scientists to better monitor changes in estuarine and marine habitats of JBNERR. The habitat map created by BB represents one such product in a suite of deliverables designed to support the management of JBNERR. In particular, these products include:

- A classification manual
- Description of the methods used to create the habitat maps
- Source datasets, including acoustic and optical imagery
- Ground validation field data
- Derived datasets, including GIS files of benthic habitats

Collectively, these products give JBNERR an increased technical capacity for management and stewardship of the reserve, including: (1) evaluating the efficacy of management actions, (2) designing monitoring sampling plans, (3) assessing the impacts of human-uses, and (4) supporting the process of coastal and marine spatial planning (CMSP). In addition to supporting the management of JBNERR, this shallow-water mapping effort is part of a larger Conservation Effects Assessment Project (CEAP) to explore the environmental effects that upland agricultural practices and conservation measures have on estuarine and coral reef ecosystems. This map may be used as a baseline for comparing future habitat maps (created using the same procedures outlined here) in order to quantify changes in the extent of seagrass beds, mangroves, coral or other habitat features. This comparison would allow managers to better understand the impact of new agricultural practices or conservation measures on the downstream benthic marine environment.

2.2. BENTHIC HABITAT CLASSIFICATION SCHEME

A habitat classification scheme allows scientists to systematically group habitat types based on common ecological characteristics. The initial task in any mapping effort is to develop a classification scheme by clearly identifying and defining discrete habitat classes. This scheme is subsequently used to guide the delineation and attribution of polygons during the mapping process. It is, consequently, critical for map users to have an understanding of the classification system, its structure and its definitions. This understanding allows users to decide on the appropriate uses for, and limitations of, the habitat map.

The Jobos Bay shallow-water habitat classification scheme defines benthic communities based on five primary coral reef ecosystem attributes: 1) broad geographic zone, 2) geomorphological structure, 3) dominant biological cover, 4) amount of live coral cover, and 5) percent hardbottom. Habitat features are described by varying levels of detail (*i.e.*, major and minor categories nested within them), so users can refine the information depicted by habitat map to best suit their research or management needs. In total, 93 unique concatenations of zone, major structure, detailed structure, percent hard bottom, major cover, percent cover and live coral cover were identified from the optical and acoustic imagery. The thematic accuracy of these classes is unknown because a statistically robust accuracy assessment was not conducted. Thus, all users should independently analyze this habitat map according to their own needs and standards to determine its limitations and usability. Other habitat

maps created using the same mapping protocol, however, reported overall thematic accuracies of greater than 88% for major geomorphological structure and cover classes, and greater than 70% for detailed geomorphological structure and biological cover classes (Battista *et al.*, 2007a,b; Zitello *et al.*, 2009; Bauer *et al.*, 2010).

2.2.1. Comparison to Previous NOAA Habitat Classification Schemes

Many important factors were considered when developing the shallow-water habitat classification scheme for Jobos Bay. These factors included: (1) how it would dovetail with existing classification schemes for marine habitats; (2) what limitations were associated with the optical imagery and with the acoustic imagery; (3) what would be an appropriate minimum mapping unit (MMU); (4) how much quantitative *in situ* underwater video would be needed to create a habitat map; and (5) how best to create a habitat map using both optical and acoustic imagery sources.

In order to simplify this process, the habitat classification scheme implemented in Jobos Bay was based on the recently updated classification scheme developed by NOAA to map shallow-water (≤ 30 m) benthic habitats around Vieques, Puerto Rico (Bauer *et al.*, 2010). Specifically, the geographic zones, major and detailed geomorphological structure and biological cover types were the same for both habitat maps (Table 2.1), although some habitat types were present in Vieques which were not present in Jobos Bay. Also, both classification schemes had the same the MMU (*i.e.*, 1,000 m²) and cover attributes were based on dominant type. That being said, it is important to note that the Vieques map was created from optical imagery, whereas the Jobos Bay map was created from both optical and acoustic imagery.

Table 2.1. The classification scheme used to classify benthic habitats in and around JBNERR in 2010. This classification scheme was modeled after the one used in Vieques, Puerto Rico (Bauer *et al.*, 2010). Classes with a line through them were not present in Jobos Bay.

Geographic Zone	Geomorphological Structure	Biological Cover
Back Reef	Coral Reef and Hardbottom (Hard)	Major Cover
Bank/Shelf	Aggregate Reef	Algae
Bank/Shelf-Escarpment	Aggregated Patch Reefs	Coralline Algae
Channel	Individual Patch Reef	Live Coral
Dredged	Pavement	Mangrove
Fore Reef	Pav. w/ Sand Channels	No Cover
Lagoon	Reef Rubble	Seagrass
Land	Rhodoliths	Unclassified
Reef Crest	Rock/Boulder	Unknown
Reef Flat	Spur and Groove	Percent Major Cover
Salt Pond	Unknown	10% ≤ 50%
Shoreline Intertidal	Unconsolidated Sediment (Soft)	50% ≤ 90%
Unknown	Mud	90% ≤ 100%
	Sand	N/A
	Sand w/ Scattered Coral & Rock	Unknown
	Unknown	Percent Coral Cover
	Other Delineations	0% ≤ 10%
	Artificial	10% ≤ 50%
	Land	50% ≤ 90%
	Unknown	90% - 100%
		N/A
		Unknown

While the map created for Jobos is similar to the one created for Vieques, it is fundamentally different from the benthic habitat map created in 2001 by NOAA for all of Puerto Rico (Kendall *et al.*, 2001). The primary difference between NOAA's 2001 and 2010 habitat maps is the separation of biological cover from habitat structure, as well as the addition of more detailed structure classes due to the higher resolution of the source imagery and much smaller geographic scope of the map project.

In addition, the 2010 classification scheme includes a map attribute called *Percent Coral Cover*. This attribute describes the percent live coral cover for a habitat feature at the scale of diver observation in the water, without regard to dominant biological cover. It is important to note that *Percent Coral Cover* refers only to the hardbottom component of any mapped polygon (and not to the entire polygon itself). For instance, an attribution of "percent hardbottom equals 50%≤70% and live coral equals 10%≤50%" indicates that 10%≤50% of the hardbottom within that polygon is colonized by live coral.

2.2.2. Geographic Zones

Eleven distinct and non-overlapping geographic zone types were mapped by visually interpreting optical and acoustic imagery. Zone refers to each benthic community's geographic location. It does not address a polygon's substrate or biological cover types. For example, the zone *Fore Reef* is often located adjacent to a *Reef Crest* on the seaward side. However, neither *Fore Reef* nor *Reef Crest* zone types describe the structural or biological habitat within them. Additionally, the location of particular zone types may change depending on whether the system is a barrier reef, fringing reef or when no emergent reef crest is present (Figures 2.2, 2.3 and 2.4, respectively). Habitats or features with areas smaller than the MMU or minimum mapping unit (1,000 m²) were not considered. A brief description of each geographic zone is provided in the following text.

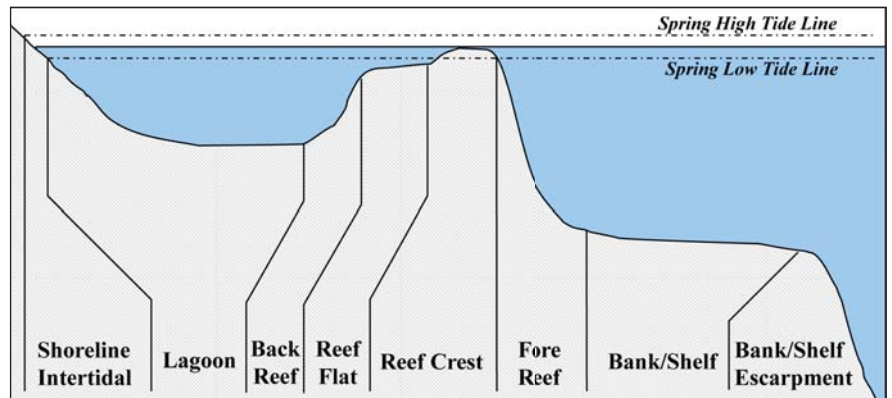


Figure 2.2. Cross-section of zone types when a barrier reef is present. The reef is separated from the shore by a relatively wide, deep lagoon.

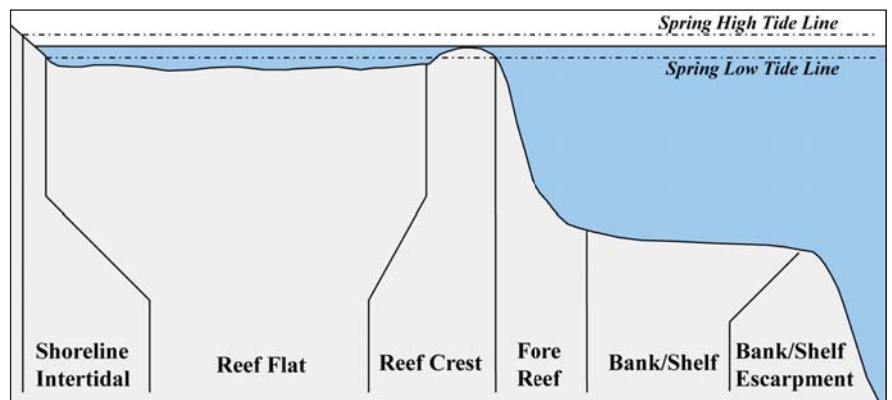


Figure 2.3. Cross-section of zone types when a fringing reef is present. The reef platform is continuous with the shore.

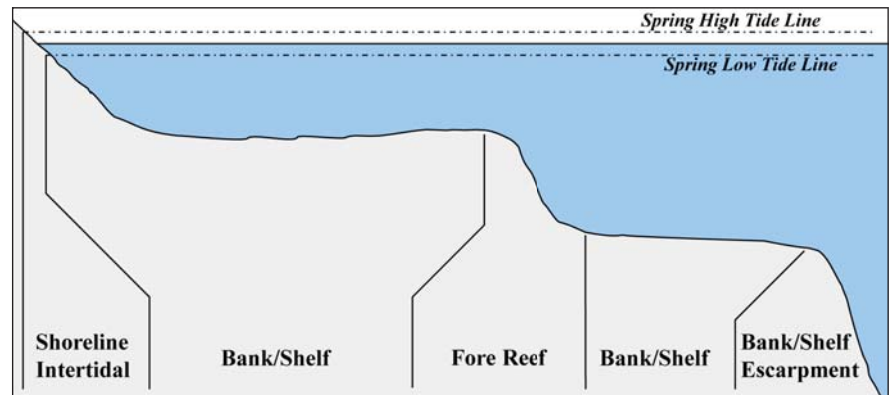


Figure 2.4. Cross-section of zone types when no emergent reef crest is present.

Back Reef

Area immediately landward of a *Reef Crest* that slopes downward towards the seaward edge of a *Lagoon floor* or *Bank/Shelf*. This zone is present only when a *Reef Crest* exists (Figure 2.5).



Figure 2.5. The red polygons (left) outline examples of the geographic zone, Back Reef, west of Cayos Caribes. The photograph (right) depicts the same area from the ground. Photo: NOAA Center for Coastal Monitoring and Assessment (CCMA).

Bank/Shelf

Deeper water area (relative to the shallow water in a lagoon) extending offshore from the seaward edge of the *Fore Reef* or shoreline to the beginning of the escarpment where the insular shelf drops off into deep, oceanic water. If no *Reef Crest* is present, the *Bank/Shelf* is the flattened platform between the *Fore Reef* and deep open ocean waters or between the *Shoreline Intertidal* zone and open ocean (Figure 2.6).



Figure 2.6. The yellow polygon highlights the location of the geographic zone, Bank/Shelf, south of Cayos de Barca.

Dredged

Area in which natural geomorphology is disrupted or altered by excavation or dredging (Figure 2.7).

Fore Reef

Area along the seaward edge of the *Reef Crest* that slopes into deeper water to the landward edge of the *Bank/Shelf* platform. Features not associated with an emergent *Reef Crest* (but still having a seaward-facing slope that is significantly greater than the slope of the *Bank/Shelf*) are also designated as *Fore Reef* (Figure 2.8).



Figure 2.7. The red polygon outlines an example of the geographic zone, Dredged, northwest of Arrecife Moreas.

Lagoon

Shallow area (relative to the deeper water of the *Bank/Shelf*) between the *Shoreline Intertidal* zone and the *Back Reef* of a reef or a barrier island. This zone is typically protected from the high-energy waves commonly experienced on the *Bank/Shelf* and *Reef Crest* zones (Figure 2.9).

Land

Terrestrial features at or above the spring high tide line. Shoreline delineations describing the boundary between land and submerged zones are established at the wrack line where possible or the wet line at the time of imagery acquisition (Figure 2.10). The wrack line is a line of organic and/or anthropogenic debris (above the mean high tide line) that has been deposited by previous higher than normal tides.



Figure 2.8. The green polygon highlights the location of the geographic zone, Fore Reef, just south of Cayos de Barca.



Figure 2.9. The red polygons (left) outline examples of the geographic zone, Lagoon, near Puerto de Jobos. The photograph (right) depicts the same area from the ground. Photo: NOAA CCMA.



Figure 2.10. The red polygon (left) outline an example of the geographic zone, Land, near Puerto de Jobos. The photograph (right) was taken looking northeasterly from inside Bahia de Jobos. Photo: NOAA CCMA.

Reef Crest

The flattened, emergent (especially during low tides) or nearly emergent segment of a reef. This zone of high wave energy lies between the *Fore Reef* and *Back Reef* or *Reef Flat* zones. Breaking waves are often visible in overhead imagery at the seaward edge of this zone (Figure 2.11).

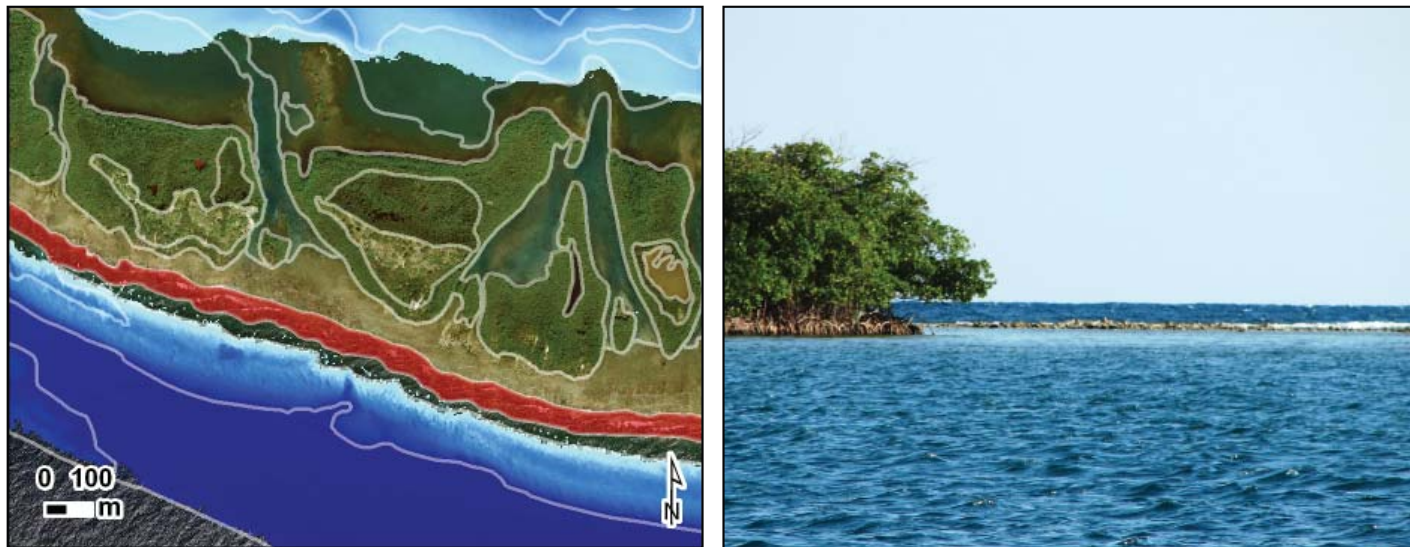


Figure 2.11. The red polygon (left) highlights the location of the geographic zone, Reef Crest, south of Cayos de Barca. The photograph (right) depicts an example of the zone, Reef Crest, in Jobos Bay. Photo: NOAA CCMA.

Reef Flat

Shallow, semi-exposed area with little relief between the *Shoreline Intertidal* zone and the *Reef Crest* of a fringing reef. This broad, flat area often exists immediately landward of a *Reef Crest* and may extend to the shoreline or drop into a *Lagoon*. This zone is protected from the high-energy waves commonly experienced on the *Bank/Shelf* and *Reef Crest* zones (Figure 2.12).



Figure 2.12. The red polygon (left) outline an example of the geographic zone, Reef Flat, near Cayos Caribes. The photograph (right) depicts the same area from the ground. Photo: NOAA CCMA.

Salt Pond

Enclosed area immediately landward of the shoreline with a permanent or intermittent flooding regime of saline to hypersaline waters (Figure 2.13).

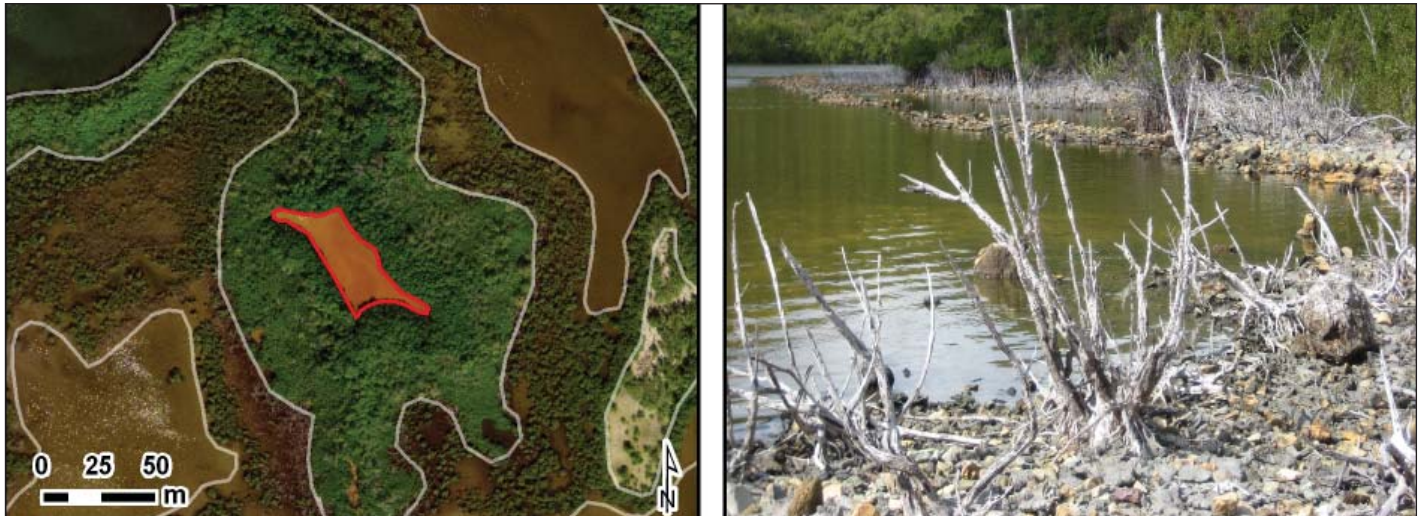


Figure 2.13. The red polygon (left) outline an example of the geographic zone, Salt Pond, near Cayo Puerca. The photograph (right) depicts a salt pond from the ground. Photo: NOAA CCMA.

Shoreline Intertidal

Area between the spring high tide line (or landward edge of emergent vegetation when present) and lowest spring tide level. Emergent segments of barrier reefs are excluded from this zone. Typically, this zone is narrow due to the small tidal range in the U.S. Caribbean (Figure 2.14).



Figure 2.14. The red polygons (left) outline examples of the geographic zone, Shoreline Intertidal, near Central Aguirre. The photograph (right) was taken among the mangroves inside JBNERR. Photo: NOAA CCMA.

2.2.3. Geomorphological Structure Types

Thirteen distinct and non-overlapping geomorphological structure types were mapped by visually interpreting optical and acoustic imagery. Geomorphological structure refers to a feature's dominant physical composition and does not address geographic location (e.g., in a *Lagoon*). Structure types are defined in a collapsible hierarchy ranging from three major classes (*Coral Reef and Hardbottom*, *Unconsolidated Sediment*, and *Other Delineations*), to thirteen detailed classes (*Aggregate Reef*, *Aggregated Patch Reefs*, *Individual Patch Reef*, *Pavement*, *Pavement with Sand Channels*, *Rock/Boulder*, *Spur and Groove*, *Mud*, *Sand*, *Sand with Scattered Coral and Rock*, *Artificial*, *Land* and *Unknown*). Habitats or features with areas smaller than the MMU or minimum mapping unit (1,000 m²) were not considered.

Coral Reef and Hardbottom

Coral reef and Hardbottom habitats are areas on the seafloor with solid substrates, including bedrock, boulders and/or the deposition of calcium carbonate by reef building organisms. Substrates typically have no sediment cover, but a thin veneer of sand or mud may be present at times. Detailed structure classes include *Aggregate Reef*, *Aggregated Patch Reefs*, *Individual Patch Reef*, *Pavement*, *Pavement with Sand Channels*, *Rock/Boulder*, *Spur and Groove*, *Mud*, *Sand*, *Sand with Scattered Coral and Rock*, *Artificial* and *Land*.

Aggregate Reef

Continuous, high-relief coral formation of variable shapes lacking sand channels of *Spur and Groove*. Includes linear coral formations that are oriented parallel to the shelf edge (Figure 2.15).

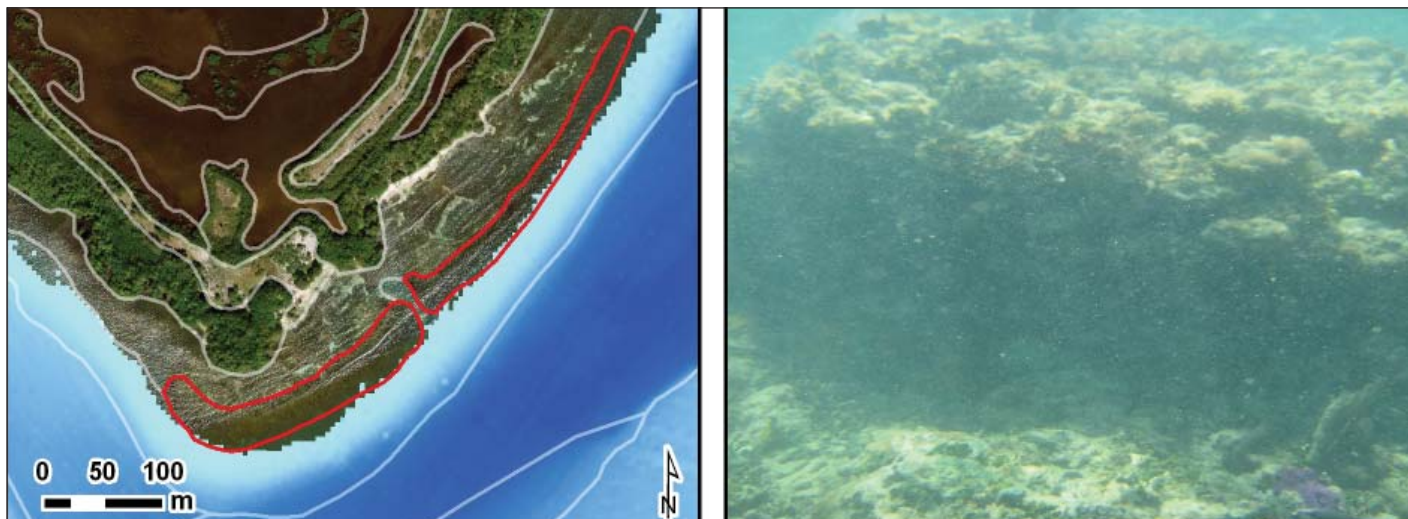


Figure 2.15. The red polygons (left) outline examples of the detailed structure type, Aggregate Reef, near Punta Colchones. The underwater photograph (right) depicts an example of aggregate reef in Jobos Bay. Photo: NOAA CCMA.

Aggregated Patch Reefs

Aggregated Patch Reefs have the same defining characteristics as an *Individual Patch Reef*. However, this class refers to clustered patch reefs that cover $\geq 10\%$ of the entire polygon, but are too small (less than the MMU) or are too close together to map individually. Where aggregated patch reefs share sand halos, the halo is included in the polygon (Figure 2.16). If the density of small or aggregated coral heads is $< 10\%$ of the entire polygon, this structure type is described as *Sand with Scattered Coral and Rock*.

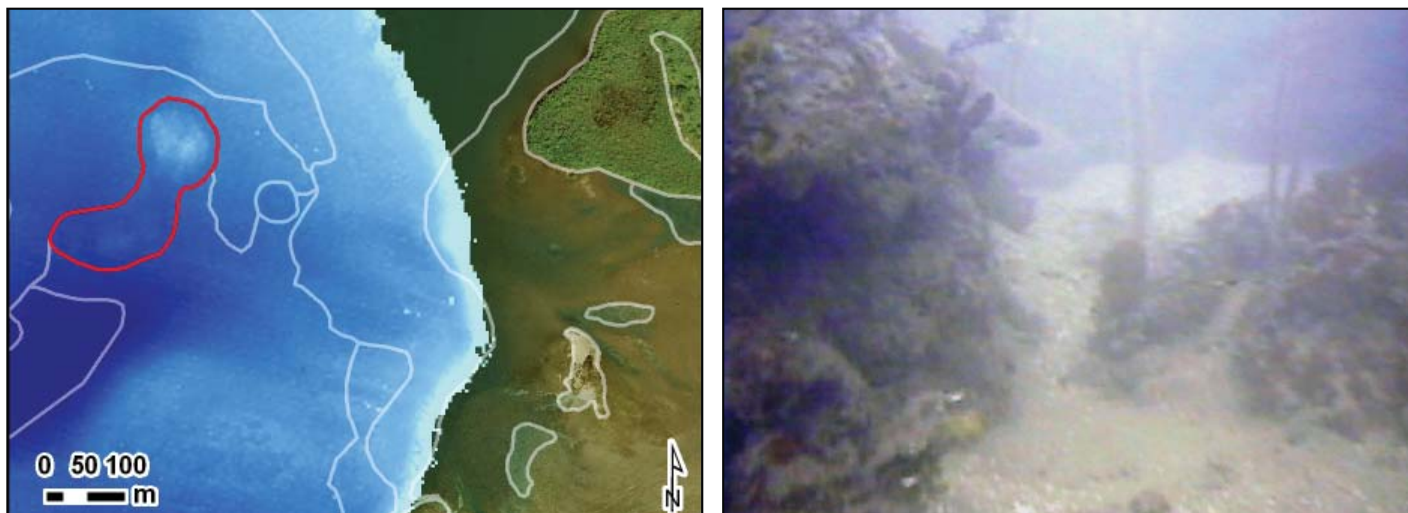


Figure 2.16. The red polygon (left) outlines an example of the detailed structure type, Aggregated Patch Reefs, near Boca del Infierno. The underwater photograph (right) depicts an example of aggregated patch reefs in Jobos Bay. Photo: NOAA CCMA.

Individual Patch Reef

Individual patch reefs are coral formations that are isolated from other coral reef formations by bare sand, seagrass or other habitats and that have no organized structural axis relative to the contours of the shelf edge. They are characterized by a roughly circular or oblong shape with a vertical relief of one meter or more in relation to the surrounding seafloor (Figure 2.17). *Individual Patch Reefs* are larger than or equal to the MMU.

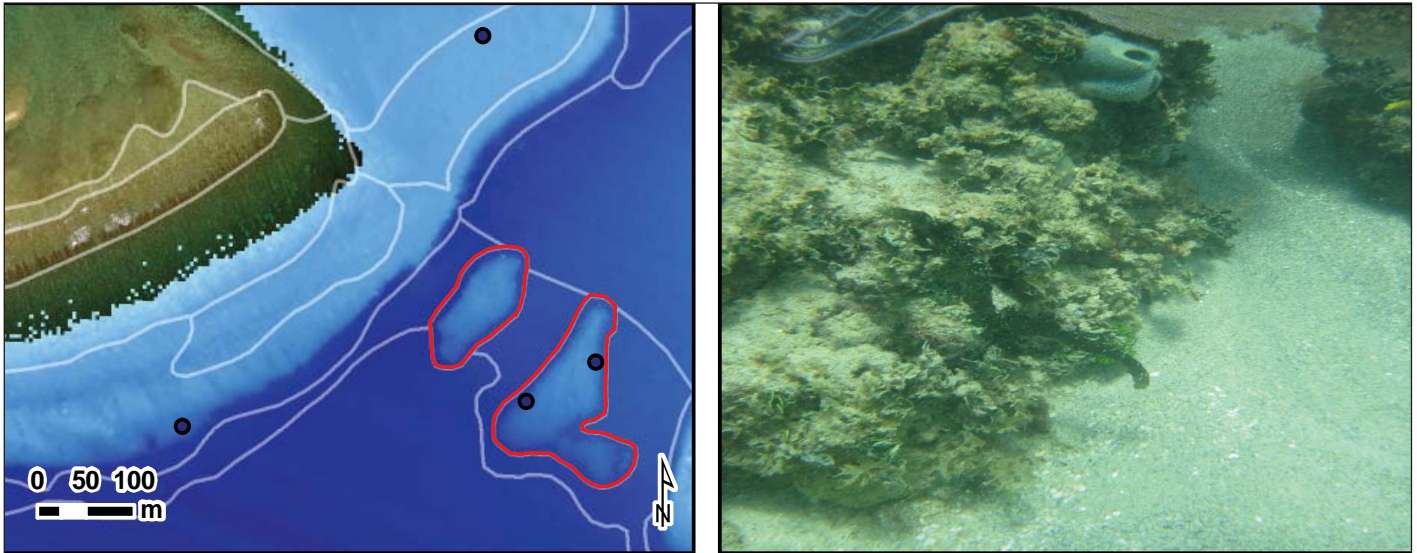


Figure 2.17. The red polygons (left) outline examples of the detailed structure type, Individual Patch Reef, near Cayos de Pájaros. The underwater photograph (right) depicts an example of an individual patch reef in Jobos Bay. Photo: NOAA CCMA.

Pavement

Flat, low-relief or sloping solid carbonate rock with little or no fine-scale rugosity that is covered with algae, hard coral, gorgonians, zoanths or other sessile vertebrates that are dense enough to partially obscure the underlying surface. On less colonized *Pavement* features, rock may be covered by a thin sand veneer or turf algae (Figure 2.18).

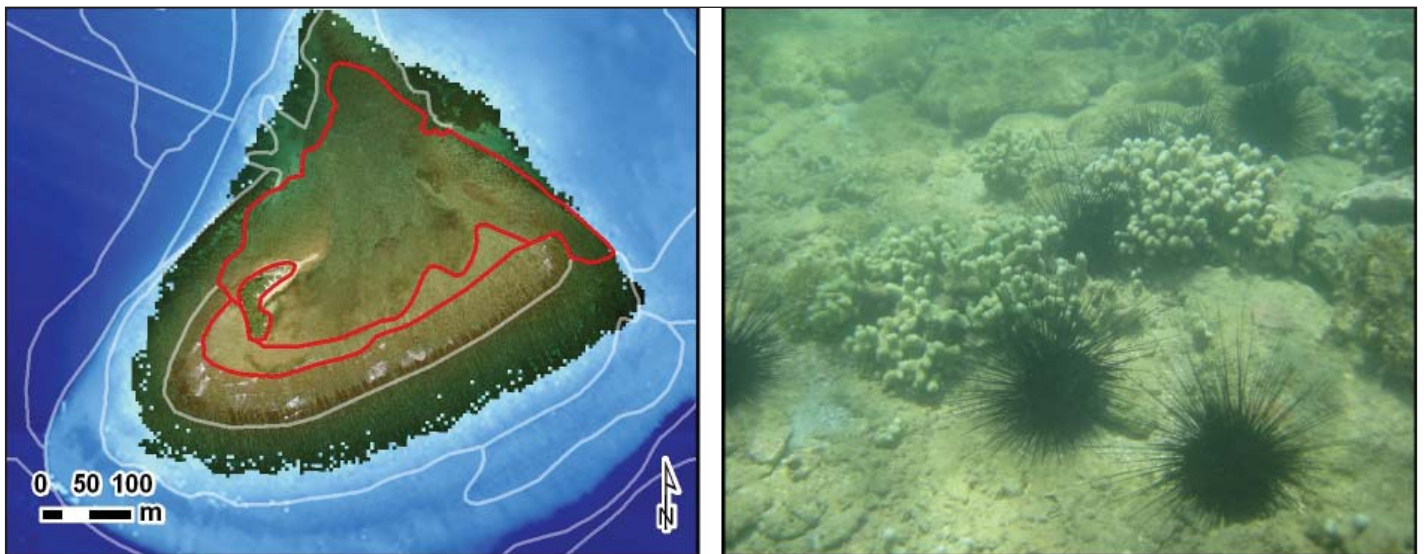


Figure 2.18. The red polygon (left) outlines an example of the detailed structure type, Pavement, near Cayo Morrillo. The underwater photograph (right) depicts an example of pavement habitat in Jobos Bay. Photo: NOAA CCMA.

Pavement with Sand Channels

Pavement with Sand Channels have the same defining characteristics as *Pavement*, in addition to having periodic sand/surge channels oriented perpendicular to the *Bank/Shelf Escarpment*. The sand/surge channels of this feature have low vertical relief and are typically erosional in origin. This habitat type occurs in areas exposed to moderate wave surge such as the *Bank/Shelf* zone (Figure 2.19).

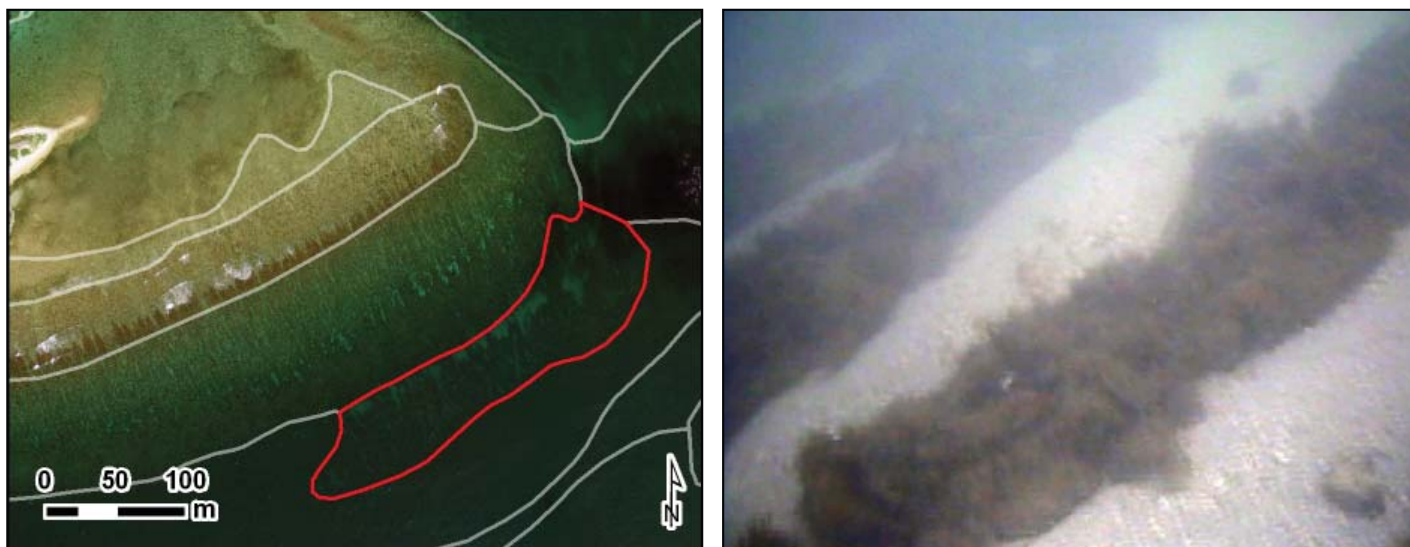


Figure 2.19. The red polygon (left) outlines an example of the detailed structure type, *Pavement with Sand Channels*, near Cayos de Pájaros. The underwater photograph (right) depicts an example of *pavement with sand channels* habitat in Jobos Bay. Photo: NOAA CCMA.

Rock/Boulder

Aggregation of solid carbonate blocks extending offshore from the island bedrock or loose carbonate fragments that have been detached and transported from their native beds (Figure 2.20). Individual boulders range in diameter from 0.25-3 m as defined by the Wentworth scale (Wentworth, 1922).



Figure 2.20. The red polygon (left) outlines an example of the detailed structure type, *Rock/Boulder*, east of Punta Pozuelo. The underwater photograph (right) depicts an example of *rock/boulder* habitat in Jobos Bay. Photo: NOAA CCMA.

Spur and Groove

Structure having alternating sand and coral formations that are oriented perpendicular to the shore or reef crest. The coral formations (spurs) of this feature typically have a high vertical relief (approximately 1 m or more) relative to pavement with sand channels and are separated from each other by 1-5 m of sand or hardbottom (grooves), although the height and width of these elements may vary considerably (Figure 2.21). This habitat type typically occurs in the *Fore Reef* or *Bank/Shelf Escarpment* zone.



Figure 2.21. The red polygon (left) outlines an example of the detailed structure type, Spur and Groove, on the western side of Cayos de Barca. The underwater photograph (right) depicts an example of spur and groove habitat in Jobos Bay. Photo: NOAA CCMA.

Unconsolidated Sediment

Areas on the seafloor consisting of small particles (<0.25 m) with less than 50% cover of large stable substrate. Detailed structure classes include: *Mud*, *Sand* and *Scattered Coral and Rock*.

Mud

Fine sediment often associated with river discharge and build-up of organic material in areas sheltered from high-energy waves and currents (Figure 2.22). Particle sizes range from <1/256-1/16 mm (Wentworth, 1922).

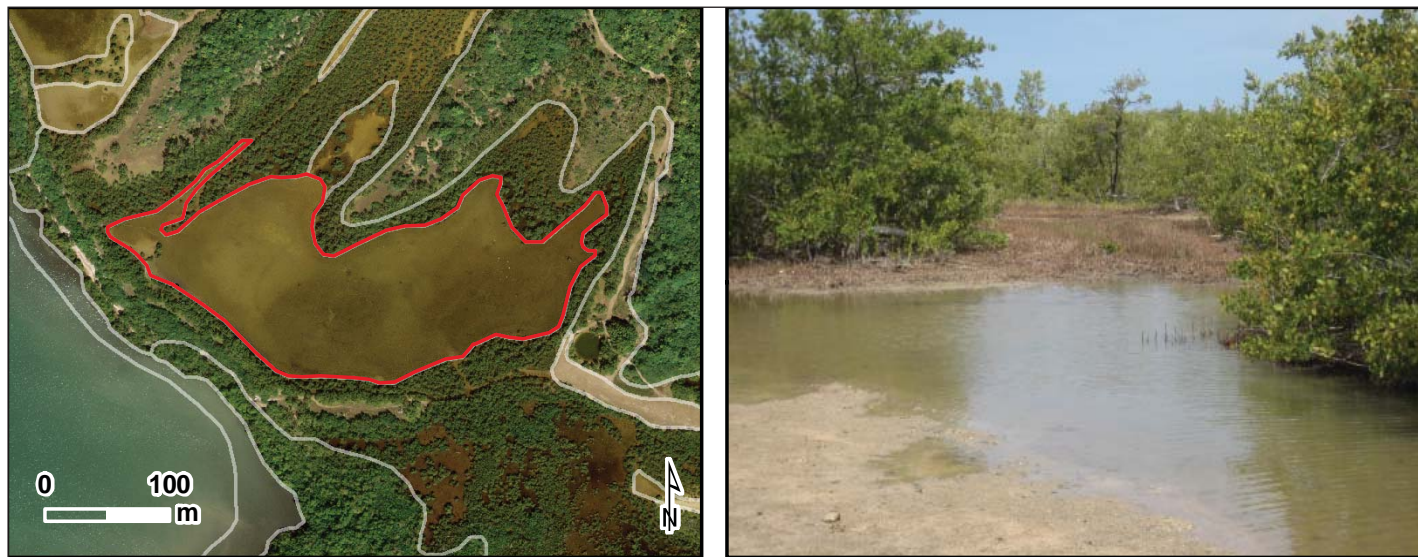


Figure 2.22. The red polygons (left) outline examples of the detailed structure type, Mud, west of Punta Pozuelo. The photograph (right) was taken in the same area on the ground. Photo: NOAA CCMA.

Sand

Coarse sediment typically found in areas exposed to currents or wave energy (Figure 2.23). Particle sizes range from 1/16–256 mm, including pebbles and cobbles (Wentworth, 1922).



Figure 2.23. The red polygons (left) outline examples of the detailed structure type, Sand, southeast of Las Mareas. The underwater photograph (right) depicts an example of sand habitat in Jobos Bay. Photo: NOAA CCMA.

Sand with Scattered Coral and Rock

Areas where $\geq 10\%$ of the entire polygon is covered by sand and $< 10\%$ of the entire polygon is covered by scattered rocks or small, isolated coral heads that are too small to be delineated individually (Figure 2.24). If the density of small coral heads is $\geq 10\%$ of the entire polygon, this structure type is described as *Aggregated Patch Reefs*.

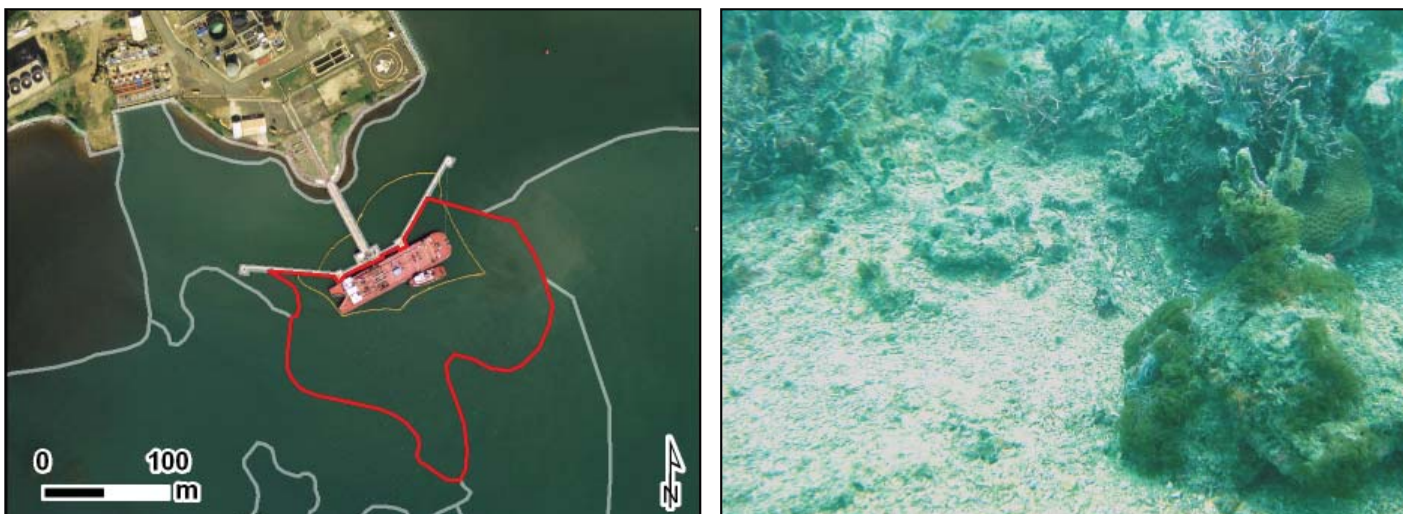


Figure 2.24. The red polygon (left) outlines an example of the detailed structure type, Sand with Scattered Coral and Rock, southeast of Las Mareas. The underwater photograph (right) was taken at this same location. Photo: NOAA CCMA.

Other Delineations

Any other type of structure not classified as *Coral Reef and Hardbottom* or *Unconsolidated Sediment*. Usually related to the terrestrial environment and/or anthropogenic activity. Detailed structure classes include *Land* and *Artificial*.

Artificial

Man-made habitats such as submerged wrecks, large piers, submerged portions of rip-rap jetties, and the shoreline of islands created from dredge spoil (Figure 2.25).



Figure 2.25. The red polygon (left) outlines an example of the detailed structure type, Artificial, near Central Aguirre. The photograph (right) was taken at this same location. Photo: NOAA CCMA.

Land

Terrestrial features at or above the spring high tide line (Figure 2.26).

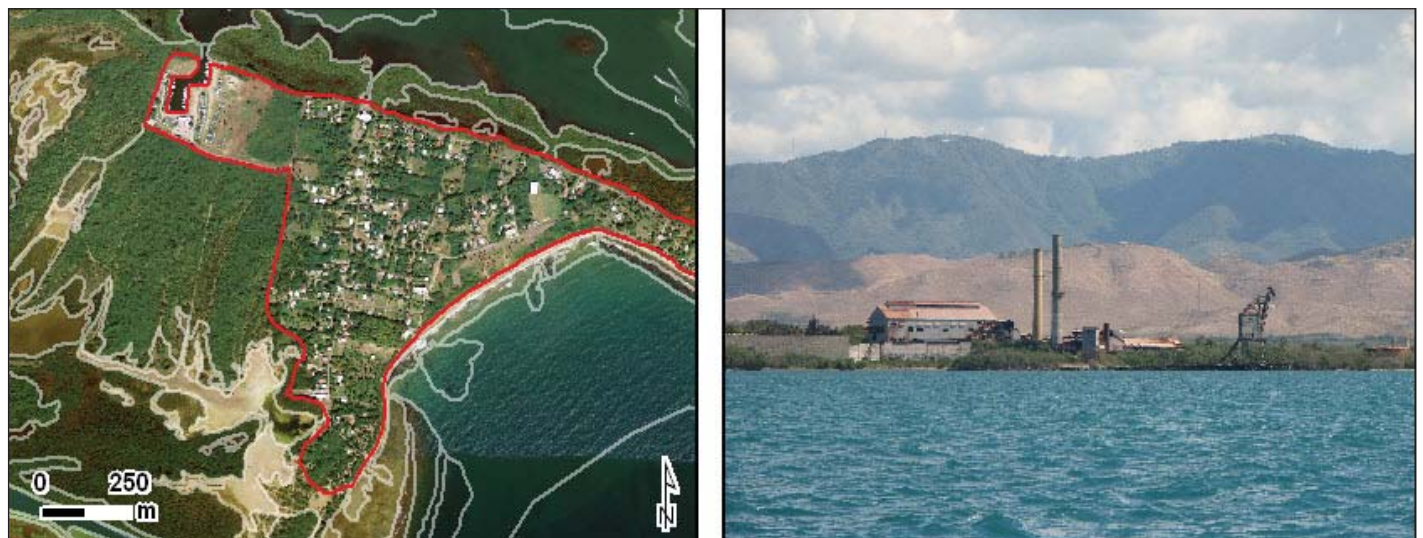


Figure 2.26. The red polygon (left) outlines an example of the detailed structure type, Land, near Punta Pozuelo. The photograph (right) taken looking westward towards Central Aguirre. Photo: NOAA CCMA.

Unknown

Major and/or detailed structure that is indistinguishable in the optical imagery due to water depth, turbidity, cloud cover, wave action, sun glint or other interference with the optical signature of the seafloor; it also maybe indistinguishable in the acoustic imagery due to noise in the bathymetry and/or backscatter or other interference with the acoustic signature of the seafloor (Figure 2.27).

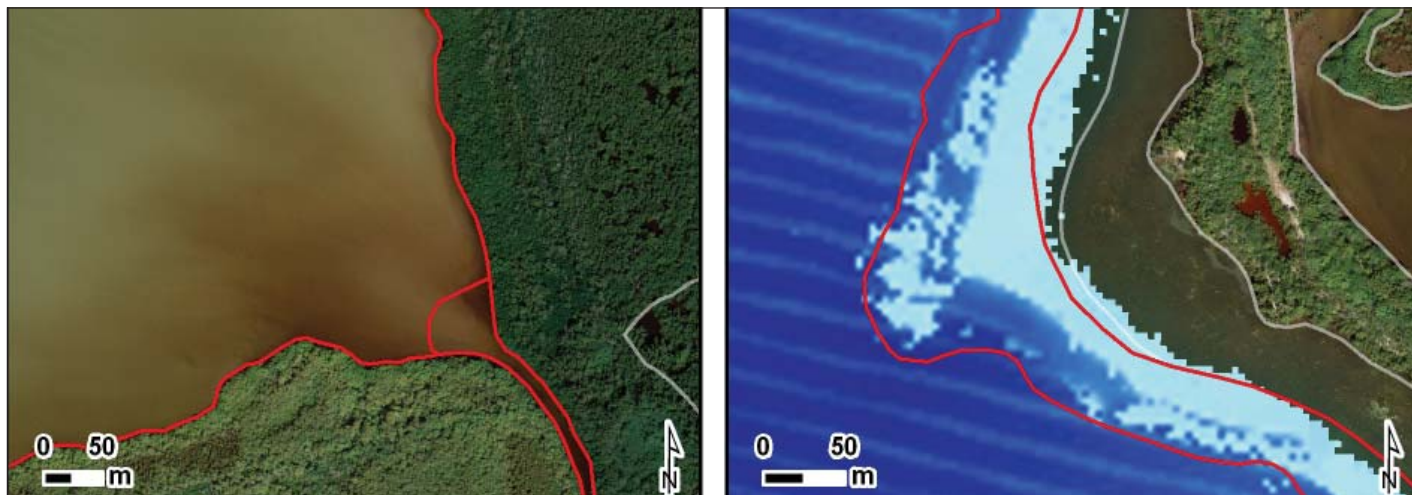


Figure 2.27. The red polygons (left) outline examples of an unknown detailed structure types due to turbidity in the optical imagery. The red polygon (right) outlines an example of an unknown detailed structure type due to noise in the acoustic imagery.

2.2.4. Biological Cover Classes

Twelve unique (*i.e.*, major plus detailed) biological cover classes were mapped by visually interpreting optical and acoustic remotely sensed imagery. Biological cover denotes the dominant biological component colonizing the surface of the feature. It does not describe the location (*e.g.*, on the *Bank/Shelf* or in a *Lagoon*) or structure (*e.g.*, *Sand*) of the feature. Habitat features smaller than the MMU were not considered. Six major cover types were identified from the optical and acoustic imagery (*i.e.*, *Algae*, *Seagrass*, *Mangrove*, *No Cover*, *Unclassified* and *Unknown*) and combined with three modifiers describing the distribution of the dominant cover within the polygon (*i.e.*, $10\% \leq 50\%$, $50\% \leq 90\%$, and $90\% - 100\%$). It is important to note that this modifier represents a measure of patchiness of the biological cover at the scale of delineation. It does not denote the density of organisms observed by divers in the water. For example, a seagrass bed can be described as covering 90%-100% of a given polygon, but may have sparse densities of shoots when observed by divers. Figure 2.28 illustrates how patchiness was used to assign a biological percent cover.

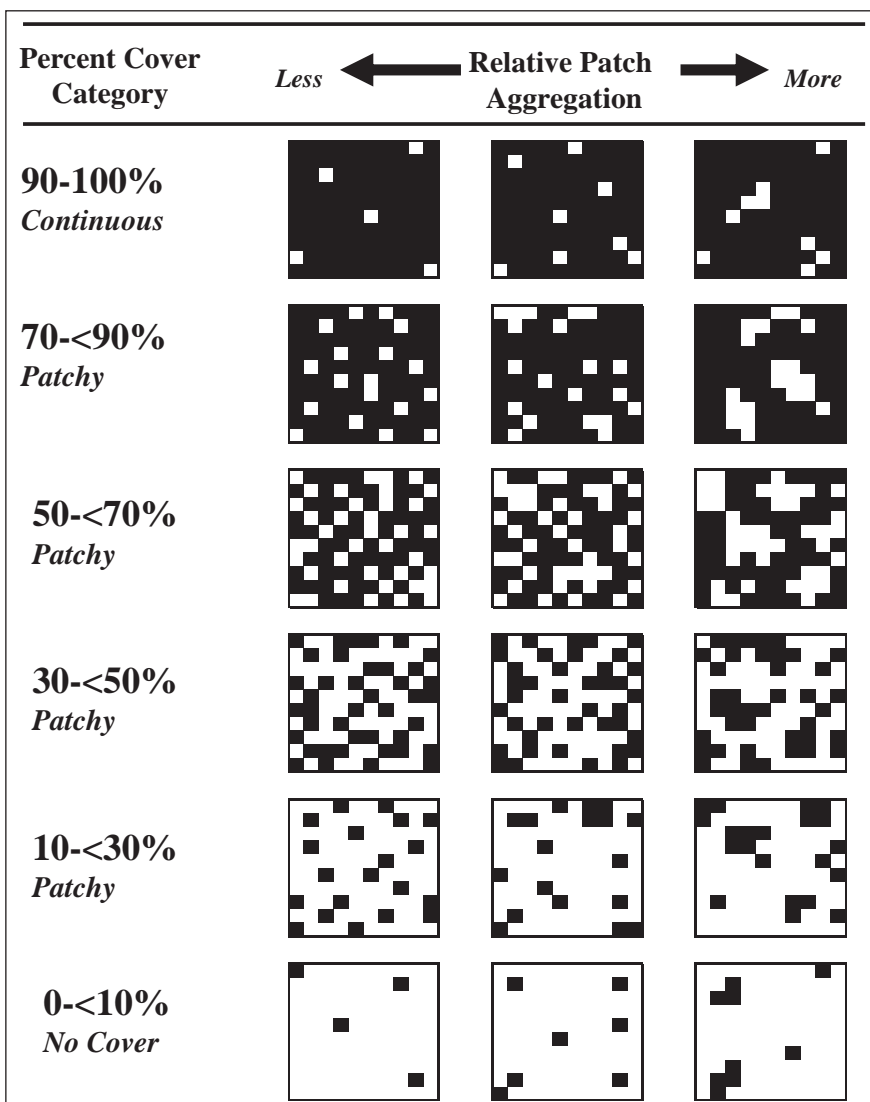


Figure 2.28. This chart outlines the process used to visually estimate patchiness when assigning a percent biological cover value to a polygon. Note that the 18 large squares are the size of a minimum mapping unit (MMU).

Major Cover

Algae

Substrates with 10% or greater distribution of any combination of numerous species of red, green, or brown algae. May be turf, fleshy, filamentous species. Occurs throughout many zones, especially on hard bottoms with low coral densities and soft bottoms in deeper waters on the *Bank/Shelf* zone (Figure 2.29).

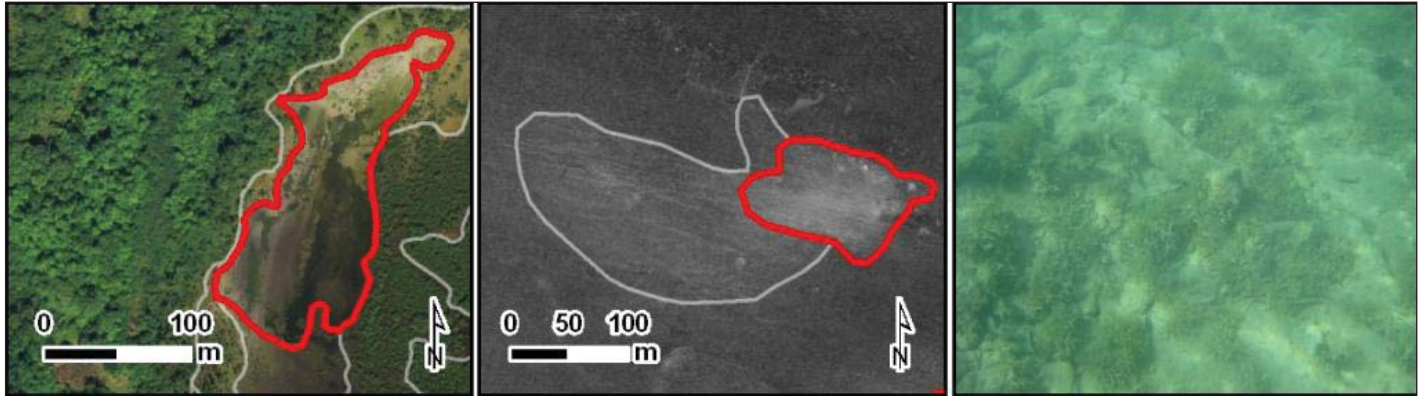


Figure 2.29. The red polygon in the map (left) and red polygon in the map (center) depict examples of the biological cover type, Algae, as seen in the optical and acoustic images, respectively. The underwater photograph (right) depicts an example of algal habitat in Jobos Bay. Photo: NOAA CCMA.

Mangrove

This habitat is comprised of semi-permanently, seasonally or tidally flooded coastal areas occupied by any species of mangrove (Figure 2.30). Mangrove trees are halophytes; plants that thrive in and are especially adapted to salty conditions. In the U.S. Caribbean, there are three species of mangrove trees: red mangrove (*Rhizophora mangle*), black mangrove (*Avicennia germinans*), and white mangrove (*Laguncularia racemosa*); another tree, buttonwood (*Conocarpus erectus*) is often associated with the mangrove formation. Red mangrove grows at the water's edge and in the tidal zone. Black mangrove and white mangrove grow further inland in areas where flooding occurs only during the highest tides. This habitat type is usually found in the *Shoreline Intertidal* zone.



Figure 2.30. The red polygons outline examples of the biological cover type, Mangroves. The photographs (center and right) depict examples of mangrove habitat in Jobos Bay. Photo: NOAA CCMA.

No Cover

Substrates not covered with a minimum of 10% of any of the other biological cover types. This habitat is usually associated with *Mud* or *Sand*. Overall, *No Cover* is estimated at 90%-100% of the bottom with the possibility of some very low density biological cover (Figure 2.31).

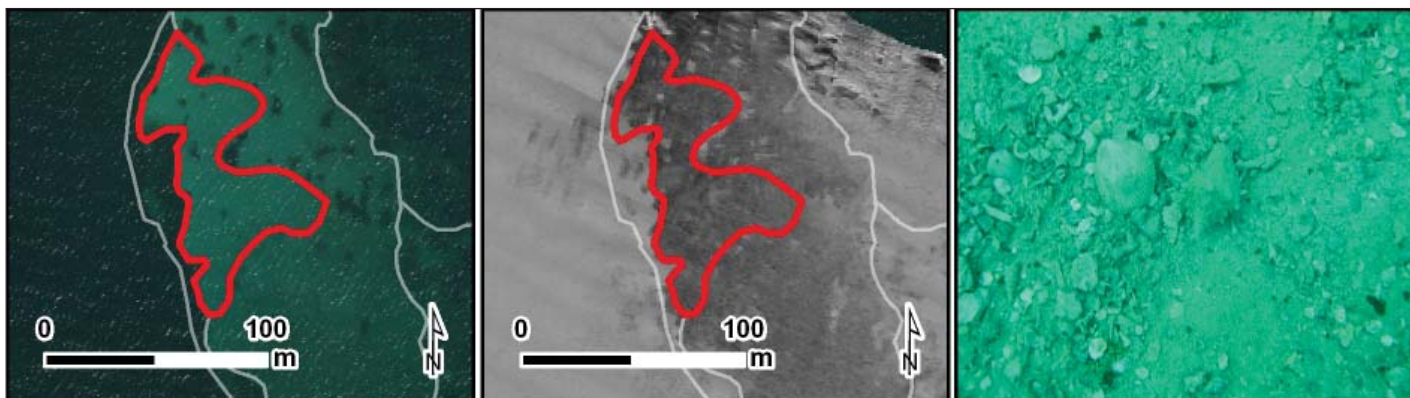


Figure 2.31. The red polygon in the map (left) and red polygon in the map (center) depict examples of the biological cover type, *No Cover*, as seen in the optical and acoustic images, respectively. The underwater photograph (right) depicts an example of habitats colonized by little or no biological organisms in Jobos Bay. Photo: NOAA CCMA.

Seagrass

Habitat dominated by any single species of seagrass (e.g., *Syringodium* sp., *Thalassia* sp., *Halophila* sp.) or a combination of several species (Figure 2.32).

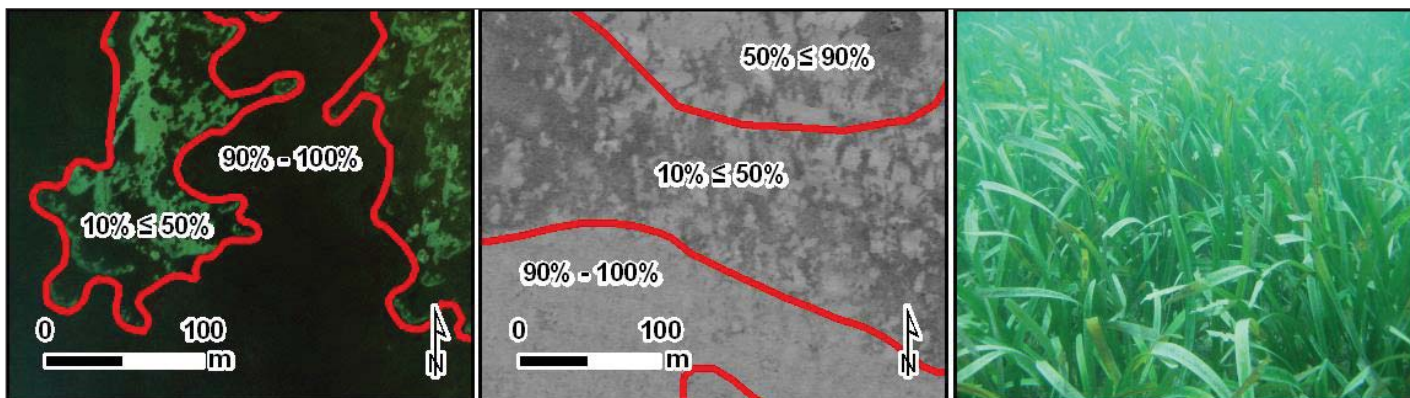


Figure 2.32. The red polygon in the map (left) and red polygon in the map (center) depict examples of the biological cover type, *Seagrass*, as seen in the optical and acoustic images, respectively. The underwater photograph (right) depicts an example of seagrass habitats in Jobos Bay. Photo: NOAA CCMA.

Unclassified

A different biological cover type, such as upland, deciduous forest, that is not included in this habitat classification scheme dominates the area. Most often used on polygons defined as *Land* with terrestrial vegetation.

Unknown

Biological cover that is indistinguishable in the optical imagery due to water depth, turbidity, cloud cover, wave action, sun glint or other interference with the optical signature of the seafloor; it also may be indistinguishable in the acoustic imagery due to noise in the bathymetry and/or backscatter or other interference with the acoustic signature of the seafloor.

Percent Major Cover

$10\% \leq 50\%$

Discontinuous cover of the major biological type with breaks in coverage that are too diffuse to delineate or result in isolated patches of a different dominant biological cover that are too small to be mapped as a different feature (*i.e.*, smaller than the MMU). Overall cover of the major biological type is estimated at $10\% \leq 50\%$ of the polygon feature (Figure 2.33).

$50\% \leq 90\%$

Discontinuous cover of the major biological type with breaks in coverage that are too diffuse to delineate or result in isolated patches of a different dominant biological cover that are too small to be mapped as a different feature (*i.e.*, smaller than the MMU). Overall cover of the major biological type is estimated at $50\% \leq 90\%$ of the polygon feature (Figure 2.33).

$90\% - 100\%$

Major biological cover type covering 90% or greater of the substrate. May include areas of less than 90% major cover on 10% or less of the total area that are too small to be mapped independently (*i.e.*, smaller than the MMU; Figure 2.33).

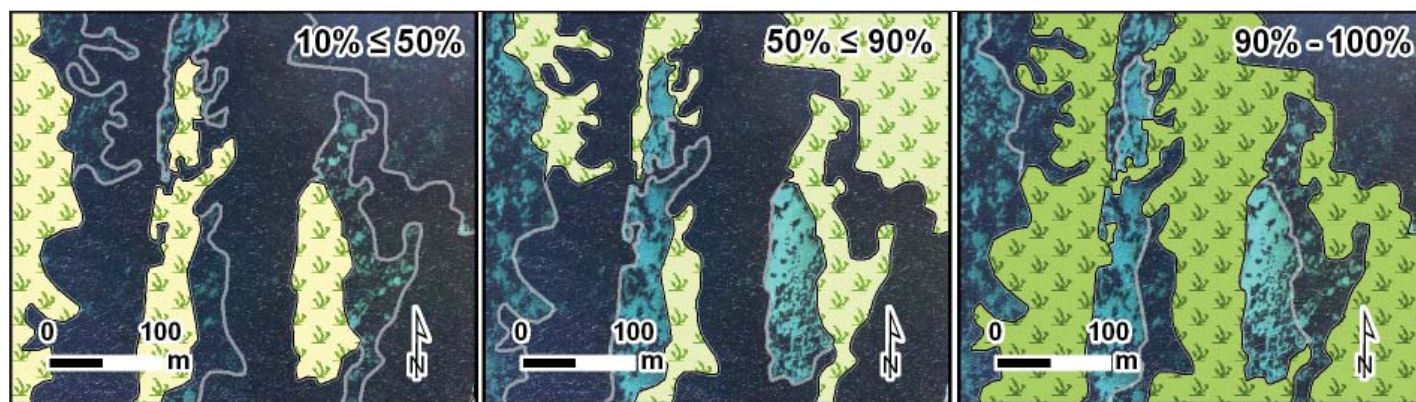


Figure 2.33. The symbolized polygons in the maps (right, center and left) have $10\% \leq 50\%$, $50\% \leq 90\%$ and $90\% - 100\%$ of their area covered by seagrass, respectively.

Not Applicable (N/A)

An estimate of percent cover is not appropriate for this particular major biological cover class (*e.g.*, for Land polygons). Regularly accompanies the use of Unclassified as the major biological cover.

Unknown

Percent estimate of the biological cover that is indistinguishable in the optical imagery due to water depth, turbidity, cloud cover, wave action, sun glint or other interference with the optical signature of the seafloor; it also maybe indistinguishable in the acoustic imagery due to noise in the bathymetry and/or backscatter or other interference with the acoustic signature of the seafloor.

2.2.5. Live Coral Cover Classes

Four distinct and non-overlapping percent live coral classes were mapped by visually interpreting optical and acoustic remotely sensed imagery. This attribute is an additional biological cover modifier denoting the abundance live coral (both scleractinian and octocorals; Figure 2.34), even when it was not the dominant cover type within a polygon. In order to provide resource managers with additional information about corals, four range classes were used (*i.e.*, $0\% \leq 10\%$, $10\% \leq 50\%$, $50\% \leq 90\%$, and $90\% - 100\%$). Habitat features are classified into these range classes based on the amount of combined scleractinian and octocoral present in a polygon. Scleractinian coral and octocorals were combined because they could not be reliable separated in the remotely sensed imagery.

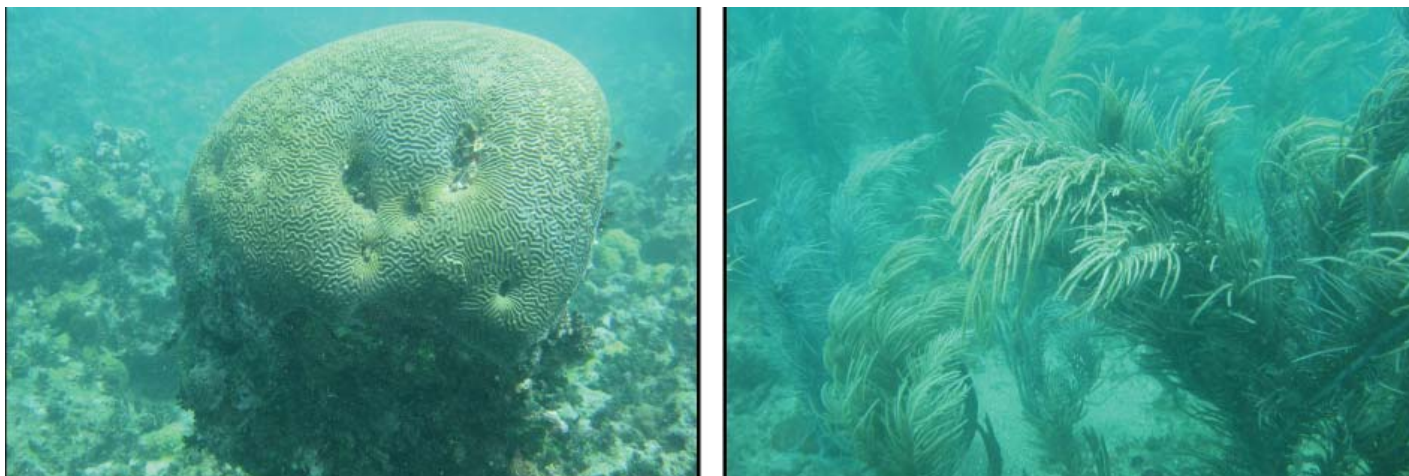


Figure 2.34. Both scleractinian and octocorals are included when estimating live coral cover. Typical corals of Jobos Bay include the scleractinian symmetrical brain coral (*Diploria strigosa*; left) and several octocorals including sea plumes (*Gorgoniidae*; right). Photos: NOAA CCMA.

Live coral cover describes the percent coral cover on hardbottom features at a fine spatial scale (*i.e.*, diver scale). It is important to note that this metric is different from percent biological cover, which denotes the patchiness of biological organisms at the scale of the habitat feature. Due to these varying scales of interpretation, the percent biological cover and percent live coral cover modifiers are not additive, and in many cases, they will sum to greater than 100%. For instance, an aggregate reef can have continuous (90%-100%) cover of algae at the polygon scale, as well as 10%-50% density of coral at the diver scale.

$0\% \leq 10\%$

Live coral cover of less than 10% of hardbottom substrate at a scale several meters above the seafloor (Figure 2.35a).

$10\% \leq 50\%$

Live coral cover between 10% and 50% of hard bottom substrate at a scale several meters above the seafloor (Figure 2.35b).

$50\% \leq 90\%$

Live coral cover between 50% and 90% of hard bottom substrate at a scale several meters above the seafloor. No Figure is provided because this class was not present in the area that was mapped in Jobos Bay.

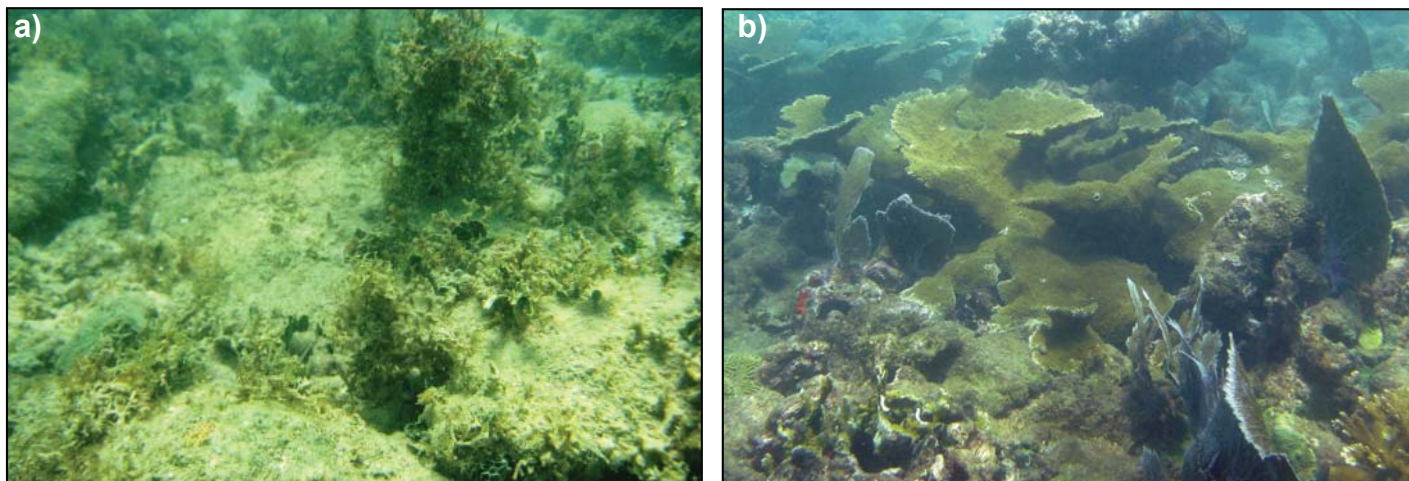


Figure 2.35. (a) An example of the presence of live coral in the $0\% \leq 10\%$ cover range; and (b) an example of the presence of live coral in the $10\% \leq 50\%$ cover range. Photos: NOAA CCMA.

90% - 100%

Continuous live coral consisting of 90% or greater cover of the hard bottom substrate at a scale several meters above the seafloor. No Figure is provided because this class was not present in the area that was mapped in Jobos Bay.

Unknown

Percent estimate of coral cover that is indistinguishable in the optical imagery due to water depth, turbidity, cloud cover, wave action, sun glint or other interference with the optical signature of the seafloor; it also maybe indistinguishable in the acoustic imagery due to noise in the bathymetry and/or backscatter or other interference with the acoustic signature of the seafloor.

2.3. BENTHIC HABITAT CREATION

Benthic habitats of the near-shore marine environment of Jobos Bay, Puerto Rico were created by delineating and classifying habitat features visible in optical and acoustic remotely sensed imagery. Optical and acoustic imagery have both been successfully used to derive the location, extent and attributes of marine habitats (Kendall *et al.*, 2001, 2005; Kostylev *et al.*, 2001; Battista *et al.*, 2007a,b; Prada *et al.*, 2008; Bauer *et al.*, 2010). NOAA scientists were able to accurately and reliably delineate the boundaries of features in the imagery using Geographic Information System (GIS) software. Field investigations were conducted in order to link signatures in the imagery with habitat features on the seafloor. This process provides natural resource managers and researchers with spatially accurate maps of seafloor features and their associated ecological characteristics.

2.3.1 General Mapping Approach

NOAA's approach to near-shore habitat mapping of estuarine and marine environments was a five-step process:

1. Imagery Acquisition – The first step in map creation was the acquisition and processing of high-resolution remotely sensed imagery. Optical imagery (*i.e.*, aerial orthophotographs) and acoustic data were collected in order to map the full geographic extent of Jobos Bay.
2. Habitat Boundary Delineation – A draft benthic habitat map was generated by manually delineating habitat features that were clearly visible in the optical and acoustic remotely sensed imagery.
3. Ground Validation (GV) – Habitat features in the map with unknown optical or acoustic signatures were explored by NOAA scientists using underwater cameras. This information was analyzed and the initial maps were edited to generate a second draft map for Jobos Bay.
4. Expert Review – The second draft map was reviewed online by local marine biologists, scientists and resource managers to qualitatively assess the maps thematic accuracy.
5. Final Product Creation – A final benthic habitat map for Jobos Bay was generated by correcting inaccuracies identified during the expert review.

2.4. REMOTELY SENSED IMAGERY

Remotely sensed imagery is a valuable tool for natural resource managers and researchers because it provides a permanent record of the location and extent of seafloor habitats. Generally in clear, tropical waters, optical imagery can be used to identify, delineate and classify seafloor habitat features from the shoreline to water depths of approximately 30 m. However, consistently poor water clarity inhibited the delineation and classification of habitat features from optical imagery for some areas in

Jobos Bay. Acoustic imagery was collected in these turbid areas to supplement the aerial photographs and provide source imagery from which to delineate and classify benthic habitats. Descriptions of the optical and acoustic source images are provided in the proceeding text.

2.4.1. Acquisition and Processing of the Optical Imagery

High resolution optical imagery provides precise and robust data with spectral and spatial resolutions suitable for shallow water benthic mapping. In order to map the benthic habitats of JBNERR, sixteen aerial orthophotographs were obtained from the U.S. Army Corps of Engineers (USACE) covering the Jobos Bay region (Figure 2.36). These 16 aerial photographs were mosaiced together to produce one seamless orthophoto image. An orthophoto is a remotely sensed, optical image in which the horizontal displacement of features in the image has been mathematically removed. The USACE collected these 16 natural color orthophotos using an ADS40 digital sensor on November 26 and 27, 2006. This collection was part of a larger effort to map the islands of Puerto Rico, Culebra and Vieques, and St. Thomas, St. John and St. Croix in the U.S. Virgin Islands (USVI) from November 2006 through March 2007. During this acquisition, aerial photographs were acquired at an altitude of 8,650 feet above ground level (AGL) with 30% sidelap between all adjacent flight lines. The ADS40 digital sensor captured the imagery at a 0.3x0.3 m spatial resolution and 12-bit (4,096 colors) radiometric resolution. This radiometric resolution was reduced to 8-bits (256 colors) during post processing in order to more effectively color balance the different images. The horizontal accuracy of these orthophotos was determined by using a GPS to measure in situ the position of distinct features in the imagery, and to compute a root mean square error (RMSE). In addition to ground control points, sample points were taken from overlapping areas of adjacent image strips to ensure that the location of adjacent images matched. All of the orthophotos were referenced to the State Plane Puerto Rico / US Virgin Islands (Zone 5200), North American Datum (NAD) 83, Geodetic Reference System (GRS) 80, Units Meters horizontal coordinate system.

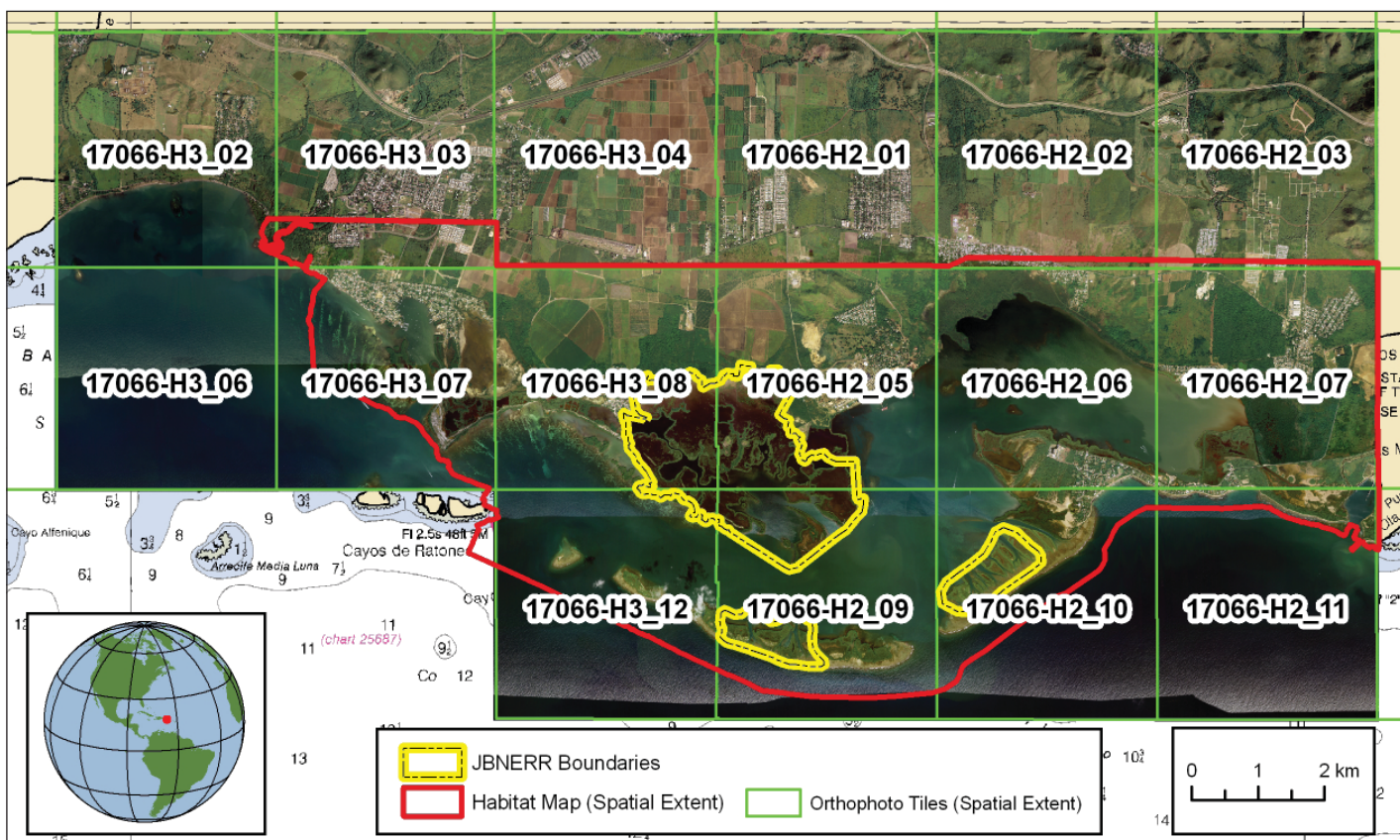


Figure 2.36. In order to map JBNERR, sixteen aerial orthophotographs were obtained from the U.S. Army Corps of Engineers (USACE) covering the Jobos Bay region. These 16 aerial photographs were mosaiced together to produce one seamless orthophoto image.

2.4.2. Acquisition of the Acoustic Imagery

Benthic habitats in shallow (≤ 30 m), perpetually turbid marine environments are challenging to characterize because conventional mapping technologies (e.g., satellite imagery, light detection and ranging and multibeam echosounders) are either unable to, or inefficient for, comprehensively mapping these areas. The use of interferometric sonars, also called phase differencing bathymetric sonars (PDBS), may fill this informational gap where conditions are not ideal for the operation of other sensors. Like other sonars, PDBS actively emit pulses of sound and record the return to gather co-located bathymetric and intensity information about the seafloor (Figure 2.37). Unlike other sonars, however, PDBS collect these spatially coincident datasets over wide swaths in shallow-waters, up to 12 times the depth versus 3 to 5 times the depth for multibeam echosounder systems (Gostnell, 2005). PDBS are able to collect wide swaths in shallow-waters because they are not beam forming but rather, they accurately measure depths by precisely measuring the phase offsets of acoustic returns (Denbigh, 1989; Gostnell, 2005). In addition to calculating depth, PDBS systems also collect information about the intensity of the returns. These individual measurements are used to create images of the seafloor, describing its hardness and roughness. The resulting acoustic images (i.e., bathymetry and intensity) are valuable tools for natural resource managers and researchers because they provide baseline information on the location and extent of seafloor habitats in turbid waters and in deep waters beyond the limits of optical imagery (i.e., approximately 30 m).

A PDBS system, called the Teledyne Benthos C3D (200 kHz) Lightweight Pole Mount (LPM; Figure 2.38), was used to acquire acoustic imagery in the Jobos Bay region. Bathymetric and intensity data were collected aboard the JBNERR's research vessel (R/V) *Jurel* from 4/7/2009 to 4/21/2009. The bathymetric and intensity datasets were logged in .hsx format using Hypack 2009

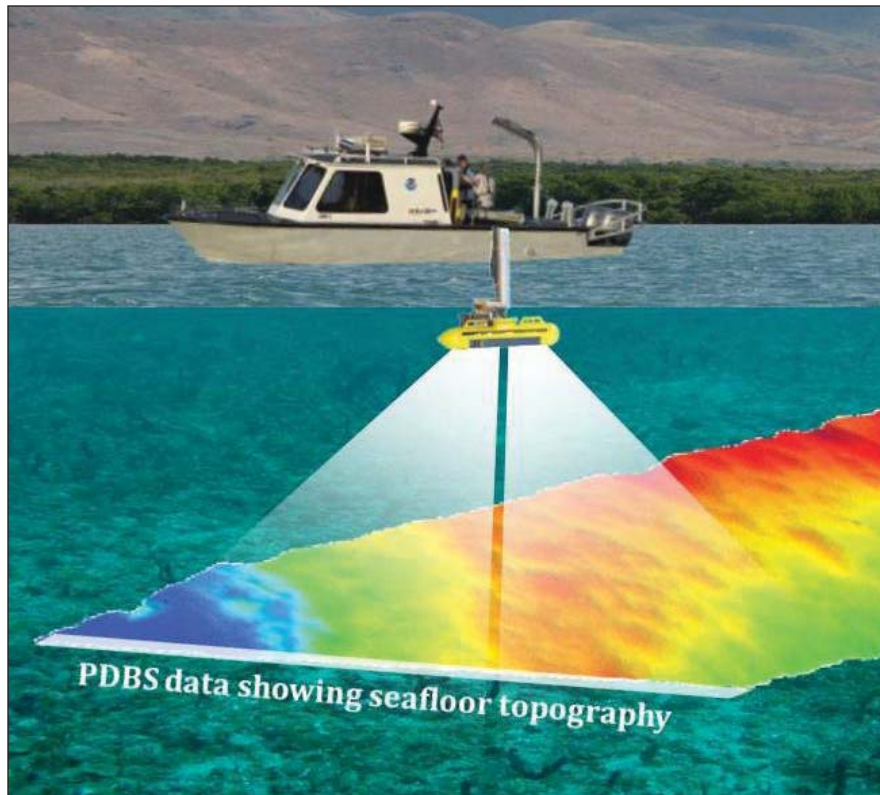


Figure 2.37. Diagram illustrating the collection of acoustic data using an interferometric sonar (phase differencing bathymetric sonars or PDBS). This acoustic dataset was integrated with underwater photographs and video to habitat mapping to create a benthic habitat map for persistently turbid areas in Jobos Bay.



Figure 2.38. The Teledyne Benthos C3D (200 kHz) LPM PDBS was pole-mounted on the R/V *Jurel*. This system was used to collect bathymetry and intensity imagery in Jobos Bay. Photo: NOAA CCMA.

software. Line spacing provided a bathymetry surface with 100% bottom coverage and an intensity surface with 200% bottom coverage. Heave, roll, pitch and heading correctors were collected using an Ixsea Octans gyrocompass and integrated motion sensor. Sound velocity profiles were acquired with a hand held conductivity, temperature and depth (CTD) profiler. Horizontal and vertical positions were obtained using a Trimble DSM 232 GPS receiver. Soundings were referenced to the NAD of 1983, Universal Transverse Mercator 19 North (NAD83 UTM 19N) horizontal coordinate system. Sounding depths were left in NAD83 ellipsoidal heights.

2.4.3. Processing of the Acoustic Imagery

Bathymetry

The .hsx lines were imported into CARIS Hydrographic Image Processing System (HIPS) & Sidescan Image Processing System (SIPS) v7.0. After being imported, sound velocity profiles (taken every four hours of the full water column) were used to correct the speed of sound in the converted lines based on previous in time. Zero tides were applied to the Hydrographic Data Cleaning System (HDGS) data, leaving the bathymetry surface referenced to NAD83 ellipsoid heights. The HDGS lines were subsequently merged, and TPU (total propagated uncertainty) was calculated. A Bathymetry with Associated Statistical Error (BASE) surface was then created at a 4x4 m spatial resolution using Combined Uncertainty and Bathymetry Estimator (CUBE) with the following parameters: (1) IHO S-44 Special Order specifications (2) density & locale disambiguation method and (3) 0 - 100 m depth filter. Additional fliers were manually rejected in subset editor. Existing data holidays were filled by interpolation, using the following parameters: 1 iteration, matrix size of 5, 10 neighbors. The final, interpolated 4x4 m bathymetry surface exported from CARIS and converted to a GeoTIFF in ArcMap (Figure 2.39).

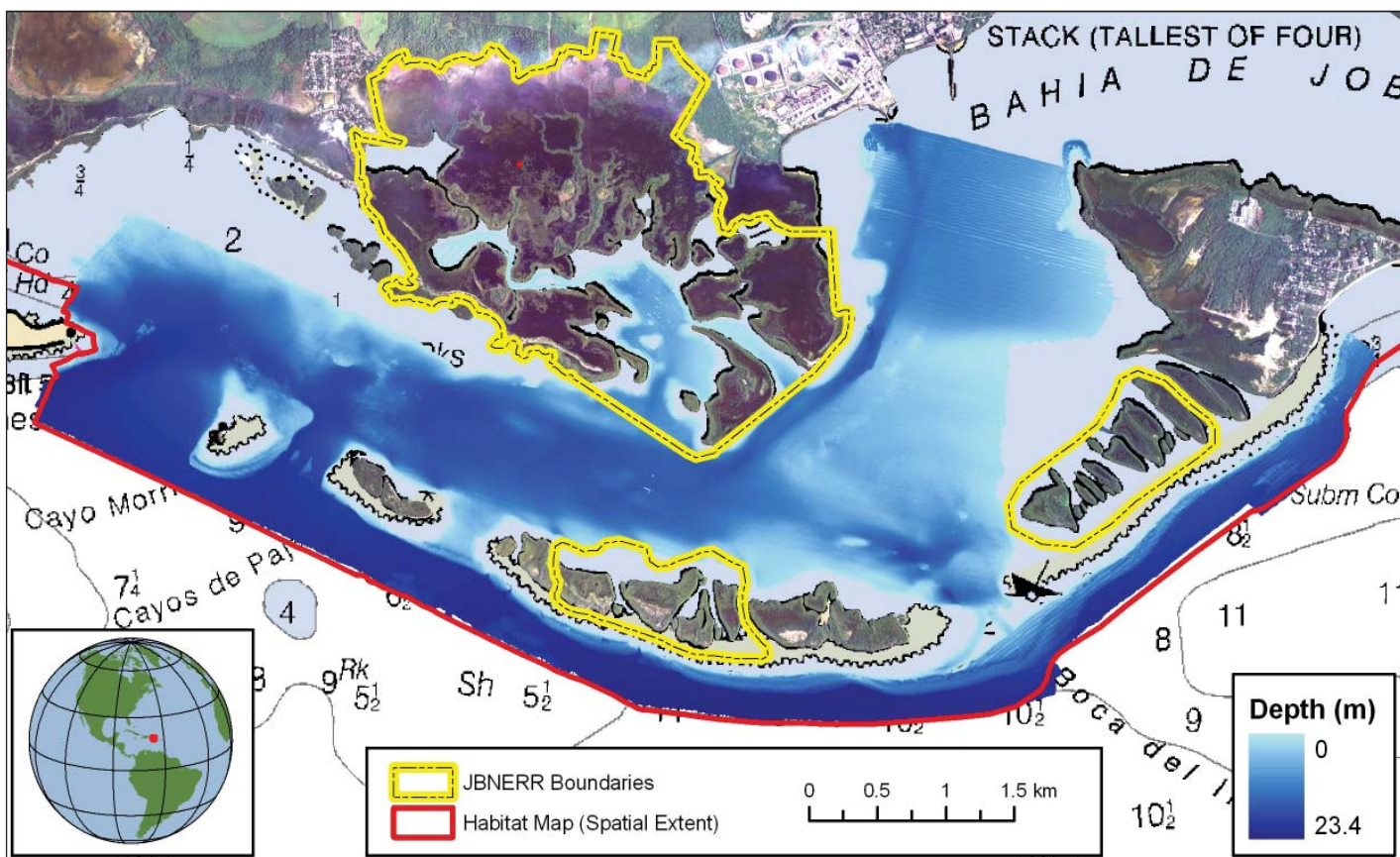


Figure 2.39. Acoustic information was collected in persistently turbid areas in Jobos Bay to support habitat mapping. This Figure shows the bathymetry surface (i.e., depths) collected by the C3D PDBS.

Intensity

An intensity surface was created using Hypack 2009 Geocoder module (Fonseca and Calder, 2005). In order to do so, the same .hsx files were imported into Geocoder. They were then geometrically corrected for navigation attitude, transducer attitude and local seafloor slope using the final bathymetric surface exported from CARIS. They were also radiometrically corrected for changes in acquisition gains, power levels, pulse widths, incidence angles and ensonification areas. Visual artifacts (e.g., noisy lines, dark or light striping, *etc.*) were manually removed. All other soundings were preserved during these corrections and edits, allowing the full resolution data to be used to create the final mosaic. The final 1x1 m intensity surface was exported from Geocoder as an 8-bit (0-255 value) GeoTIFF (Figure 2.40).

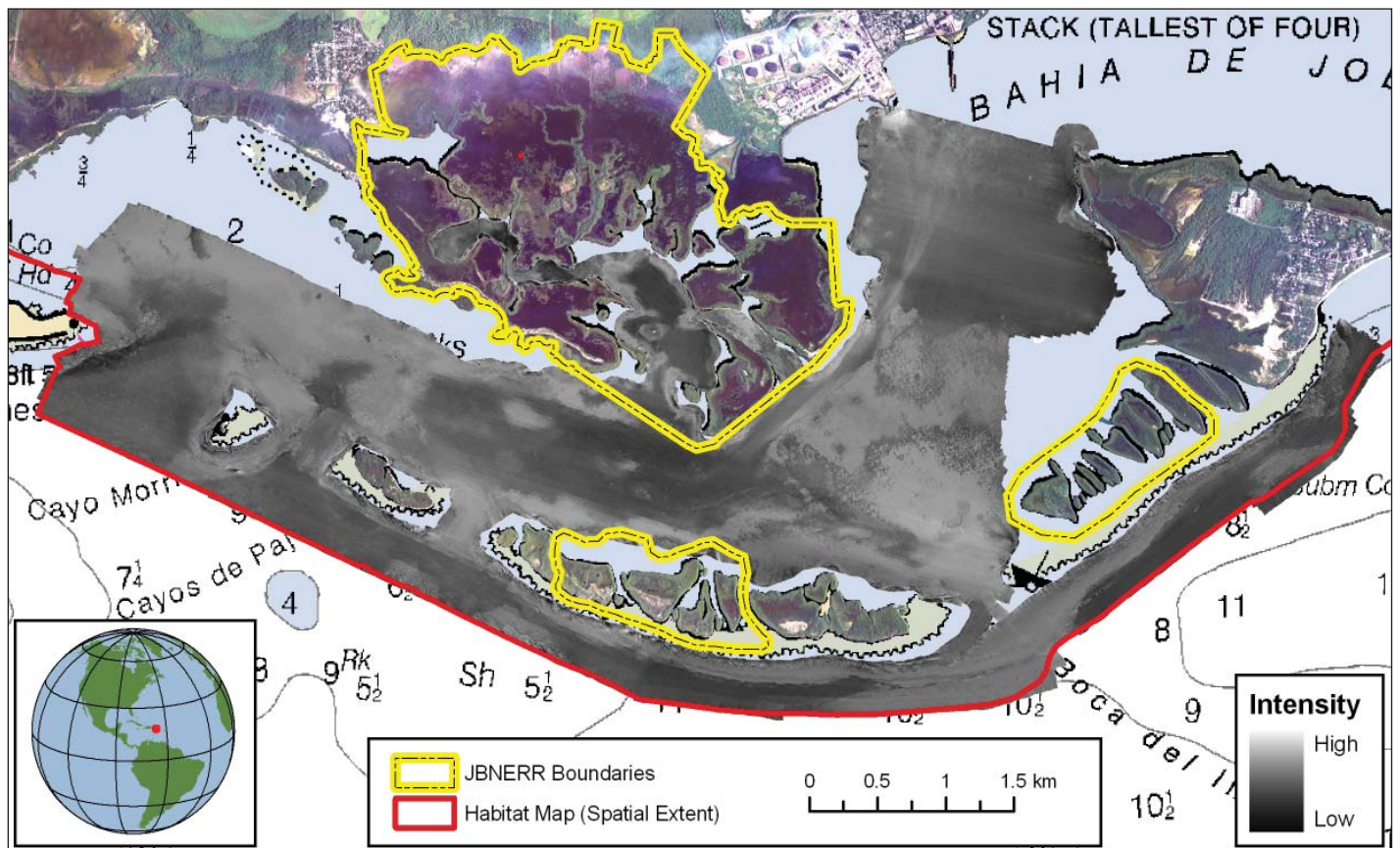
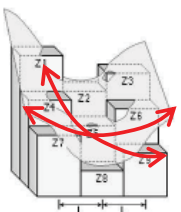
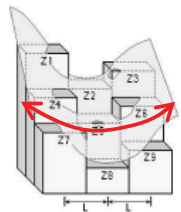
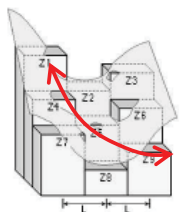
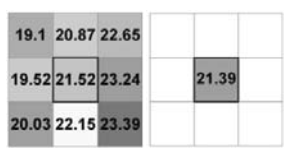
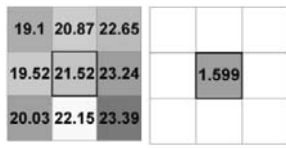
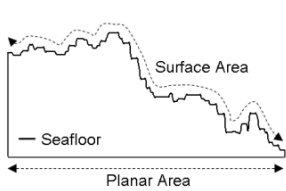
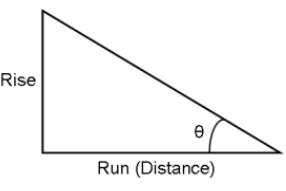
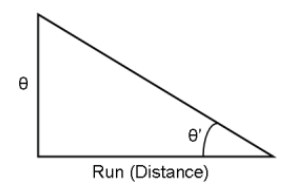


Figure 2.40. This Figure shows the intensity surface collected by the C3D PDBS.

Creating Derivative Surfaces

A suite of eight metrics were derived from the final bathymetry surface, in order to characterize the complexity and structure of the seafloor. These metrics specifically included: (1) mean depth, (2) standard deviation of depth, (3) curvature, (4) plan curvature, (5) profile curvature, (6) rugosity, (7) slope, and (8) slope of slope. Each of these metrics had a spatial resolution of 4x4 m. They were calculated using a square 3x3 cell neighborhood, where the pixel in the middle of the neighborhood was assigned the calculated value. These metrics are described in more detail in Table 2.2.

Table 2.2. Descriptions of the morphometrics used to characterize the complexity of the seafloor in and around JBNERR. The GIS tools used to derive these metrics from the PDBS bathymetry surface are also included in the table.

Dataset	Unit	Description	Formula	Tool
	1/100 z units - = concave + = convex	Rate of change in curvature across the surface highlighting ridges, crests and valleys (3 x 3 cell neighborhood)	$-2(D + E) * 100$ Where: D is $[(Z4 + Z6)/2 - Z5] / L2$ E is $[(Z2 + Z8)/2 - Z5] / L2$	Curvature function in ArcGIS 3D Analyst
	1/100 z units - = concave + = convex	Curvature of the surface perpendicular to the slope direction (3 x 3 cell neighborhood)	$-2(D + E) * 100$ Where: D is $[(Z4 + Z6)/2 - Z5] / L2$ E is $[(Z2 + Z8)/2 - Z5] / L2$	Plan curvature function in ArcGIS 3D Analyst
	1/100 z units - = convex + = concave	Curvature of the surface in the direction (3 x 3 cell neighborhood)	$-2(D + E) * 100$ Where: D is $[(Z4 + Z6)/2 - Z5] / L2$ E is $[(Z2 + Z8)/2 - Z5] / L2$	Profile curvature function in ArcGIS 3D Analyst
	Meters	Average water depth (3 x 3 cell neighborhood)	$\Sigma \text{ depth} / n \text{ grid cells}$	Focal statistic in ArcGIS Spatial Analyst
	Meters	Dispersion of water depth values about the mean (3 x 3 cell neighborhood)	$\sigma = \sqrt{\text{VAR}}$	Focal statistic in ArcGIS Spatial Analyst
	Ration value	Ratio of surface area to planar area (3 x 3 cell neighborhood)	See Jenness (2002, 2004) and Wright <i>et al.</i> (2005)	Benthic Terrain Mapper toolbox
	Degrees	Maximum rate of change in slope between cell and 8 neighbors (3 x 3 cell neighborhood)	$\tan \theta = \text{rise} / \text{distance}$	ArcGIS Spatial Analyst's slope function
	Degrees of degrees	Maximum rate of maximum slope change between cell and eight neighbors (3 x 3 cell neighborhood)	$\tan \theta' = \theta / \text{distance}$	ArcGIS Spatial Analyst's slope function

These eight complexity surfaces were subsequently stacked, and exported to create one image with several different bands (each band representing a specific metric). This image was then transformed into its' first three principal components (PCA; Pearson, 1901; Hotelling, 1933; Figure 2.41) in ENVI 4.7. This transformation reduced the dimensionality of the dataset by removing information that was redundant among the different bands. The resulting three band PCA image only contained information that uniquely described the complexity and structure of the seafloor (Table 2.3).

Table 2.3. The amount (%) of variance in a principal component that is explained by a single complexity surface. For example, the plan curvature surface contributed 11.11%, 2.32% and 40.67% of the information contained in the transformed image's first, second and third principal components, respectively.

	PC number		
	1	2	3
Bathymetry	11.11	25.04	10.51
Bathymetry (Mean)	11.11	24.60	12.09
Bathymetry (Stdev)	11.11	12.47	1.33
Curvature	11.11	2.40	29.47
Curvature (Plan)	11.11	2.32	40.67
Curvature (Profile)	11.11	0.02	1.03
Rugosity	11.11	4.29	0.03
Slope	11.11	13.22	1.89
Slope of Slope	11.11	15.63	2.97

Each of these three bands were converted from 16-bit, floating point values to 8-bit, integer values, so that they could be imported into ArcMap 9.3 for visual analysis. The final PCA surface had a spatial resolution of 4x4 m.

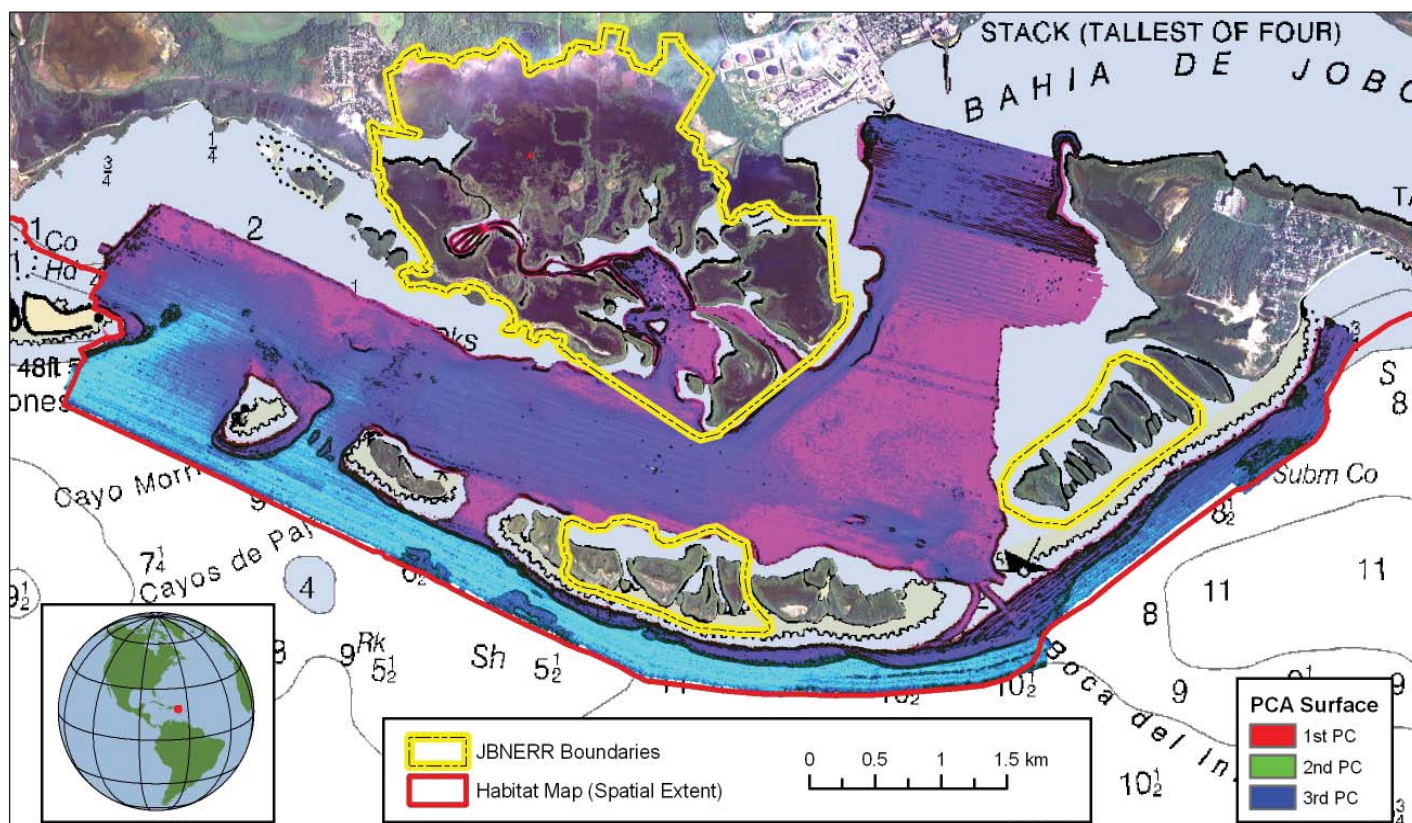


Figure 2.41. A suite of eight complexity metrics was derived from the bathymetry surface in order to characterize the complexity and structure of the seafloor. This figure shows the first three principal components derived from these eight complexity metrics.

2.5. HABITAT FEATURE IDENTIFICATION AND DELINEATION

2.5.1. Habitat Feature Identification

In order to create a habitat map for Jobos Bay, habitat boundary identification, delineation and attribution techniques were adopted from Kendall *et al.* (2001) and Costa *et al.* (2009). In particular, habitat boundaries were delineated around distinct optical and acoustic signatures that correlated with

habitat types in the classification scheme (described in Sections 2.2 to 2.5). These distinct signatures had unique colors, textures and shapes that distinguished them from the surrounding seafloor. In places where the optical and acoustic imagery overlapped, habitat features were clearly visible in both imagery sources (Figure 2.42). Brightness, contrast and histogram stretching of the source imagery were often manipulated in ArcGIS to enhance the interpretability of some subtle features and boundaries. This was particularly helpful when using the optical imagery to identify habitats in deeper water where differences in color and texture between adjacent features were more subtle. Particular caution was used when interpretation was performed from stretched images, since results from color and brightness manipulations were sometimes misleading. Additional ancillary datasets were also consulted to improve the understanding of particular areas. These data types included previously-completed habitat maps (Kendall *et al.*, 2001), bathymetry, nautical charts, and imagery from different time periods.

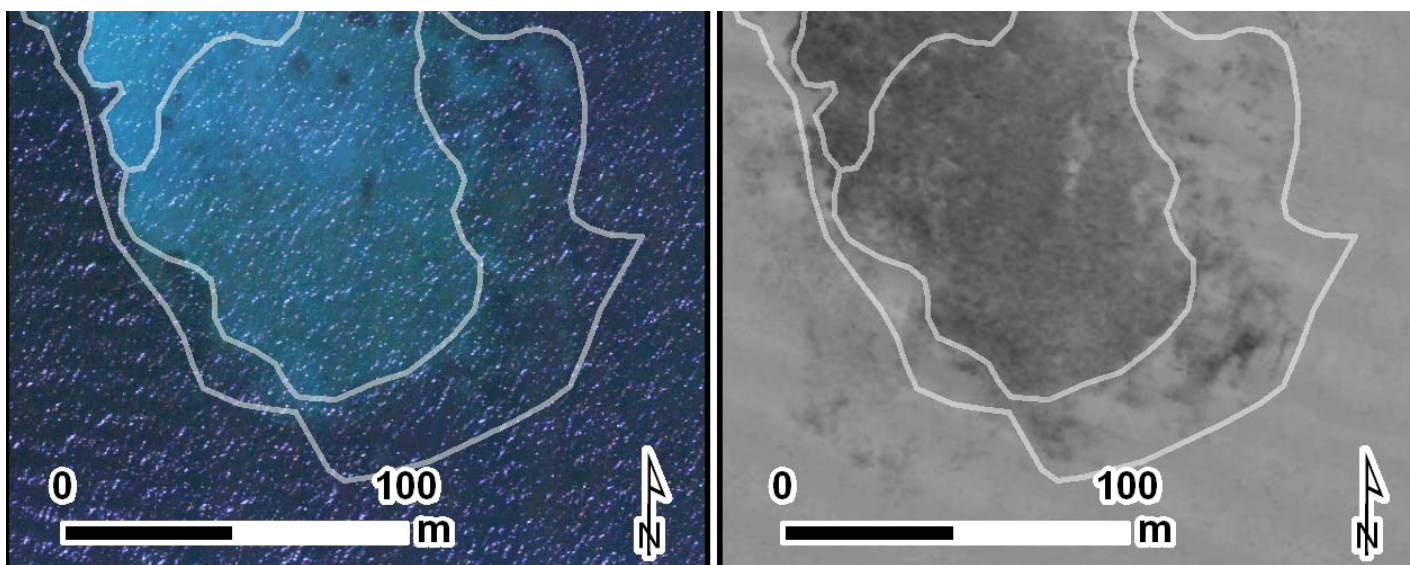


Figure 2.42. These maps denote an example of sand habitat with different amounts of seagrass in the optical (left) and acoustic (right) imagery. Habitat features were identified by their distinct optical and/or acoustic signatures. These unique colors, intensities, textures and/or shapes distinguished them from the surrounding seafloor.

2.5.2. Habitat Feature Delineation

The Jobos Bay benthic habitat map was created in ArcMap 9.3 using the Habitat Digitizer Extension (Buja, 2008a). The Habitat Digitizer Extension is a GIS tool that allows a user to delineate and attribute polygon features from geo-referenced images. A custom classification scheme (described in Section 2.2) was imported and used to attribute polygons by visual interpretation. This allowed the cartographer to rapidly and dynamically delineate and classify habitat features on the fly, significantly improving the efficiency with which habitat maps are developed.

Using the Habitat Digitizer, habitat features were often delineated by first digitizing a large boundary polygon (such as the shoreline) and then appending new polygons to the initial boundary polygon. Another technique was to draw one large polygon around a homogenous feature and then split it into smaller polygons based on percent cover type. This approach was often used for seagrass beds of varying patchiness. Regardless of the digitizing approach, critical digitizing parameters were set in advance (using the Habitat Digitizer), in order to standardize the scale and size of feature delineation. These parameters specifically included: (1) the MMU, which was set to 1,000 m², and (2) the digitizing scale, which was set to 1:2,000. Setting the MMU ensured a uniform minimum polygon size, whereas setting a uniform digitizing scale ensured a consistent level of habitat polygon boundary detail. The cartographer was allowed to zoom in and out to varying scales when assessing an area, but always returned to 1:2,000 before delineating a feature.

2.6. HABITAT FEATURE ATTRIBUTION (GROUND VALIDATION)

Extensive field work is needed to create high-quality benthic habitat maps because it enhances the accuracy of habitat attribution and (to a lesser degree) habitat delineation. A team of NOAA field scientists visited predetermined locations to explore and verify existing habitat information on the seafloor. These “ground validation” (GV) locations were targeted by the cartographer to satisfy the following objectives:

1. Explore features in the imagery with unknown or confusing optical or acoustic signatures
2. Confirm that the habitat type correlated with a particular optical or acoustic signature remained consistent throughout the entire study area

To achieve this first objective, the cartographer placed GV points in features with unknown habitat types. These points were important for understanding the habitat class associated with these distinct but unknown remotely sensed signatures. To achieve the second objective, the cartographer placed GV points in habitat features with known habitat types distributed throughout the entire spatial extent of the mapped area. These points were important to the GV process because the same habitat type may exhibit slightly different signatures in different parts of the study area. A single habitat type may exhibit slightly different optical signatures because they occur at different depths (e.g., a polygon attributed as “Sand, No Cover 90-100%” at 5 m depth will look slightly different than one at 25 m depth). Similarly, a single habitat type may exhibit slightly different acoustic signatures because different polygons will contain varying amounts of structural and biological cover heterogeneity within them (e.g., polygons attributed as “Sand” contains varying amounts of sand, mud, algae and seagrass).

Ground validation data were collected from May 13-17, 2009 at 168 sites in the Jobos Bay region (Figure 2.43) onboard the R/V *Jurel* provided by JBNERR. A combination of underwater video (155 sites), surface observations (eight sites), free diving and snorkeling (five sites) were used to survey the ecological characteristics at each location (Figure 2.44). GV sites were navigated to using a hand-

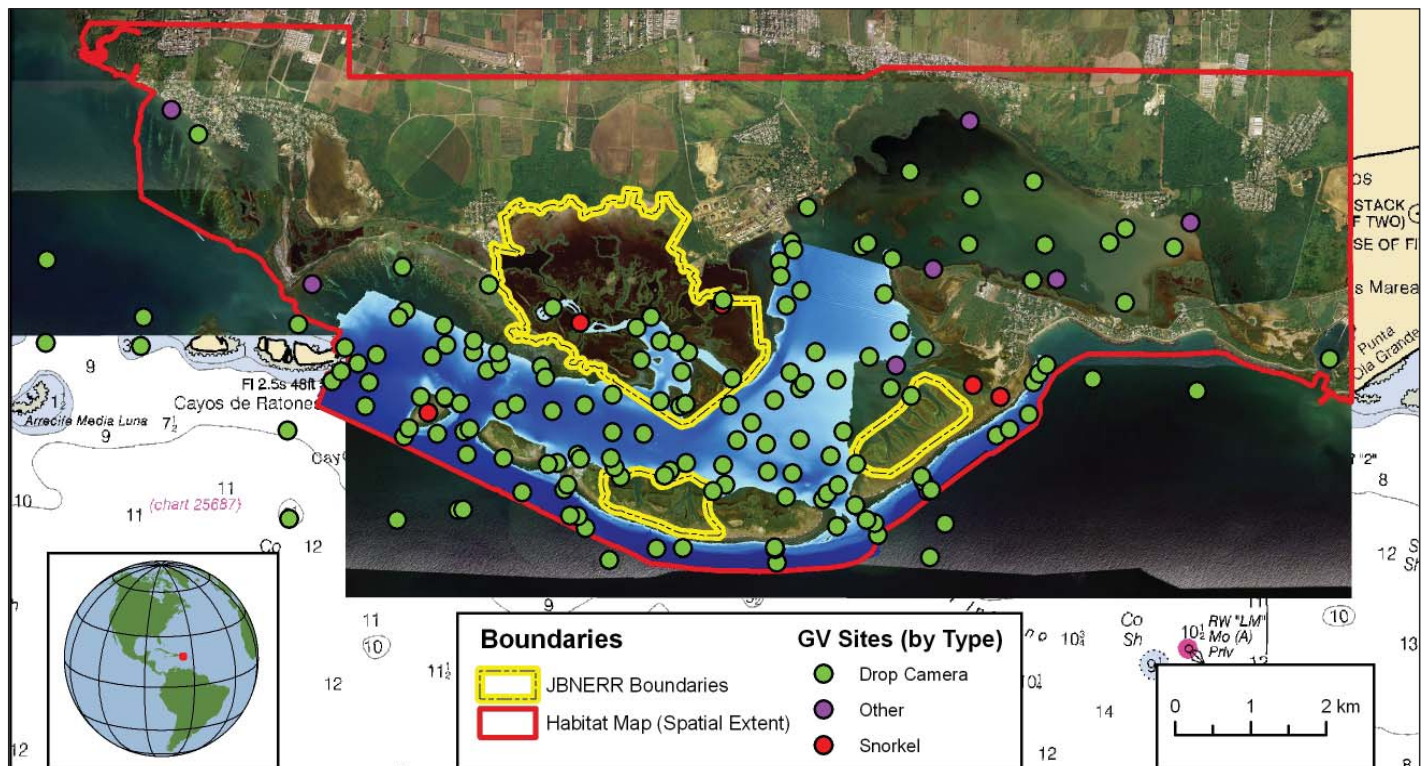


Figure 2.43. A combination of underwater video (155 sites), surface observations (eight sites), free diving and snorkeling (five sites) were used to survey the ecological characteristics at each location. This information was analyzed (in concert with the optical and acoustic imagery) to classify each polygon in the habitat map.

held WAAS-enabled GPS unit. The vessel was maneuvered to within 5 m of the target location. Once in position, NOAA scientists would concurrently deploy a SeaViewer Sea-Drop 950 camera (attached to a down weight and 300 feet of line), and begin logging a waypoint on a Trimble GeoXT GPS receiver. While on site, the vessel's position was captured as an epic (*i.e.*, point) approximately every 5-10 seconds depending on the number of satellites detected by the GPS antennae. The underwater video was recorded onto mini-video tapes using a video recorder. The camera operator adjusted the camera lens to get a downward view of the seafloor approximately 2 m from the bottom, and a side view of the seafloor. This allowed for accurate measurements of percent biological cover and a broader scale understanding of the structure at each site. No attempt was made to standardize the amount of time the camera was on the seafloor. In fact, it was often advantageous to drift across habitat transitions, as it allowed the cartographer to understand the ecotone at many locations.



Figure 2.44. SeaViewer Sea-Drop 950 camera (left) was used in combination with snorkeling, free diving and surface observations via a look bucket (right) to ground truth 168 discrete seafloor locations. Photos: <http://www.ub88.org/> (left), NOAA CCMA (right).

While the camera was recording video of the seafloor, an observer viewed the video real-time on a laptop and classified the major/detailed geomorphological structure, major/detailed biological cover, and percent coral for each site. Waterproof field maps (depicting the draft habitat map and source imagery) were used to visually link signatures in the imagery with the in situ habitats seen in the video. In many cases, suggestions on boundary delineation and habitat classifications were made directly on the field maps with permanent marker. Once back in the office, Trimble Pathfinder Office software was used to post process and differentially correct the raw GPS data to the CORS at Coamo, Puerto Rico (PRN4). The underwater video was converted from the mini-tapes to softcopy form using Final Cut Pro software. The classification of each GPS location (completed in the field) was then reviewed in conjunction with the associated underwater video and/or photos (as well as the optical and acoustic imagery) to develop a final classified set of GV points (Figure 2.45).



Figure 2.45. The classification of each GPS location (completed in the field) was then reviewed in conjunction with the associated underwater video and/or photos, as well as the optical and acoustic imagery, to develop a final classified set of GV points.

2.7. EXPERT REVIEW

Before the Jobos Bay habitat map was considered final and ready for release, a panel of local experts reviewed the map online. In particular, local marine biologists, coral reef scientists and resource managers from a variety of organizations (including the U.S. Department of Agriculture [USDA], Forest Service, the U.S. Fish and Wildlife Service, NOAA, University of Puerto Rico and JBNERR) were invited to review the habitat map online from August 31 to September 7, 2010. Using an online web GIS interface (Buja, 2010), experts were asked to comment on the habitat classification scheme, habitat boundary delineations and polygon attributes of the draft maps in order to improve the quality and accuracy of the final map products. The reviewers also commented on the utility of these maps for management and research purposes. Some suggestions were made to change the class type of individual polygons, based on their local knowledge of the seafloor. These comments were incorporated into the final map after the expert review had concluded. Additionally, two independent scientists within the BB reviewed the underwater video, source imagery and map product to qualitatively confirm the classifications assigned to each habitat polygon. The final map was then reviewed for topological errors before being finalized. This process is described in the proceeding section.

2.8. GIS QUALITY CONTROL

All GIS deliverable products generated throughout the mapping process were examined for attribution and topological errors. Particular attention was given to polygon geometry and attribution of the benthic habitat map, as well as to the attribution of each GV point. Multipart, sliver and void polygons were all removed using standard ArcGIS Spatial Analyst tools. Two custom ArcGIS extensions were employed to identify the following conditions:

1. Adjacency – polygons that shared a common boundary and exact attribute combination that were delineated separately (Buja, 2008b);
2. Overlap – polygons sharing the same geographic space, thus violating mutual exclusion (Buja, 2008c).

Errors resulting from either of these GIS routines were corrected on draft maps and eliminated in the final product. A visual inspection of attributes on a feature-by-feature basis was conducted to correct for any misspellings or illogical attribute combinations. These quality assessments and controls ensured that the GIS data from this work were topologically clean and free of attribution errors. In addition, metadata summaries were prepared in a Federal Geographic Data Committee (FGDC) format for all GIS products that were supplied during final delivery.

2.9. CONCLUSIONS

NOAA's BB, with support from the USDA, NOAA's Coral Reef Conservation Program (CRCP), NERRS and JBNERR, has completed a benthic habitat map for the estuarine and shallow-water marine environment in Jobos Bay, Puerto Rico. While no independent accuracy assessment was conducted for this habitat map, the final map was reviewed by local experts to qualitatively validate its spatial and thematic accuracy. Additionally, other habitat maps created using the same mapping protocol reported overall thematic accuracies of greater than 88% for major geomorphological structure and cover classes, and greater than 70% for detailed geomorphological structure and biological cover classes (Battista *et al.*, 2007a,b; Zitello *et al.*, 2009; Bauer *et al.*, 2010). As a result, these digital map products can be used with confidence by scientists and resource managers for a multitude of different applications. The scientific and management communities have used previous NOAA benthic habitat maps to structure monitoring programs, support management decisions, and establish and

manage marine conservation areas. The final deliverables for this project are available to the public by request. Brief descriptions of these deliverables are listed in Table 2.4.

2.9.1. Map Summary Statistics

In total, 35.7 km² of the seafloor and 14.1 km² of the intertidal shoreline in and around JBNERR were mapped. The entire 8.3 km² area inside the JBNERR boundaries was mapped to the detailed structure level. Figures 2.46 through 2.50, depict

the geographic zone, detailed structure, percent hardbottom, detailed biological cover and coral cover of the area mapped in Jobos Bay. Several patterns emerged when examining the summary map statistics for the total mapped area, as well as the mapped area inside and outside the Reserve boundaries (Figures 2.51-5.56). In particular, *Shoreline Intertidal* constituted 65% of the area inside JBNERR (excluding land), whereas only about 21% of the area outside JBNERR and 28% of the total area was classified as *Shoreline Intertidal*. *Unconsolidated Sediment*, specifically *Mud*, constituted the majority of the total mapped area, as well as the majority of the mapped areas inside and outside the JBNERR boundaries. After *Mud*, *Sand* was the second most dominant detailed structure type for all three areas. *Individual Patch Reefs*, *Aggregated Patch Reefs* and *Aggregate Reef* comprised 3.1% of the total mapped area, 3.5% of the mapped area outside the JBNERR, and 0.1% of the mapped area inside the JBNERR. The 0.02 km² of Artificial detailed structure type denotes the presence of several industrial piers outside of the JBNERR boundaries.”

Although the majority of these three mapped areas had the same structure type, they were dominated by different biological covers. In particular, approximately 41% of the area inside JBNERR was colonized by mangroves, with 90% - 100% being the most common of the three density classes. Of the remaining 59% of the Reserve, 18% was colonized by seagrass, 5% by algae, 4% was land and 32% was uncolonized by biological organisms. The habitat distributions were slightly different outside the JBNERR boundaries. In particular, about 33% of the of the area (excluding land) outside JBNERR boundaries was dominated by seagrass with 50%≤90% being the most common of the three density classes. Substrates with little or no biological cover and substrates with algae were also prevalent outside the Reserve. *Mangroves* constituted about 21% of the mapped area outside JBNERR. In terms of coral cover, the majority (>94%) of the areas inside and outside JBNERR were colonized by 0%≤10% live scleractinian and/or soft corals. It is important to note, however, that the mapped area outside the JBNERR had 2.46 km² of seafloor with 10%≤50% live coral.

Table 2.4. Final deliverables for NOAA’s habitat map of Jobos Bay, Puerto Rico.

Item	Format	Quantity
Benthic Habitat Map	GIS	1
Habitat Symbology Layers	GIS	5
Optical Data (Images)	GIS	17
Acoustic Data (Images)	GIS	11
Ground Validation Dataset	GIS	2
Photos of Seafloor	.jpeg	155
Video of Seafloor	.mov	149
FGDC-compliant Metadata for GIS Files	Text	31
Online Interactive Map Project	Online	1
Final Report	PDF	1

2 - Benthic Habitat Mapping

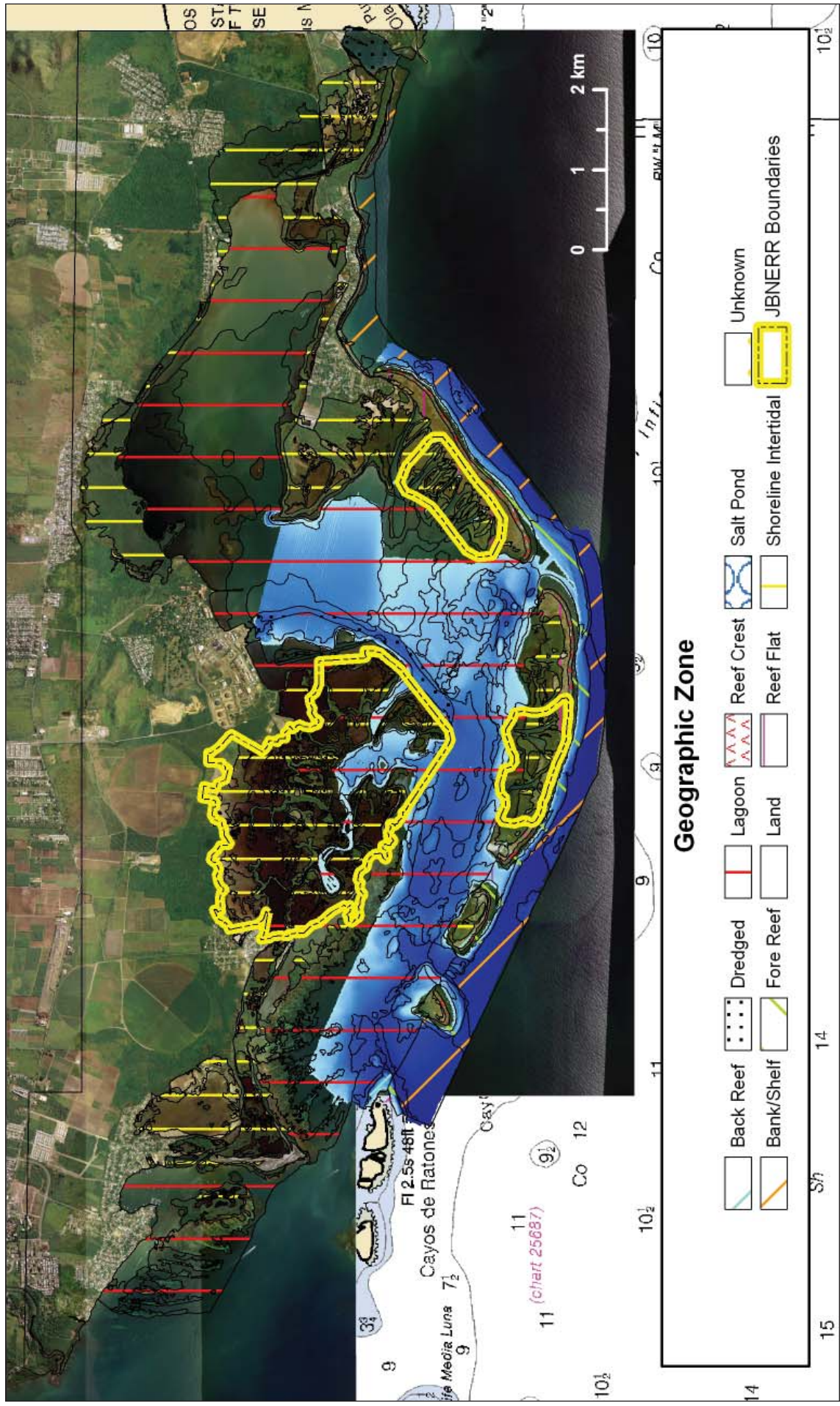


Figure 2.46. Map of geographic zone types in Jobos Bay, Puerto Rico.

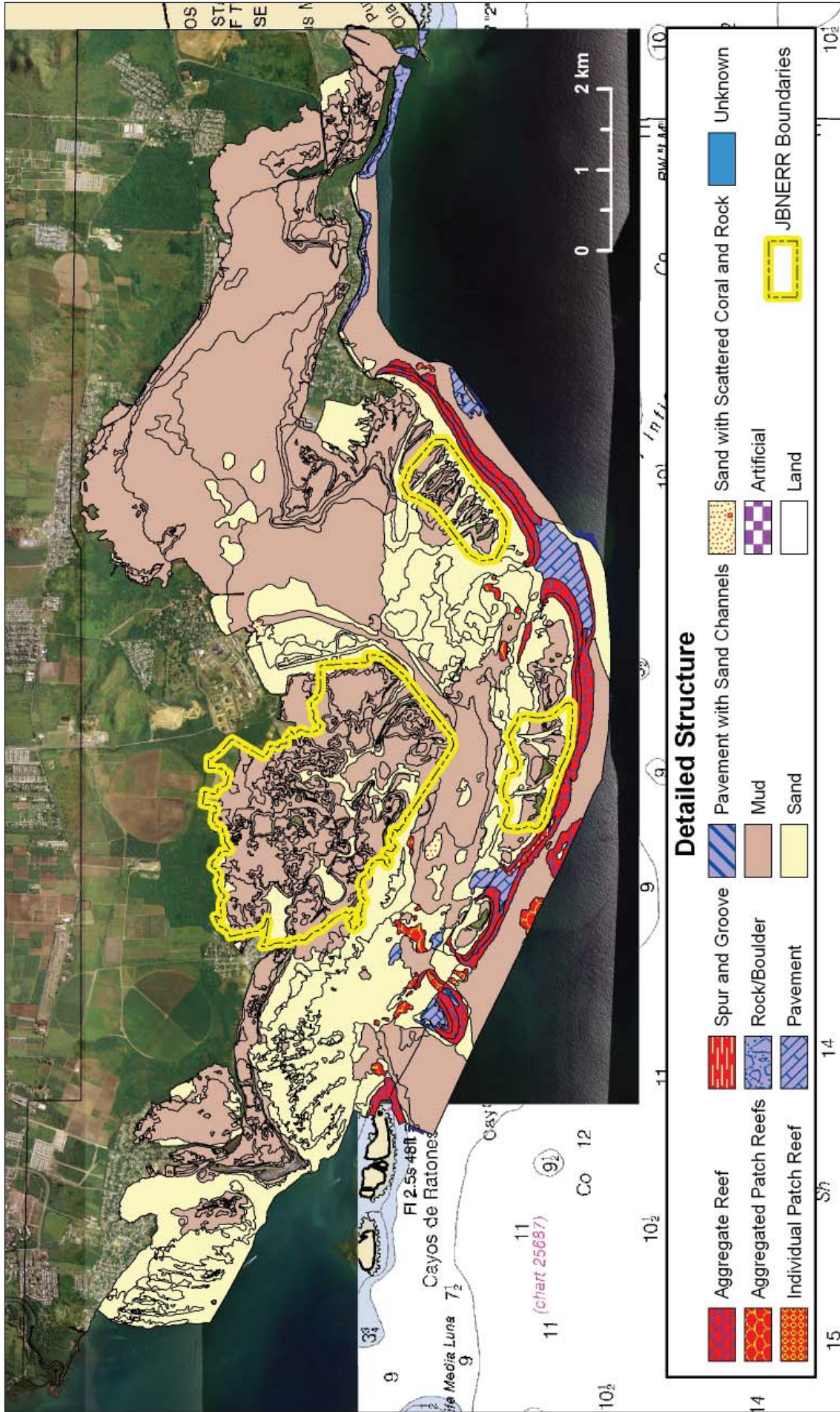


Figure 2.47. Map of geomorphological structure types in Jobos Bay.

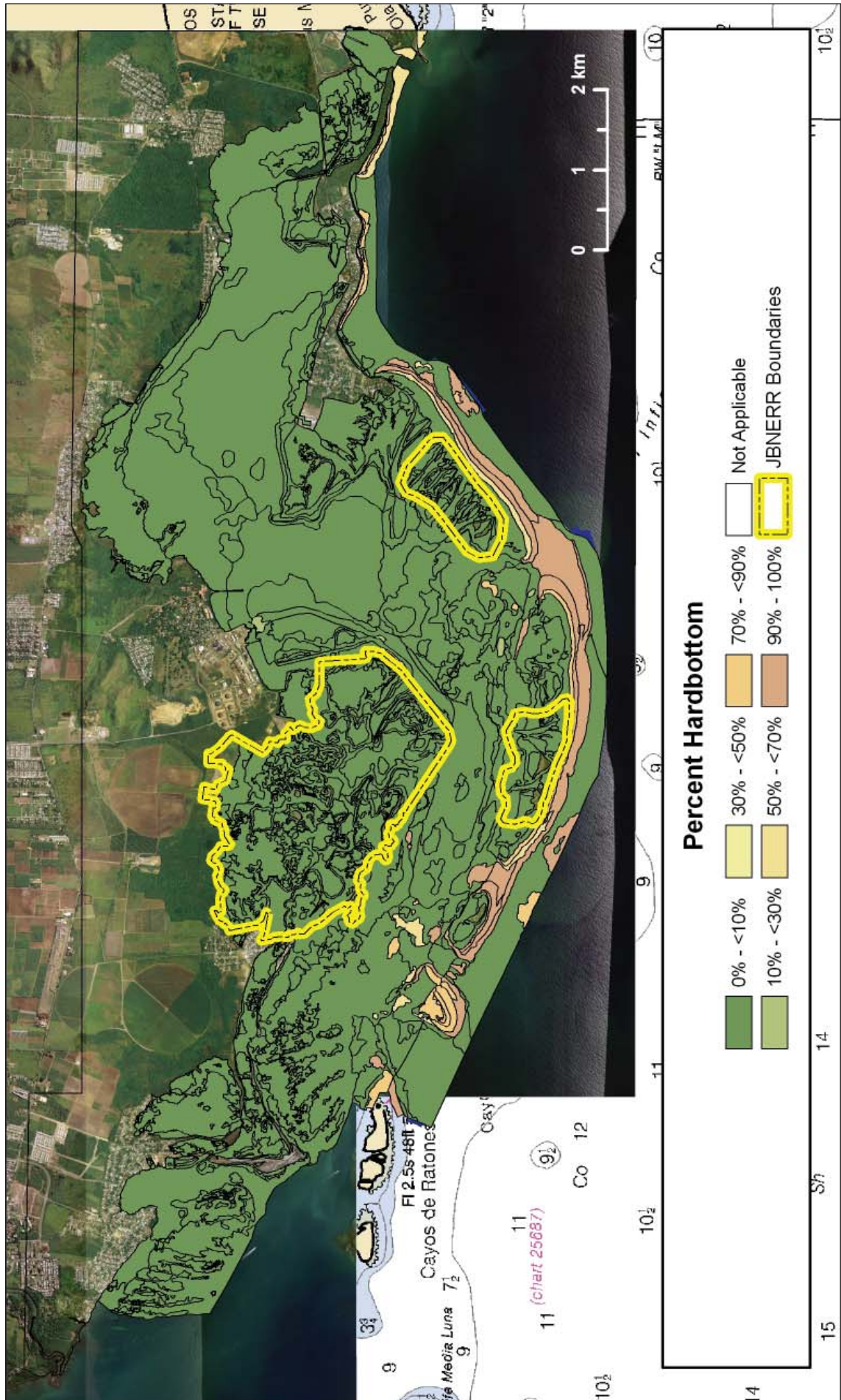


Figure 2.48. Map of percent Hardbottom class types in Jobos Bay.

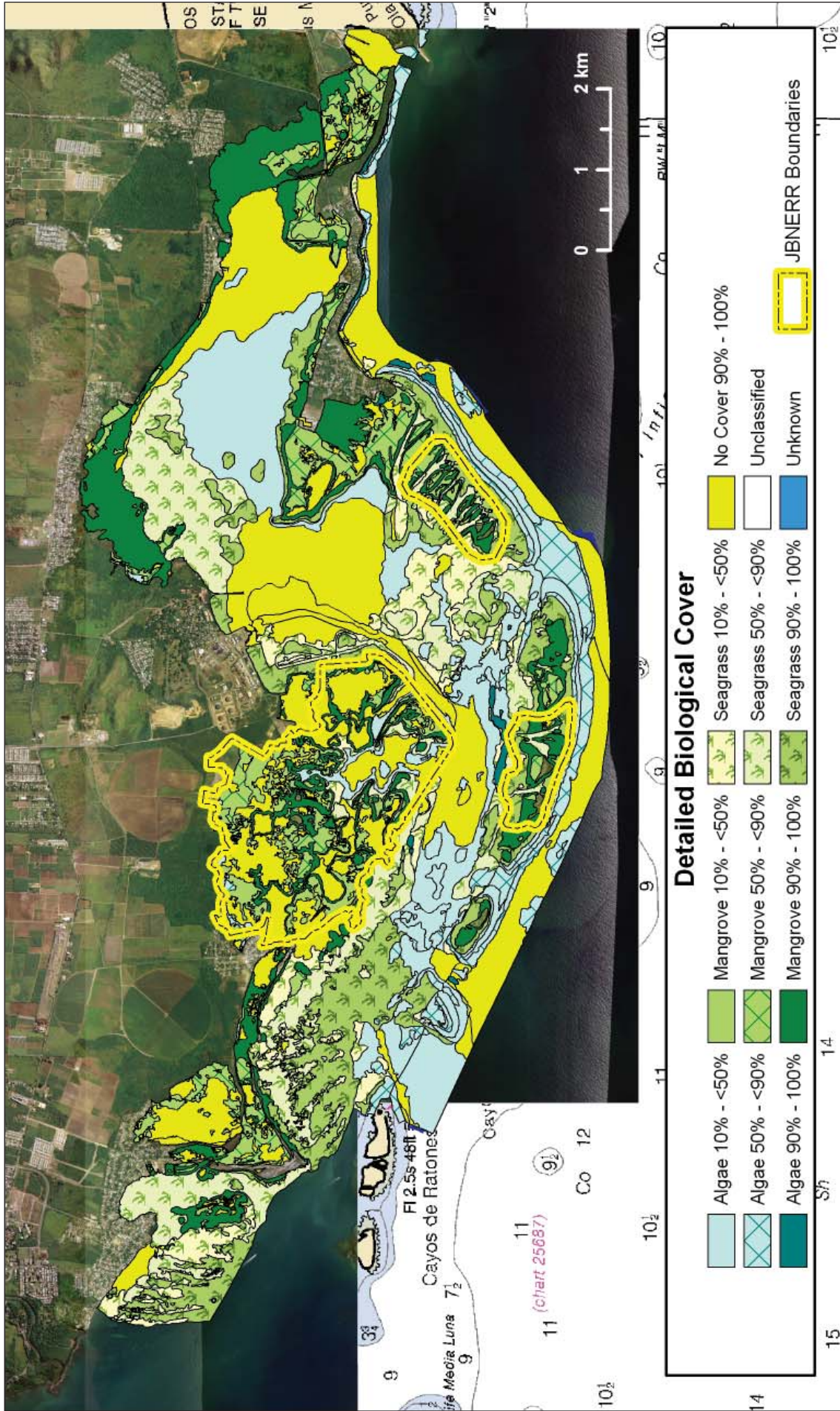


Figure 2.49. Map of major and detailed biological cover types in Jobos Bay.

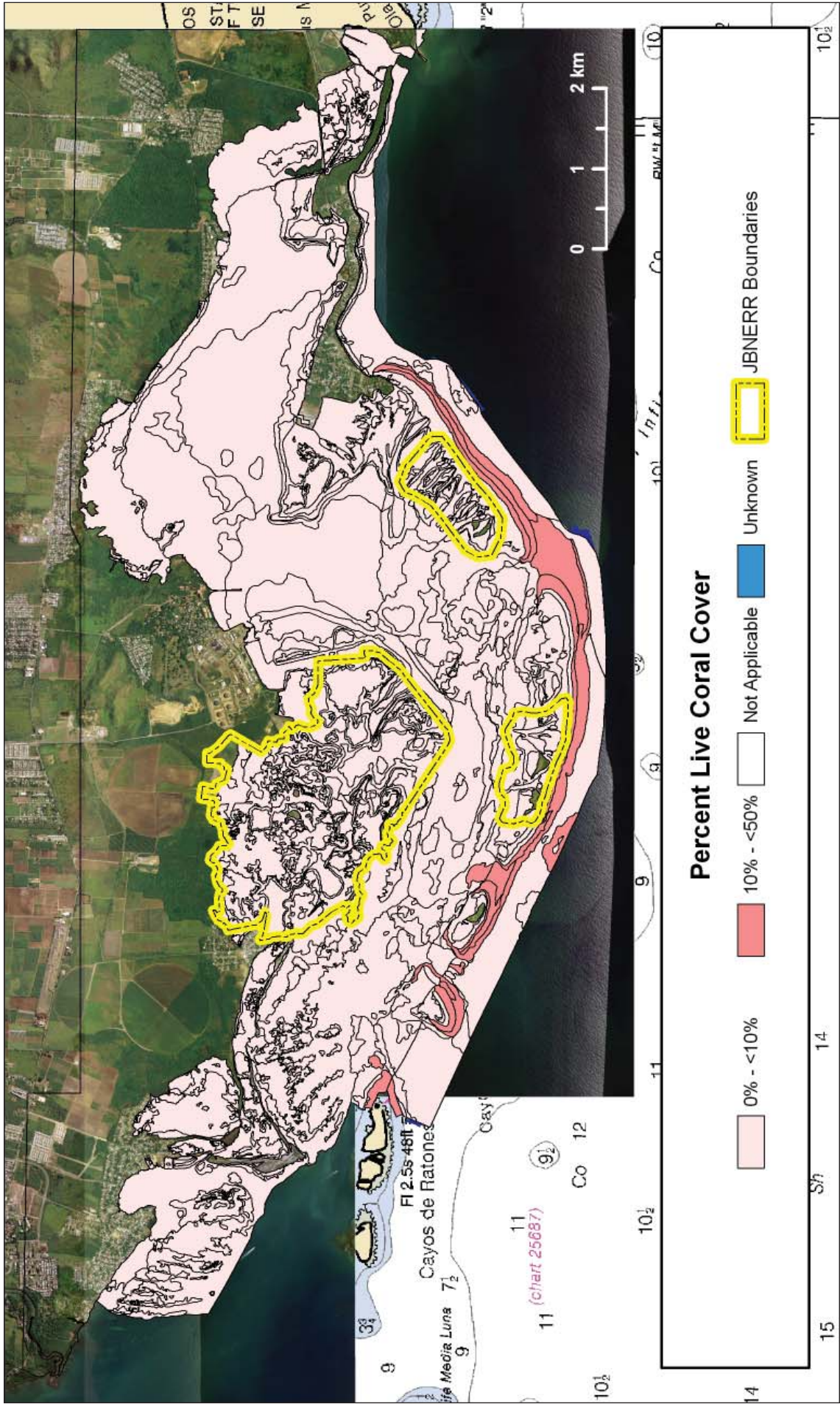


Figure 2.50. Map of percent live coral cover types in Jobos Bay.

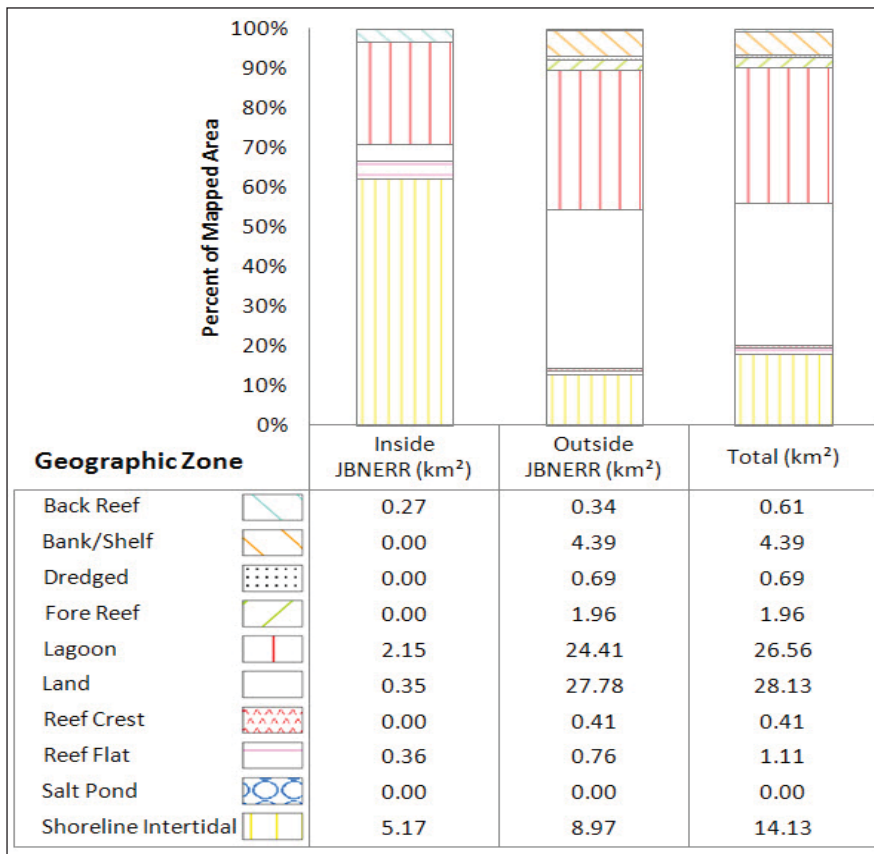


Figure 2.51. Summary statistics describing the total amount of mapped area by geographic zone types. These numbers are further divided into the amount of mapped area inside and outside the JBNERR.

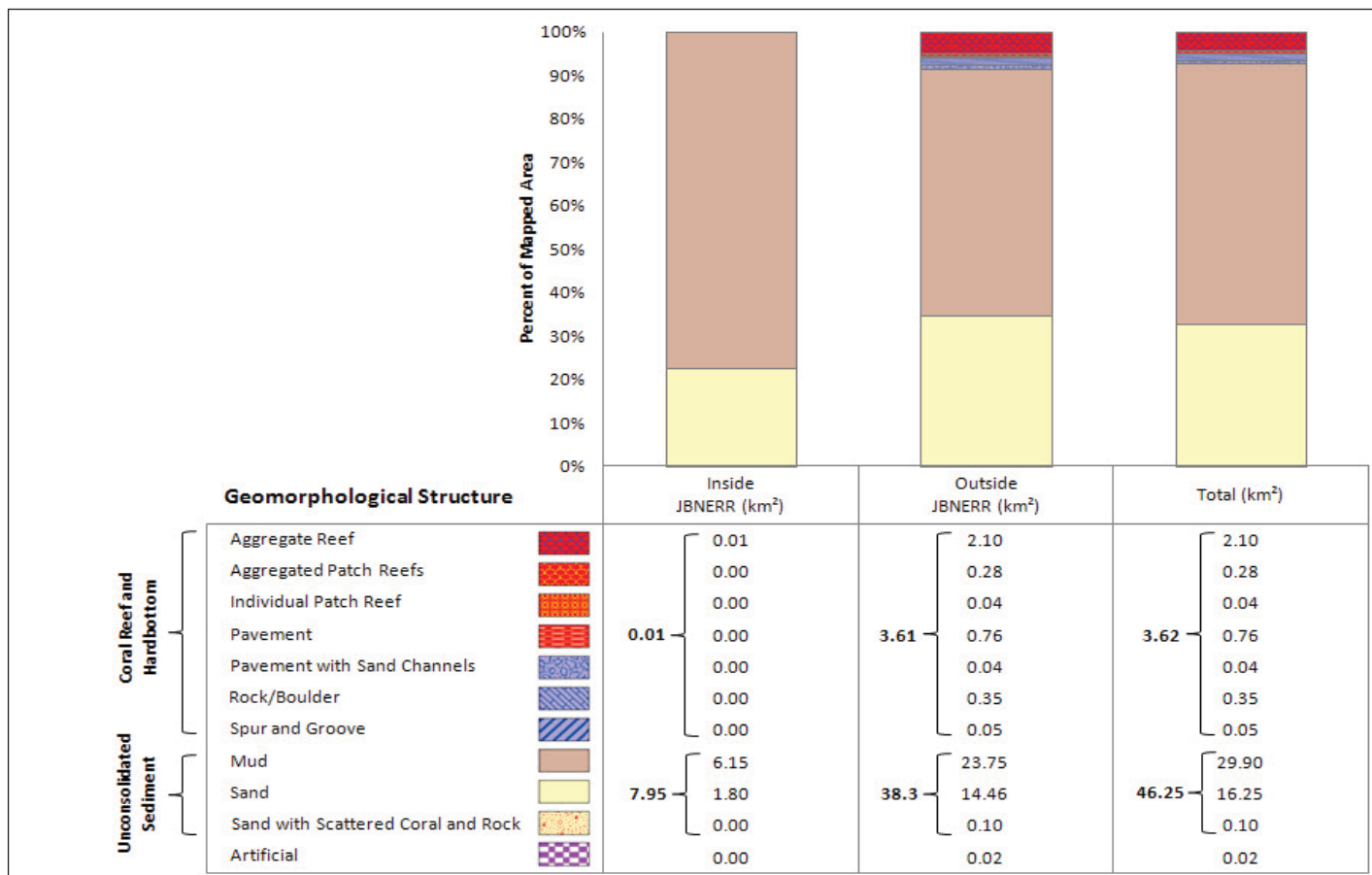


Figure 2.52. Summary statistics describing the total amount of mapped area by major and detailed structure types. These numbers are further divided into the amount of mapped area inside and outside the JBNERR.

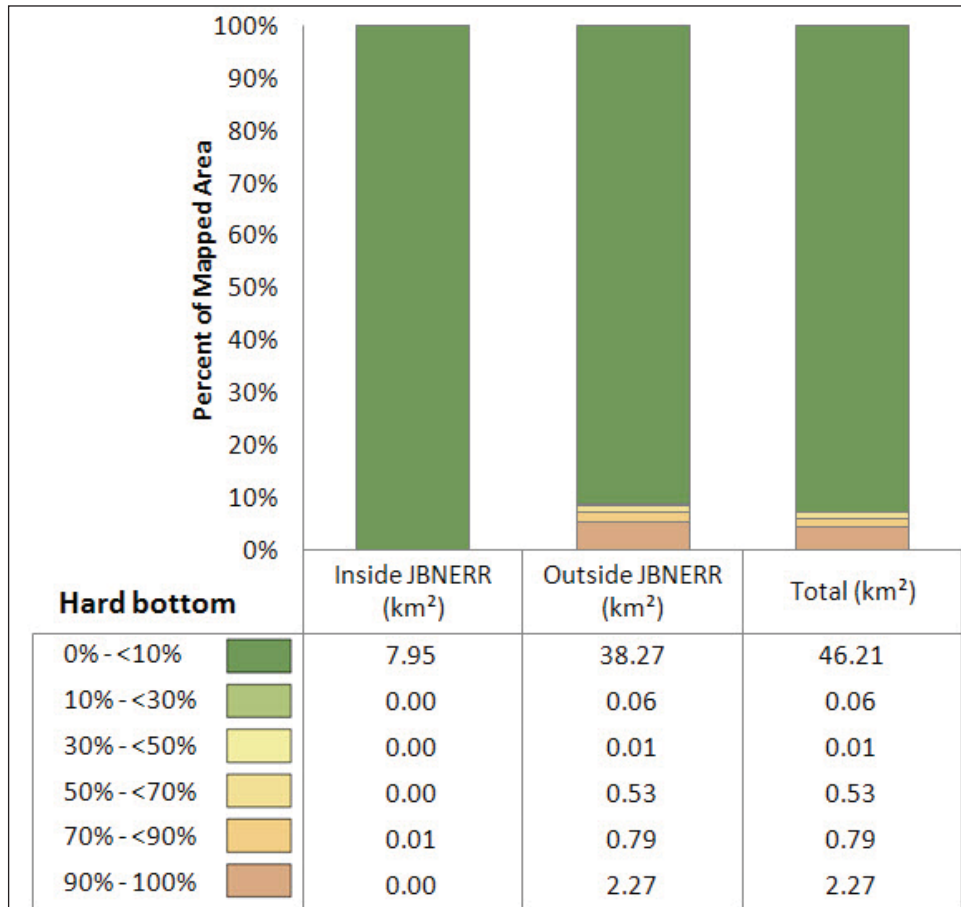


Figure 2.53. Summary statistics describing the total amount of mapped area by percent hardbottom class types. These numbers are further divided into the amount of mapped area inside and outside the JBNERR.

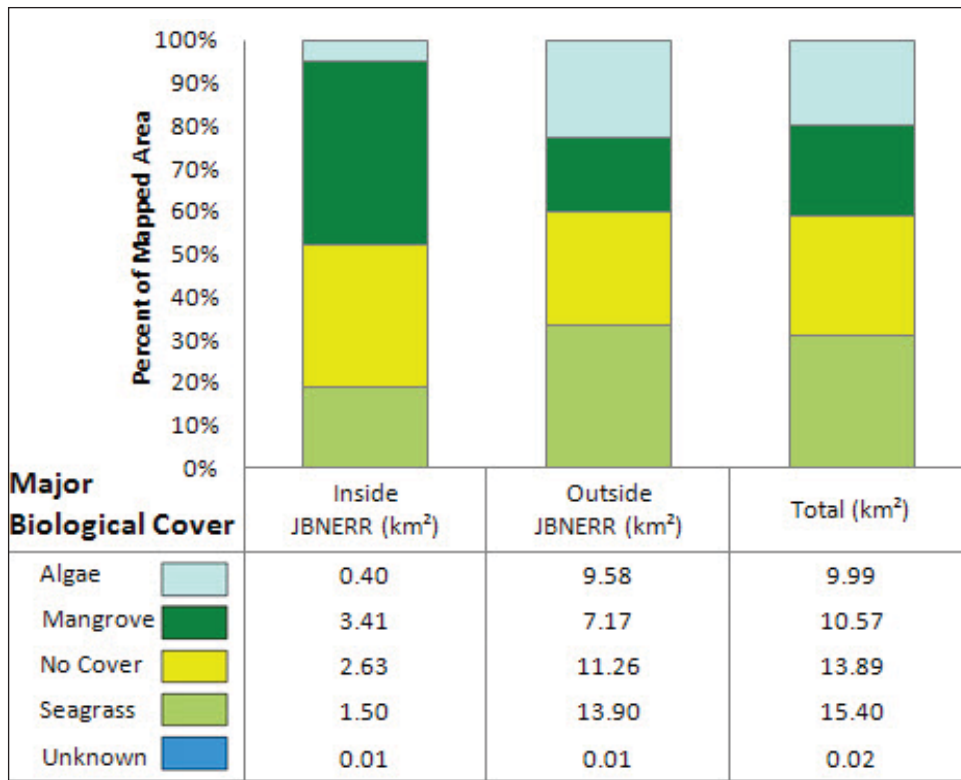


Figure 2.54. Summary statistics describing the total amount of mapped area by major biological cover types. These numbers are further divided into the amount of mapped area inside and outside the JBNERR.

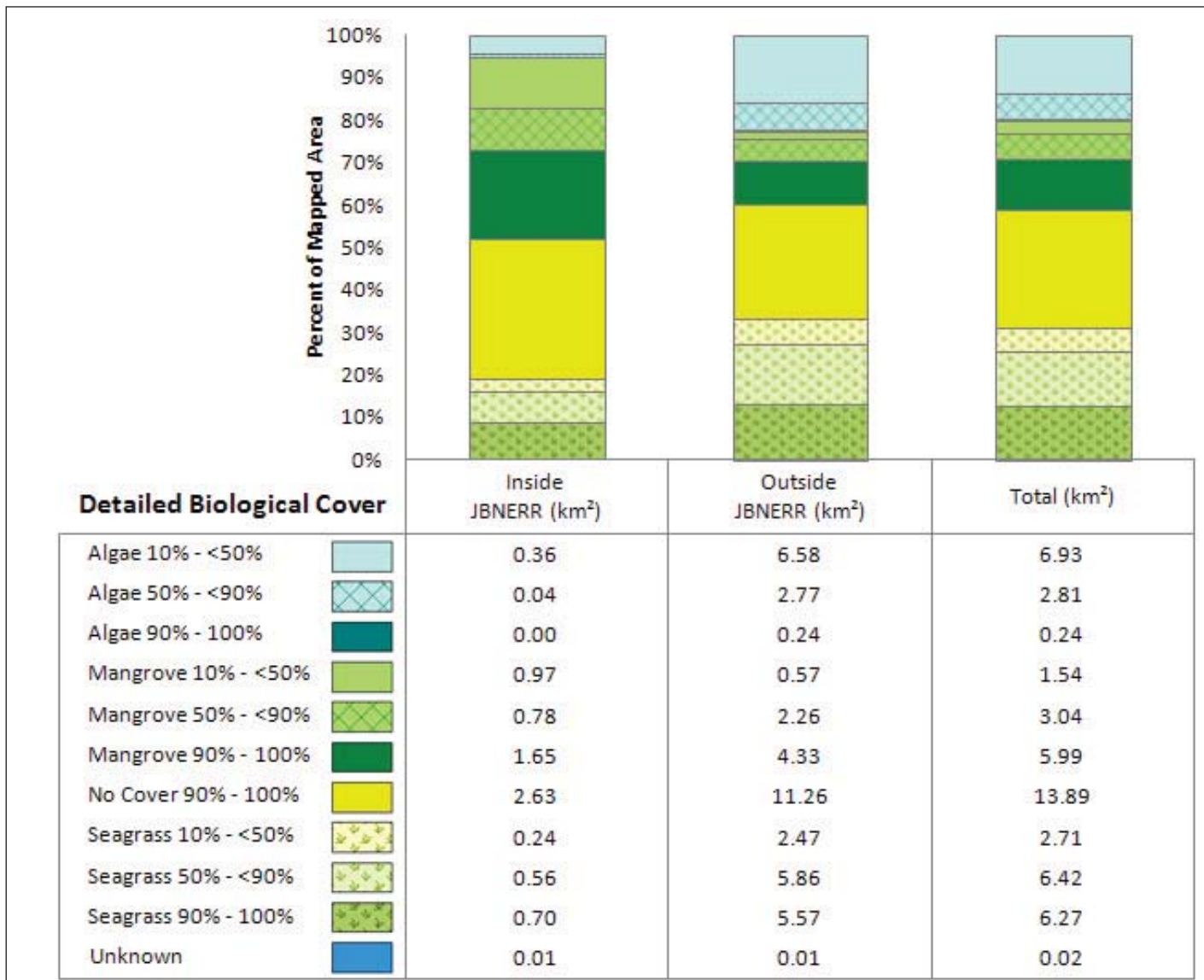


Figure 2.55. Summary statistics describing the total amount of mapped area by detailed biological cover types. These numbers are further divided into the amount of mapped area inside and outside the JBNERR.

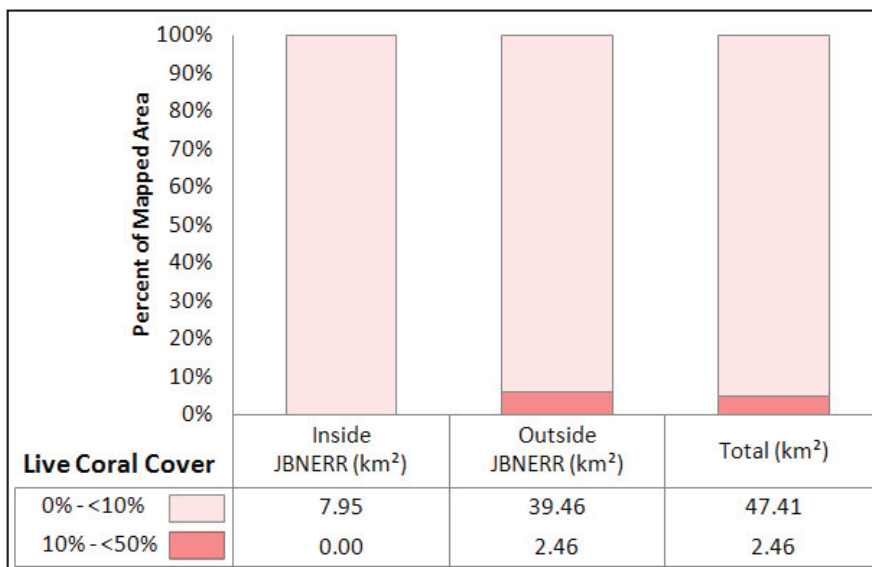


Figure 2.56 Summary statistics describing the total amount of mapped area by percent coral cover types. These numbers are further divided into the amount of mapped area inside and outside the JBNERR.

2.9.2. Comparison to Previous NOAA Habitat Maps of Jobos Bay

The 2010 mapping effort described in this chapter marks the second time NOAA has mapped the shallow-water marine benthic habitats of Jobos Bay. However, several improvements were made in the 2010 map versus the 2001 map (Kendall *et al.*, 2001). These improvements specifically include the use of: (1) a new classification scheme with a higher thematic resolution, (2) a finer scale of delineation, and (3) a smaller minimum mapping unit (Table 2.5). These improvements were possible

due to the use of higher resolution optical imagery and to the mapping of a much smaller project area. In addition to these enhancements, more of the seafloor within Jobos Bay was mapped in 2010 than in 2001 (*i.e.*, approximately 78 km² versus 56 km², respectively; Figure 2.57). More seafloor was

Table 2.5. Comparison of map and feature characteristics for the 2001 and 2010 benthic habitat maps.

		NOAA Mapping Effort	
		2001	2010
Map	Optical Imagery Acquisition Date	1999	2010
	Spatial Resolution of Optical Imagery (m)	2.40	0.30
	Scale of Delineation	1:6,000	1:2,000
	MMU (m ²)	4,046	1,000
Feature	Number of Polygons	230	817
	Number of Polygons <4,046 m ²	-	261
	Mean Area of Polygons (m ²)	0.25	0.10
	Total Mapped Area (km ²)	55.89	78.00
	Mean Perimeter of Polygons (km)	2.88	1.74
	Total Perimeter of Polygons (km)	653	1,422

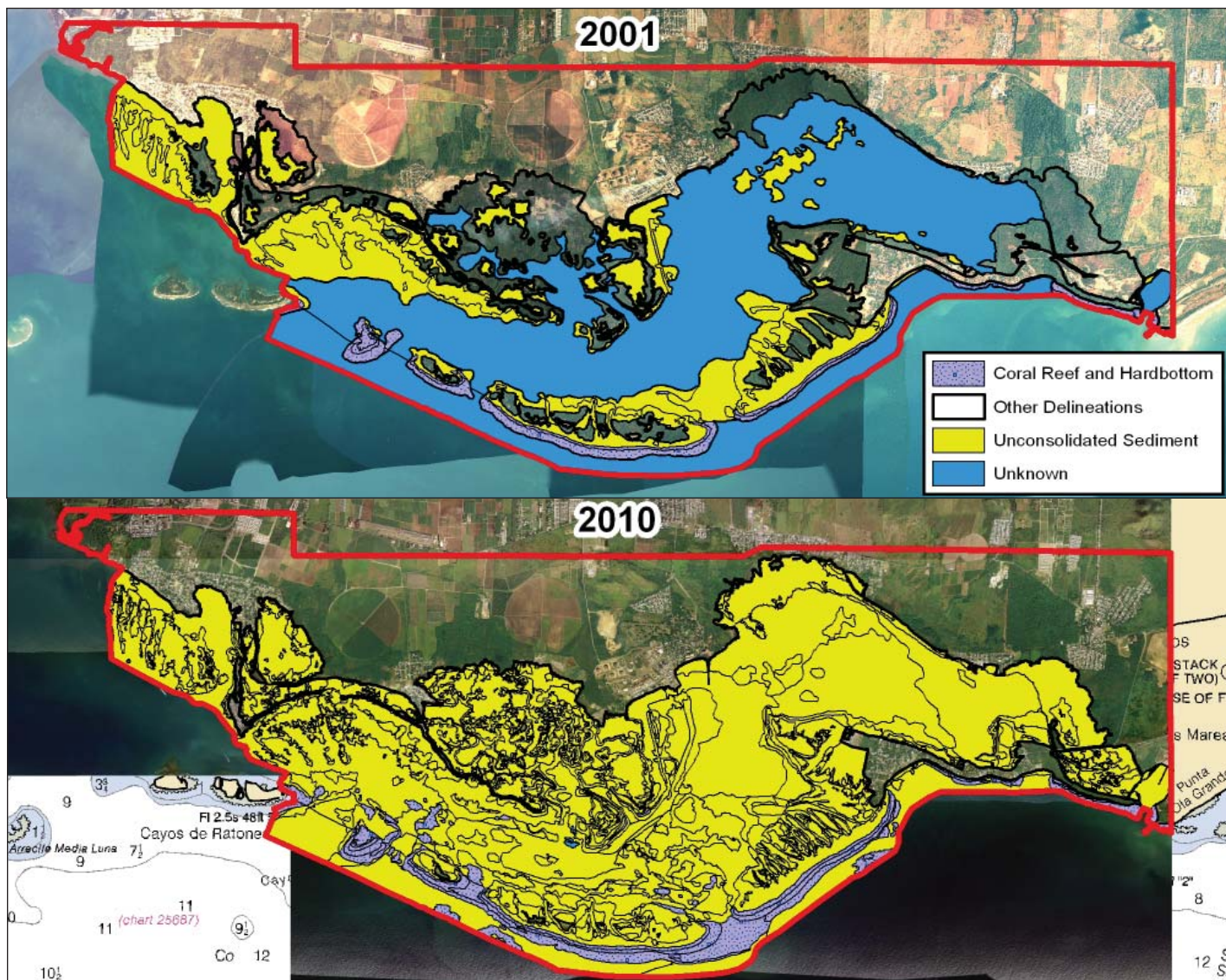


Figure 2.57. Maps of the major geomorphological structure types mapped in 2001 and in 2010. Note the large area that was characterized as “Unknown” in 2001.

mapped in 2010 because acoustic imagery was collected and used to characterize areas that were previously obscured by turbidity in the 2001 mapping effort.

Periodic re-mapping of an area can serve as an important monitoring tool. Although the different classification schemes and MMUs prohibit a quantitative comparison between the 2001 and 2010 maps for several reasons (Kendall and Miller, 2008), there appear to be some changes in biological cover on softbottom between the two time periods. For example, areas immediately east of Punta Arenas experienced some loss and regrowth of seagrass between 1999 (when the previous source imagery was taken) and 2007 (when the new source imagery was taken; Figure 2.58).

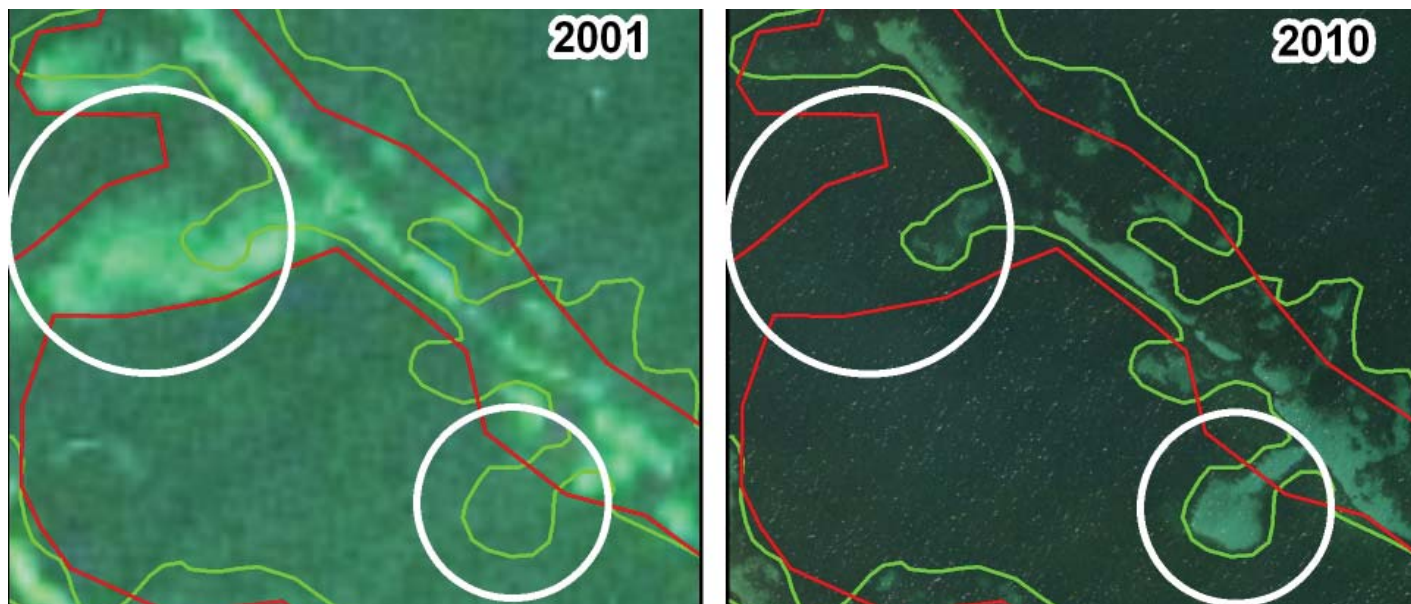


Figure 2.58. Periodic re-mapping of an area can serve as an important monitoring tool. These maps (developed in 2001 and 2010) show the loss and regrowth of seagrass (denoted by the white circles) southeast of Punta Arenas.

In addition to the localized loss and regrowth of seagrass beds, several square kilometers (approximately 4.7 km²) of seagrass that were previously unmapped (due to turbidity) were characterized in the new habitat map. These previously unmapped seagrass beds were primarily found in the shallows east of Cayo Puerca, north of Punta Rodeo and north of Cayo Morrillo and Cayos de Pájaros (Figure 2.59). A more detailed, visual comparison of the 1999 and 2007 imagery and 2001 and 2010 habitat maps may reveal additional fine scale habitat changes, helping managers to better understand how

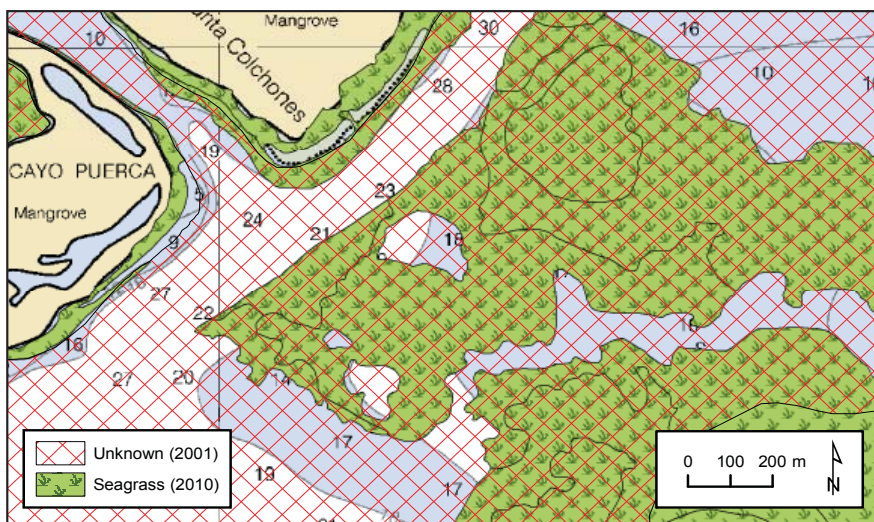


Figure 2.59. Several square kilometers (approximately 4.7 km²) of previously unmapped seagrass (due to turbidity) were characterized in the new habitat map east of Cayo Puerca, north of Punta Rodeo and north of Cayo Morrillo and Cayos de Pájaros.

benthic communities have changed in the last decade, and possibly to better understand how benthic communities will change during the next decade in the Jobos Bay.

ACKNOWLEDGEMENTS

Funding for this mapping effort was provided by NOAA's CRCP and the Natural Resources Conservation Service (NRCS). This work would not have been possible without the numerous people who shared their data, time and expertise throughout this process. In particular, we appreciate the support of the JBNERR staff, especially Angel Dieppa. We also appreciate the support of Jay Lazar and David Bruce from NOAA's Chesapeake Bay Office (CBO) for collecting the acoustic data. Also, many thanks to Adam Zitello, Tim Battista and Chris Caldow for helping to collect ground validation data in the field. Matthew Kendall, Matthew Poti, Angel Dieppa and Jorge "Reni" García-Sais provided useful comments and editorial assistance.

REFERENCES

Battista, T.A., Costa, B.M., and S.M. Anderson. 2007a. Shallow-water benthic habitats of the main eight Hawaiian islands. NOAA Technical Memorandum NOS NCCOS 61 (Online). http://ccma.nos.noaa.gov/products/biogeography/hawaii_cd_07/welcome.html (Accessed 17 February 2011).

Battista, T.A., Costa, B.M., and S.M. Anderson. 2007b. Shallow-Water Benthic Habitats of the Republic of Palau. NOAA Technical Memorandum NOS NCCOS 59 (Online). <http://ccma.nos.noaa.gov/products/biogeography/palau/htm/overview.html> (Accessed 17 February 2011).

Bauer, L.J., M.S. Kendall, A.G. Zitello, and T. Battista. 2010. Chapter 2: Benthic Habitats of Vieques, Puerto Rico. pp. 9-46. In: L.J. Bauer and M.S. Kendall (eds.). An Ecological Characterization of the Marine Resources of Vieques, Puerto Rico Part II: Field Studies of Habitats, Nutrients, Contaminants, Fish, and Benthic Communities. NOAA Technical Memorandum NOS NCCOS 110. Silver Spring, MD. 174 pp.

Buja, K. 2008a. Habitat digitizer extension for ArcGIS v5. Biogeography Branch, Center for Coastal Monitoring and Assessment, National Centers for Coastal Ocean Science, National Ocean Service, National Oceanic and Atmospheric Administration. (Online) <http://ccma.nos.noaa.gov/products/biogeography/digitizer/welcome.html> (Accessed 17 February 2011).

Buja, K. 2008b. Find adjacent features. ESRI Support Center. (Online) <http://arcscripsts.esri.com/details.asp?dbid=15805> (Accessed 10 June 2011).

Buja, K. 2008c. Find overlapping polygons. ESRI Support Center. (Online) <http://arcscripsts.esri.com/details.asp?dbid=15198> (Accessed 10 June 2011).

Buja, K. 2010. BIOMapper (Biogeography Integrated Online Mapper) for Jobos Bay, Puerto Rico. Biogeography Branch, Center for Coastal Monitoring and Assessment, National Centers for Coastal Ocean Science, National Ocean Service, NOAA. (Online) <http://ccma.nos.noaa.gov/products/biogeography/biomapper/biomapper.html?id=JobosBay> (Accessed 17 February 2011).

Costa, B.M., L.J. Bauer, T.A. Battista, P.W. Mueller and M.E. Monaco. 2009. Moderate-Depth Benthic Habitats of St. John, U.S. Virgin Islands. NOAA Technical Memorandum NOS NCCOS 105. Silver Spring, MD. 57 pp.

Denbigh, P.N. 1989. Swath Bathymetry: Principles of Operation and an Analysis of Errors. IEEE Journal of Oceanic Engineering 14(4): 289-298.

Department of Natural and Environmental Resources (DNER). 2002. Jobos Bay Estuarine Profile: A National Estuarine Research Reserve. Puerto Rico DNER and National Oceanic and Atmospheric Administration, Office of Ocean and Coastal Resource Management, Estuarine Reserve Division. 107 pp.

Fonseca, L. and B. Calder. 2005. Geocoder: an efficient backscatter map constructor. Proceedings of the U.S. Hydrographic Conference 2005. San Diego, CA.

García-Sais, J., R. Appeldoorn, T. Battista, L. Bauer, A. Bruckner, C. Caldow, L. Carrubba, J. Corredor, E. Diaz, C. Lilyestrom, G. García-Moliner, E. Hernández-Delgado, C. Menza, J. Morell, A. Pait, J. Sabater, E. Weil, E. Williams, and S. Williams. 2008. The State of Coral Reef Ecosystems of Puerto Rico. pp. 75-116. In: J.E. Waddell and A.M. Clarke (eds.). The State of Coral Reef Ecosystems of the United States and Pacific Freely Associated States: 2008. NOAA Technical Memorandum NOS NCCOS 73. Silver Spring, MD. 569 pp.

Gostnell, K. 2005. Efficacy of an Interferometric Sonar for Hydrographic Surveying: Do Interferometers Warrant an In-Depth Examination? The Hydrographic Journal 118: 17-24.

Hotelling, H. 1933. Analysis of a complex of statistical variables into principal components. The Journal of Educational Psychology 24(6): 417-441.

Jenness, J. 2002. ArcView 3.x extension: Surface Areas and Ratios from Elevation Grid v1.2. (Online) http://www.jennessent.com/arcview/surface_areas.htm (Accessed 17 February 2011).

Jenness, J. 2004. Calculating landscape surface area from digital elevation models. Wildlife Society Bulletin 32: 829-839.

Kendall, M.S., C.R. Kruer, K.R. Buja, J.D. Christensen, M. Finkbeiner, R.A. Warner, and M.E. Monaco. 2001. Methods Used to Map the Benthic Habitats of Puerto Rico and the U.S. Virgin Islands. NOAA Technical Memorandum NOS NCCOS CCMA 152. Silver Spring, MD. 46 pp.

Kendall, M.S., O.P. Jensen, C. Alexander, D. Field, G. McFall, R. Bohne, and M.E. Monaco. 2005. Benthic Mapping Using Sonar, Video Transects, and an Innovative Approach to Accuracy Assessment: A Characterization of Bottom Features in the Georgia Bight. Journal of Coastal Research 21(6): 1154-1165.

Kendall, M.S. and T. Miller. 2008. The Influence of Thematic and Spatial Resolution on Maps of a Coral Reef Ecosystem. Marine Geodesy 31: 75-102.

Kostylev, V.E., B.J. Todd G.B.J. Fader, R.C. Courtney, G.D.M. Cameron, and R.A. Pickrill. 2001. Benthic habitat mapping on the Scotian Shelf based on multibeam bathymetry, surficial geology and sea floor photographs. Marine Ecology Progress Series 219: 121-137.

Pearson, K. 1901. On lines and planes of closest fit to systems of points in space. Philosophical Magazine Series 6. 2:11, 559-572.

Pittman, S.J., S.D. Hile, C.F.G. Jeffrey, R. Clark, K. Woody, B.D. Herlach, C. Caldow, M.E. Monaco, R. Appeldoorn. (2010). Coral reef ecosystems of Reserva Natural La Parguera (Puerto Rico): Spatial and temporal patterns in fish and benthic communities (2001-2007). NOAA Technical Memorandum NOS NCCOS 107. Silver Spring, MD. 202 pp.

Prada, M.C., R.S. Appeldoorn, and J.A. Rivera. 2008. Improving Coral Reef Habitat Mapping of the Puerto Rico Insular Shelf Using Side Scan Sonar. *Marine Geodesy*. 31: 49-73.

Wentworth, C.K. 1922. A scale of grad and class terms for clastic sediments. *Journal of Geology* 30(5): 377-392.

Wright, D.J., E.R. Lundblad, E.M. Larkin, R.W. Rinehart, J. Murphy, L. Cary-Kothera, and K. Draganov. 2005. Arc-GIS Benthic Terrain Modeler (BTM). Corvallis, Oregon.

Zitello, A.G., L.J. Bauer, T.A. Battista, P.W. Mueller, M.S. Kendall and M.E. Monaco. 2009. Shallow-Water Benthic Habitats of St. John, U.S. Virgin Islands. NOAA Technical Memorandum NOS NCCOS 96. Silver Spring, MD. 53 pp.

Chapter 3



Baseline Characterization of Fish Communities, Associated Benthic Habitats and Marine Debris of Jobos Bay

Laurie Bauer^{1,2,3}, Christopher F.G. Jeffrey^{1,2} and Kimberly Roberson¹

3.1. INTRODUCTION

The Jobos Bay marine ecosystem is comprised of a complex mosaic of habitats, including mangrove, seagrass beds, and coral reefs that span both subtidal and intertidal areas (Chapter 2). This habitat complexity is most evident in the central portion of the bay. An extensive network of mangroves is present, both as basin and fringe forests lining the shore, and as overwash islets and cays lining the southern edge of the bay (Figure 3.1). The remainder of the Bay is composed mostly of unconsolidated sediments while coral reef and hardbottom line the seaward edge of the cays.



Figure 3.1. Gray snapper (*Lutjanus griseus*) amongst mangrove roots. Photo: NOAA Center for Coastal Monitoring and Assessment (CCMA).

Despite Jobos Bay's ecological importance and designation as a NOAA National Estuarine Research Reserve (NERR), marine fish and benthic communities within and outside the Bay are not well characterized. In the 1970s, studies were conducted evaluating potential impacts of the Aguirre thermoelectrical power plant on the Bay's marine resources, including fish and benthic organisms (PRNC, 1975). More recent studies, which also focus on the assessment of marine communities under varying influence of the Aguirre plant, include García and Castro (1997) and García-Sais *et al.* (2003). As part of an overall profile of the Jobos Bay National Estuarine Research Reserve (JBNERR or Reserve), DNER (2002) provided a fish and invertebrate species inventory and highlighted the need for further inventory and monitoring.

As described in Chapter 1, an aim of the Conservation Effect and Conservation Project (CEAP) is to quantify the environmental benefits of conservation practices applied by landowners which are expected to reduce inputs of pollutants derived from land-based sources into Jobos Bay. In support of this broad effort, this assessment used established monitoring protocols (Pittman *et al.*, 2008, 2010) to spatially characterize fish assemblages, benthic communities, and marine debris across all habitats (reef/hardbottom, unconsolidated sediments, mangrove) within Jobos Bay that may be affected by changing land-use practices. Characterization of the Jobos Bay marine ecosystem will provide a foundation for evaluating expected changes in marine biota, benthic habitats, water quality, and biogeochemistry following implementation of agricultural conservation practices in the adjacent watershed. The data presented here will serve as a baseline to monitor future changes in benthic cover, population estimates and size spectra of fish over time. In addition, the data collected may be utilized by JBNERR for developing a spatially-explicit long-term monitoring program within the Reserve and for informing future management decisions.

¹ Center for Coastal Monitoring and Assessment, National Centers for Coastal Ocean Science, National Ocean Service, National Oceanic and Atmospheric Administration

² Consolidated Safety Services, Inc., under NOAA Contract No. DG133C07NC0616

³ Corresponding author: Laurie.Bauer@noaa.gov

3.2. METHODS

3.2.1. Site Selection

To assist in monitoring coral reef resources and to achieve a better understanding of fish-habitat relationships in the U.S. Caribbean, the Center for Coastal Monitoring and Assessment (CCMA) Biogeography Branch^A (BB) developed a fish and macroinvertebrate monitoring protocol to provide fishery-independent and size-structured survey data needed to comprehensively assess faunal populations and communities (Menza *et al.*, 2006). In addition, a complementary benthic composition survey was developed to support studies of fish-habitat relationships. These data collection activities are core components of CCMA's Coral Reef Ecosystem Monitoring (CREM) project, which are used to quantify long-term changes in fish species and assemblage diversity, abundance, biomass and size-structure in southwest Puerto Rico (Pittman *et al.*, 2010) and the Buck Island Reef National Monument (BIRNM) in St. Croix, U.S. Virgin Islands (USVI; Pittman *et al.*, 2008).

Using these established CREM protocols, field surveys were conducted from June 7-14, 2009 to characterize the fish communities and associated habitats in Jobos Bay. Sites were selected using a random-stratified survey design with habitat type (hardbottom, unconsolidated sediments, mangrove) and location (inshore, offshore, shelf, see Figure 3.2) as the main strata. These strata were chosen to ensure adequate spatial distribution of sites among all available habitats. The number of sites selected within each strata was determined based on logisitics and results from statistical analyses of variance (Menza *et al.*, 2006). As the new benthic habitat map produced in Chapter 2 was not completed at the time, a previous NOAA benthic habitat map (Kendall *et al.*, 2001) was used as the basis for site stratification, and draft classifications were created for portions of the offshore region that had been classified as "unknown" in the 2001 map. The "hardbottom" strata comprised bedrock, pavement, rubble, and coral reef, while the "unconsolidated sediments" stratum comprised seagrasses and macroalgal beds, as well as uncolonized sand and mud. The "mangrove" stratum comprised the seaward edge of mangrove

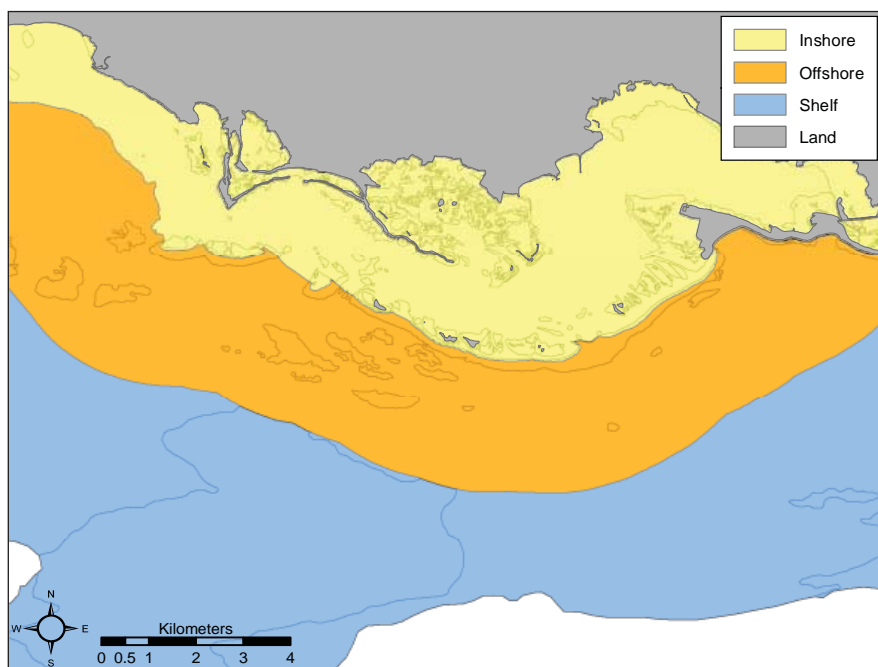


Figure 3.2. Inshore, offshore, and shelf regions used to stratify survey locations.



Figure 3.3. Diver collecting data on benthic habitat composition. Photo: NOAA CCMA

^A The Biogeography Branch is a part of National Oceanic and Atmospheric Administration (NOAA), National Ocean Service (NOS), National Centers for Coastal Ocean Science (NCCOS), Center for Coastal Monitoring and Assessment (CCMA).

habitat able to be surveyed with these visual underwater survey methods.

3.2.2. Field methods

The surveys of benthic features, fish communities, marine debris and macroinvertebrates were conducted within a 25x4 m transect (100 m²), along a random heading (Pittman *et al.*, 2008, 2010). Two divers performed the survey at each site. One diver was responsible for visual counts and size estimation of fish species. The second diver quantified benthic features, macroinvertebrates and marine debris (Figure 3.3).

Benthic habitat composition

The habitat diver first assigned an overall bottom type (*i.e.*, hardbottom, unconsolidated sediments, or mangrove) to each transect based on *in situ* observation. Data on the percent cover of abiotic and biotic composition at each survey site were recorded within five 1 m² quadrats placed randomly along the 25x4 m transect so that one quadrat falls within every 5 m interval along the transect. The quadrat was placed at each randomly chosen meter mark and systematically alternated from side to side along the transect tape (Figure 3.4). Several variables were measured to characterize benthic composition and structure (Table 3.1). The quadrat was divided into 100 smaller 10x10 cm squares with string (1 small square = 1% cover) to help the diver with estimation of percent cover. Percent cover was determined by looking at the quadrat from above and visually estimating percent cover in a two dimensional plane. The information recorded included:

1. Abiotic cover - the percent cover (to the nearest 1%) of four abiotic substrate categories (hardbottom, sand, rubble, fine sediments/silt) was estimated within each 1 m² quadrat. The maximum height of the hardbottom was also measured.

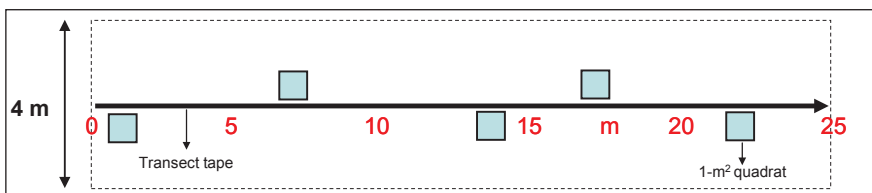


Figure 3.4. Schematic representation of the placement of the 1 m² quadrat along a 25 m transect tape during fish and benthic substrate surveys.

Table 3.1. Abiotic and biotic variables measured in five quadrats along fish transects in Jobos Bay.

Parameter	Measurements		
	Cover (%)	Height (cm)	Abundance (#)
Abiotic			
Hardbottom	X	X	
Sand	X		
Rubble	X		
Fine sediment/silt	X		
Rugosity			
Water depth			
Biotic			
Corals (by species)	X		
Macroalgae	X	X	
Seagrass (by species)	X	X	
Gorgonians			
Sea rods, whips and plumes	X	X	X
Sea fans	X	X	X
Encrusting form	X		
Sponges			
Barrel, tubes, rope, vase	X	X	X
Encrusting form	X		
Other benthic macrofauna			
Anemones and hydroids	X		X
Tunicates and zoanthids	X		
Mangroves			
Prop roots			X
Prop roots colonized by algae			X
Prop roots colonized by sponges			X
Prop roots colonized by other biota			X

2. Biotic cover - the percent cover (to the nearest 0.1%) of algae, seagrass, live corals, sponges, gorgonians, and other biota was estimated within each 1 m² quadrat. Taxa were identified to the following levels: stony coral-species, seagrass-species, algae-morphological group, sponge-morphological group, and gorgonians-morphological group. For stony and fire corals, the percentage of bleached coral and diseased/dead coral was estimated to the nearest 0.1 percent.
3. Maximum canopy height - the maximum canopy height of sponges, gorgonians, and soft algal groups was recorded to the nearest 1 cm in each quadrat.
4. Number of individuals - the number of individual upright sponges, gorgonians, non-encrusting anemones, and non-encrusting hydroids was recorded in each quadrat.
5. Rugosity – for hardbottom sites, rugosity was measured by placing a 6 m chain at two randomly selected positions, ensuring no overlap, along the 25 m belt transect. The chain was positioned along the centerline of the transect such that it followed the substrate's relief, and the straight-line horizontal distance covered by the chain was measured.

Mangrove habitat data

At mangrove sites, the survey was conducted close to the prop roots and as far into the mangroves as possible, up to 2 m and then out to the edge of the mangrove overhang such that the total area surveyed was still 100 m². In this case, some of the survey may necessarily fall on seagrass habitat. This is allowed as the mangrove habitat is defined as a transition zone habitat. In addition to the habitat data collected above, further mangrove data are collected including number of prop roots, number of prop roots colonized by algae, number of prop roots colonized by sponges and number of prop roots colonized by other biota (tunicates, anemones, zoanthids, *etc.*).

Macroinvertebrate counts

The habitat diver counted the abundance of spiny lobsters (*Panulirus argus*), long-spined urchins (*Diadema antillarum*), and the abundance/maturity of queen conchs (*Eustrombus gigas*) within the 25x4 m transect at each site. The maturity of each conch was determined by the presence (mature) or absence (immature) of a flared lip.

Fish census

Fish surveys were conducted along the 25x4 m transect (100 m²) using a fixed survey duration of 15 minutes regardless of habitat type or complexity. The number of individuals per species was recorded in 5 cm size class increments up to 35 cm using visual estimation of fork length. Individuals greater than 35 cm were recorded as an estimate of the actual fork length to the nearest centimeter.

Marine debris

The number and type of marine debris within the 100 m² transect were recorded. The size of marine debris and the area of habitat that it was affecting were estimated, as well as a note about any flora or fauna that were colonizing the debris item.

3.2.3. Data Analysis

Benthic Habitat

While many benthic variables were measured during the surveys, data analyses for this report focused primarily on describing differences among major habitat types and broad-scale spatial patterns in the percent cover of the sessile biotic components as described in Table 3.1. Multiple quadrat measurements within each site transect were averaged and cumulative coral species richness was calculated for each survey location. Domain-wide estimates of abiotic and biotic cover variables were

computed employing methods described by Cochran (1977) for a stratified sampling design (SAS v9.1, Proc SurveyMeans). In addition, data were plotted in ArcGIS (v9.3, ESRI) to examine broad spatial patterns in the benthic cover variables.

Fish Assemblages

A summary table of all species observed in this characterization was created (Appendix A, Table A.1). Domain-wide estimates for several metrics were computed employing methods described by Cochran (1977). Percent occurrence, mean density and biomass (per 100 m²) and corresponding standard errors (SE) were calculated for each species. Mean density and biomass were also calculated for each family and trophic group for the overall survey area. Trophic groups include piscivores, herbivores, invertivores, and zooplanktivores and were defined for each species based on diet information from Randall (1967). However, it is important to note that these groups are not mutually exclusive because many fish species can be classified into two or more of these groups based on diet. Biomass was calculated using published length-weight relationships based on the formula,

$$W = \alpha L^{\beta}$$

where L is length in centimeters and weight is in grams. The midpoint of each size class was used for L values, and the actual length was used for fish >35 cm. For fish in the 0-5 cm size class, 3 cm was used as the mid-point because we do not typically observe fish <1 cm). Values for the α and β coefficients were obtained from FishBase (Froese and Pauly, 2008). Biomass for species with no published length-weight relationships was calculated using terms for the closest congener with most similar morphology.

Species diversity was calculated using the Shannon Index (H'), a measure that incorporates both richness and evenness:

$$H' = \sum p_i (\log_e p_i)$$

where p_i is the relative abundance of each species.

Select variables (density, biomass, richness, and diversity) were compared among bottom type to characterize any potential differences related to major habitat type. As the assumptions of normality and homogeneity of variance were not met non-parametric Wilcoxon tests were used. When the overall test was significant, non-parametric multiple pairwise comparisons were used to determine whether pairs of habitats were significantly different (Zar, 2010). Data were plotted in ArcGIS to examine broad spatial patterns in the fish metrics.

In addition, select families and species of commercial and/or ecological interest were selected for further examination. For each species/family, a summary of the species distribution, mean density and biomass among strata, and size frequency is provided. Juveniles/subadults were identified based on length at maturity information provided by FishBase (Froese and Pauly, 2008), García-Cagide *et al.* (1994) and Ault *et al.* (2008). Fish less than the mean length at maturity were classified as juveniles/subadults. Where length at maturity was unknown, 1/3 of maximum size was used as a proxy as in Pittman *et al.* (2008, 2010).

Differences and similarities in species composition were examined using multivariate statistical techniques (Primer v.6, Clarke and Warwick, 2001). Data were square-root transformed prior to analysis, and one outlier site was removed due to extremely low abundance (one fish). Data were arranged in a species abundance by site data matrix, which was used to construct a triangular matrix of the percentage similarity in community composition between all pairs of sites using the Bray-Curtis Coefficient. The coefficient is a measure of how similar samples are to each other, ranging from

0% (complete dissimilarity) to 100% (complete similarity). Next, non-metric multidimensional scaling (nMDS) was used to place samples in a two-dimensional configuration such that the rank order of the distances between the samples agreed with the rank-order of the similarities from the Bray-Curtis matrix. Sites were coded by habitat strata for examination of visual patterns of between site similarity. These factors were also used to test for significant differences in similarity using Analysis of Similarities (ANOSIM), a multivariate, non-parametric version of ANOVA. Finally, similarity percentages (SIMPER) were calculated to identify the species that contributed most to the differences between strata.

3.3. RESULTS AND DISCUSSION

Although 72 sites were originally proposed, several sites were not surveyed due to very low visibility. Exceptionally poor visibility prohibited all planned surveys (eight total) in Rincón Bay, the northwest portion of the study area. Visibility was also poor and prohibited most surveys within the eastern portion of central Jobos Bay. In addition, one site at a dock in the landward reaches of Mar Negro was not surveyed due to water quality concerns. A total of 45 sites were surveyed: 20 on hardbottom, 15 on unconsolidated sediments, and 10 in mangrove (Figure 3.5). Only four sites fell within the boundaries of JBNERR.

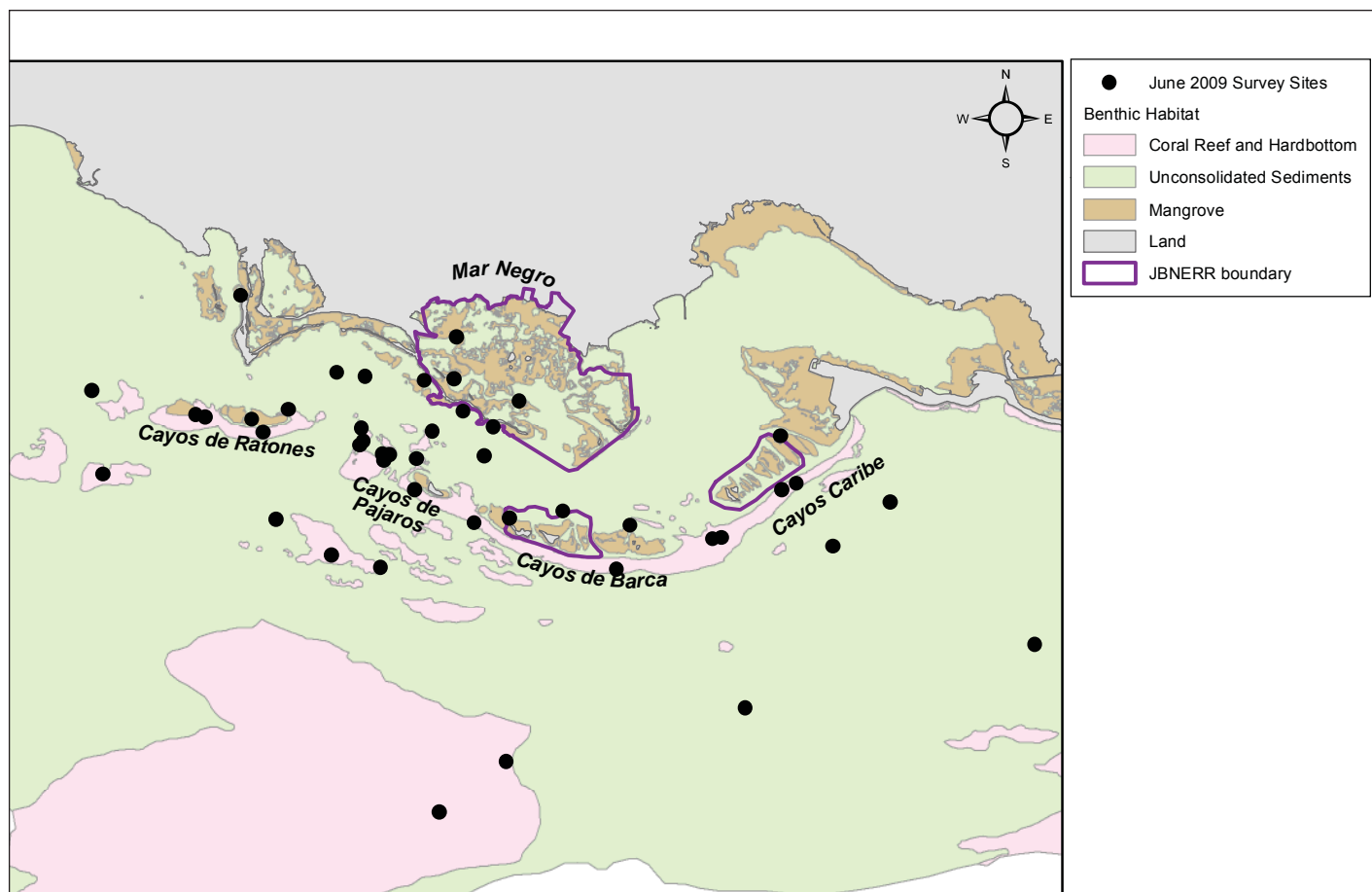


Figure 3.5. Benthic habitat strata and site locations of the June 2009 survey of benthic habitat composition, fish communities, and marine debris. The boundaries of the Jobos Bay National Estuarine Research Reserve (JBNERR) are shown for reference.

3.3.1. Benthic habitat

Abiotic composition

Five sites stratified as hardbottom surveys were designated as unconsolidated sediment by the diver, and were subsequently grouped with the unconsolidated sediment surveys in the data analysis. This likely occurred due to the heterogeneity of some hardbottom structure types (e.g., aggregated patch reefs, pavement with sand channels).

As expected, sites conducted on hardbottom habitat were predominantly composed of hardbottom substrate, with smaller amounts of rubble, sand and fine sediment (Figures 3.6a). Many unconsolidated sediment sites were dominated by fine sediment, while a few locations in the west-central portion of the bay, as well as those located furthest offshore, were composed of sand and rubble substrates (Figures 3.6b). Most mangrove sites were also characterized by fine sediments, although a few locations were more typified by sand and rubble (Figures 3.6c).

Biotic composition

On hardbottom sites, turf algae accounted for the highest mean percent cover ($36.3 \pm 4.8\%$), followed by macroalgae ($15.3 \pm 2.6\%$), hard (scleractinian) corals ($6.5 \pm 1.2\%$), sponges ($4.4 \pm 1.0\%$), gorgonians ($4.4 \pm 0.9\%$), and zoanthids ($4.4 \pm 3.3\%$; Figure 3.7a). Other algae groups included crustose coralline algae (CCA; $3.5 \pm 1.3\%$), cyanobacteria and filamentous algae ($2.2 \pm 1.1\%$), and rhodoliths ($0.5 \pm 0.5\%$). Small amounts of the hydroid *Millepora* spp. (fire coral), were also present ($0.2 \pm 0.1\%$). Bare, uncolonized substrate averaged $28.7 \pm 5.3\%$. Rugosity ranged from 0.01-0.42 and averaged 0.22 (± 0.02). Sites with highest rugosity were typically located on sloping fore reef seaward of the cays (Figure 3.8).

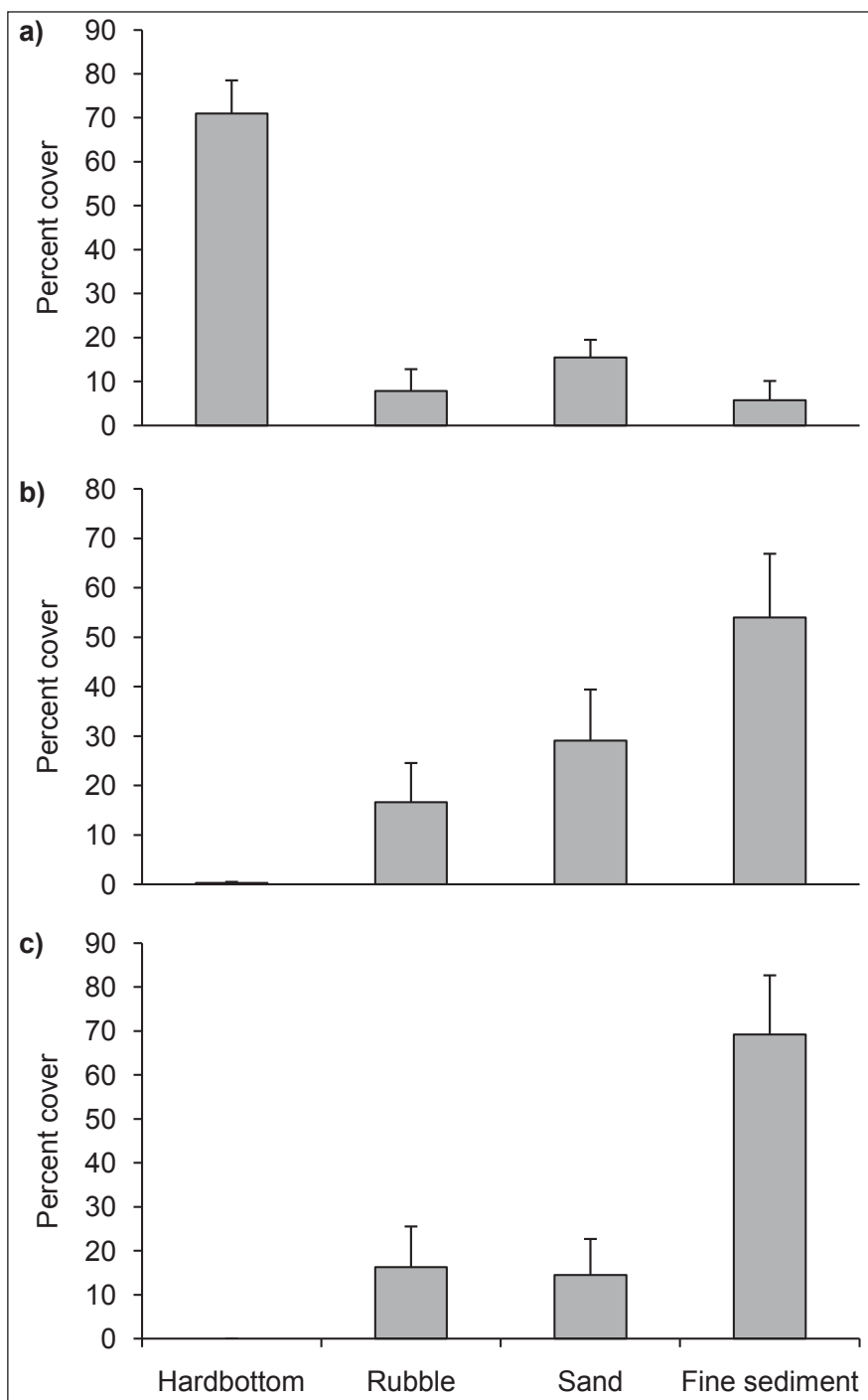


Figure 3.6. Mean (\pm SE) percent cover of abiotic substrate across a) hardbottom, b) unconsolidated sediment, and c) mangrove sites.

Unconsolidated sediment sites were characterized by an assemblage of submerged aquatic vegetation and low levels of benthic fauna. Macroalgae accounted for the highest mean percent cover ($11.6 \pm 6.4\%$), followed by seagrass ($6.9 \pm 3.0\%$), turf algae ($5.8 \pm 4.4\%$), rhodoliths ($4.5 \pm 4.1\%$), CCA ($3.0 \pm 2.7\%$), and cyanobacteria/filamentous algae ($1.8 \pm 1.2\%$; Figure 3.7b). The average amount of bare substrate ($65.8 \pm 8.5\%$) was considerably higher than on hardbottom.

The majority of the substrate in mangrove habitat ($78.9 \pm 8.4\%$) was characterized as uncolonized, with variable amounts of cyanobacteria and filamentous algae ($12.8 \pm 7.6\%$), turf algae ($4.4 \pm 4.4\%$), and macroalgae ($3.3 \pm 1.6\%$; Figure 3.7c). Seagrass cover was generally low, averaging less than one percent.

Live scleractinian coral cover varied widely across the survey area (Figure 3.9), ranging from 0-21.8%. Sites inside the Bay tended to be characterized by low cover, while aggregate reef adjacent to the cays was characterized by higher than average coral cover. However, coral cover only exceeded 10% in four surveys. The site with the highest total cover was located on an offshore patch of hardbottom southwest of Cayos de Ratones. Recent work by García and Castro (1997) and García-Sais *et al.* (2003) also detected low coral cover in the inshore areas but upwards of 15-20% on reefs offshore of Cayos Caribe and Cayos de Barca.

The coral community observed in the study was represented by 24 species, 22 of which were observed on hardbottom. Species richness ranged from 0-13 species at individual sites. The spatial pattern was similar to that of that of live coral cover- sites within the bay tended to be characterized by low species richness, while aggregate reef adjacent to the cays and offshore hardbottom tended to have higher richness (Figure 3.10). The most abundant coral was *Porites astreoides* (mustard hill coral), followed by *Siderastrea siderea* (massive starlet coral), *Montastraea cavernosa* (great star coral), and the *Montastraea annularis* complex (boulder star coral; Figure 3.11). Two additional species not included in Figure 3.11, *Manicina areolata* (rose coral) and *Oculina diffusa* (diffuse ivory bush coral), were observed only on unconsolidated sediments. Neither *Acropora palmata* (elkhorn coral) or *Acropora cervicornis* (staghorn coral), both of which are listed as threatened under the Endangered Species Act (ESA), were observed in any survey quadrat; however *A. palmata* and *A. cervicornis* were observed outside survey quadrats at one and two sites, respectively. Both sites were located along the fore reef of Cayos Caribe.

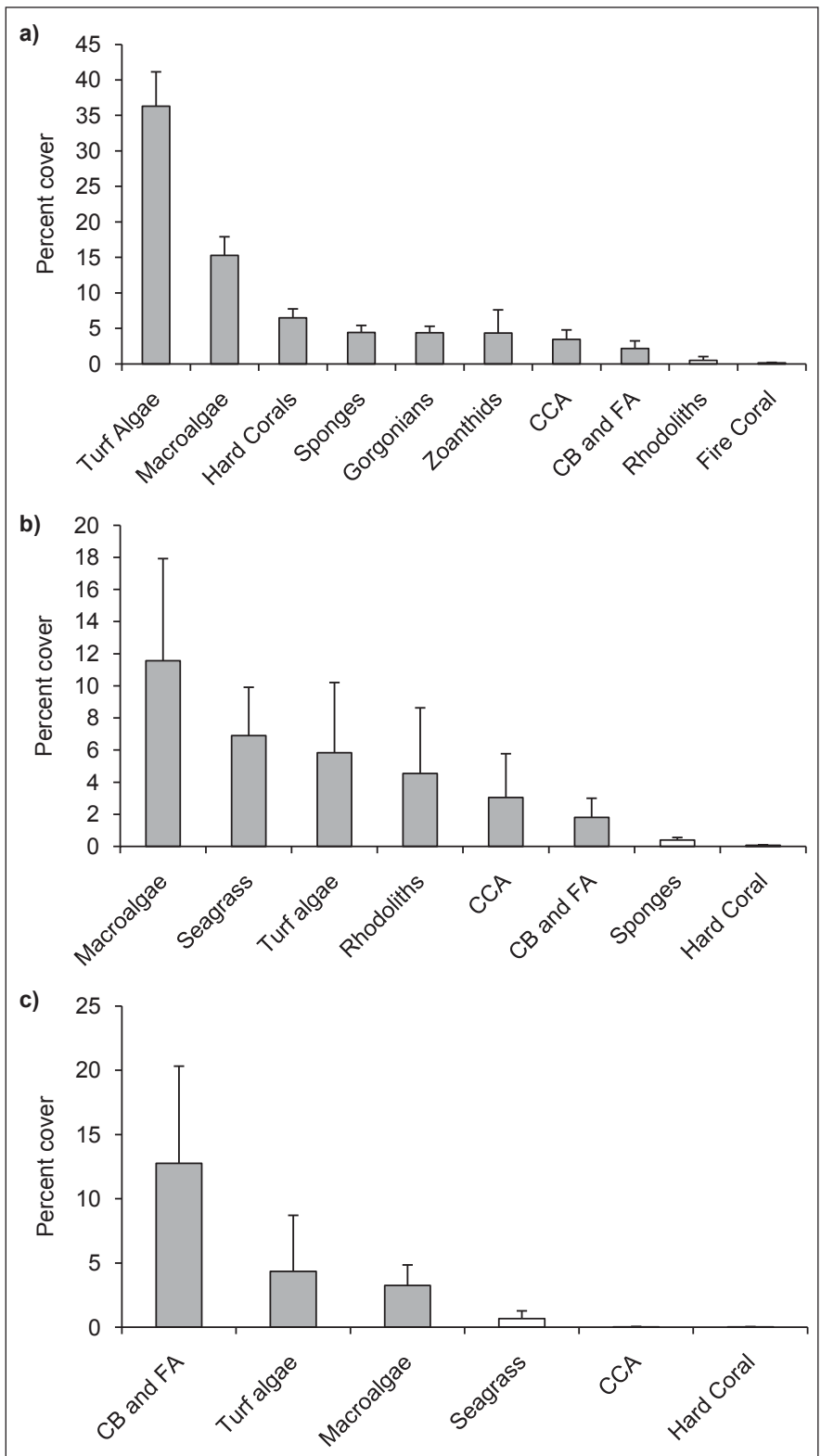


Figure 3.7. Mean (\pm SE) percent cover for key components of the benthic community across a) hardbottom, b) unconsolidated sediments, and c) mangrove sites.

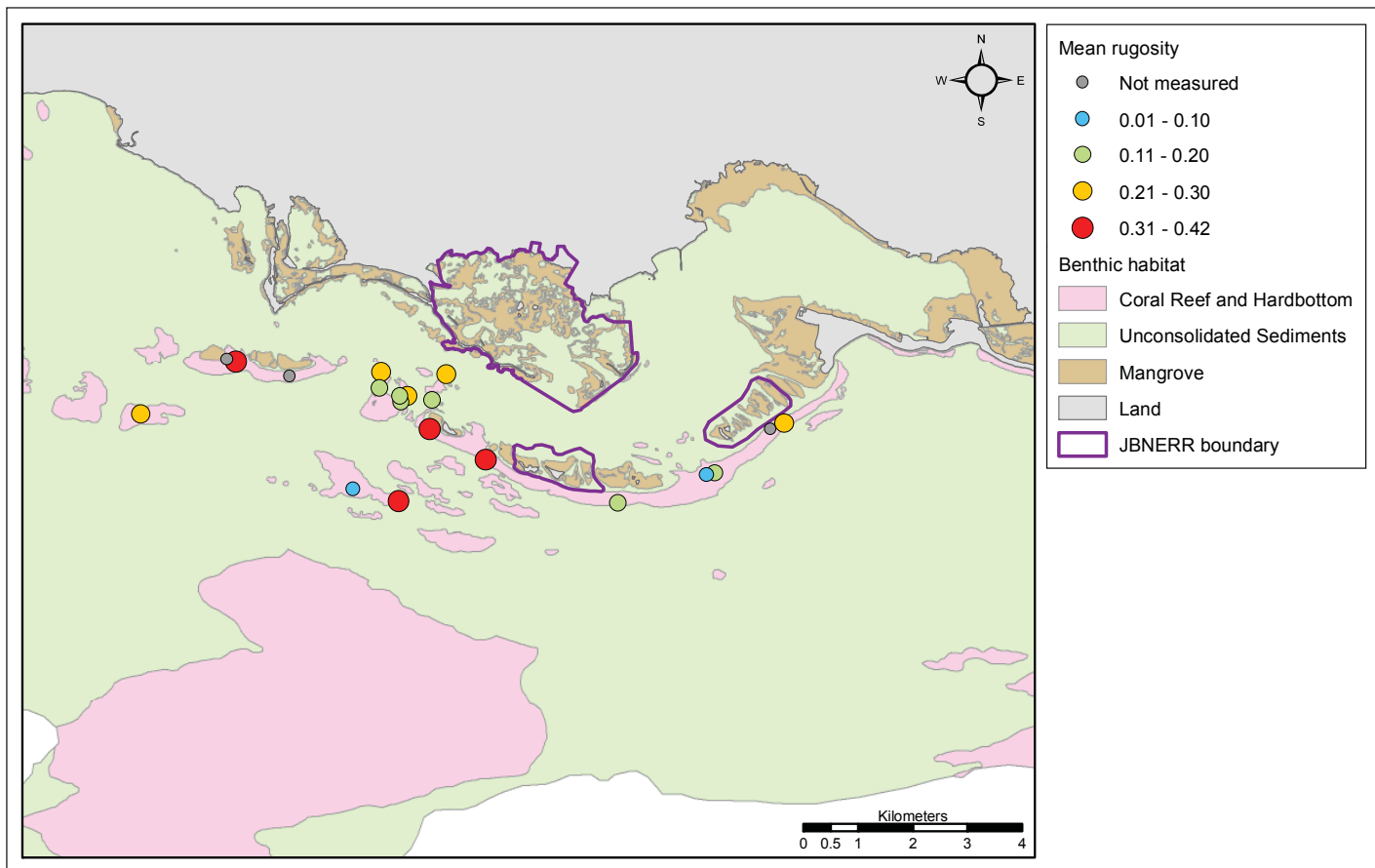


Figure 3.8. Mean rugosity (hardbottom sites only).

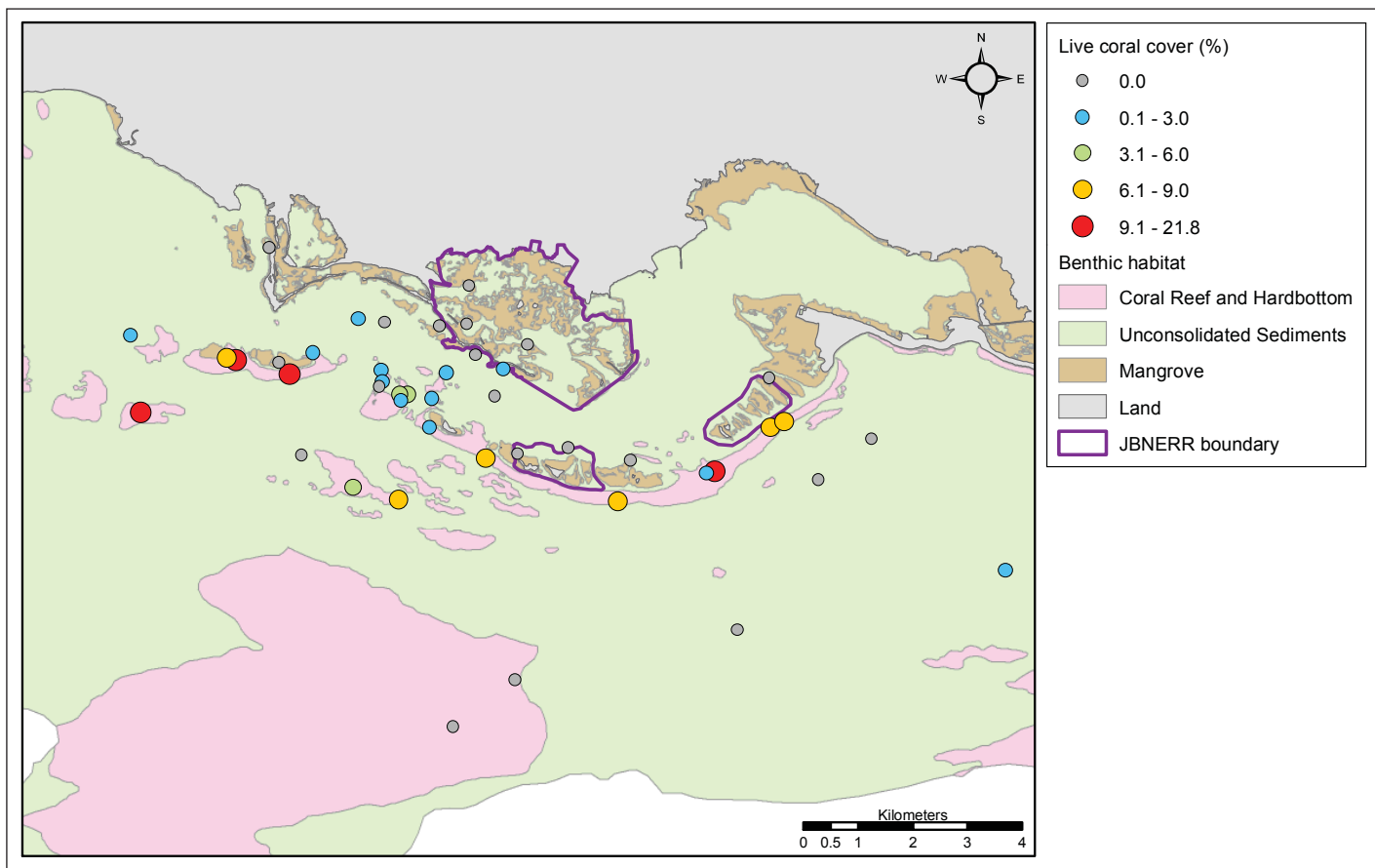


Figure 3.9. Percent live coral cover.

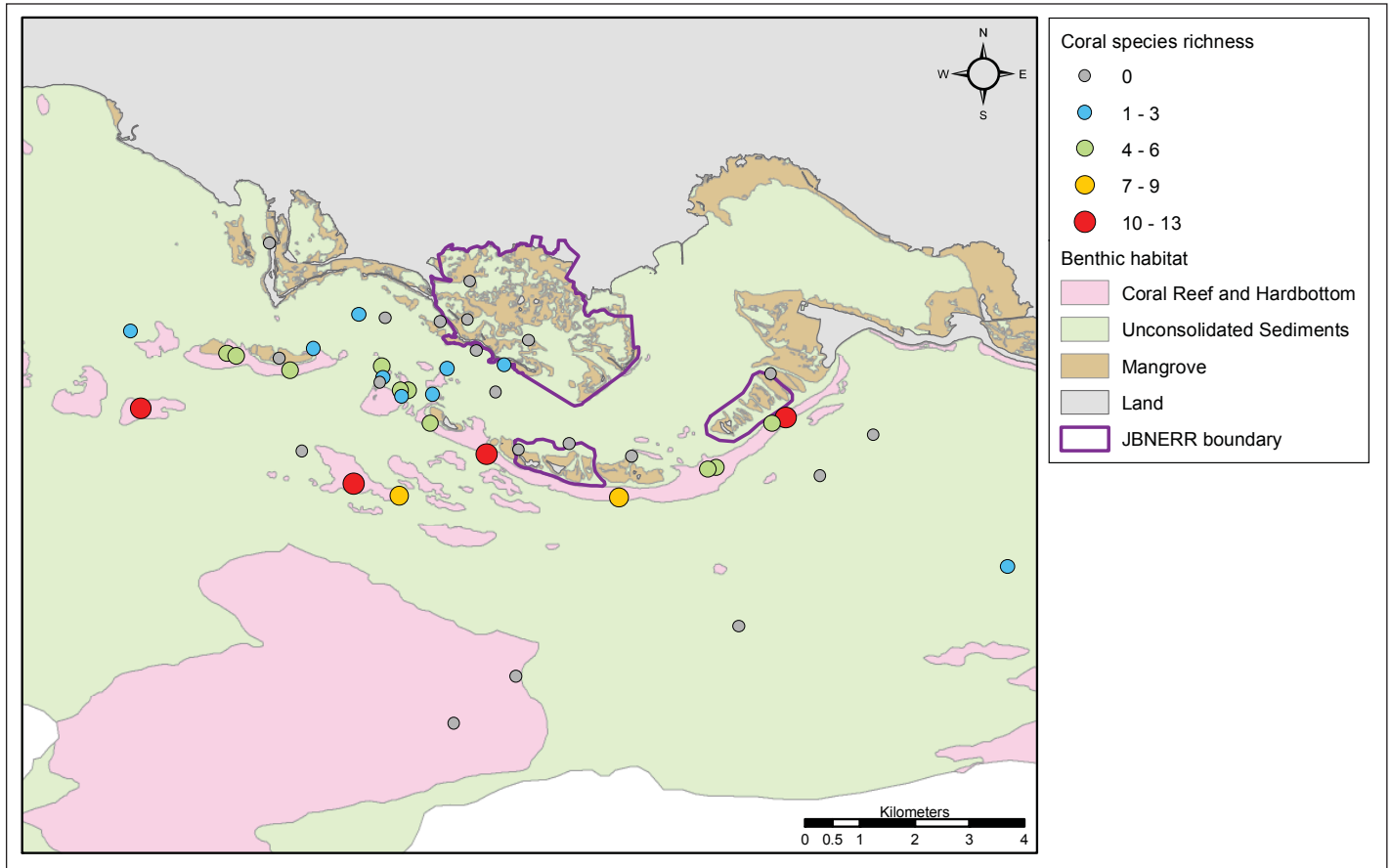


Figure 3.10. Coral species richness.

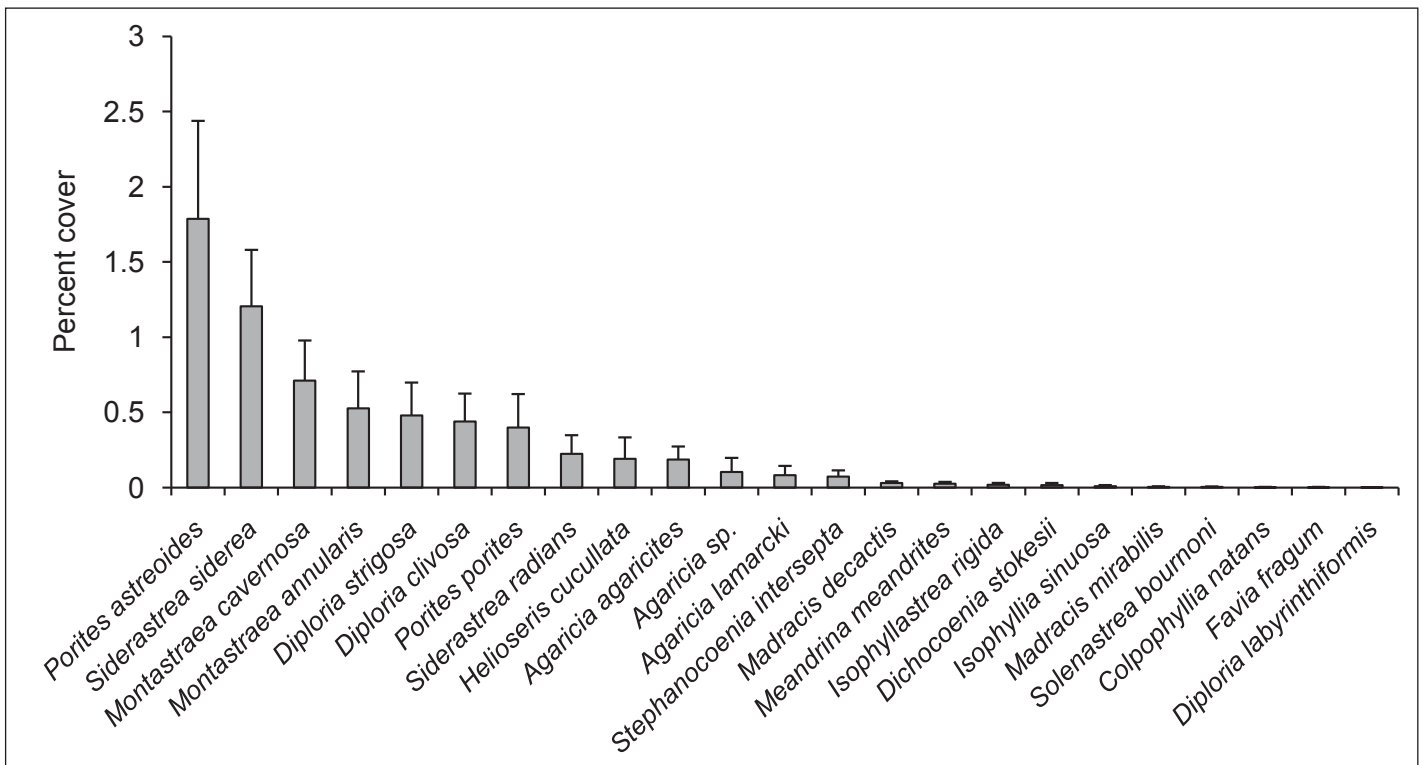


Figure 3.11. Mean (\pm SE) percent cover of coral species across hardbottom sites. Species identified as *Montastraea annularis* refer to the *M. annularis* complex.

Gorgonian cover ranged from 0-12.3% and exhibited similar spatial patterns to hard coral cover (Figure 3.12). Sites on aggregate reef adjacent to the cays, as well as one location farther offshore, exhibited the highest gorgonian cover. Encrusting gorgonians were the dominant gorgonian type on hardbottom in terms of percent cover, averaging $2.2 \pm 0.6\%$, followed by sea plumes/rods/whips ($1.6 \pm 0.5\%$), and sea fans ($0.6 \pm 0.2\%$). Sea plumes/rods/whips were also more abundant than sea fans in the average number of individuals/m² ($2.0 \pm 0.5/\text{m}^2$ vs. $0.6 \pm 0.3/\text{m}^2$).

Sponge cover ranged from 0-15.5% and did not exhibit distinctive spatial patterns (Figure 3.13). Sites with percent cover >10% were located on hardbottom near and south of Cayos de Pájaros. Barrel/tube/vase sponges accounted for the majority of percent cover on hardbottom ($3.1 \pm 0.9\%$), while encrusting sponge comprised a smaller component of the sponge community ($1.3 \pm 0.4\%$). This pattern was also true for unconsolidated sediment sites, although both sponge morphologies were present in much smaller amounts (barrel/tube/vase = $0.4 \pm 0.2\%$; encrusting = 0.02 ± 0.01).

Macroalgae cover ranged from 0-95.6% and was distributed across all areas (Figure 3.14). The site with the highest macroalgal cover was located in unconsolidated sediments within the lagoon, but overall macroalgal cover was generally greater on hardbottom than unconsolidated sediments and mangrove. Turf algae was a ubiquitous component of the reef community and was recorded in all but one hardbottom survey (Figure 3.15). CCA was typically present in small amounts but higher values were present in surveys near Cayos de Ratones and at the study site furthest offshore (Figure 3.16). The site furthest from shore was also characterized by cover of filamentous algae/cyanobacteria >15% (Figure 3.17). This category was characterized by wide variations in cover, ranging from 0-76.6%. Higher cover was particularly associated with mangrove surveys within Jobos Bay (Figure 3.17).

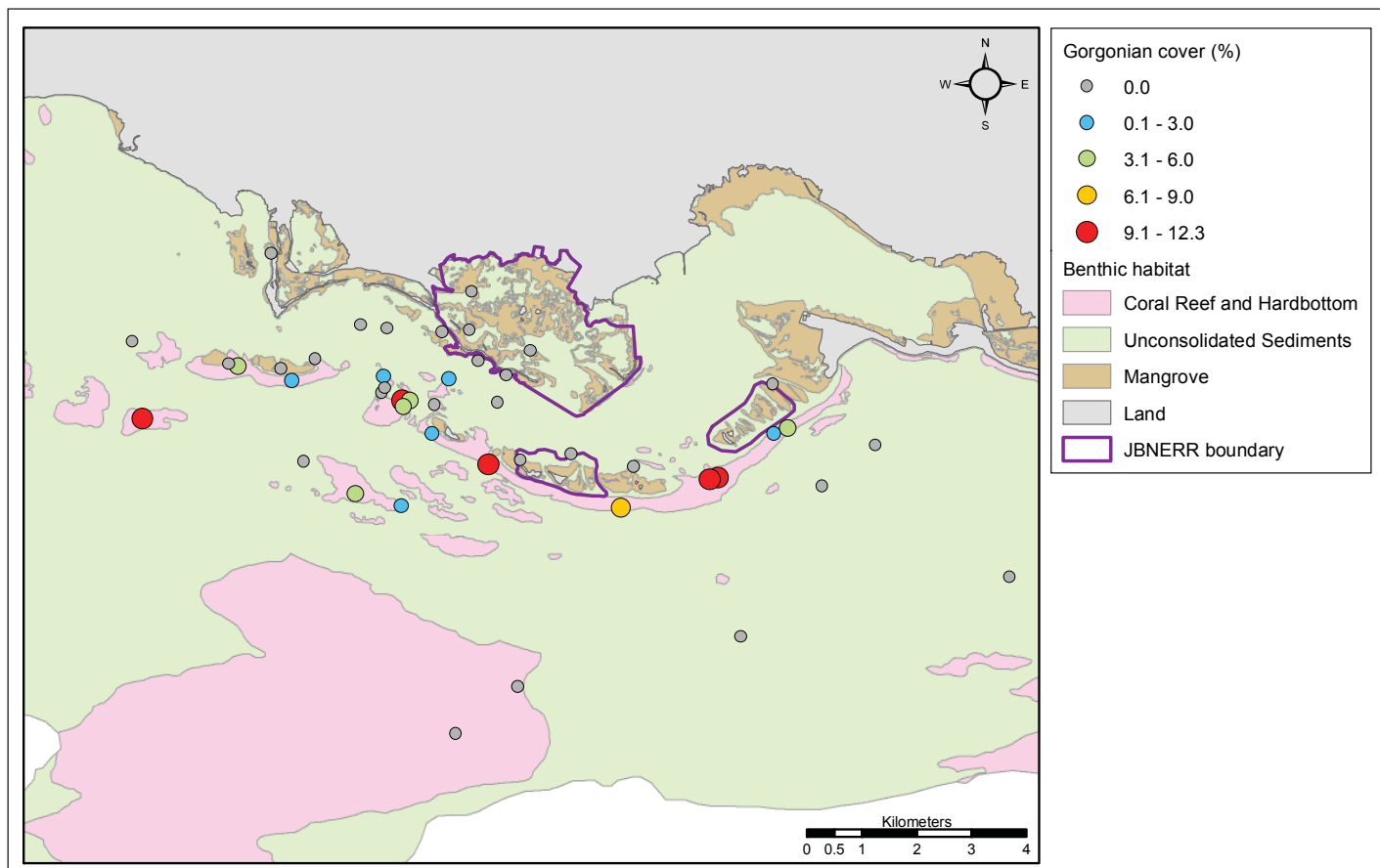


Figure 3.12. Percent gorgonian cover.

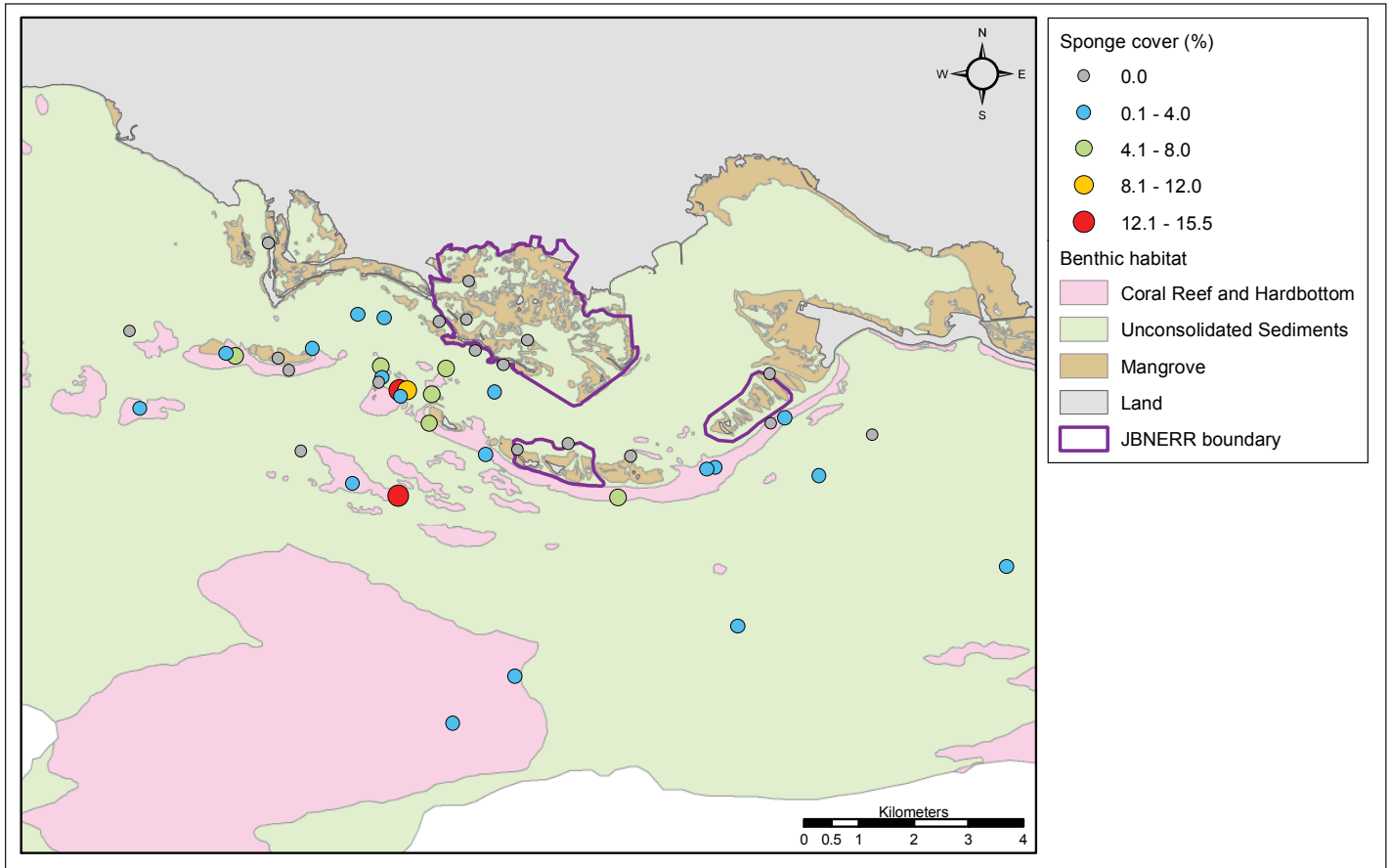


Figure 3.13. Percent sponge cover.

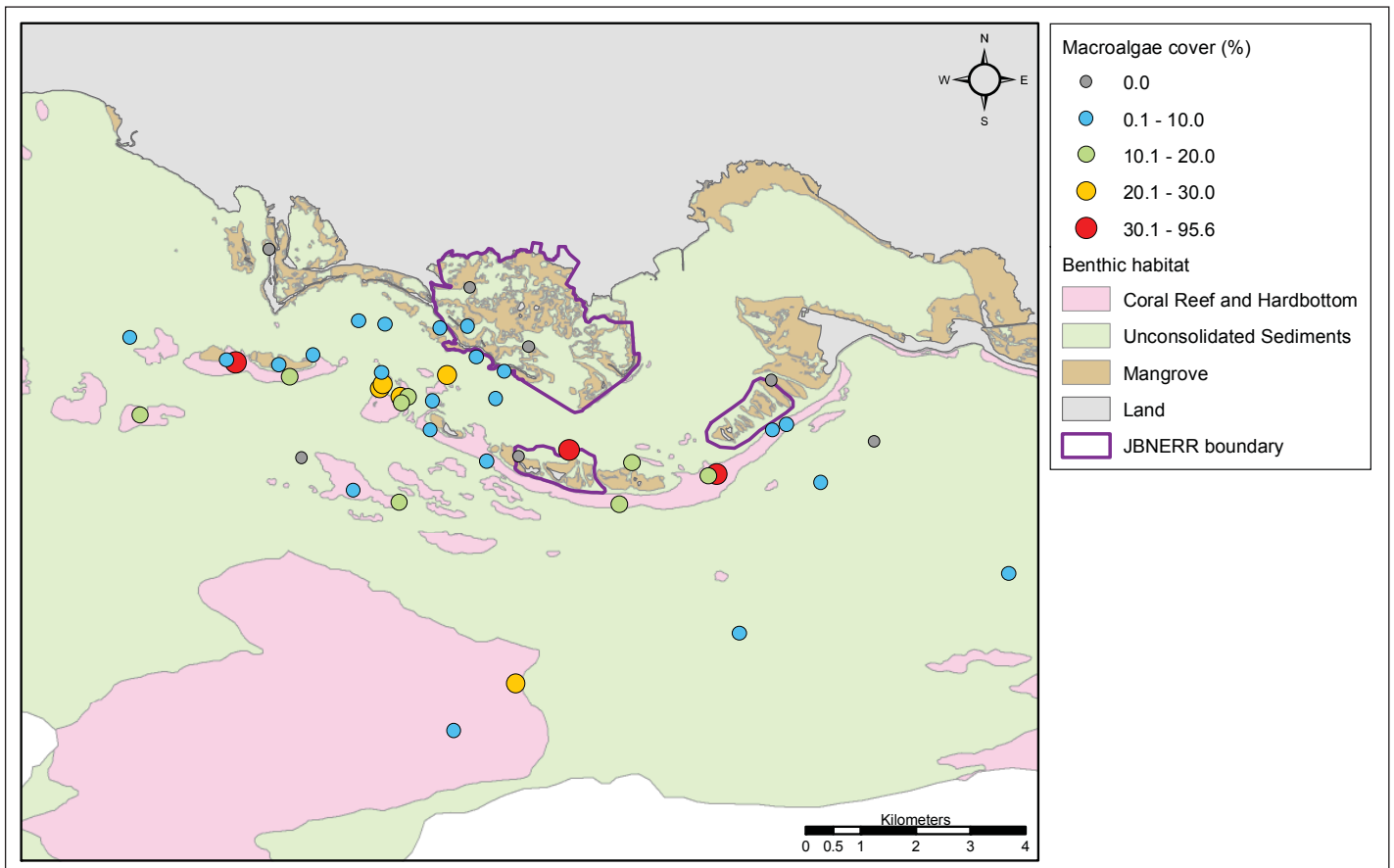


Figure 3.14. Percent macroalgae cover.

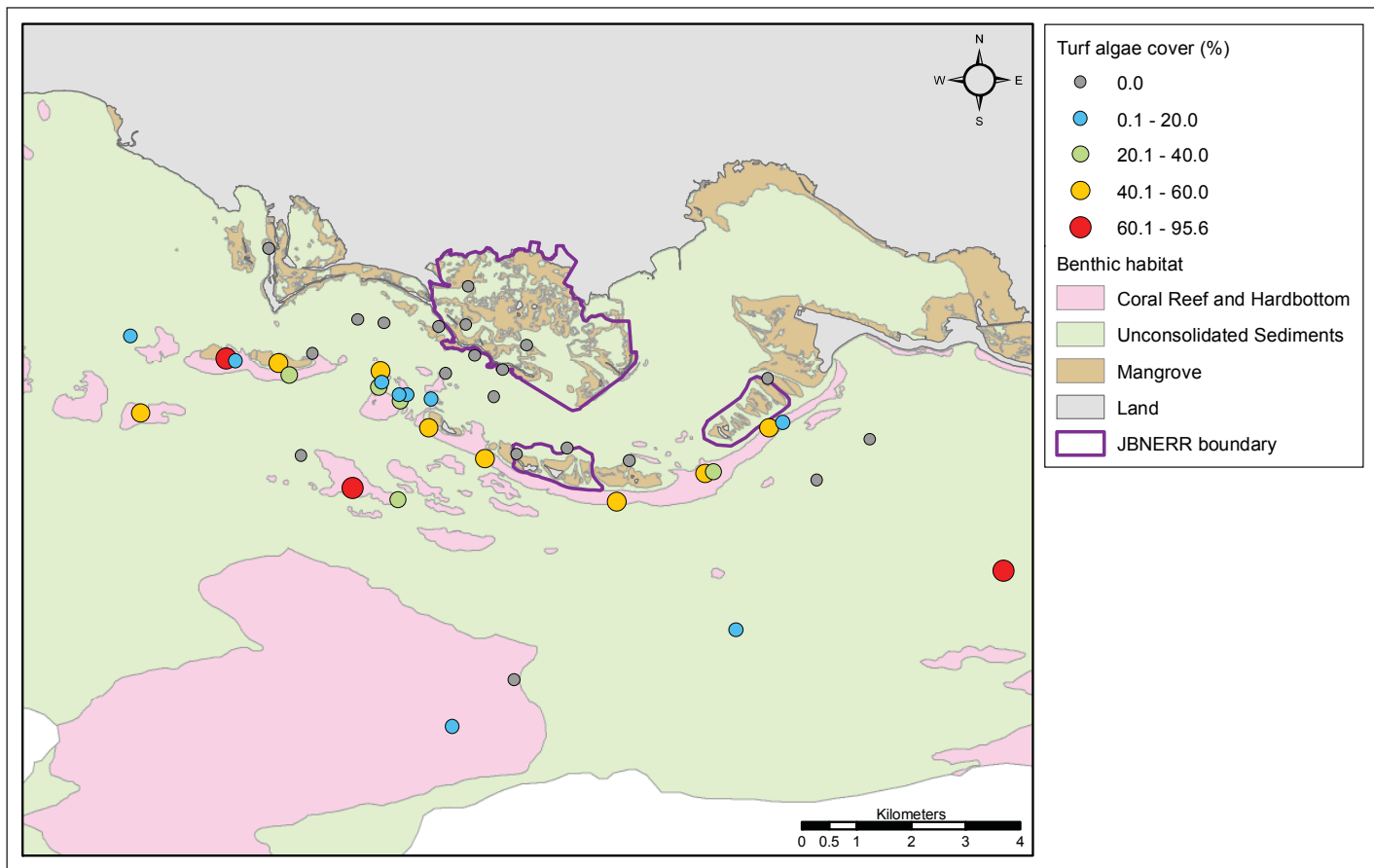


Figure 3.15. Percent turf algae cover.

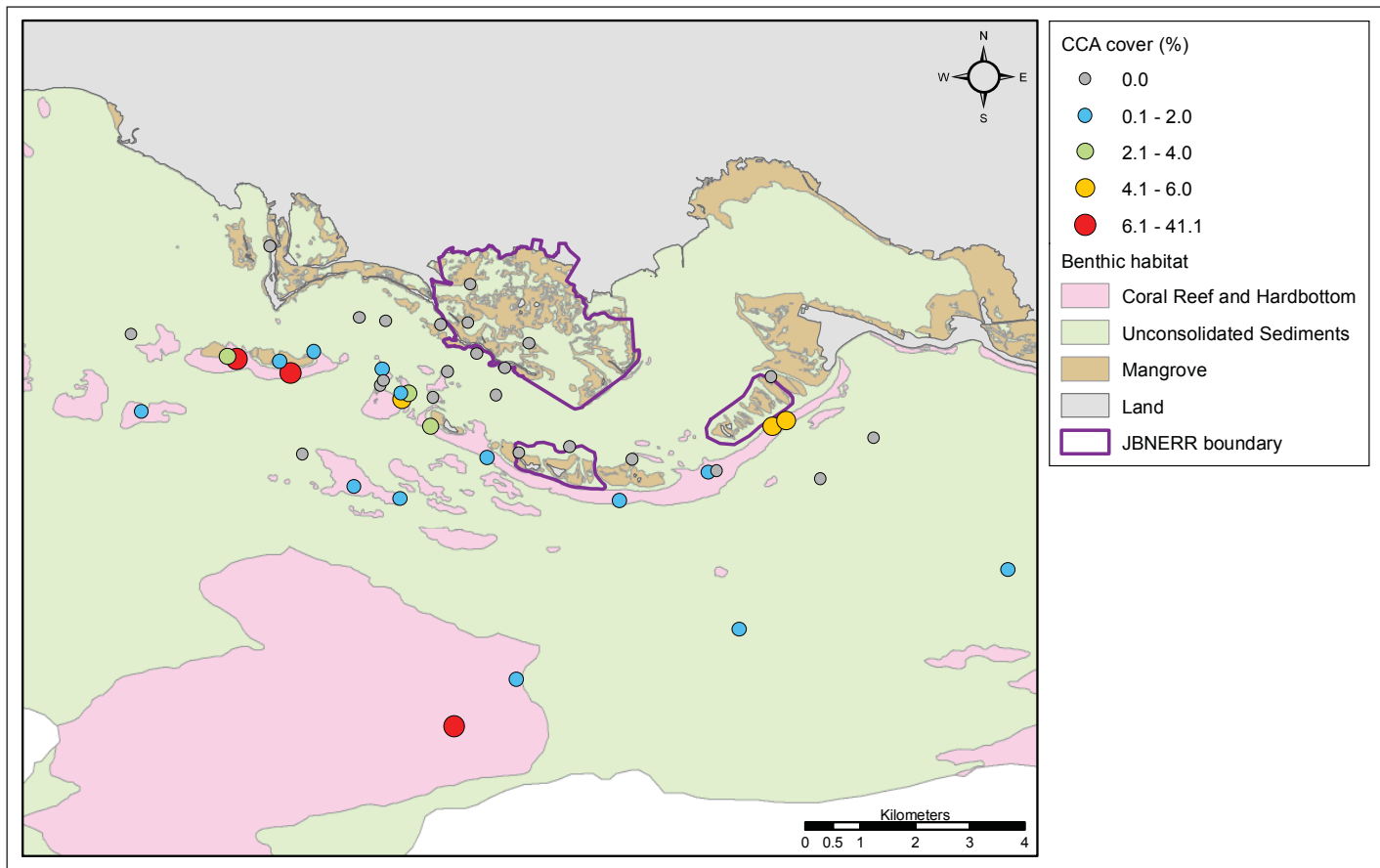


Figure 3.16. Percent crustose coralline algae (CCA).

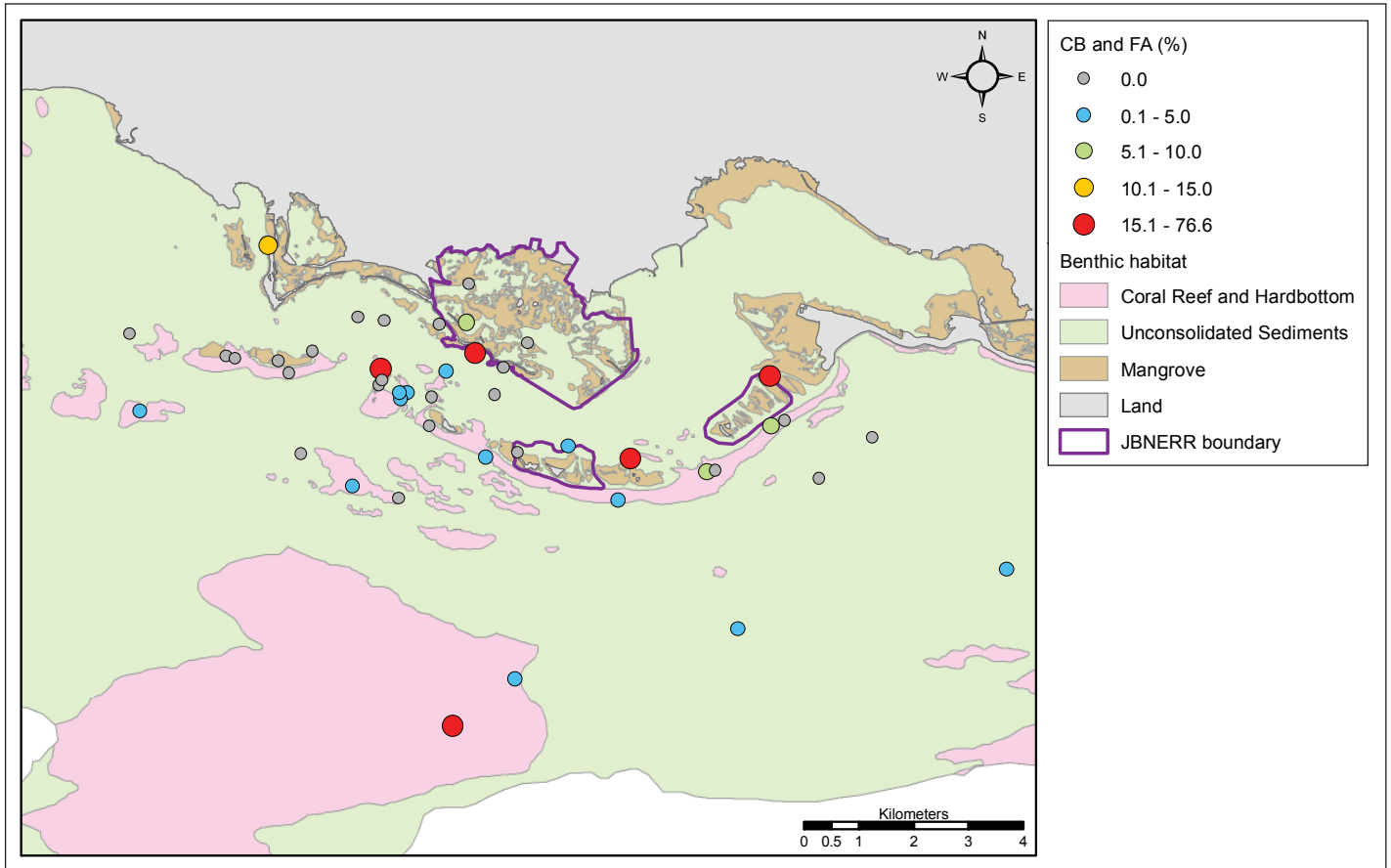


Figure 3.17. Percent cover of filamentous algae (FA) / cyanobacteria (CB).

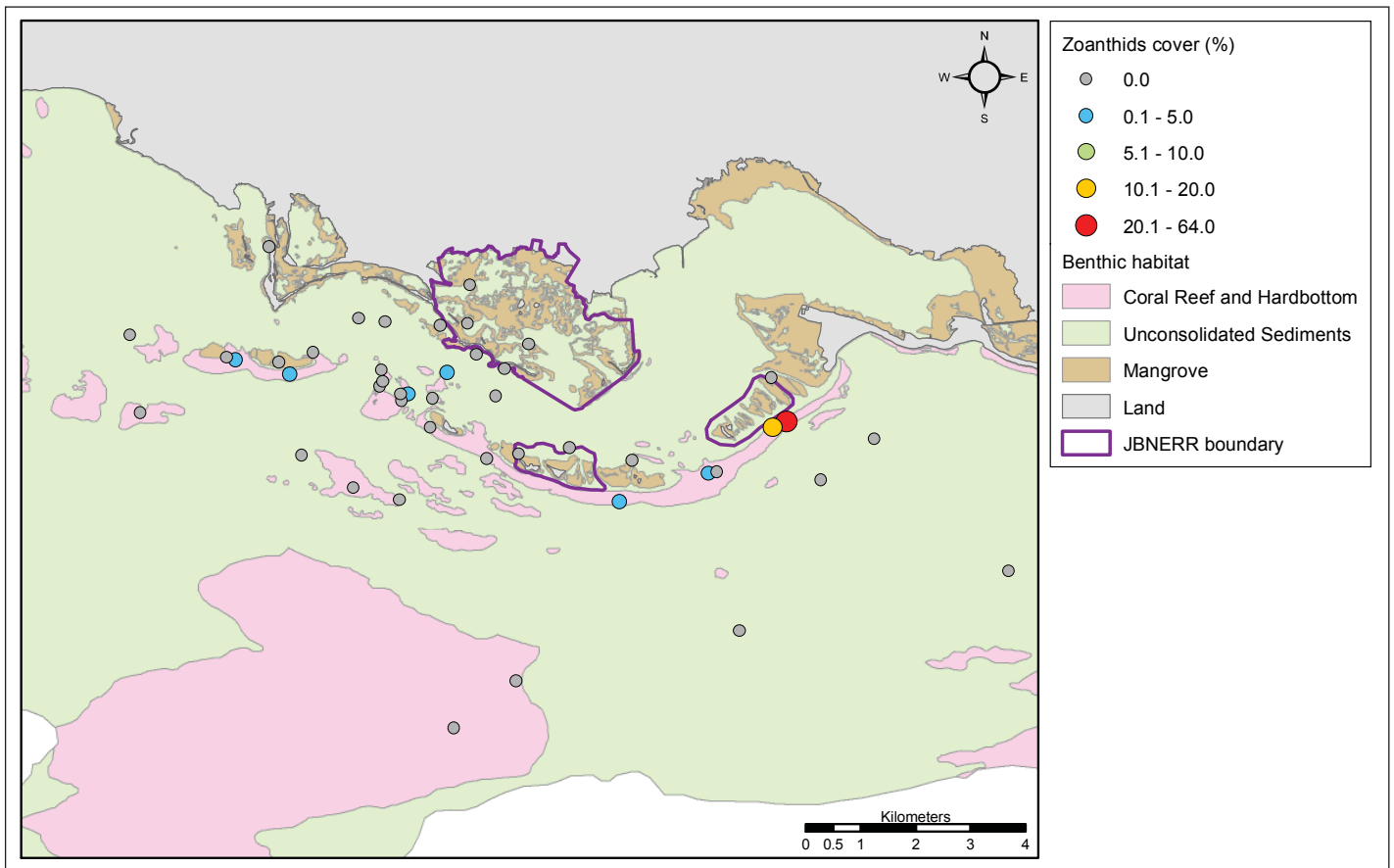


Figure 3.18. Percent cover of zoanthids.

Other benthic taxa (anemones, tunicates, zoanths) were recorded infrequently and generally in small amounts. Highest percent cover of zoanths was present on reef adjacent to Cayos Caribe (Figure 3.18). In one survey, zoanths covered 64% of the substrate (Figure 3.19).

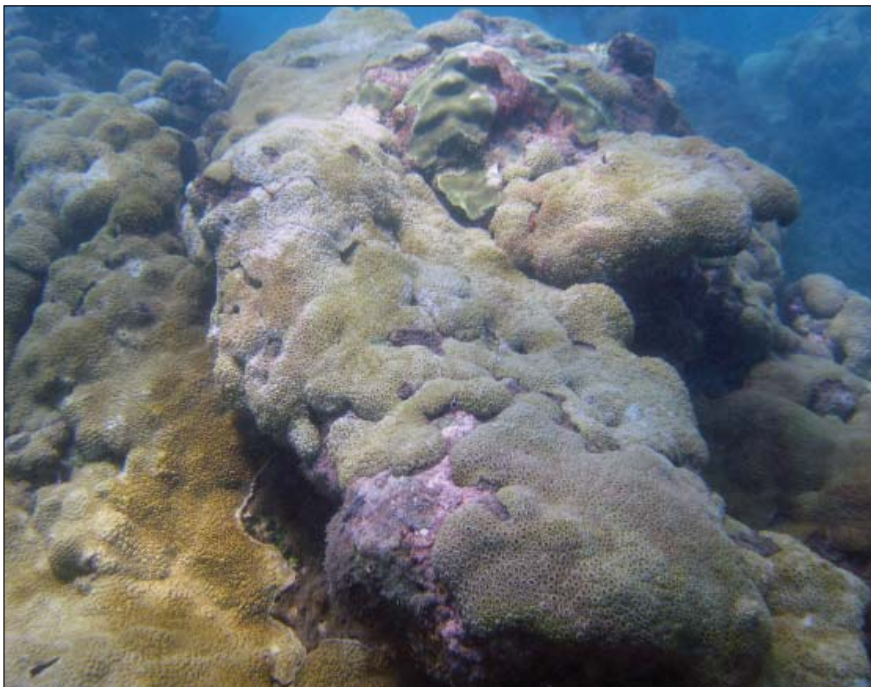


Figure 3.19. Zoanthid cover. Photo: NOAA CCMA.

Seagrass was present primarily within Jobos Bay across unconsolidated sediment habitat and a limited number of mangrove surveys (Figure 3.20). *Thalassia testudinum* accounted for the highest mean percent cover on unconsolidated sediments, followed by *Halophila decipiens* and *Syringodium filiforme* (Figure 3.21). A fourth seagrass species, *Halodule wrightii*^B, was uncommon. In mangrove habitat, the only species recorded was *T. testudinum*.

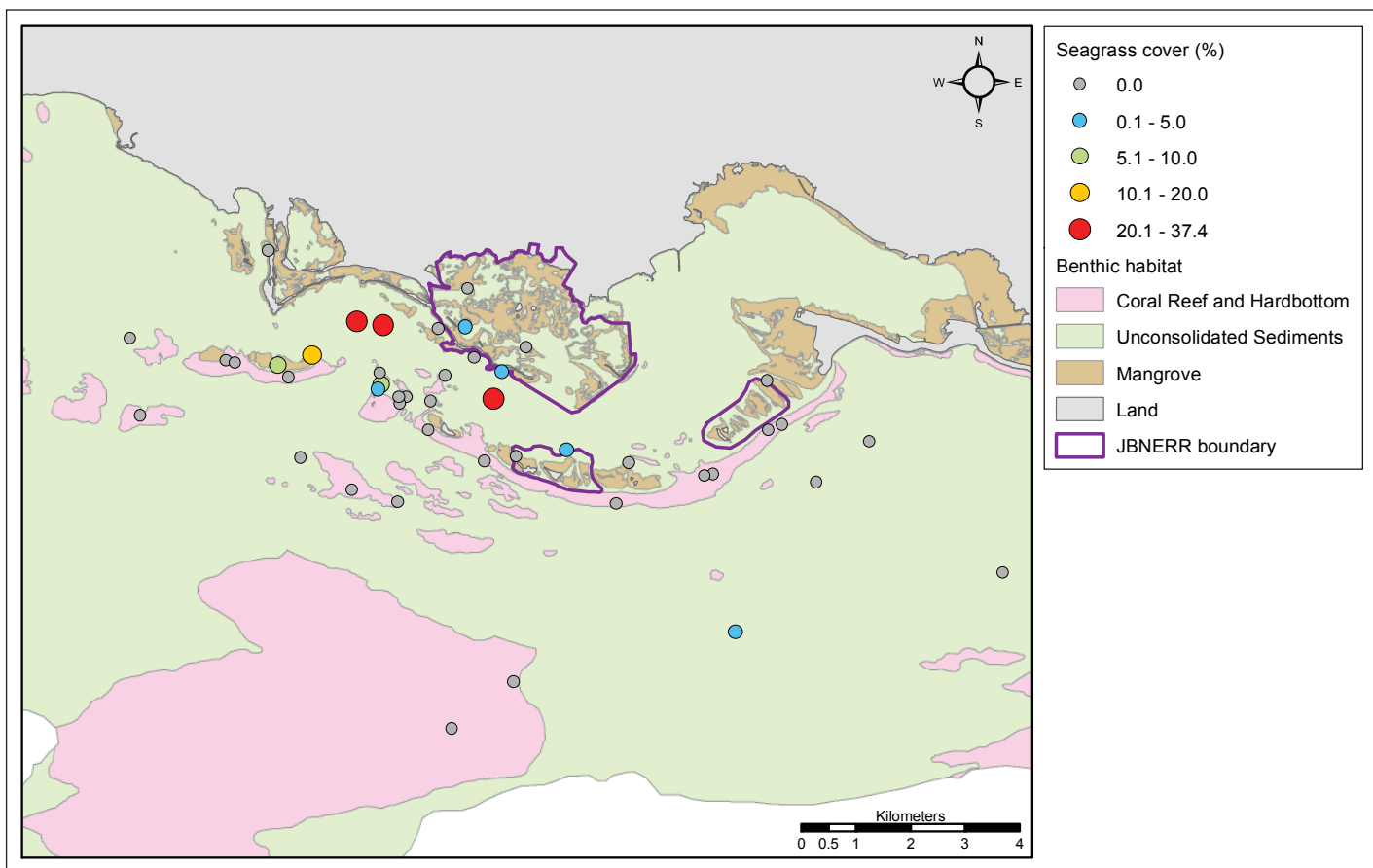


Figure 3.20. Percent seagrass cover.

^B The taxonomic name for *Halodule wrightii* has been recently changed to *Halodule beaudettei* (<http://www.itis.gov/index.html>); however, the original name will be used in this document as it is more widely known.

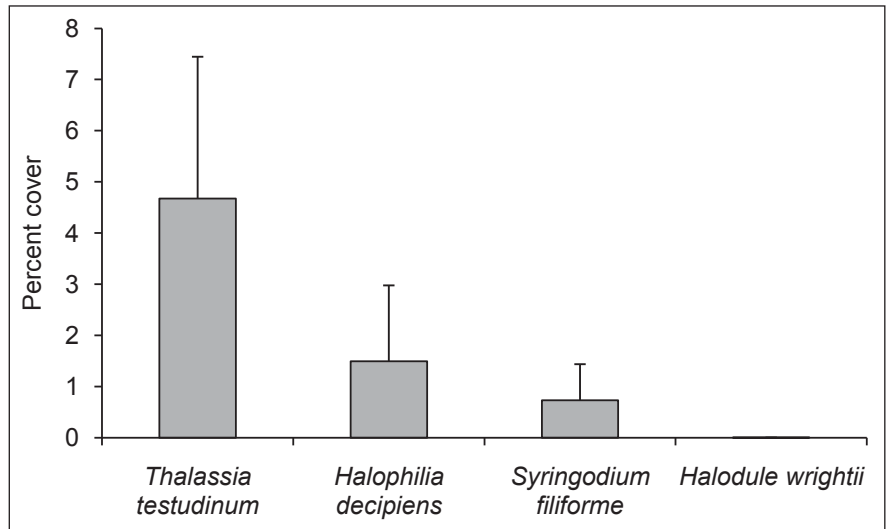


Figure 3.21. Mean (±SE) percent cover of seagrass species across unconsolidated sediment sites.

3.3.2. Fish assemblages

Community metrics

The fish community observed in the Jobos Bay study included 34 taxonomic families represented by 112 species (Appendix A, Table A.1). Fish species richness ranged from 1 to 27 species per site. Richness was generally highest on hardbottom sites, particularly on reefs south of Cayos de Ratones, Cayos de Pájaros and Cayos de Barca (Figures 3.22a and 3.23). Species diversity follows a similar trend (Figures 3.22b and 3.24). Results of a non-parametric analysis indicate that both richness and Shannon diversity were significantly greater on hardbottom compared with both unconsolidated sediments and mangrove ($p < 0.05$).

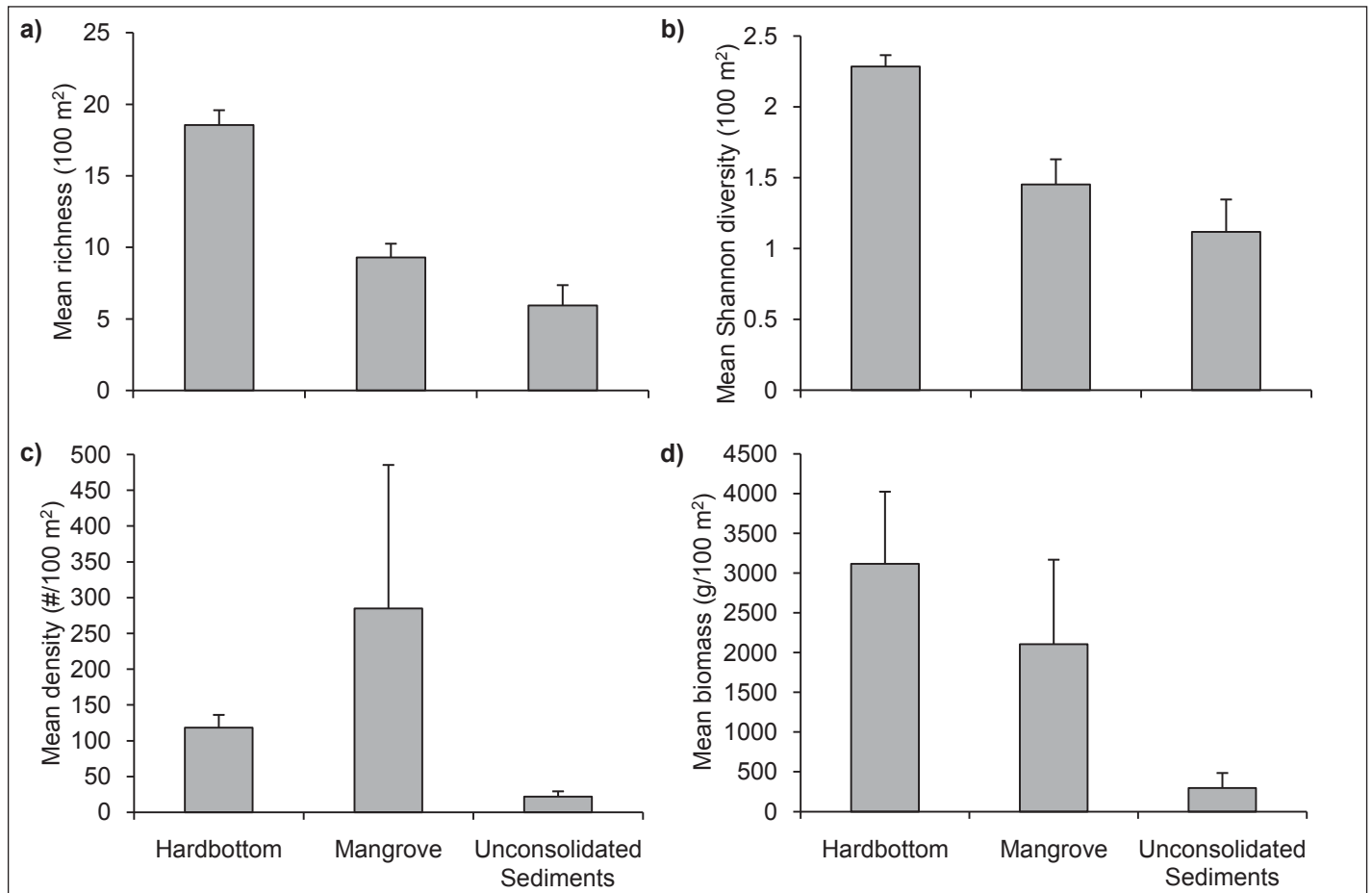


Figure 3.22. Mean (±SE) fish species a) richness, b) Shannon diversity, c) density, and d) biomass by habitat type.

Total fish density was significantly greater on hardbottom and mangrove habitats in comparison to unconsolidated sediments ($p < 0.05$), but did not significantly vary between hardbottom and mangrove. Although average fish density was highest on mangrove, there was also a large degree of variability (Figure 3.22c). The site with the highest fish density in the study area was located in mangrove habitat on Cayos de Ratones, where over 2000 individuals per 100 m² (primarily *Jenkinsia* sp.) were observed (Figure 3.25). Three additional locations of high fish density (> 100 individuals/100m²) were located in mangrove and reefs surrounding Cayos de Ratones. In general, density tended to be higher on hardbottom sites located on the fore reefs of the cays than at the offshore locations (Figure 3.25). Fish density was consistently low on unconsolidated sediments; in 60% of surveys on this habitat, ≤ 10 individuals were observed.

Overall, hardbottom supported the highest levels of total fish biomass, whereas mangroves supported intermediate levels of biomass (Figures 3.22d and 3.26). Surveys on unconsolidated sediment were typically characterized by low levels of biomass. Similar to fish density, total fish biomass was significantly greater on hardbottom and mangrove habitats in comparison to unconsolidated sediments ($p < 0.05$), but did not significantly vary between hardbottom and mangrove. Surveys with the highest total biomass include hardbottom sites in close proximity to the cays and a mangrove site in the lagoon. At two of the three surveys characterized by biomass > 10000 g/100 m², the high biomass was largely attributed to the presence of a southern stingray (*Dasyatis americana*) and great barracuda (*Sphyraena barracuda*), respectively.

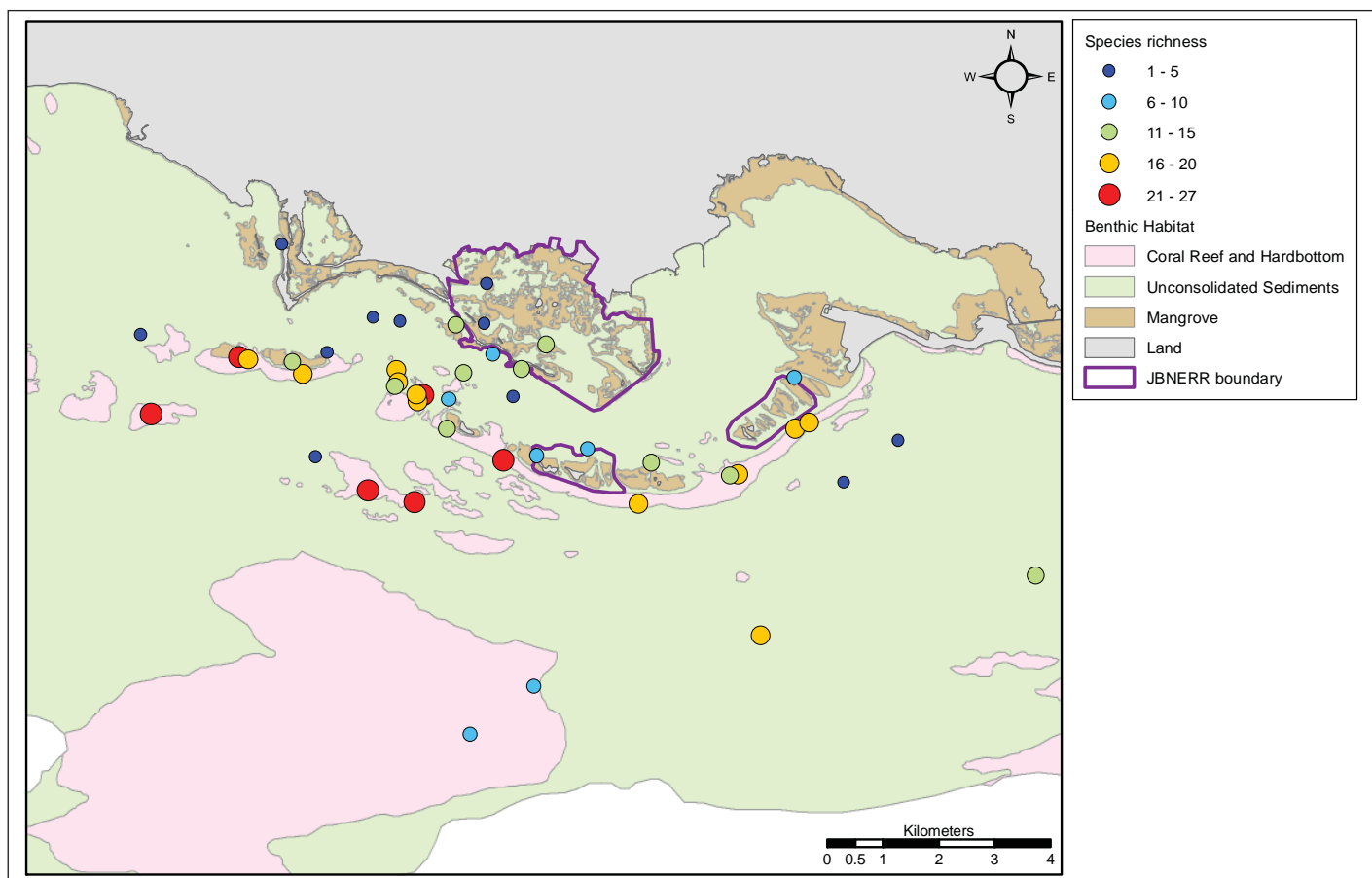


Figure 3.23. Fish species richness.

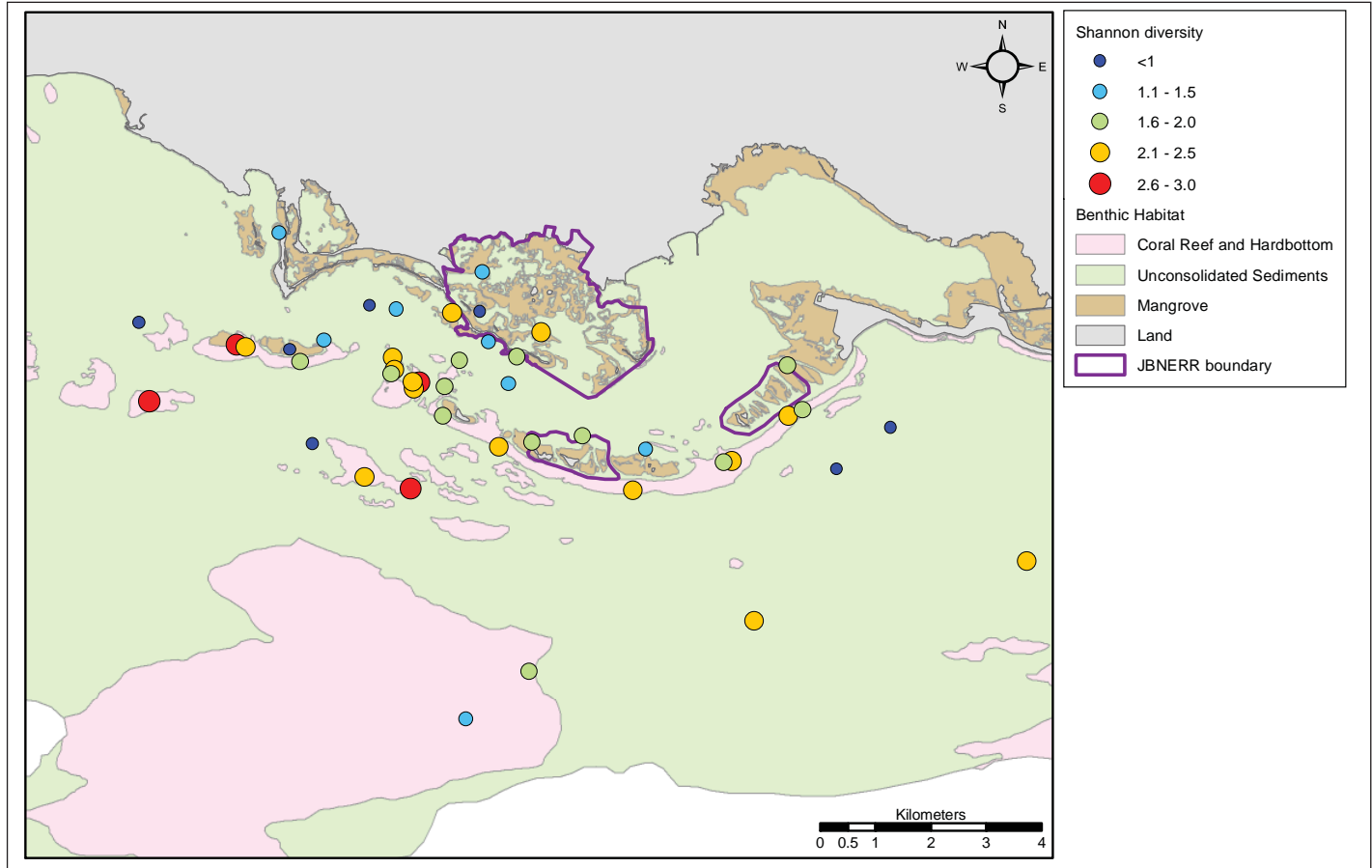


Figure 3.24. Fish species diversity.

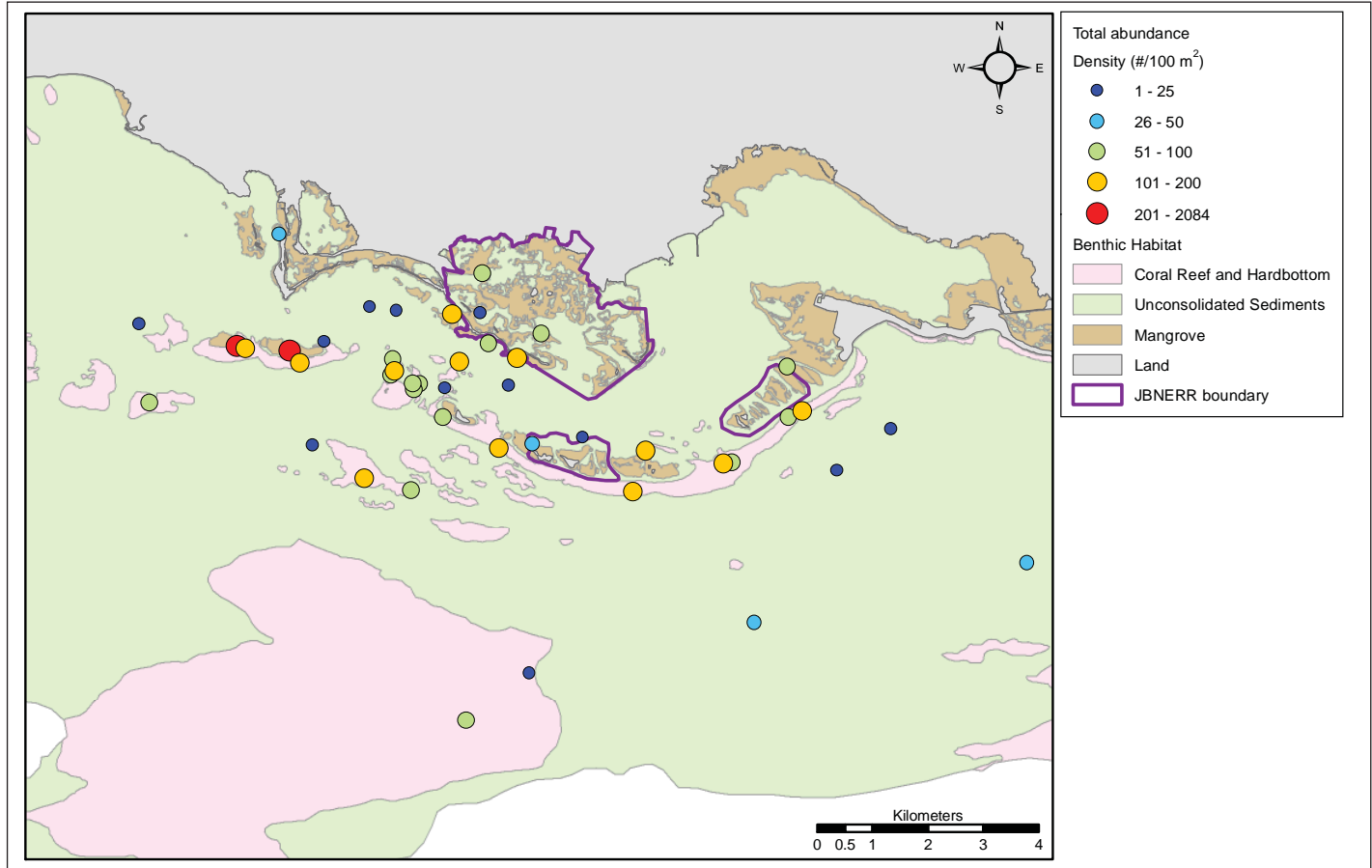


Figure 3.25. Total fish density.

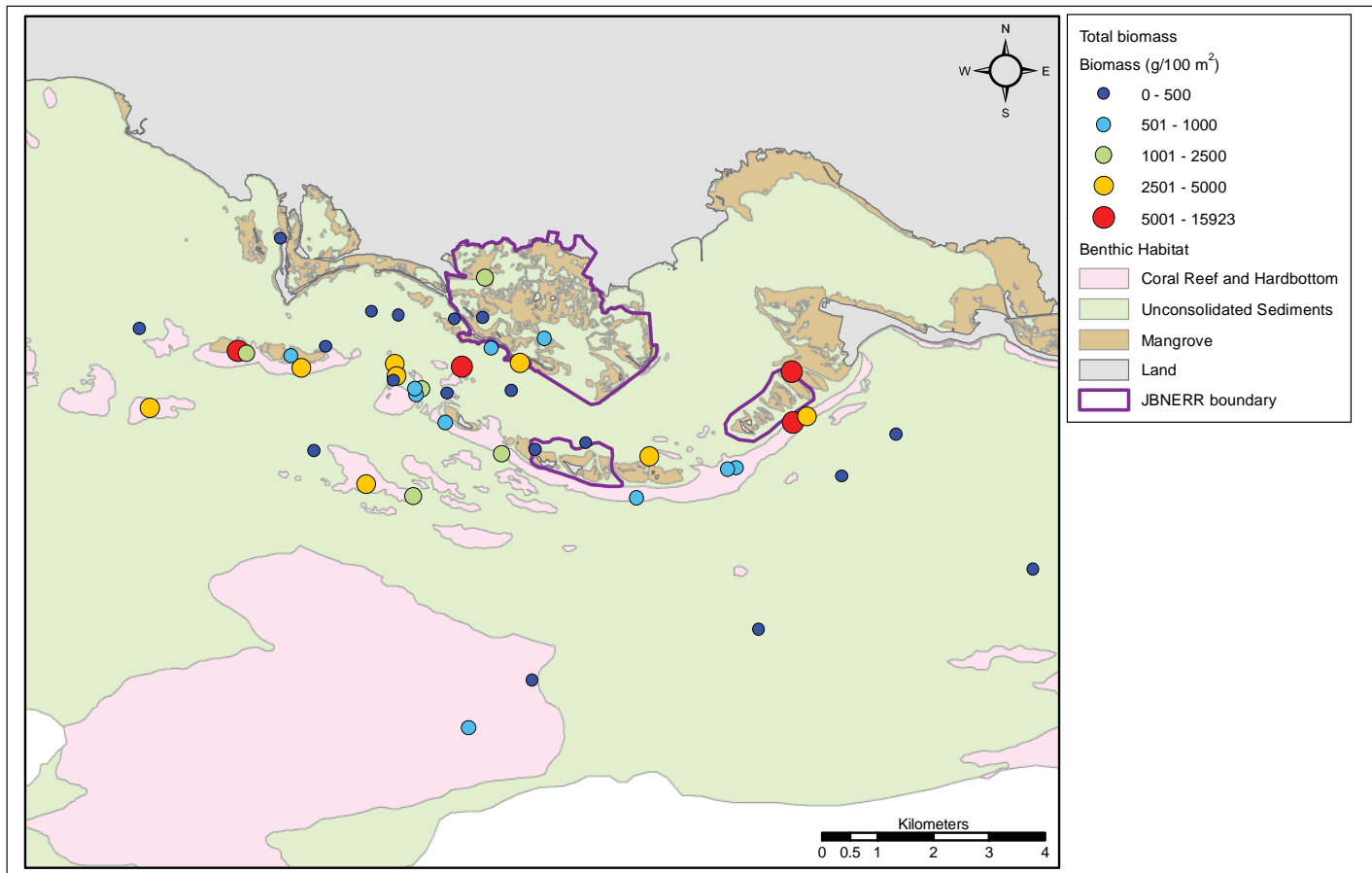


Figure 3.26. Total fish biomass.

The nMDS and ANOSIM analyses further indicate that fish assemblages in Jobos Bay differ by bottom type. There was a clear separation between hardbottom, unconsolidated sediment, and mangrove surveys (Figure 3.27). One exception was an unconsolidated sediment site among the hardbottom group. The transect was conducted in a seagrass bed in close proximity to a reef (within 4 m), which likely explains why the fish community was similar to other hardbottom samples. Mangrove and hardbottom sites tended to be highly clustered, indicating a high degree of similarity in species composition among sites within each respective habitat type. In contrast, unconsolidated sediment sites tended to be more dispersed, indicating more dissimilarity among sites within this group. Indeed, the average Bray-Curtis similarity for hardbottom and mangrove sites was 33.78 and 31.75, respectively, but only 6.92 for unconsolidated sediment surveys. Sub-habitats within unconsolidated sediment bottom include both sand and mud substrate types that can range in cover (e.g., continuous seagrass, sparse algae, no cover). Similarly, fish communities in these sub-habitats can vary widely. The results of the ANOSIM test ($R=0.581$, $p<0.001$) also indicate that there is a statistically significant difference in

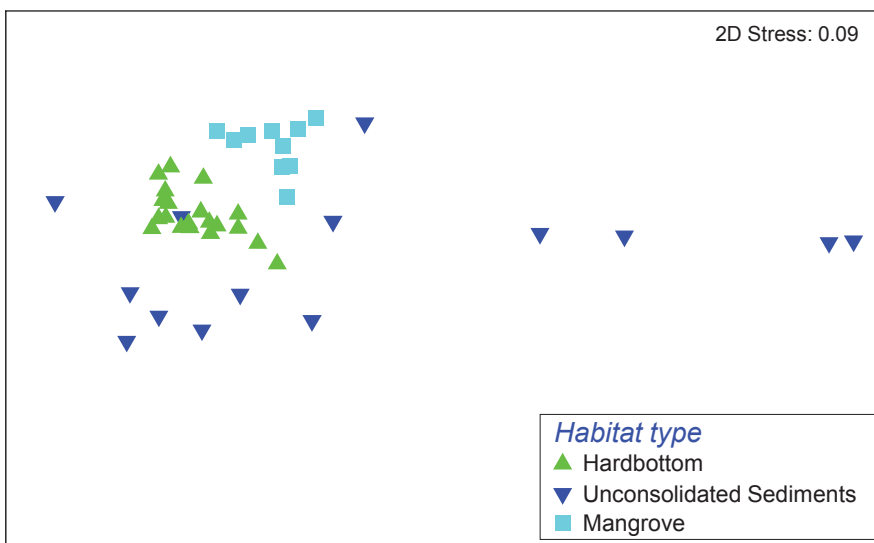


Figure 3.27. Non-metric multidimensional (nMDS) scaling ordination based on between site similarity composition using fish abundance data. Sites are color-coded by habitat type.

the ANOSIM test ($R=0.581$, $p<0.001$) also indicate that there is a statistically significant difference in

community composition among the three groups of sites. Pairwise comparisons resulted in similar or slightly higher R values for hardbottom versus unconsolidated sediments ($R=0.549$) and hardbottom vs. mangrove ($R=0.853$), but a lower value for unconsolidated sediments vs. mangrove ($R=0.336$). This indicates that hardbottom fish communities differ from both mangrove and unconsolidated sediments, but that community differences between the two latter groups are not as distinguishable. This is expected as these two habitats share some overlap; for example, mangrove surveys are conducted along the interface between the mangrove forest and the adjacent sand/mud bottom.

Trophic Groups, Families and Species

Biomass and abundance were distributed unevenly throughout trophic and taxonomic groups. The most abundant groups in terms of biomass and abundance were herbivores (H; e.g., parrotfishes, damselfishes) and invertivores (I; e.g., grunts, butterflyfishes). Piscivores (P; e.g., snappers, groupers) constituted a small percentage of total fish abundance, but constituted a greater proportion of the biomass. While there was often a large degree of variability among habitat type (Figures 3.28a,b), some general spatial patterns emerged. Results of a non-parametric analysis indicated that herbivore abundance and biomass were significantly greater on hardbottom compared to mangrove and unconsolidated sediments. Invertivore abundance and biomass were significantly greater on hardbottom and mangrove in comparison to unconsolidated sediments, but did not vary significantly between mangrove and hardbottom. Piscivore abundance and biomass were significantly greater in mangrove habitat than on hardbottom or unconsolidated sediments. Piscivores were present in all mangrove surveys, compared to 50% of the surveys on hardbottom and unconsolidated sediments.

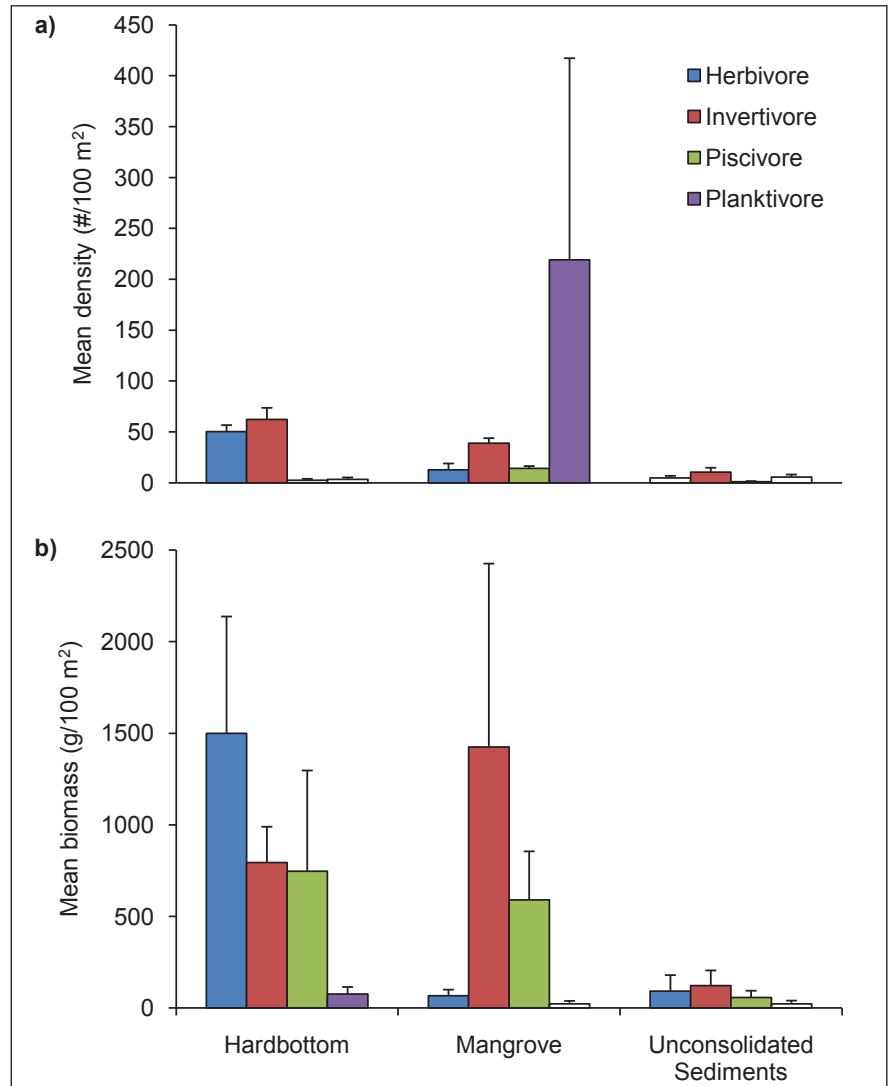


Figure 3.28. Mean (\pm SE) a) density, and b) biomass of major trophic groups by habitat type.

For each bottom type, families with the highest mean abundance and biomass were ranked and their proportional abundance/biomass was calculated (Figures 3.29a-c, 3.30a-c, and 3.31a-c). Overall, approximately 90% of individuals and biomass came from eight and nine families, respectively, but this distribution varied by bottom type.

While individuals of the wrasse (Labridae) and damselfish (Pomacentridae) families were the most numerically abundant on hardbottom, surgeonfishes (Acanthuridae) accounted for the highest proportion of biomass (Figure 3.29a-c). Other families with high proportional abundance and biomass

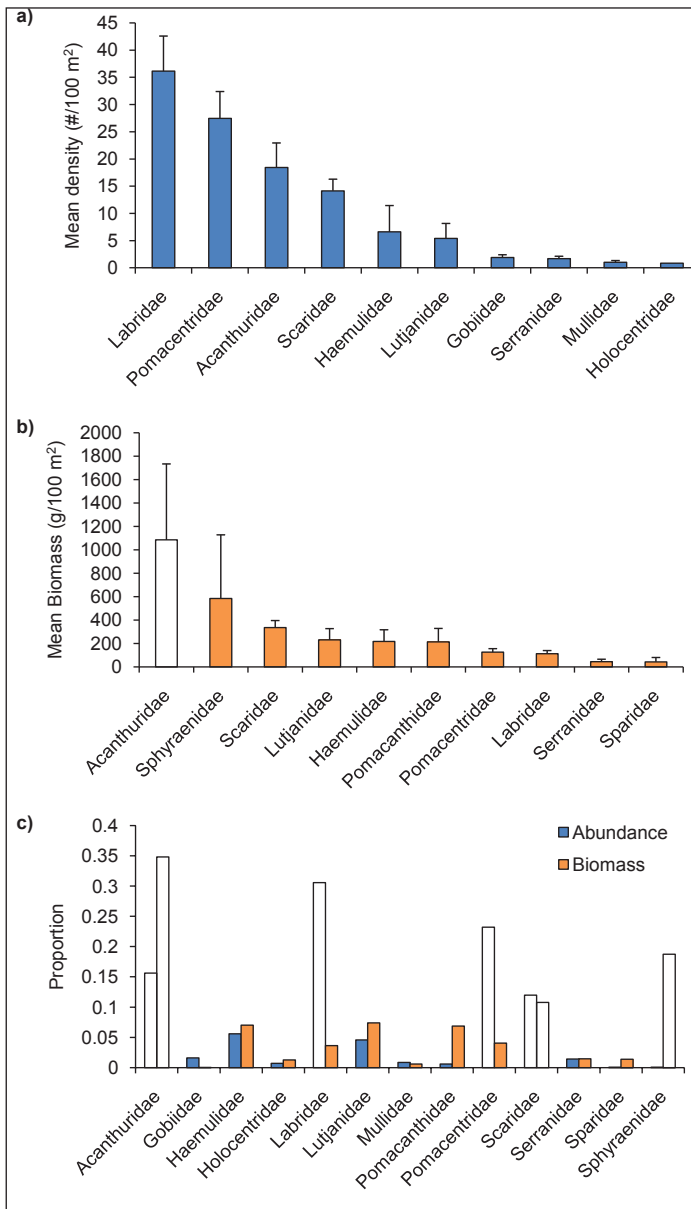


Figure 3.29. Mean (\pm SE) a) density, and b) biomass, and c) proportional distribution of abundance and biomass of major fish families across hardbottom sites.

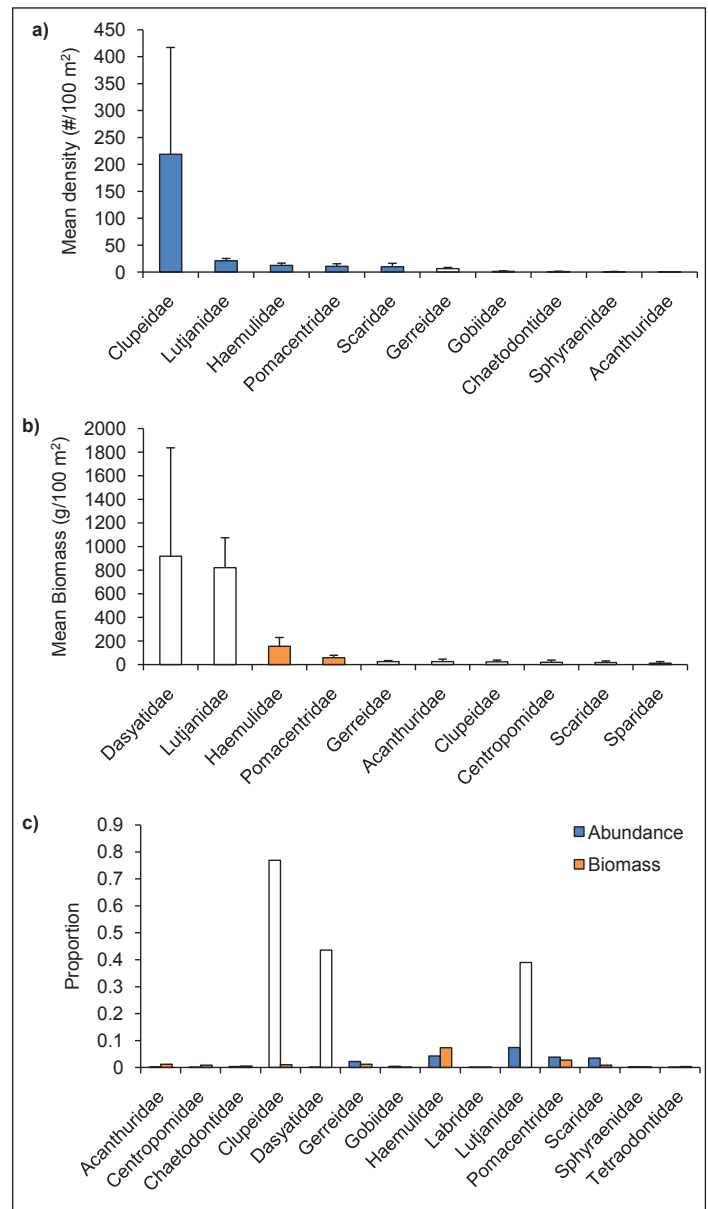


Figure 3.30. Mean (\pm SE) a) density, and b) biomass, and c) proportional distribution of abundance and biomass of major fish families across mangrove sites.

included snappers (Lutjanidae), grunts (Haemulidae) and parrotfish (Scaridae). The high proportional biomass of barracuda (Sphyraenidae) was largely due to the presence of a large great barracuda individual at one site. The most frequently observed and abundant fish species on hardbottom were the ocean surgeonfish (*Acanthurus bahianus*) and bluehead wrasse (*Thalassoma bifasciatum*), which were sighted at 90% of transects on hardbottom. Other species that ranked high in terms of frequency and density on hardbottom include damselfish species (*Stegastes* spp.) and redband and striped parrotfish (*Sparisoma aurofrenatum* and *Scarus iseri*, respectively).

Among bottom types, mangrove habitat was represented by the fewest number of families. Large schools of juvenile clupeids, which were absent on other habitats, were characteristic at several mangrove sites. Clupeids accounted for over 75% of observed individuals in mangroves, but due to their small size only a small percentage (1%) of their biomass (Figure 3.30a-c). Herring *Jenkinsia* sp. were sighted in about 50% of transects but exhibited patchy abundance where found. Due to the presence of a southern stingray in one transect, the stingrays (Family Dasyatidae) accounted for the highest proportional biomass in mangrove habitat, followed by snapper. Schoolmaster and gray snapper

(*Lutjanus apodus* and *Lutjanus griseus*, respectively) and the yellowfin mojarra (*Gerres cinerus*) all ranked high in terms of frequency, mean density and biomass.

Family abundance and biomass on unconsolidated sediments was highly variable (Figure 3.31a-c). While fishes of the groupers, hamlets and seabasses family (*Serranidae*) were most numerically abundant, individuals were typically small; consequently, the family accounted for only a small proportion of the total biomass found on this habitat. Wrasses were also numerically abundant on softbottom, while surgeonfishes accounted for the highest proportion of biomass. Overall, species composition was variable across unconsolidated sediment survey locations. Only one species, bicolor damselfish (*Stegastes partitus*), was observed in over 30% of transects in this habitat.

Several families and species of economic and ecological importance were selected for further examination. Summary information on the spatial distribution, mean density and biomass by habitat, and size frequency for select families and species are discussed and illustrated in this section.

Groupers, Hamlets and Seabasses (*Serranidae*)

Groupers, hamlets and seabasses were observed in 42% of survey transects. The family was represented by 12 species, with harlequin bass (*Serranus tigrinus*) and chalk bass (*Serranus tortugarum*) most frequently sighted.

When all serranids were included, mean density was highest on unconsolidated sediments, primarily due to chalk bass, but biomass was higher on hardbottom (Figure 3.32). Large-bodied groupers (*Cephalopholis* and *Epinephelus* spp.) were infrequent, primarily small in size, and were almost exclusively found on hardbottom (Figure 3.33). Three coney (*Cephalopholis fulva*) were sighted south of Cayos Caribe, while three graysby (*Cephalopholis cruentata*) and one red hind (*Epinephelus guttatus*) were documented in the area of Cayos de Pájaros (Figure 3.33a). All red hind and coney individuals were small adults, while graysby individuals were primarily juvenile/sub-adult.

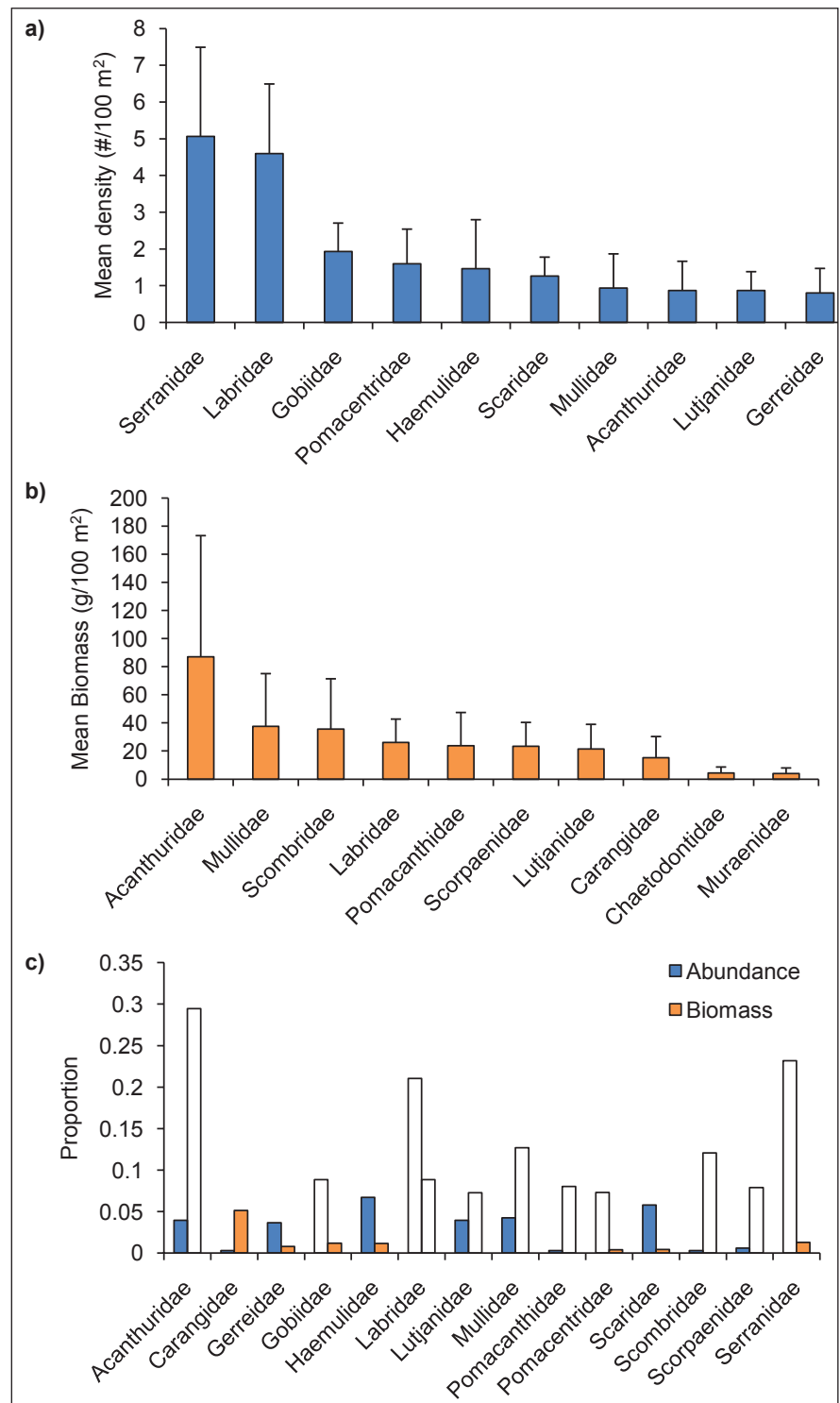


Figure 3.31. Mean (\pm SE) a) density, and b) biomass, and c) proportional distribution of abundance and biomass of major fish families across unconsolidated sediment sites.

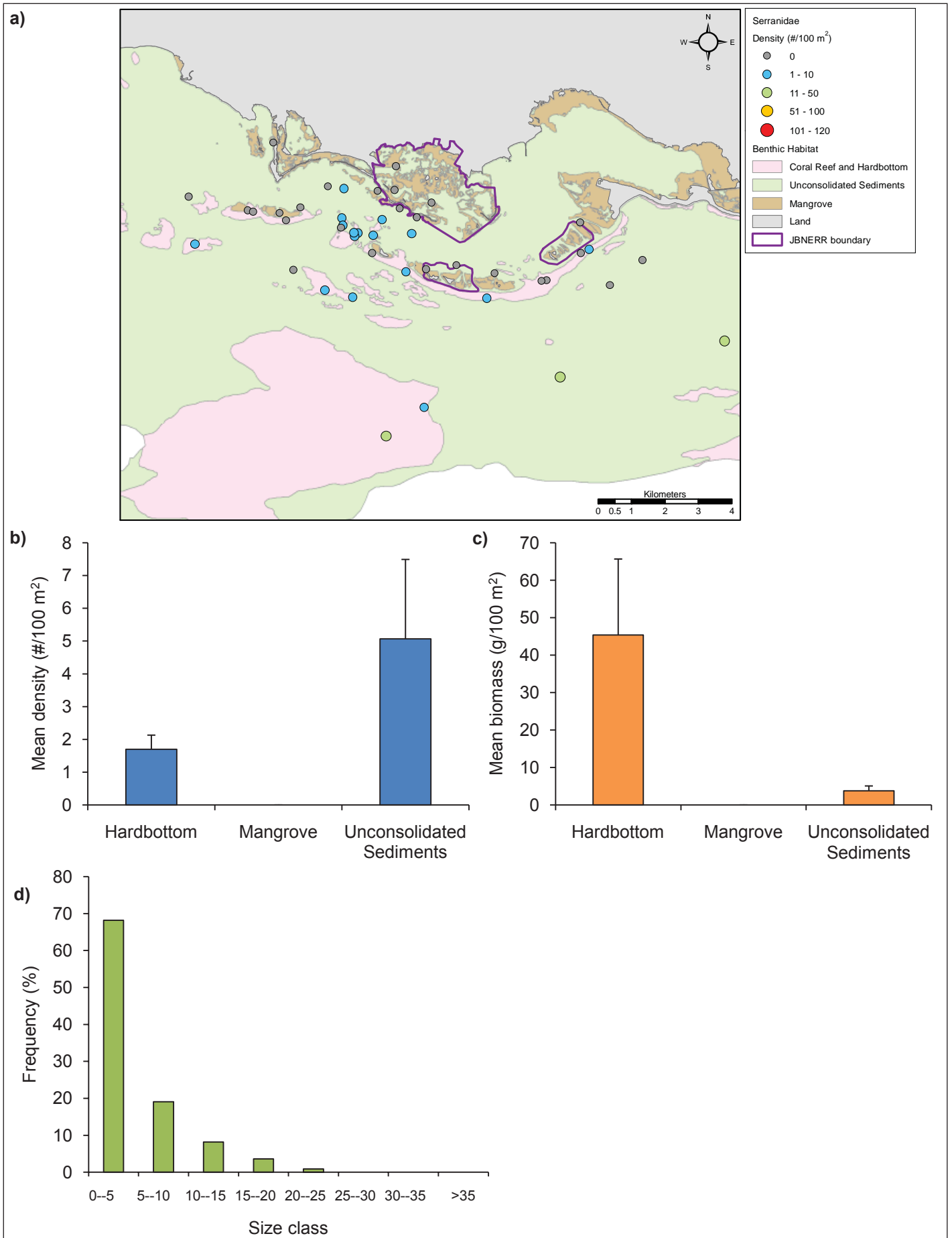


Figure 3.32. a) Spatial distribution, b) mean (\pm SE) density by habitat, c) mean (\pm SE) biomass by habitat, and d) size frequency histogram of groupers, hamlets, and seabasses (Family Serranidae).

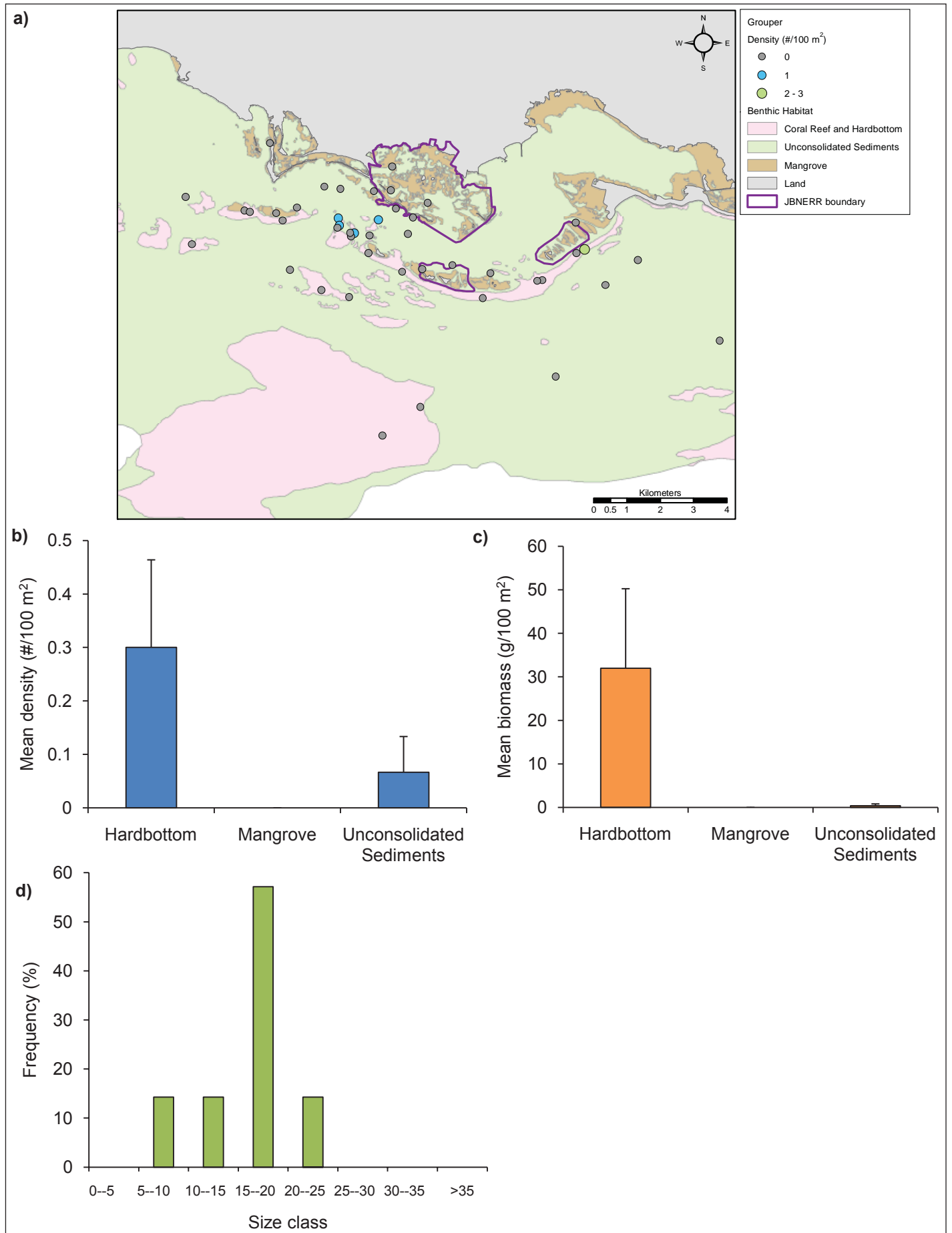


Figure 3.33. a) Spatial distribution, b) mean (\pm SE) density by habitat, c) mean (\pm SE) biomass by habitat, and d) size frequency histogram of large-bodied groupers (*Cephalopholis* and *Epinephelus* spp.).

Snappers (*Lutjanidae*)

Snappers were detected among all investigated habitats but were most abundant in mangroves and nearshore environments (Figure 3.34). Lowest abundance and biomass were observed over unconsolidated sediments. Eight Lutjanid species were documented, with schoolmaster, yellowtail (*Ocyurus chrysurus*) and gray snapper accounting for the majority of observations. The remaining species were infrequently sighted. Size frequency was skewed toward smaller size classes.

Schoolmaster were observed at 33% of survey transects and were most abundant in nearshore mangrove fringes and cays (Figure 3.35). A few individuals were observed on hardbottom habitat adjacent to the cays, while none were observed on unconsolidated sediments. The majority of schoolmaster were juveniles/subadults. All adult-sized individuals, about 4% of the total, were located on mangrove habitat.

Gray snapper were observed in 16% of surveys and were almost exclusively associated with mangrove fringes and cays (Figure 3.36). The site with the highest abundance and biomass was located in a sheltered area in the northern portion of the JBNERR. Observed individuals were comprised exclusively of juveniles/sub-adults.

In comparison to other Lutjanid species, highest abundance and biomass of yellowtail snapper were found on hardbottom habitats, while the species was largely absent from mangroves (Figure 3.37). The site with the highest abundance and biomass was offshore of Cayos de Barca. All observed individuals were juveniles/subadults.

Grunts (*Haemulidae*)

Fishes of the grunt family were present within 47% of survey transects across all habitat types. While mangrove habitat was characterized by highest mean abundance, biomass was generally higher at hardbottom habitat (Figure 3.38). The family was represented by seven species. French grunt (*Haemulon flavolineatum*) and porkfish (*Anisotremus virginicus*) were most frequently sighted and had the highest mean abundance and biomass of the Haemulid species. Tomtates (*Haemulon aurolineatum*) were infrequently observed (9% of survey transects). About 19% of observed grunts were small juveniles that could not be identified to the species level.

French grunt was present in 24% of sites. The species was most commonly observed on hardbottom and mangrove habitat in the central and western portion of the study area (Figure 3.39). The site with the highest abundance and biomass was located on hardbottom adjacent to Cayos de Ratones. No individuals were observed on softbottom. Size frequency was skewed toward the juvenile/sub-adult size classes.

Porkfish was present in 18% of survey transects. In contrast with *H. flavolineatum*, the species was most common on hardbottom and absent from mangrove habitat (Figure 3.40). The species was generally sighted in small numbers and was present both inside and outside the bay. The size distribution was about evenly divided between juveniles/sub-adults and small adults.

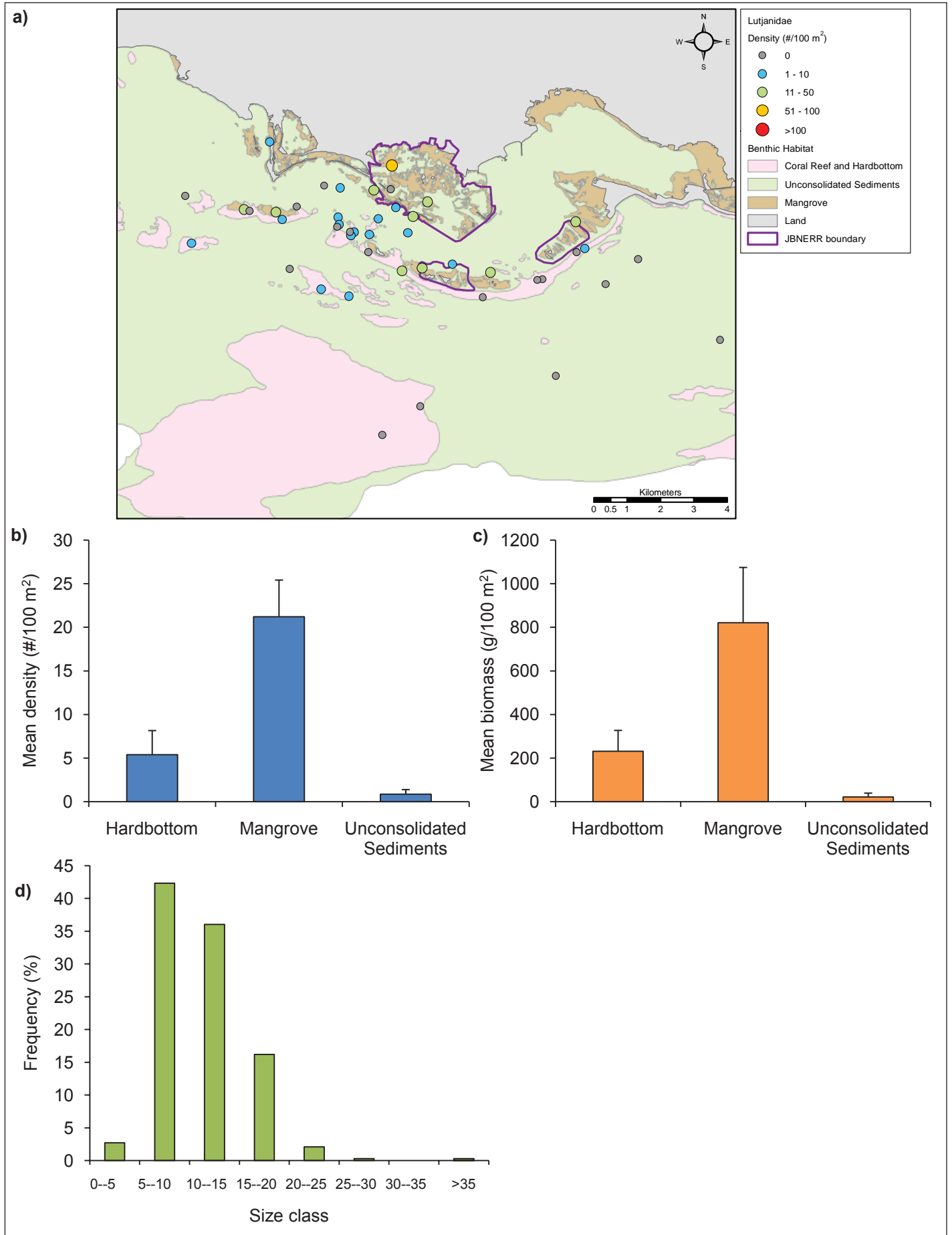


Figure 3.34. a) Spatial distribution, b) mean (\pm SE) density by habitat, c) mean (\pm SE) biomass by habitat, and d) size frequency histogram of snappers (Family Lutjanidae).

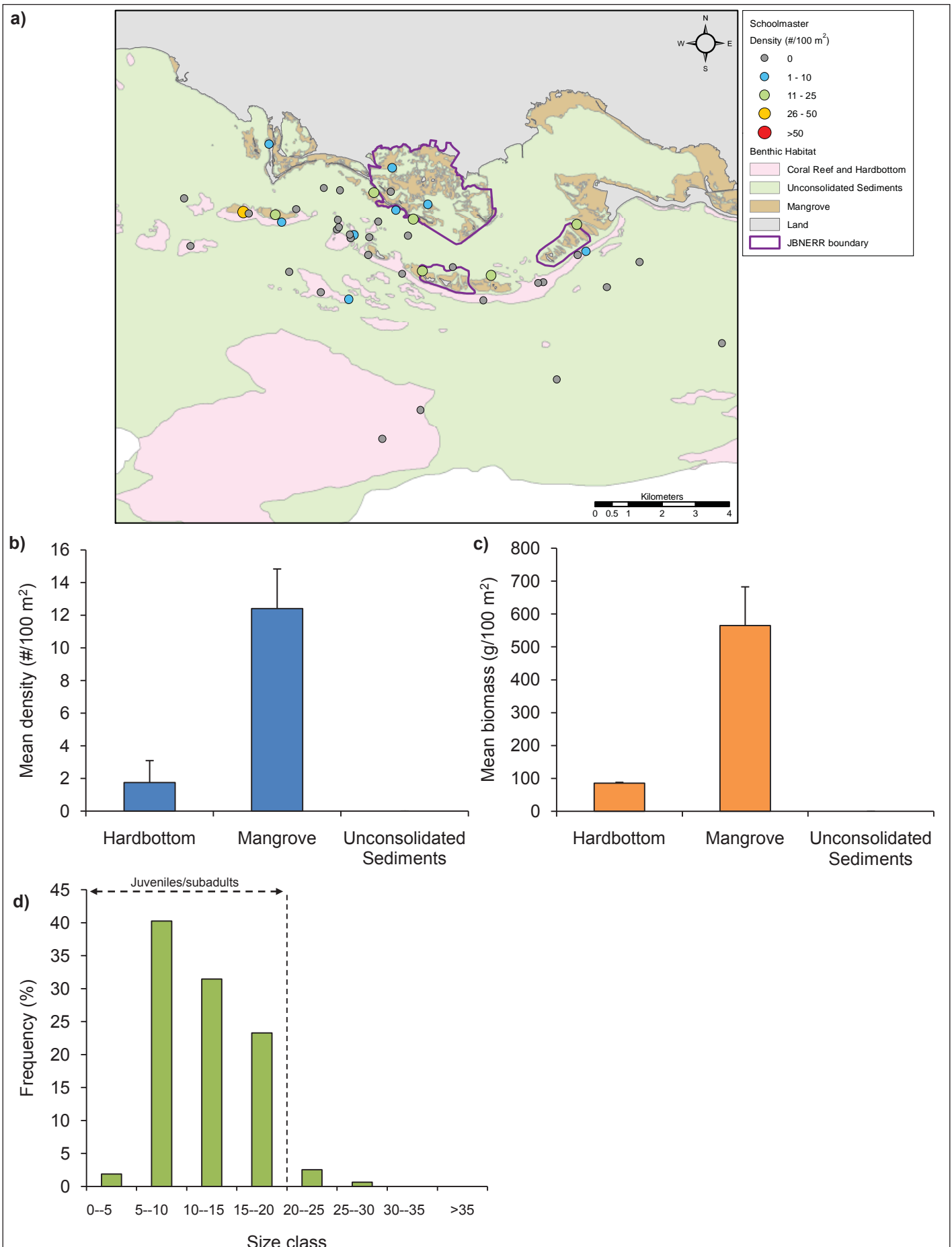


Figure 3.35. a) Spatial distribution, b) mean (\pm SE) density by habitat, c) mean (\pm SE) biomass by habitat, and d) size frequency histogram of schoolmaster (*Lutjanus apodus*).

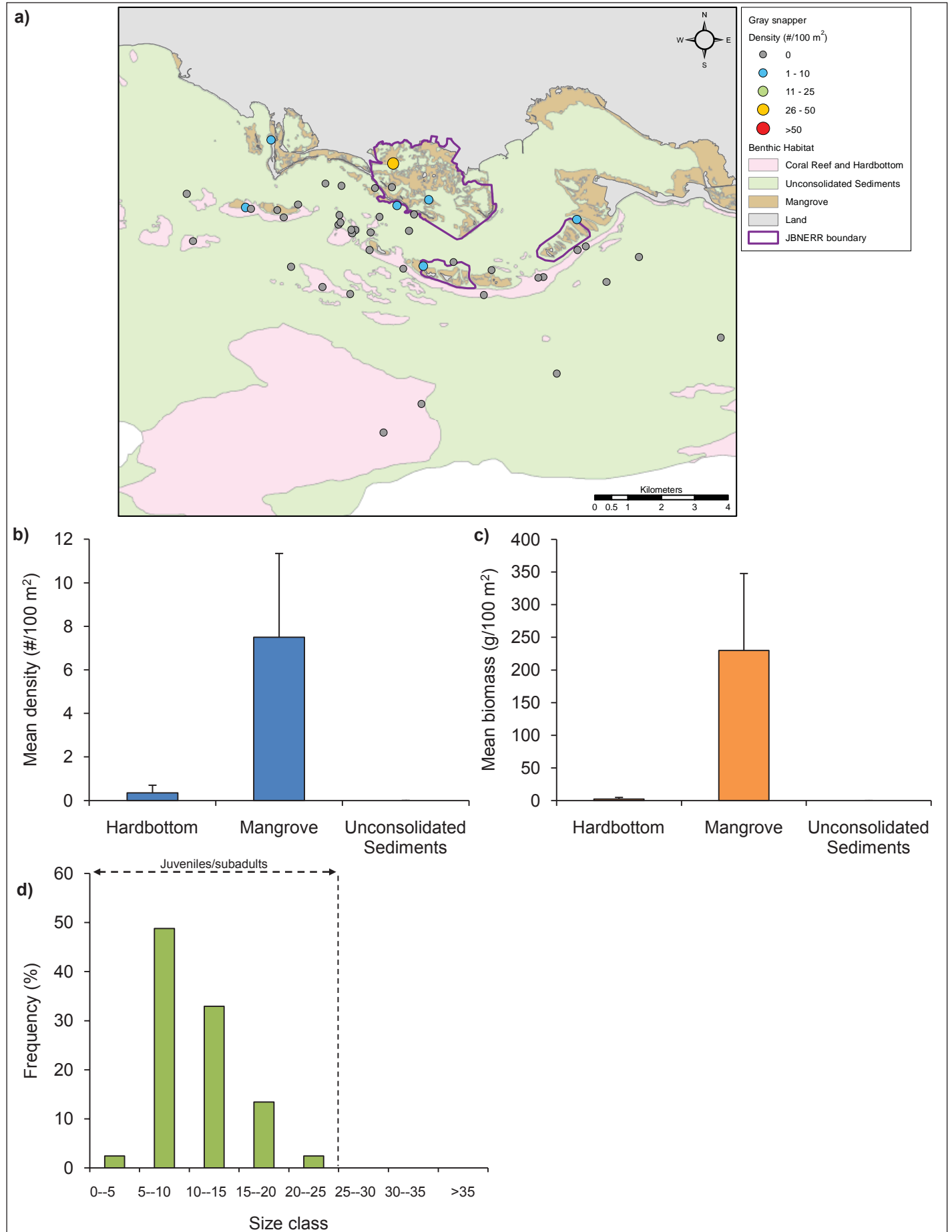


Figure 3.36. a) Spatial distribution, b) mean (\pm SE) density by habitat, c) mean (\pm SE) biomass by habitat, and d) size frequency histogram of gray snapper (*Lutjanus griseus*).

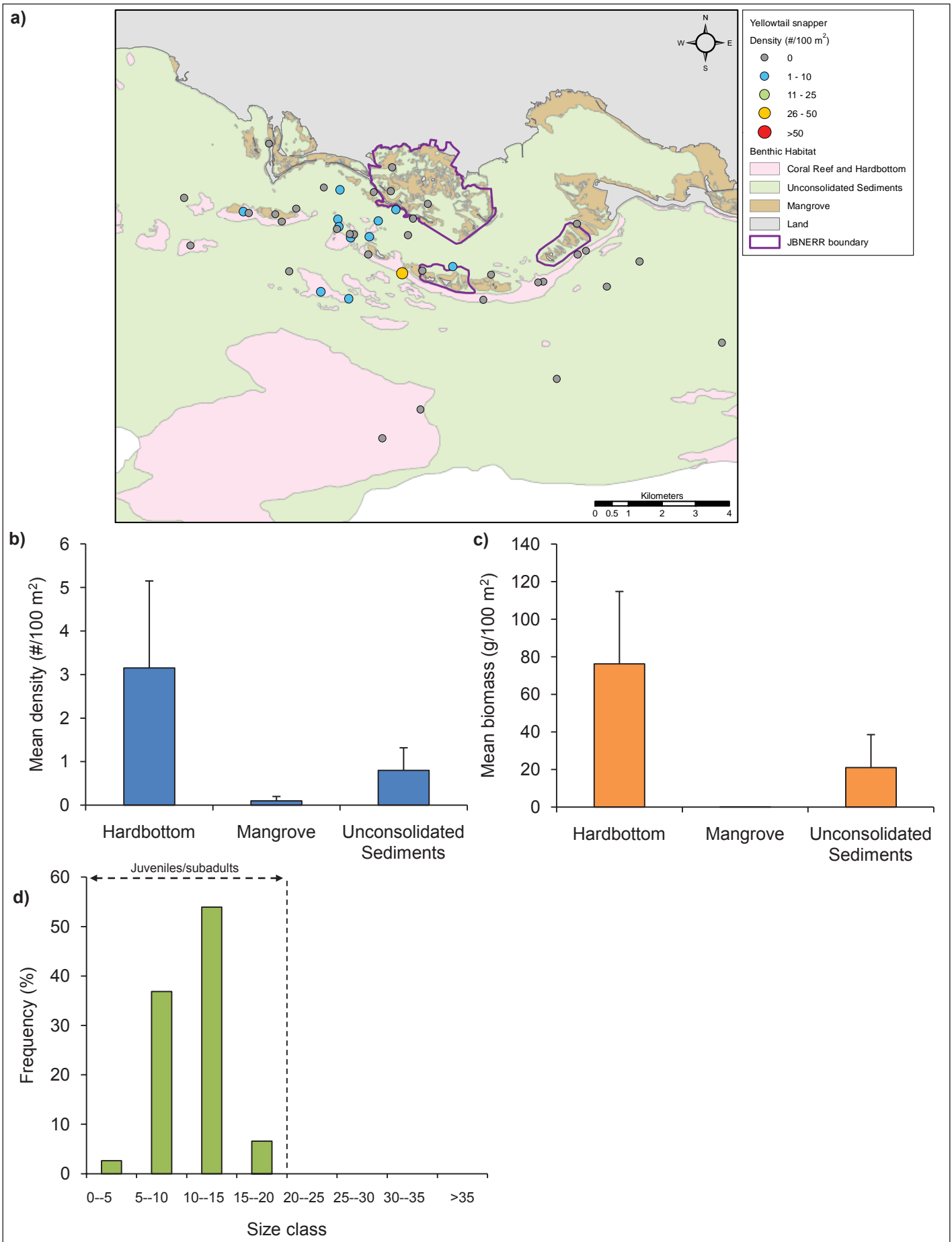


Figure 3.37. a) Spatial distribution, b) mean (\pm SE) density by habitat, c) mean (\pm SE) biomass by habitat, and d) size frequency histogram of yellowtail snapper (*Ocyurus chrysurus*).

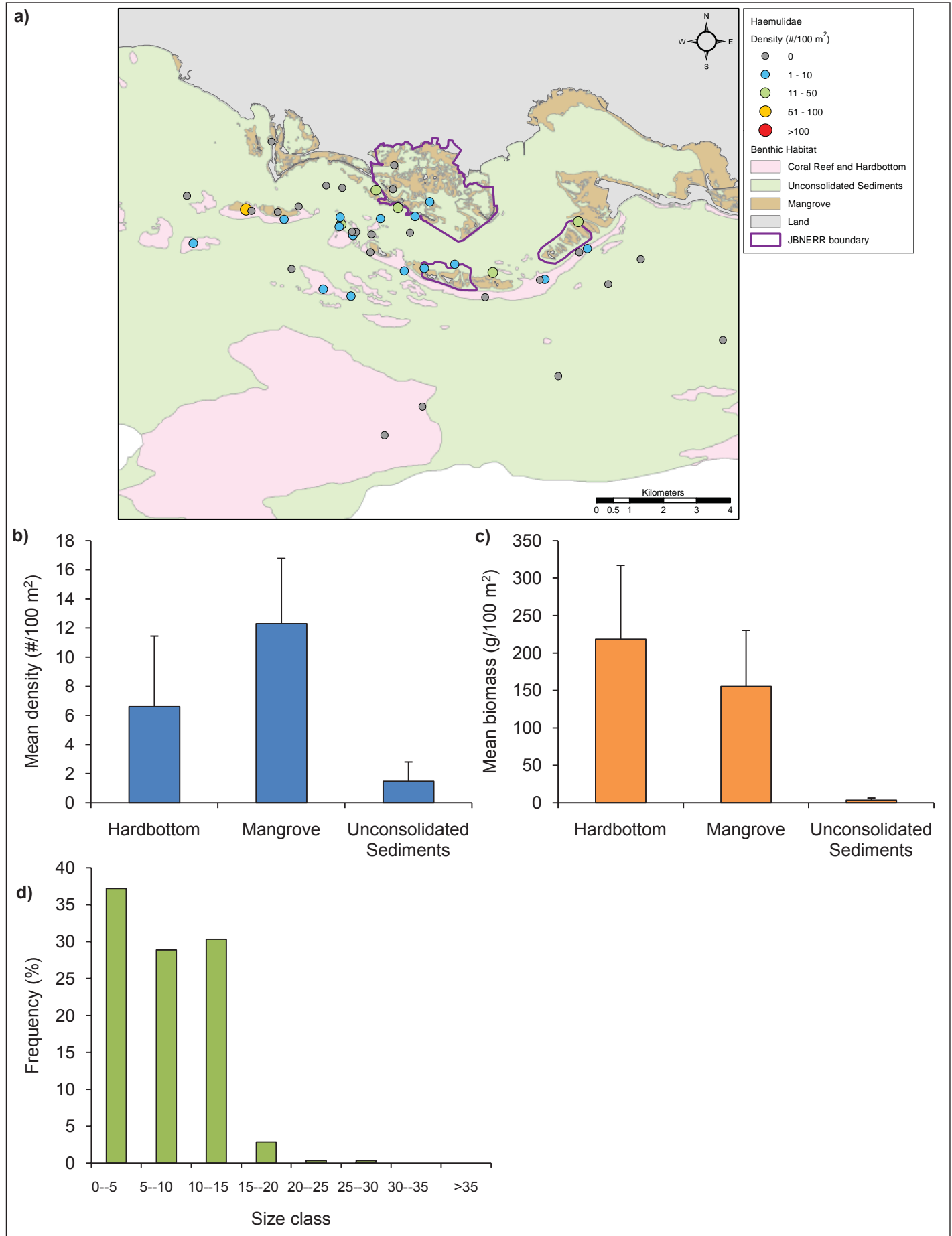


Figure 3.38. a) Spatial distribution, b) mean (\pm SE) density by habitat, c) mean (\pm SE) biomass by habitat, and d) size frequency histogram of grunts (Family Haemulidae).

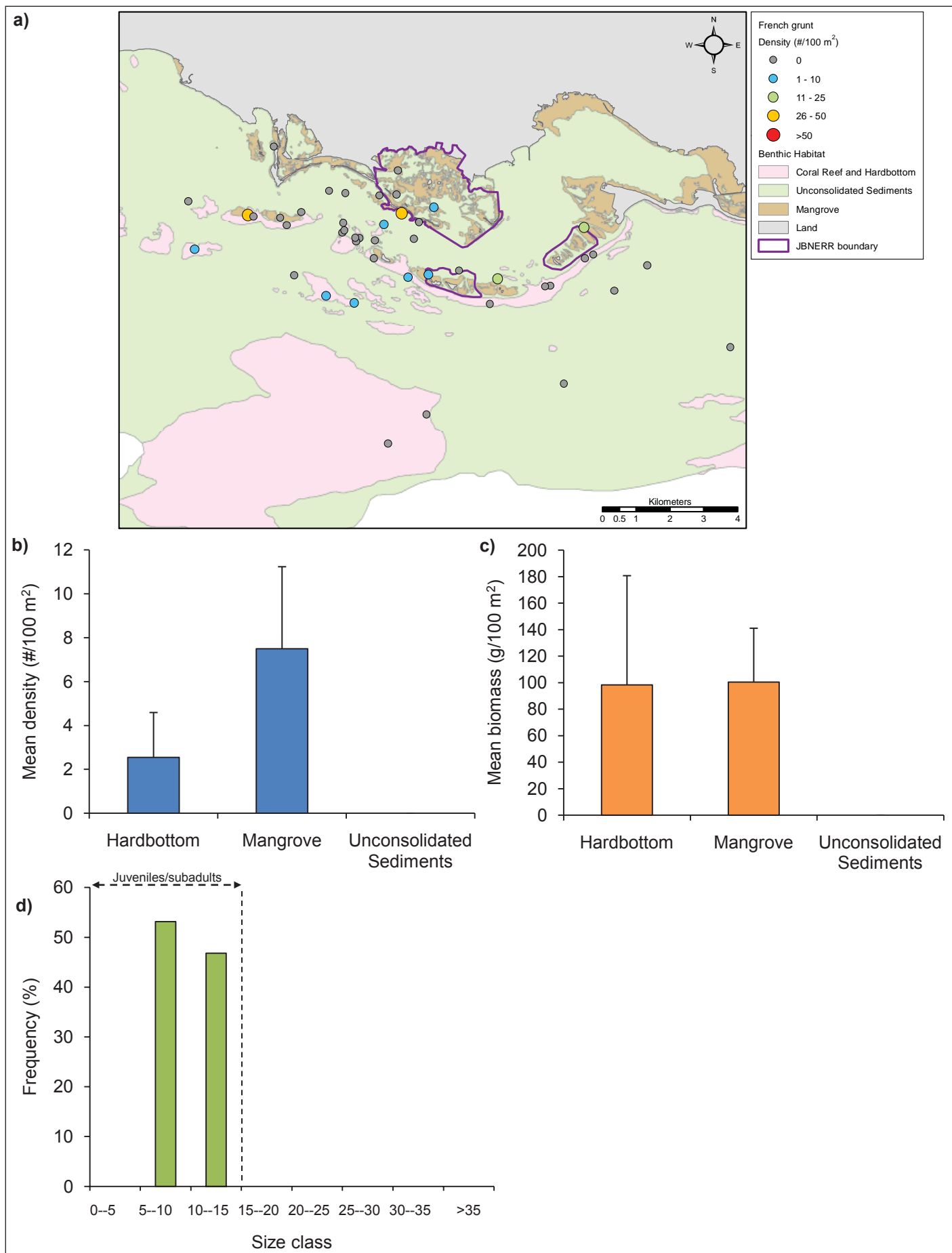


Figure 3.39. a) Spatial distribution, b) mean (\pm SE) density by habitat, c) mean (\pm SE) biomass by habitat, and d) size frequency histogram of French grunt (*Haemulon flavolineatum*).

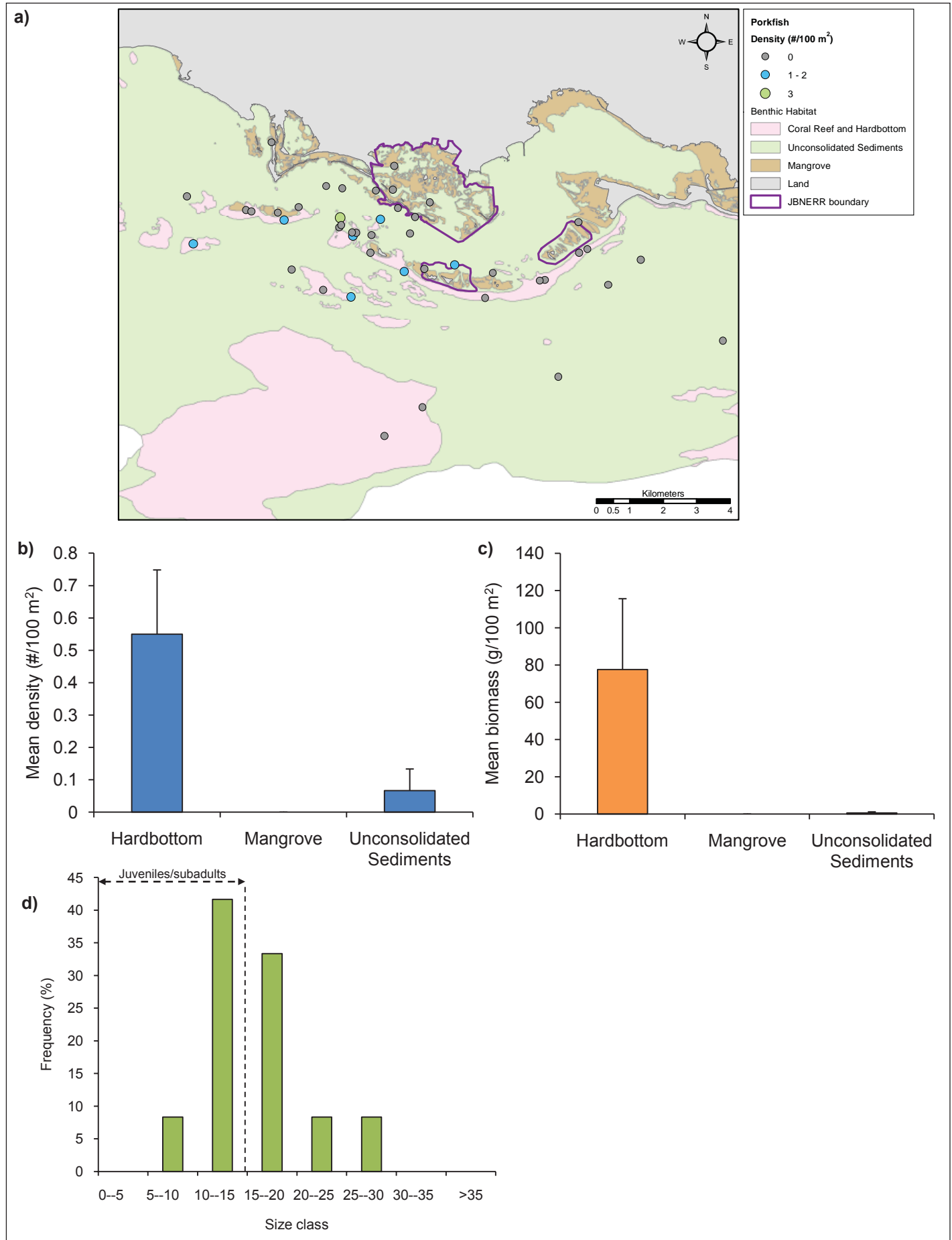


Figure 3.40. a) Spatial distribution, b) mean (\pm SE) density by habitat, c) mean (\pm SE) biomass by habitat, and d) size frequency histogram of porkfish (*Anisotremus virginicus*).

Surgeonfishes (*Acanthuridae*)

Surgeonfishes were a common member of the Jobos Bay fish community, occurring in 53% of survey transects. Acanthurids were most common on hardbottom and were present at all but one hardbottom site. Sites with the highest abundance and biomass were located on hardbottom adjacent to the cays and on a patch reef landward of Cayos de Pájaros (Figure 3.41). Abundance and biomass of surgeonfish on unconsolidated sediments and mangrove were generally low.

Ocean surgeonfish were sighted in 42% of surveys. The highest abundance and biomass were observed on hardbottom habitat, while the species was absent from mangrove (Figure 3.42). A large percentage (>40%) of individuals were small juveniles in the 0-5 cm size class, partly due to the presence of one large school of juveniles at a hardbottom site near Cayos de Pájaros. Larger juveniles/sub-adults accounted for the majority of the remainder of ocean surgeonfish individuals encountered during the surveys.

Doctorfish (*Acanthurus chirurgus*) were present in a similar percentage (40%) of surveys as ocean surgeonfish but generally in lower abundance. Highest abundance and biomass occurred on hardbottom and were highly variable among sites within this habitat. The species was infrequent on unconsolidated sediments and mangrove (Figure 3.43). High species abundance and biomass were observed at a patch reef in the lagoon behind Cayos de Pájaros. The majority of individuals were small-medium sized adults, while only 15% of individuals were juveniles/sub-adults.

Blue tangs (*Acanthurus coeruleus*) were present in 24% of surveys and were almost exclusively limited to hardbottom. The species was generally found in low abundance, with hotspots detected at two sites on fore reef adjacent to Cayos de Pájaros and Cayos Caribe (Figure 3.44). Over 60% of individuals were small adults within the 10-15 cm size class.

Parrotfishes (*Scaridae*)

Parrotfishes were a common component of the Jobos fish community, occurring in 62% of survey transects. Highest mean density was observed on hardbottom habitat, with intermediate, but variable, levels in the mangrove fringes (Figure 3.45). Biomass was also greatest on hardbottom, with lower levels on mangrove as this habitat tended to be dominated by small juveniles. Of the nine species, striped parrotfish and redband parrotfish accounted for the highest mean abundance and biomass. Approximately 80% of Scarids were <20 cm, while one large yellowtail parrotfish (*Sparisoma rubripinne*) in the 30-35 cm size class was observed.

Striped parrotfish was most common on hardbottom habitat. The species was not as frequently sighted in mangroves, but was patchily abundant where found. Areas with higher than average abundance include mangrove fringes in the lagoon and fore reef adjacent to the cays (Figure 3.46). The majority of individuals (>85%) were juveniles/sub-adults.

Redband parrotfish was almost exclusively limited to hardbottom. The species was absent from mangrove and occurred in only one survey on unconsolidated sediments (Figure 3.47). While hardbottom densities were similar to striped parrotfish, redband parrotfish biomass tended to be higher as the size distribution was skewed towards slightly larger size classes. Approximately 35% of individuals were adult-sized.

Stoplight parrotfish (*Sparisoma viride*) occurred only at hardbottom sites, generally in low densities. Otherwise there were no distinctive spatial patterns in the species distribution as it was present on reefs both within the bay and offshore of the cays (Figure 3.48). The majority of individuals were juveniles/sub-adults with a lesser percentage (17%) of fish in the smallest adult size class (15-20 cm).

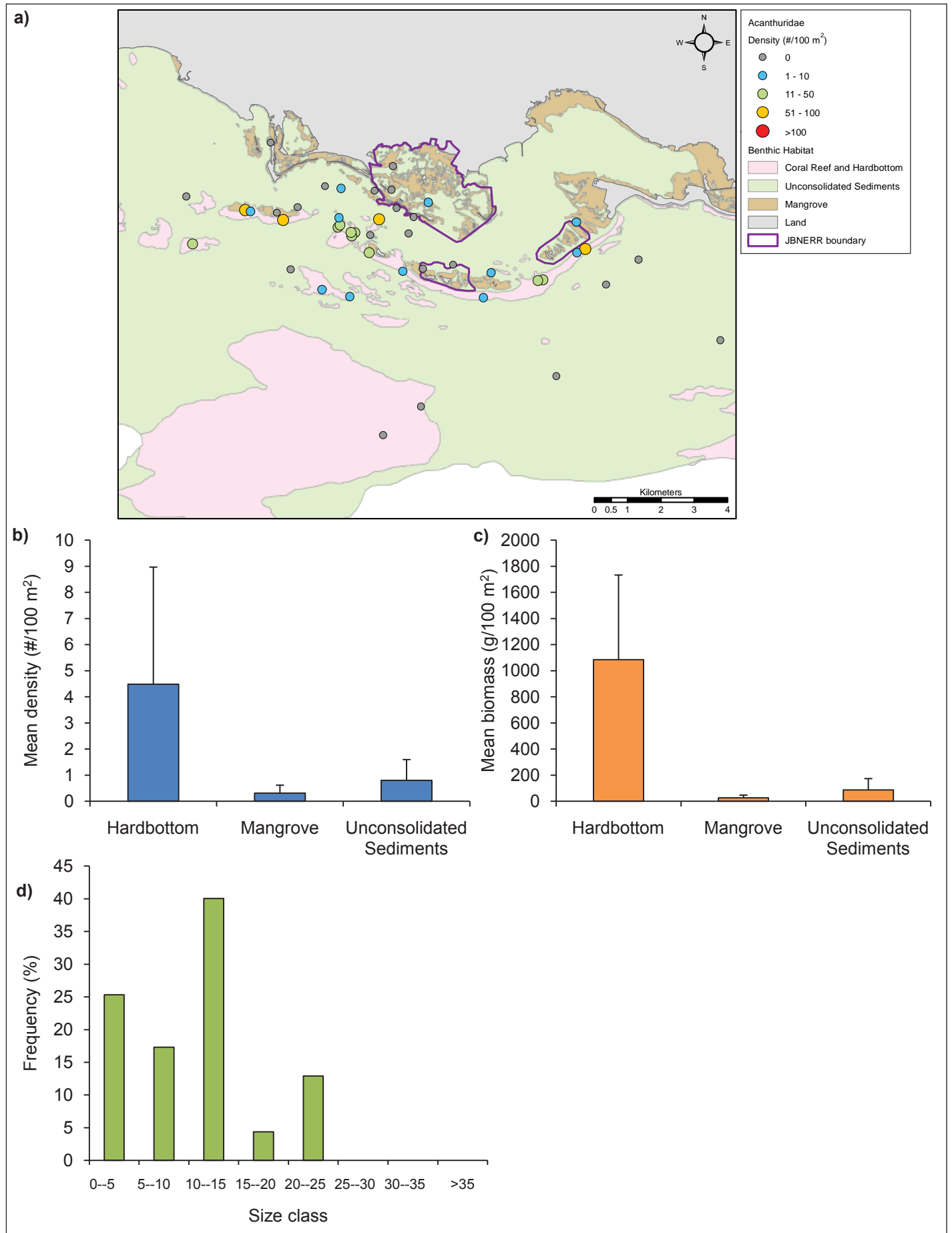


Figure 3.41. a) Spatial distribution, b) mean (\pm SE) density by habitat, c) mean (\pm SE) biomass by habitat, and d) size frequency histogram of surgeonfishes (Family Acanthuridae).

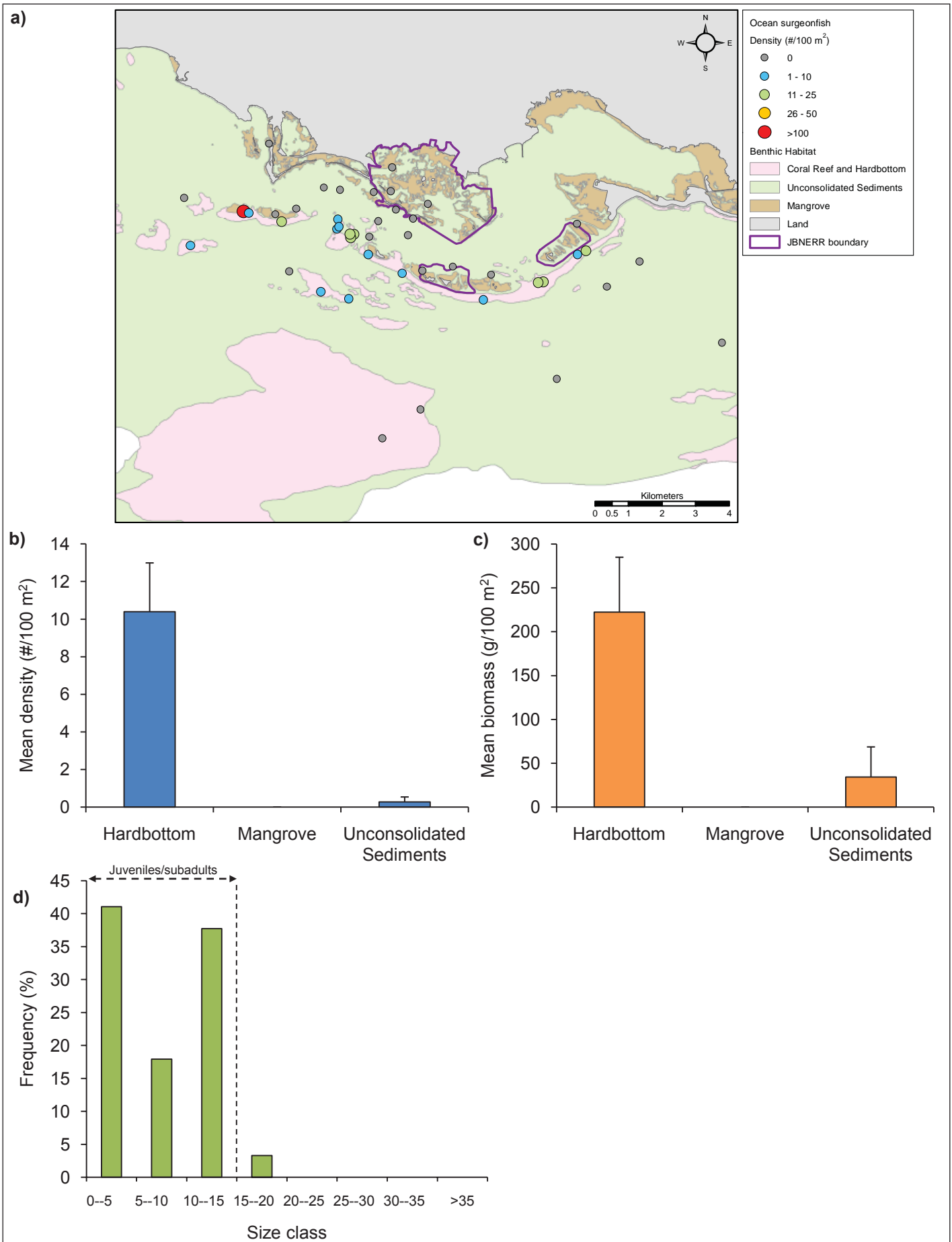


Figure 3.42. a) Spatial distribution, b) mean (\pm SE) density by habitat c) mean (\pm SE) biomass by habitat, and d) size frequency histogram of ocean surgeonfish (*Acanthurus bahianus*).

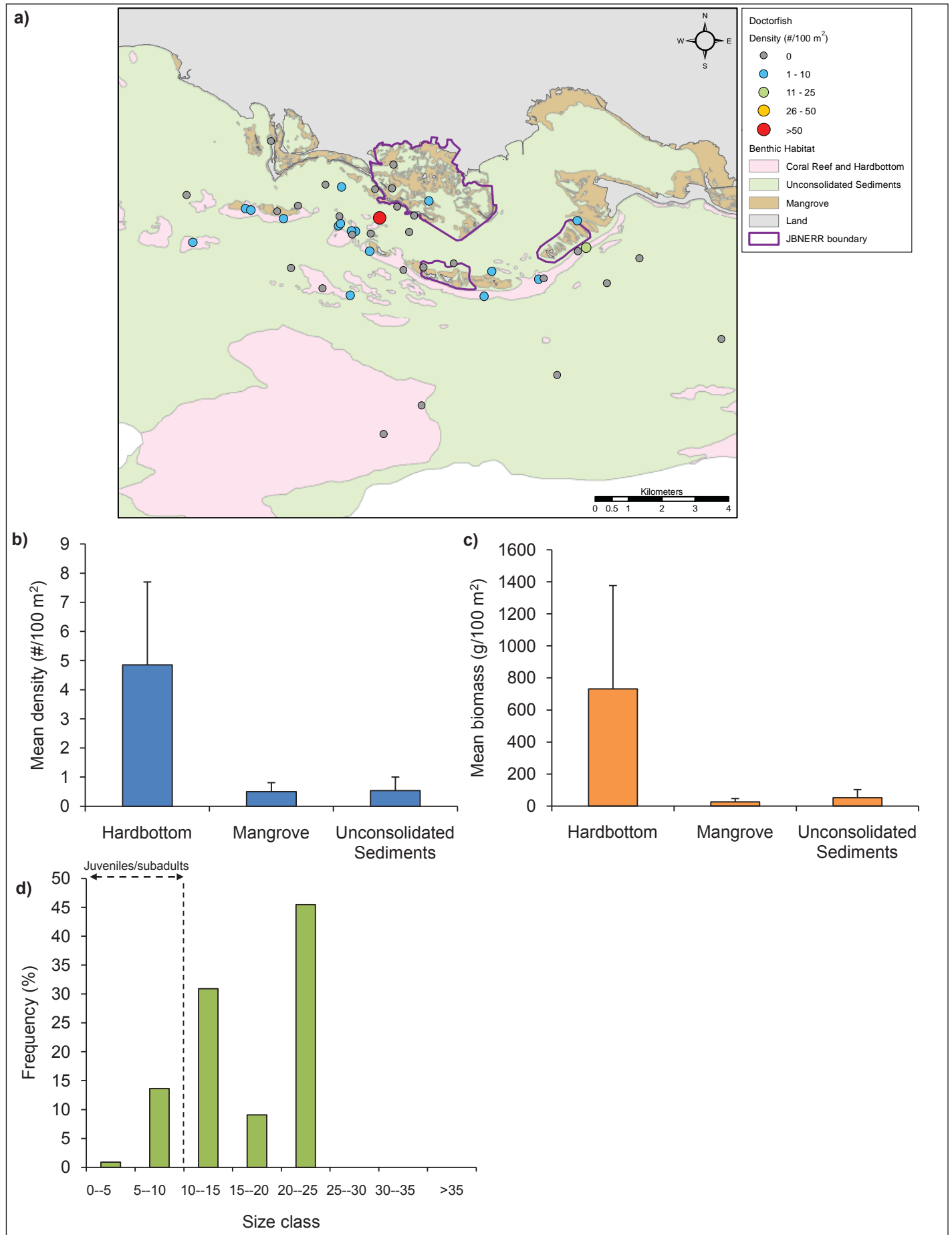


Figure 3.43. a) Spatial distribution, b) mean (\pm SE) density by habitat c) mean (\pm SE) biomass by habitat, and d) size frequency histogram of doctorfish (*Acanthurus chirurgus*).

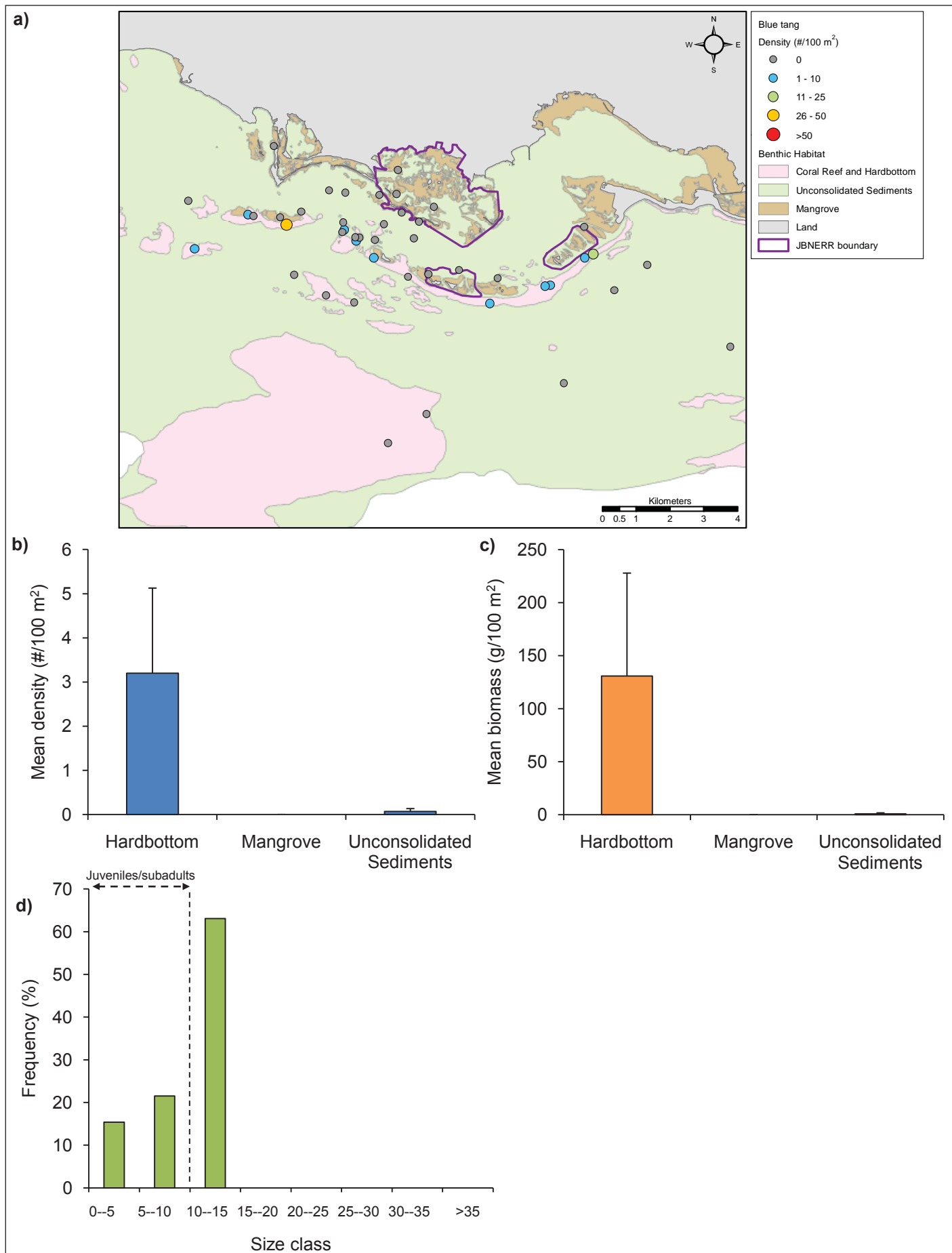


Figure 3.44. a) Spatial distribution, b) mean (\pm SE) density by habitat c) mean (\pm SE) biomass by habitat, and d) size frequency histogram of blue tang (*Acanthurus coeruleus*).

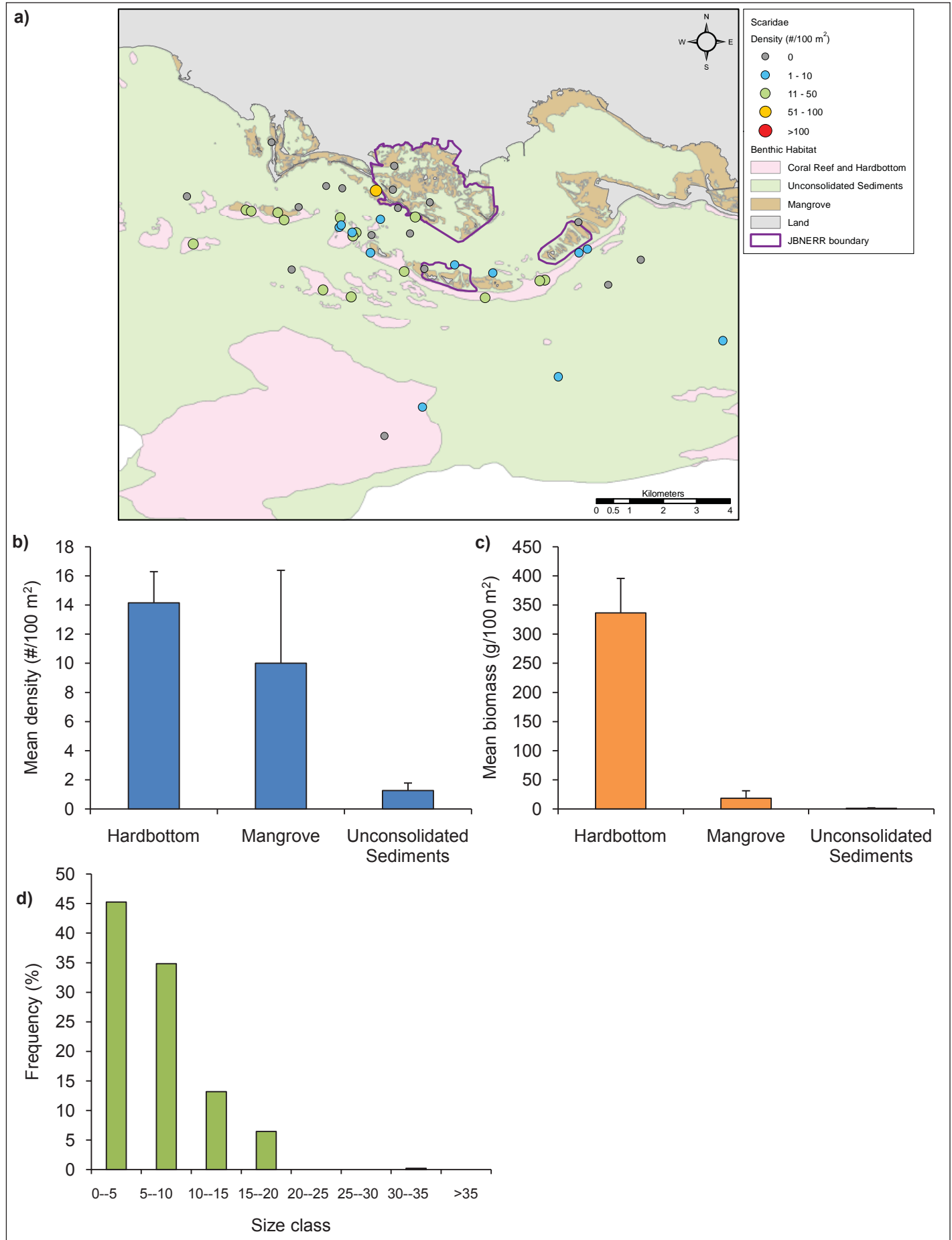


Figure 3.45. a) Spatial distribution, b) mean (\pm SE) density by habitat c) mean (\pm SE) biomass by habitat, and d) size frequency histogram of parrotfishes (Family Scaridae).

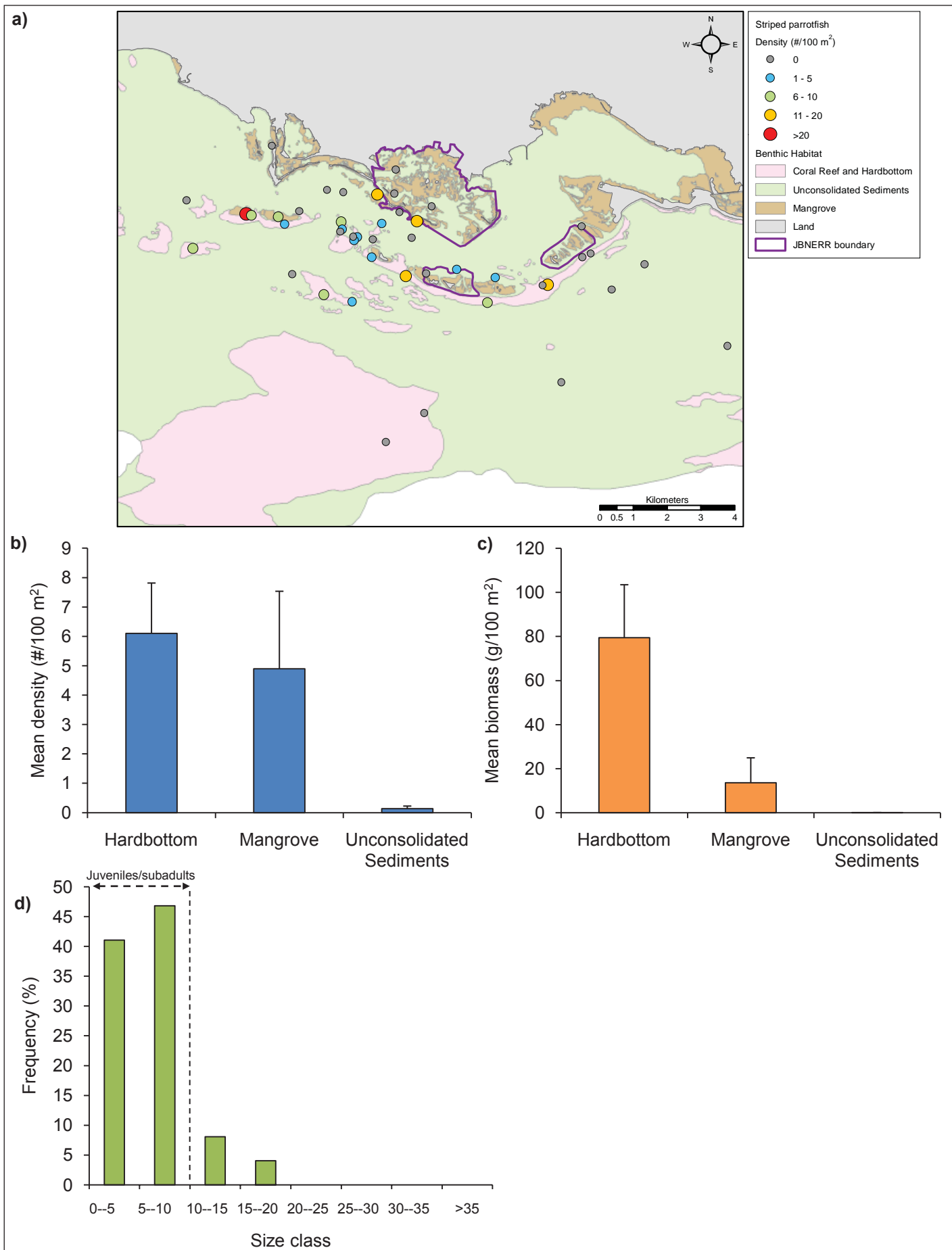


Figure 3.46. a) Spatial distribution, b) mean (\pm SE) density by habitat c) mean (\pm SE) biomass by habitat, and d) size frequency histogram of striped parrotfish (*Scarus iseri*).

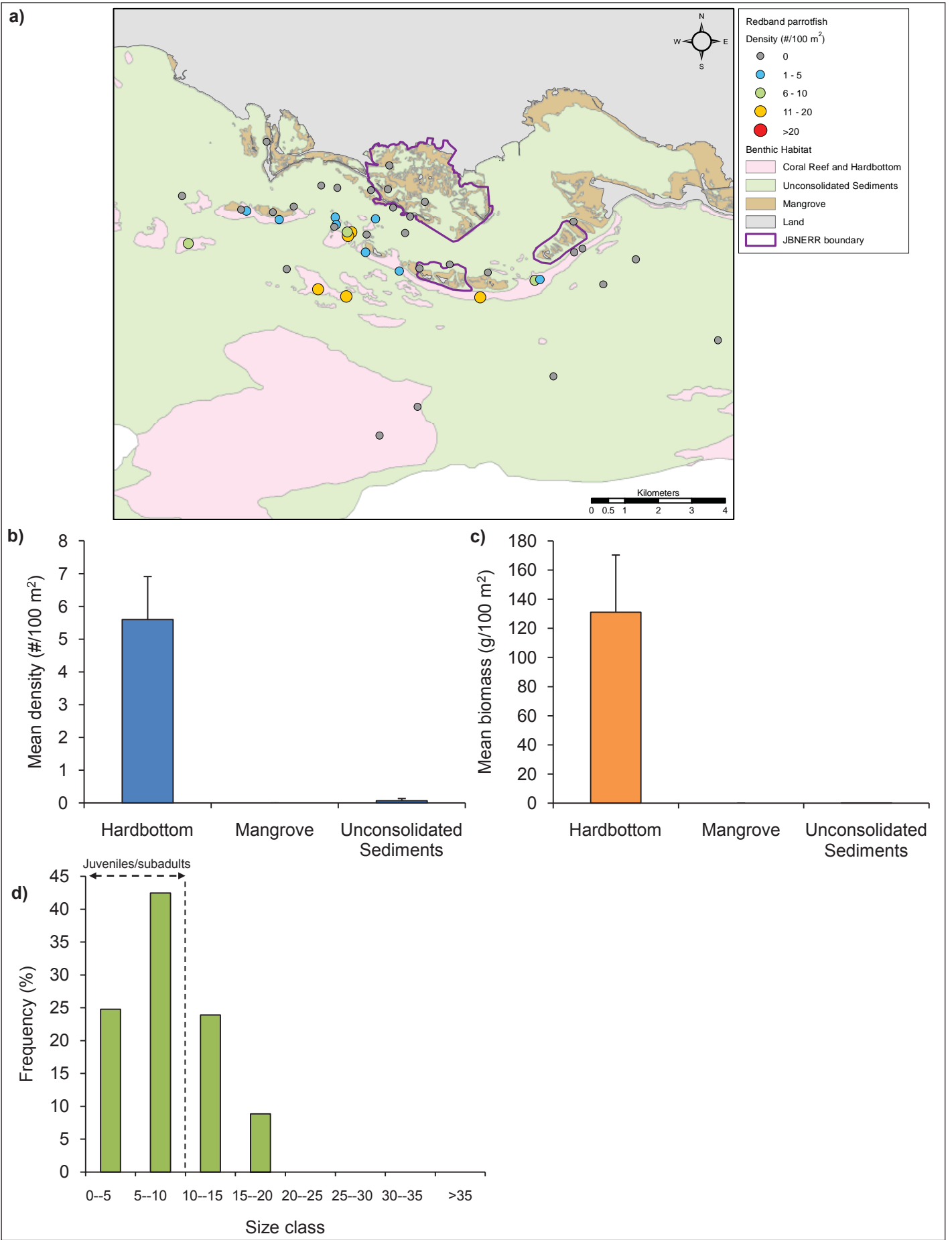


Figure 3.47. a) Spatial distribution, b) mean (\pm SE) density by habitat c) mean (\pm SE) biomass by habitat, and d) size frequency histogram of redband parrotfish (*Sparisoma aurofrenatum*).

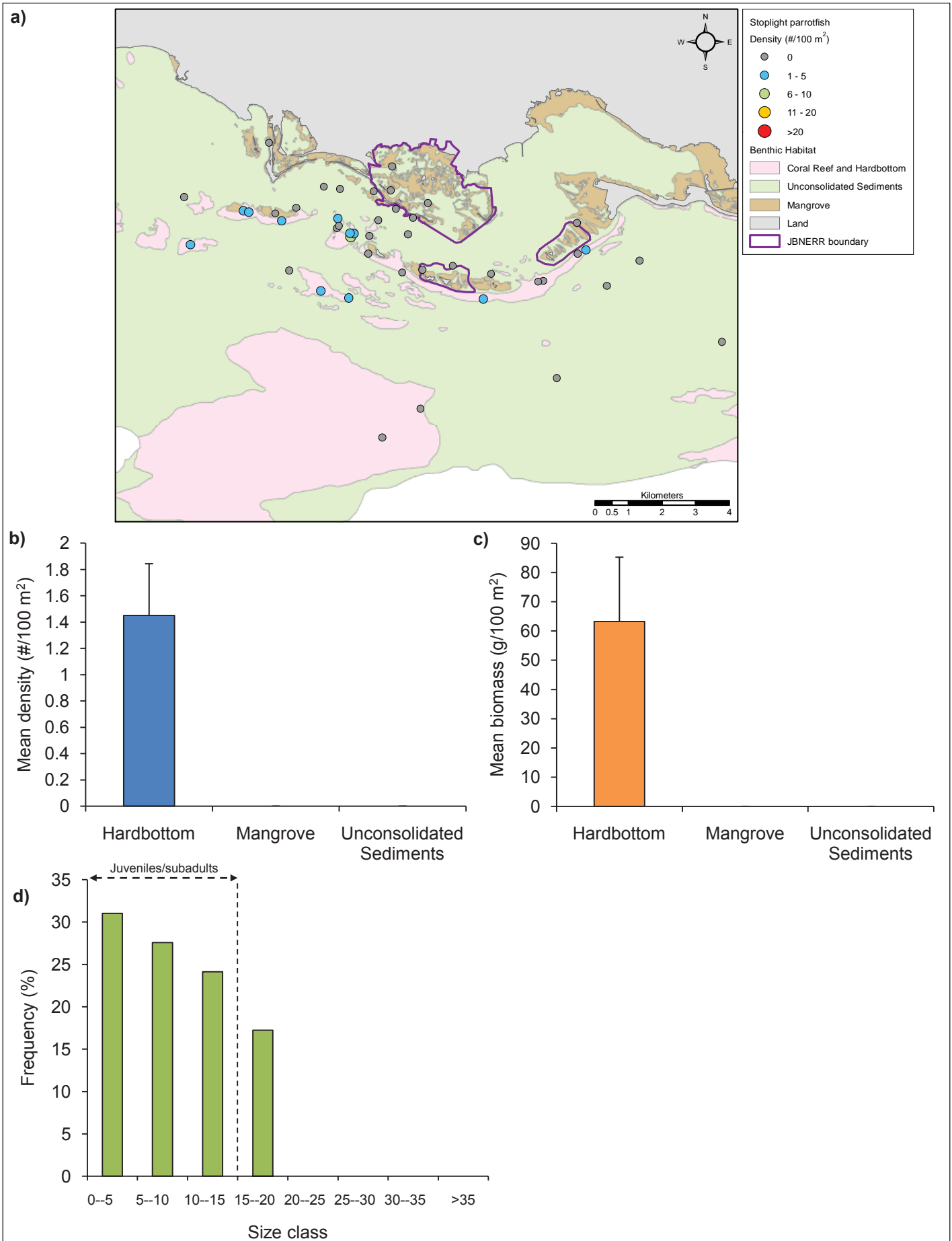


Figure 3.48. a) Spatial distribution, b) mean (\pm SE) density by habitat c) mean (\pm SE) biomass by habitat, and d) size frequency histogram of stoplight parrotfish (*Sparisoma viride*).

Wrasses (Labridae)

Wrasses were commonly sighted, occurring in 64% of surveys overall and all but two hardbottom surveys. Mean density and biomass were highest on hardbottom (Figure 3.49). Sites with particularly high density include sites on the fore reef seaward of the cays. Due to their typically small size, biomass was typically low and did not exceed 500 g/100 m² in any survey. Labrids were generally present in smaller numbers on unconsolidated sediments and were largely absent in mangroves. Eleven Labrid species were documented, with bluehead wrasse, blackear wrasse (*Halichoeres radiatus*) and slippery dick (*Halichoeres bivittatus*) accounting for the highest site frequency, density and biomass. Hogfish (*Lachnolaimus maximus*), a common species in Puerto Rico finfish fisheries, were present in only two survey transects.

Goatfishes (Mullidae)

Fishes of the goatfish family (Mullidae) were present in 27% of survey transects. The site with the highest abundance and biomass was located on unconsolidated sediments in close proximity to reef (Figure 3.50). All other occurrences of mullids were on hardbottom. The family was represented by two species, the spotted goatfish (*Pseudupeneus maculatus*), which was most common, and yellow goatfish (*Mulloidichthys martinicus*). All individuals were <15 cm in length, which is below the size at maturity for both species.

Damselfishes (Pomacentridae)

Damselfishes were present across all bottom types, occurring in 76% of survey transects. Highest abundance and biomass were found on hardbottom habitats, with intermediate levels in the fringing mangrove (Figure 3.51). Sites with a density of >50 fish/100 m² were located on reef adjacent to Cayos de Pájaros and Cayos Caribe. Nine damselfish species were found during the Jobos Bay study, with longfin damselfish (*Stegastes diencaeus*), beaugregory (*Stegastes leucostictus*) and bicolor damselfish (*Stegastes partitus*) having the greatest site frequency and accounting for the highest mean density. Damselfish species with the highest mean biomass were the longfin damselfish and beaugregory. The size frequency of damselfishes was skewed towards smaller size classes, with >65% of individuals less than 5 cm in length.

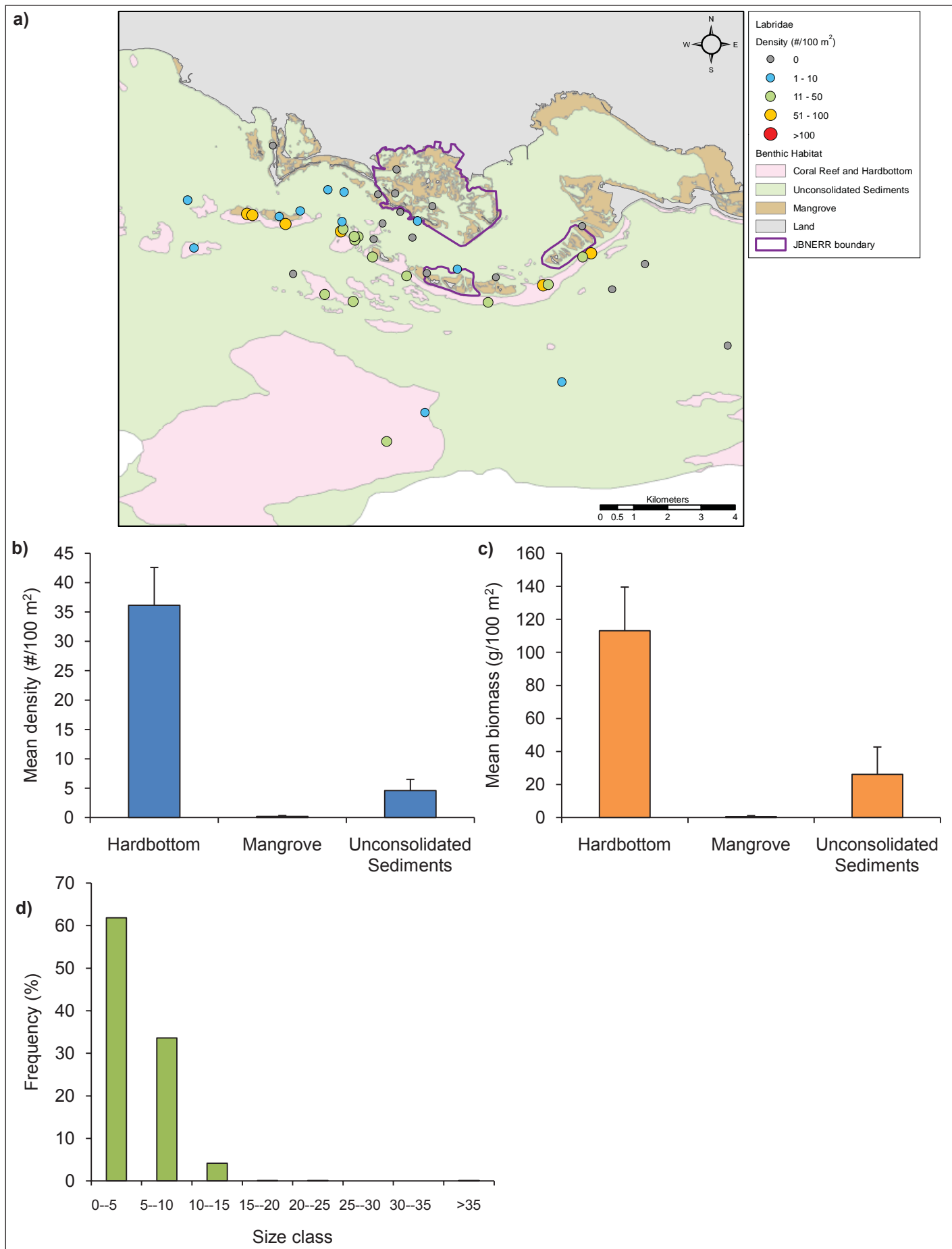


Figure 3.49. a) Spatial distribution, b) mean (\pm SE) density by habitat c) mean (\pm SE) biomass by habitat, and d) size frequency histogram of wrasses (Family Labridae).

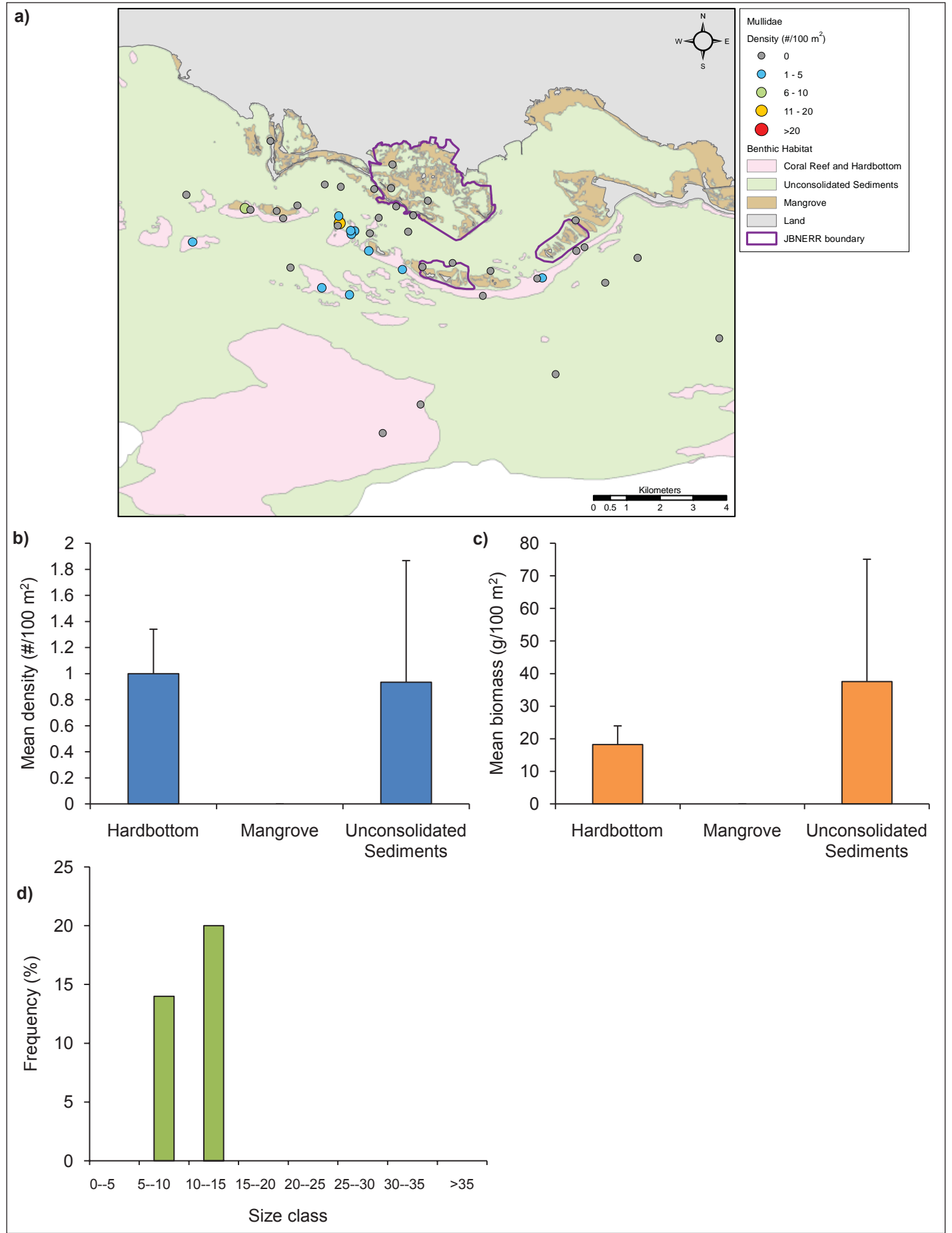


Figure 3.50. a) Spatial distribution, b) mean (\pm SE) density by habitat c) mean (\pm SE) biomass by habitat, and d) size frequency histogram of goatfishes (Family Mullidae).

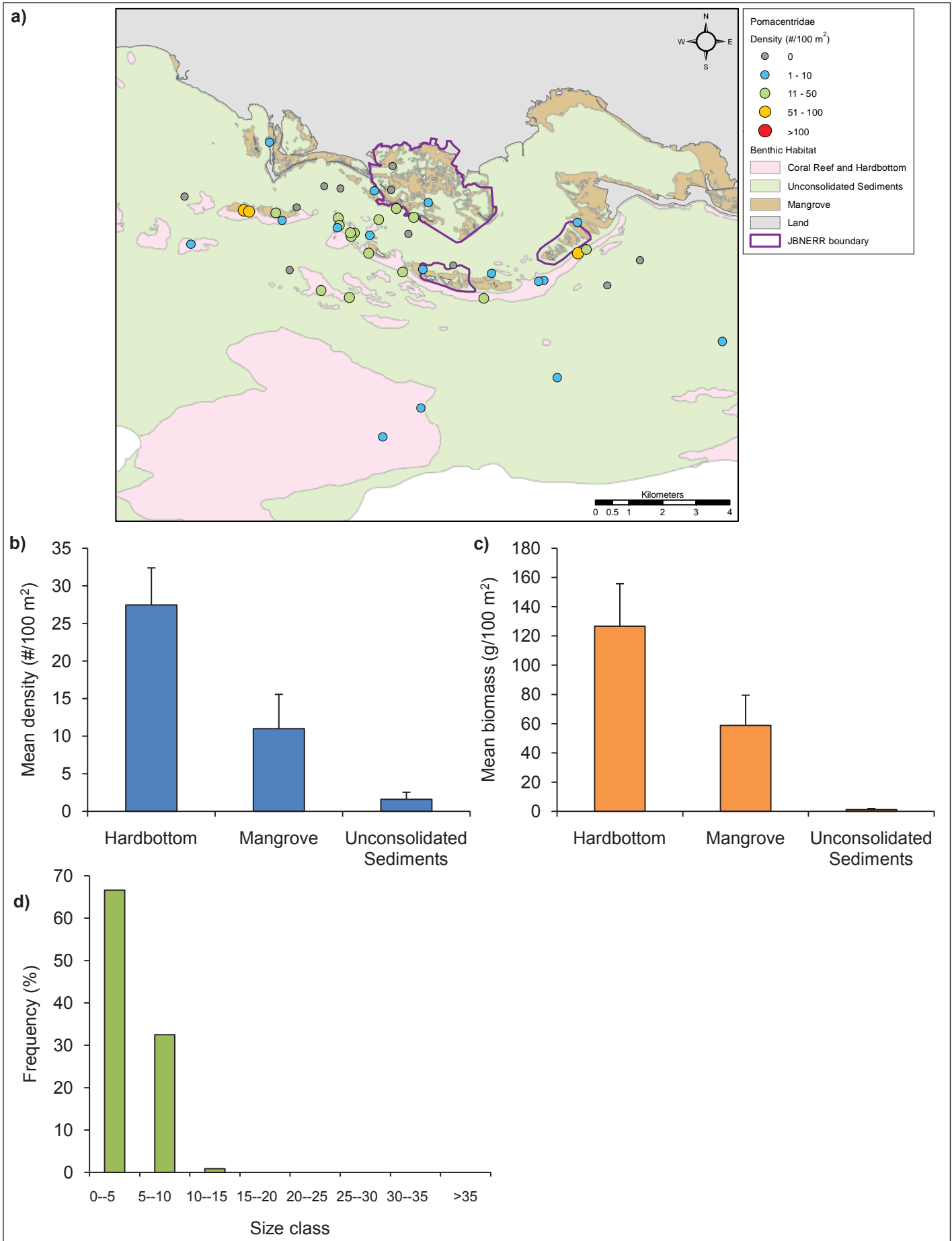


Figure 3.51. a) Spatial distribution, b) mean (\pm SE) density by habitat c) mean (\pm SE) biomass by habitat, and d) size frequency histogram of damselfishes (Family Pomacentridae).

Macroinvertebrates

No spiny lobster (*Panulirus argus*) were observed within any of the surveys. Only two queen conch (*Eustrombus gigas*) were observed in two of the 45 surveyed transects. Both conch were immature juveniles and recorded on unconsolidated sediment sites within the bay. No mature conch were observed.

A total of 129 long-spined urchins (*Diadema antillarum*) were observed in five (four hard and one soft) survey transects. Although only observed at a few sites, long-spined urchins were patchily abundant where found. Two sites accounted for approximately 97% of the total urchins recorded. Eighty-one individuals were recorded on a hardbottom survey site adjacent to Cayos de Ratones, while 44 individuals were observed at an unconsolidated sediment site in the lagoon near Cayos de Pájaros (Figure 3.52).

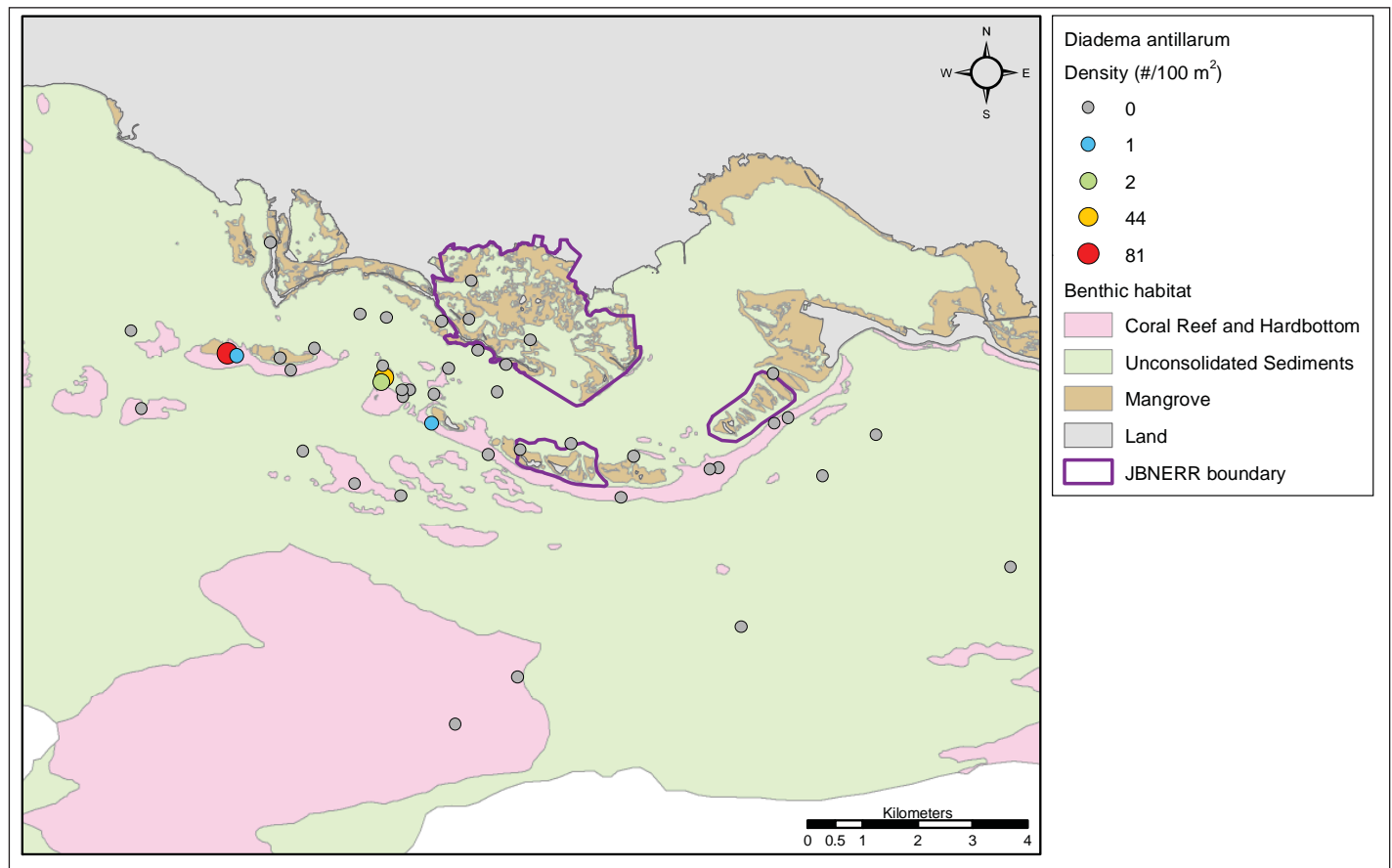


Figure 3.52. Spatial distribution of the long-spined sea urchin (*Diadema antillarum*).

Marine Debris

A total of eight marine debris items were recorded in three survey transects (Table 3.2). Items ranged from glass bottles to a tire. The majority of debris was observed in two surveys located in the mangrove cays (Figure 3.53). Several of the items were colonized by various algal groups (*i.e.*, cyanobacteria, crustose algae) and a net with rope was found entangled in the mangrove roots.

Table 3.2. Number, type, area, and degree of fouling on marine debris recorded in Jobos Bay transects.

Station	Number	Debris Type	Debris Area (cm ²)	Colonized By
1H06	1	Glass beer bottle	24	Uncolonized
1M17	2	Bottle	150	Crustose algae (CCA)
		Whistle	10	Uncolonized
		Piece of rope (used for net)	300	Uncolonized
1M30	5	Tire (tire diameter = 1 m)	7850	Cyanobacteria
		Glass soda bottle	150	Cyanobacteria
		Tin can	400	Cyanobacteria
		Net with rope	160	Entangled in mangrove roots

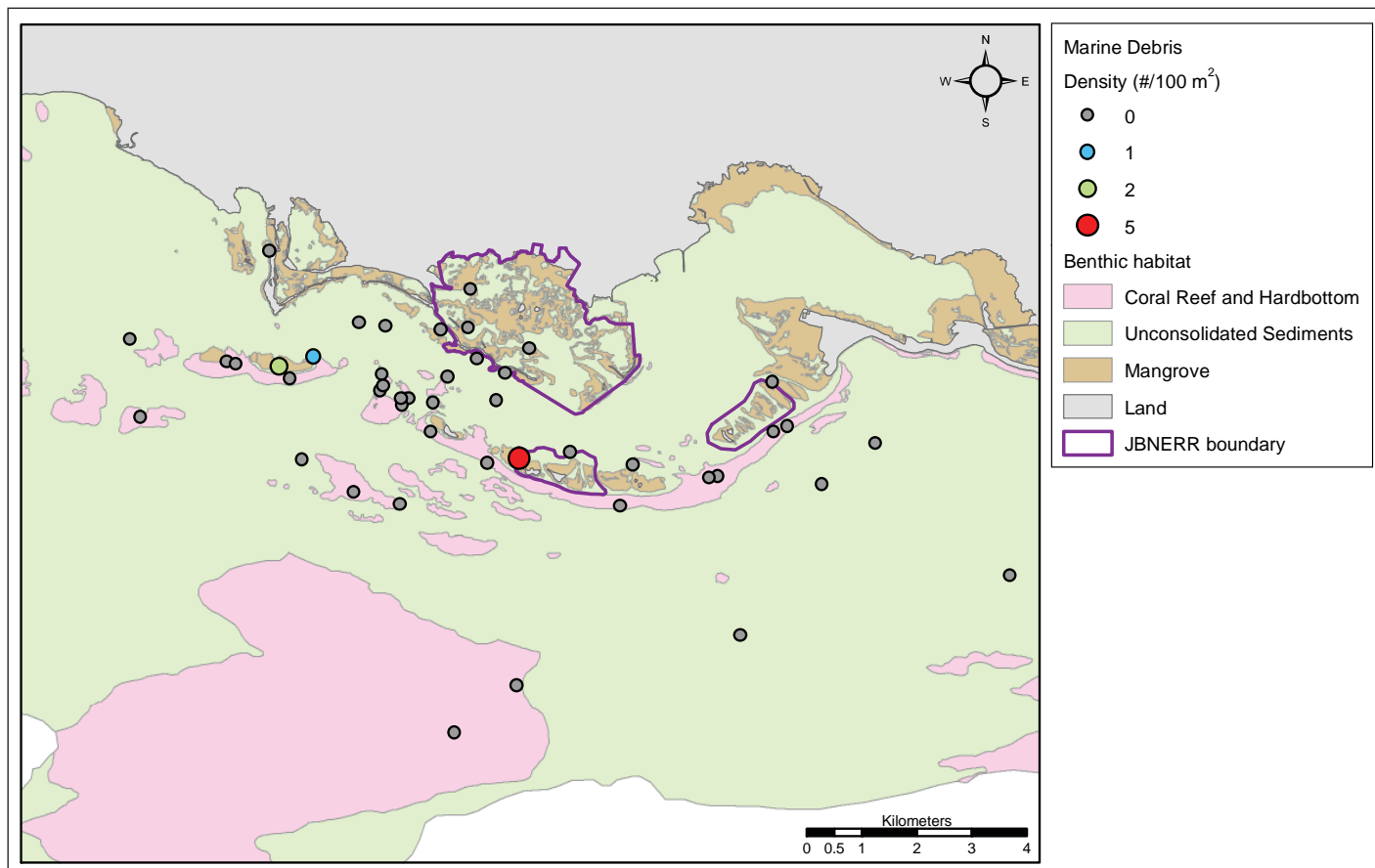


Figure 3.53. Spatial distribution of marine debris.

3.4. CONCLUSIONS

Although there are few historical studies in Jobos Bay with which to compare current conditions, the area has been subject to region-wide stresses that have affected the wider Caribbean in the last few decades, including a widespread die-off of *D. antillarum* in the 1980s, mass *Acropora* species mortality due to white band disease, coral bleaching, overfishing, and tropical cyclones. A recent meta-analysis indicates that live coral cover in the Caribbean has declined by 80% over the last three decades (Gardner *et al.*, 2003). This loss has led to a “flattening,” or decline in rugosity, of reefs over time (Alvarez-Filip *et al.*, 2009). Caribbean region-wide declines in fish abundance have also been documented (Paddack *et al.*, 2009). Elkhorn (*A. palmata*; Figure 3.54) and staghorn coral (*A. cervicornis*), which were formerly dominant reef builders in shallow and intermediate fore reef communities, respectively, have been devastated by white-band disease (Aronson and Precht, 2001). In Puerto Rico, recovery from the initial 1980’s outbreak has been limited and acroporid populations have declined significantly at locations island-wide where they were formerly abundant (Weil *et al.*, 2002). While *A. palmata* was reported to be highly abundant on the reef crest in the 1970s (PRNC 1972), it was rarely sighted in this study and absent from all survey quadrats. The presence of *Acropora* rubble at several locations observed both during this study and by García-Sais *et al.* (2003) are additional evidence of their former abundance.



Figure 3.54. Elkhorn coral (*Acropora palmata*) in Jobos Bay. Photo: NOAA CCMA.

Puerto Rican reefs experienced further declines in coral cover following the recent 2005 bleaching event (García-Sais *et al.*, 2008). In addition, local anthropogenic stresses to the Jobos Bay marine environment include thermal discharges from the Aguirre thermoelectric power plant, sewage inputs, mangrove deforestation, and runoff from agriculture and developed lands.

Reef and hardbottom benthic communities in Jobos Bay appear to be similar to other regions of Puerto Rico and the USVI. Since 2001, BB has regularly monitored habitat and fish communities using the same survey methodology in other U.S. Caribbean locations, including the BIRNM in St. Croix, USVI (Pittman *et al.*, 2008) and La Parguera in southwestern Puerto Rico (Pittman *et al.*, 2010). Additionally, a characterization of reef/hardbottom communities was recently conducted in Vieques, Puerto Rico (Bauer and Kendall, 2010). Hard coral cover in nearby La Parguera averaged $5.3 \pm 0.3\%$ over a period of seven years (2001-2007; Pittman *et al.*, 2010). The authors also detected a decreasing trend in hard coral cover over time. Similarly, hard coral cover in St. Croix averaged $5.6 \pm 0.5\%$ over 2001-2006 (Pittman *et al.*, 2008). In Vieques, measured coral cover from the 2007 survey averaged $3.4 \pm 0.5\%$ (Bauer and Kendall, 2010). At all of these locations, turf algae and macroalgae were the dominant benthic cover types on reef and hardbottom.

Additionally, fish community metrics and species composition in Jobos Bay appear to be similar to that of La Parguera in SW Puerto Rico (Pittman *et al.*, 2010). Both areas are characterized by

a diverse assemblage of benthic habitat types. In particular, both regions contain extensive networks of mangrove forest and offshore cays fringed by reef tracts. While the La Parguera study area lacks a substantial “inner bay” of similar scope as Jobos, the central and outer portions of Jobos Bay, which likely receive greater water exchange than the more protected inner bay, were primarily surveyed here. Mean total fish biomass was similar across habitat types in Jobos and La Parguera (Figure 3.55). While biomass appears to be lower in Jobos than Vieques (hardbottom only) and St. Croix (hardbottom and unconsolidated sediments only), results of non-parametric tests indicate no significant difference in biomass in the Jobos Bay region compared to the other study areas ($p > 0.05$). This is likely influenced at least in part by the lower sample size and relatively high variability in the Jobos and Vieques datasets.

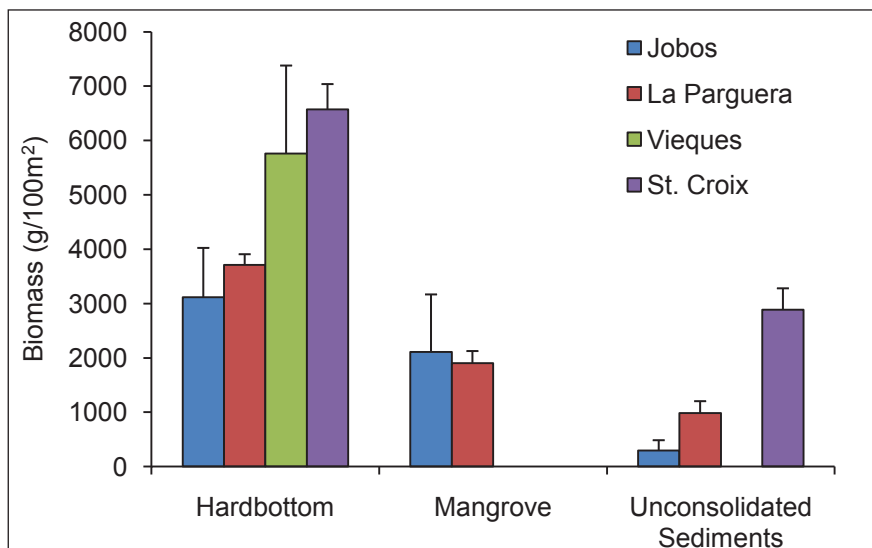


Figure 3.55. Estimated mean (\pm SE) biomass in Jobos Bay in June 2009 compared to other CCMA Biogeography Branch monitoring locations: Vieques, PR (2007; Bauer and Kendall 2010) La Parguera, PR (2001-2007; Pittman et al., 2010), St. Croix (2003-2006; Pittman et al., 2008).

While biomass appears to be lower in Jobos than Vieques (hardbottom only) and St. Croix (hardbottom and unconsolidated sediments only), results of non-parametric tests indicate no significant difference in biomass in the Jobos Bay region compared to the other study areas ($p > 0.05$). This is likely influenced at least in part by the lower sample size and relatively high variability in the Jobos and Vieques datasets.

Recent surveys of fish communities in Jobos Bay include García and Castro (1997) and García-Sais *et al.* (2003). In both studies, transects were conducted on both reef crest and deeper slope hardbottom structure near Cayos de Barca and Cayos Caribe. Similar to the findings of this characterization, the fish community consisted largely of small herbivores such as damselfish, parrotfish, and surgeonfish, and small invertivores (e.g., wrasses; García and Castro, 1997; García-Sais *et al.*, 2003). Snappers, grunts, and other species of commercial importance were generally low in abundance and small sized.

While CEAP Special Emphasis Watersheds (SEW) are distributed nationwide, only one other coastal watershed, the Choptank River in the Chesapeake Bay, has been designated a SEW. As Jobos Bay represents the first coastal SEW established in the tropics, this project represents a unique opportunity to assess the effect of agricultural conservation practices on a coral reef ecosystem. Land-based sources of pollution are widely attributed to be a contributing factor to coral reef decline (e.g., Waddell and Clarke, 2008), but identifying the relative contribution of individual anthropogenic activities to reef degradation is challenging, especially at the regional level (Downs *et al.*, 2005; Fabricius, 2005; Wolanski *et al.*, 2009). Sedimentation has been found to smother corals, lead to decreased growth rates, and reduce recruitment, but the effects vary among coral species, sediment types, and environmental conditions (see review in Fabricius, 2005). Further, linkages between chemical contaminants and coral health are poorly understood (Pait *et al.*, 2007; also see Chapter 4). Understanding these cause and effect relationships are critical to effective management and restoration practices.

Similar efforts that also seek to reduce degradation of reef environments are underway in Hawaii (Conservation Reserve Enhancement Program, <http://www.fsa.usda.gov/>) and Micronesia (Richmond *et al.*, 2007). However, there is little in the literature that demonstrates the effects of restoration efforts on a reef ecosystem. It is likely that more immediate benefits of the practices will be evident in

reduced sediment and nutrient loads to the Jobos Bay system (see Chapters 4 and 5). Improvement to biological metrics such as live coral cover and fish abundance will ultimately require a reduction in multiple stressors, many of which are present at not only local but also regional and global scales (e.g., climate change, ocean acidification, overfishing).

In addition, it should be noted that agricultural land represents only 11% of total land use within the watershed (Zitello *et al.*, 2008). However, historically almost the entire watershed was cultivated by sugar cane (see Chapter 1). Although much of this land has since been re-vegetated following the demise of sugarcane production, Zitello *et al.* (2008) noted that re-vegetated agriculture fields and pasture have a higher frequency of disturbance and don't necessarily provide the same ecosystem services as naturally vegetated lands. Ultimately, the CEAP measures are likely to be most effective if efforts are simultaneously taken to mitigate other sources of runoff into Jobos Bay.

A few caveats should be considered when interpreting the results from this study. Compared to other study locales within the CREM project, the sample size was relatively low (e.g., 45 in Jobos Bay compared to 90 surveyed annually in La Parguera). While the number of sample sites appear to be adequate to characterize differences in community metrics among the broad habitat strata, sample size was not adequate to characterize among finer scale habitats within strata, or among the three geographic strata (Inshore, Offshore, Shelf). Increased sample size would improve statistical power for detecting changes in metrics over time and should be considered when planning subsequent monitoring. Continued monitoring of permanent sites established by García-Sais *et al.* (2003) would provide further information on long-term changes in the ecosystem.

Additional challenges should be considered when conducting future monitoring of the Jobos Bay marine ecosystem. Several planned survey sites were not sampled because of high turbidity. It may be that the visual survey method by divers is not the most effective means of surveying these regions. Additionally, diving was not suitable to explore deeper (>100 ft) areas of the shelf, meaning that a potentially important part in the Jobos Bay ecosystem has not been characterized. Alternative methods (e.g., trawl nets, traps) could be explored to fully characterize fish populations in areas characterized by poor visibility or depths that exceed the limits of diving.

ACKNOWLEDGEMENTS

Funding for this work was provided by NOAA's Coral Reef Conservation Program (CRCP) and the U.S. Department of Agriculture (USDA) Natural Resources Conservation Service (NRCS). Many thanks to Captain Angel Nazario (*Aquanauta*) and his assistant Joel (Joito) Rivera and Claudio Burgos (JBNERR) for getting us safely to and from our sites. Angel Dieppa (JBNERR) provided invaluable logistical support before and during the survey. Charles Menza assisted in the collection of field data. Thanks to Matthew Kendall, Matthew Poti, Jorge "Reni" García-Sais, and Angel Dieppa for providing useful comments and editorial assistance.

REFERENCES

- Alvarez-Filip, L., N.K. Dulvy, J.A. Gill, I.M. Côte, and A.R. Watkinson. 2009. Flattening of Caribbean coral reefs: region-wide declines in architectural complexity. *Proceedings of the Royal Society B: Biological Sciences* 276: 3019-3025.
- Aronson, R.B. and W.F. Precht. 2001. White-band disease and the changing face of Caribbean coral reefs. *Hydrobiologia* 460: 25-38.

Ault, J.S., S.G. Smith, J. Luo, M.E. Monaco, and R.S. Appeldoorn. 2008. Length-based assessment of sustainability benchmarks for several coral reef fishes in Puerto Rico. *Environmental Conservation* 35(3): 221-231.

Bauer, L.J. and M.S. Kendall. 2010. Characterization of Reef and Hardbottom Habitats, Associated Reef Communities, and Marine Debris in Vieques. pp. 47-87. In: L.J. Bauer and M.S. Kendall (eds.). *An Ecological Characterization of the Marine Resources of Vieques, Puerto Rico Part II: Field Studies of Habitats, Nutrients, Contaminants, Fish, and Benthic Communities*. NOAA Technical Memorandum NOS NCCOS 110. Silver Spring, MD. 174 pp.

Clarke, K.R. and R.M. Warwick. 2001. *Change in marine communities: an approach to statistical analysis and interpretation*, 2nd Edition. PRIMER-E. Plymouth Marine Laboratory, Plymouth. 144 pp.

Cochran, W.G. 1977. *Sampling Techniques*. John Wiley and Sons, Inc., New York. 413 pp.

Department of Natural and Environmental Resources (DNER). 2002. *Jobos Bay Estuarine Profile: A National Estuarine Research Reserve*. Puerto Rico DNER and National Oceanic and Atmospheric Administration, Office of Ocean and Coastal Resource Management, Estuarine Reserve Division. 107 pp.

Downs, C.A., C.M. Woodley, R.H. Richmond, L.L. Lanning, and R. Owen. 2005. Shifting the paradigm of coral-reef 'health' assessment. *Marine Pollution Bulletin* 51: 486-494.

Fabricius, K.E. 2005. Effects of terrestrial runoff on the ecology of corals and coral reefs: review and synthesis. *Marine Pollution Bulletin* 50: 125-146.

Froese, R. and D. Pauly (eds.). 2008. *FishBase*. World Wide Web electronic publication. (Online) <http://www.fishbase.org> version (06/2008), (Accessed 10 June 2011).

García-Cagide, A., R. Claro, and B.V. Koshelev. 1994. Reproducción. pp. 187-262. In: R. Claro (ed.) *Ecología de los peces marinos de Cuba*. Instituto de Oceanología Academia de Ciencias de Cuba and Centro de Investigaciones de Quintana Roo (CIQRO) México. 525 pp.

García, J.R. and R. Castro. 1997. Survey of marine communities associated with coral reefs and seagrass beds and mangrove root habitats at Jobos Bay Natural Estuarine Research Reserve (JOBANERR). Final report prepared for Jobos Bay Natural Estuarine Research Reserve. 70 pp.

García-Sais, J.R., R. Castro, J. Sabater and M. Carlo. 2003. Survey of Marine Communities in Jobos Bay, Aguirre Power Plant. 316 Demonstration Studies. Reef Surveys, submitted to Washington Group International, Inc.

García-Sais, J., R. Appeldoorn, T. Battista, L. Bauer, A. Bruckner, C. Caldow, L. Carrubba, J. Corredor, E. Diaz, C. Lilyestrom, G. García-Moliner, E. Hernández-Delgado, C. Menza, J. Morrell, A. Pait, J. Sabater, E. Weil, E. Williams and S. Williams. 2008. The State of Coral Reef Ecosystems of Puerto Rico. pp. 75-116. In: J.E. Waddell and A.M. Clarke (eds.). *The State of Coral Reef Ecosystems of the United States and Pacific Freely Associated States: 2008*. NOAA Technical Memorandum NOS NCCOS 73. Silver Spring, MD. 569 pp.

Gardner, T., I.M. Cote, J.A. Gil, A. Grant, and A. Watkinson. 2003. Long-term region-wide declines in Caribbean corals. *Science* 301: 958-960.

Kendall, M.S., C.R. Kruer, K.R. Buja, J.D. Christensen, M. Finkbeiner, R.A. Warner, and M.E. Monaco. 2001. Methods Used to Map the Benthic Habitats of Puerto Rico and the U.S. Virgin Islands. NOAA Technical Memorandum NOS NCCOS CCMA 152. Silver Spring, MD. 46 pp.

Menza, C., J. Ault, J. Beets, C. Bohnsack, C. Caldow, J. Christensen, A. Friedlander, C. Jeffrey, M. Kendall, J. Luo, M.E. Monaco, S. Smith, and K. Woody. 2006. A guide to monitoring reef fish in the National Park Service's South Florida/Caribbean Network. NOAA Technical Memorandum NOS NCCOS 39. Silver Spring, MD. 166 pp.

Pait, A.S., D.R. Whitall, C.F.G. Jeffrey, C. Caldow, J.D. Christensen, M.E. Monaco, A.L. Mason, and J. Ramirez. 2007. Land-based sources of pollution in Southwest Puerto Rico: an assessment of chemical contaminants in coral reef ecosystem study sediments. NOAA Technical Memorandum NOS NCCOS 52. Silver Spring, MD. 112 pp.

Paddack, M.J., J.D. Reynolds, C. Aguilar, R.S. Appeldoorn, J. Beets, E.W. Burkett, P.M. Chittaro, K. Clarke, R. Esteves, A.C. Fonseca, G.E. Forrester, A.M. Friedlander, J. García-Sais, G. González-Sansón, L.K.B. Jordan, D.B. McClellan, M.W. Miller, P.P. Molloy, P.J. Mumby, I. Nagelkerken, M. Nemeth, R. Navas-Camacho, J. Pitt, N.V.C. Polunin, M.C. Reyes-Nivia, D.R. Robertson, A. Rodríguez-Ramírez, E. Salas, S.R. Smith, R.E. Spieler, M.A. Steele, I.D. Williams, C.L. Wormald, A.R. Watkinson, and I.M. Côté. 2009. Recent region-wide declines in Caribbean reef fish abundance. *Current Biology* 19: 590-595.

Pittman, S.J., S.D. Hile, C.F.G. Jeffrey, C. Caldow, M.S. Kendall, M.E. Monaco, and Z. Hillis-Starr. 2008. Fish assemblages and benthic habitats of Buck Island Reef National Monument (St. Croix, U.S. Virgin Islands) and the surrounding seascape: A characterization of spatial and temporal patterns. NOAA Technical Memorandum NOS NCCOS 71. Silver Spring, MD. 96 pp.

Pittman, S.J., S.D. Hile, C.F.G. Jeffrey, R. Clark, K. Woody, B.D. Herlach, C. Caldow, M.E. Monaco, R. Appeldoorn. 2010. Coral reef ecosystems of Reserva Natural La Parguera (Puerto Rico): Spatial and temporal patterns in fish and benthic communities (2001-2007). NOAA Technical Memorandum NOS NCCOS 107. Silver Spring, MD 202 pp.

Puerto Rico Nuclear Center (PRNC). 1972. Aguirre Power Project Environmental Studies 1972 Annual Report. PRNC-162. 464 pp.

Puerto Rico Nuclear Center (PRNC). 1975. Aguirre Environmental Studies Jobos Bay, PR, Final Report. PRNC-196. 95 pp.

Randall, J.E. 1967. Food habits of reef fishes of the West Indies. *Studies in Tropical Oceanography* (Miami) 5: 665-847.

Richmond, R.H., T. Rongo, Y. Golbuu, S. Victor, N. Idechong, G. Davis, W. Kostka, L. Neth, M. Hamnett, and E. Wolanski. 2007. Watersheds and coral reefs: Conservation science, policy, and implementation. *BioScience* 57(7): 598-607.

Waddell, J.E. and A.M. Clarke (eds.) 2008. The state of coral reef ecosystems of the United States and Pacific Freely Associated States. 2008. NOAA Technical Memorandum NOS NCCOS 73. Silver Spring, MD 569 pp.

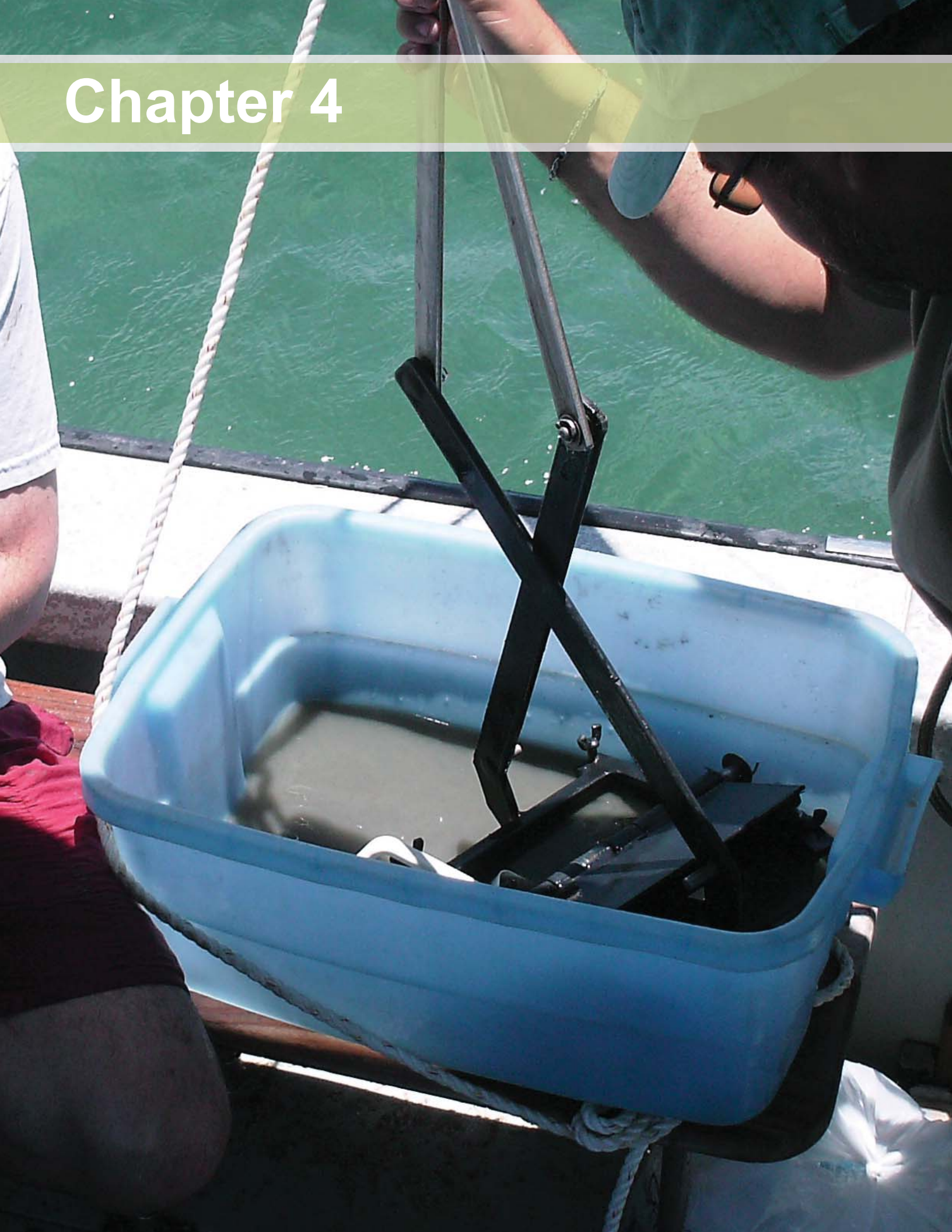
Weil, E., E.A. Hernández-Delgado, A.W. Bruckner, A.L. Ortiz, M. Nemeth, and H. Ruiz. 2002. Distribution and status of Acroporid coral (Scleractinia) populations in Puerto Rico. pp. 71-98. In: A.W. Bruckner (ed.). Proceedings of the Caribbean Acropora Workshop: Potential application of the U.S. Endangered Species Act as a conservation strategy. NOAA Technical Memorandum NMFS-OPR-24. Silver Spring, MD. 199 pp.

Wolanski, E., J.A. Martinez, and R.H. Richmond. 2009. Quantifying the impact of watershed urbanization on a coral reef: Maunalua Bay, Hawaii. *Estuarine, Coastal and Shelf Science* 84: 259-268.

Zar, JH. 2010. *Biostatistical Analysis (Fifth Edition)*. Pearson Prentice Hall, New Jersey. 944 pp.

Zitello, A.G., D.R. Whitall, A. Dieppa, J.D. Christensen, M.E. Monaco, and S.O. Rohmann. 2008. Characterizing Jobos Bay, Puerto Rico: A watershed modeling analysis and monitoring plan. NOAA Technical Memorandum NOS NCCOS 76. 81 pp.

Chapter 4



Contaminants in Sediments and Coral Tissues of Jobos Bay

David R. Whitall^{1,5}, Anthony S. Pait¹, Dennis Apeti¹, Angel Dieppa², Sarah E. Newton^{1,3}, Lia Brune^{1,4}, Chris Caldow¹, Andrew L. Mason¹ and John Christensen¹

4.1. INTRODUCTION

The goal for this component of the ecosystem characterization of Jobos Bay was to quantify the level of chemical contaminants in sediments from the Bay and in coral tissues from the surrounding coral reef ecosystems.

The objectives were to:

1. Collect and analyze sediments from sites from the Bay, including within the Jobos Bay National Estuarine Research Reserve (JBNERR or Reserve), for organic (e.g., hydrocarbons) and inorganic (e.g., trace elements, typically metals) contaminants;
2. Collect and analyze samples of mustard hill coral (*Porites astreoides*) for presence and magnitude of the same organic and inorganic contaminants.

4.2. METHODS

4.2.1. Sampling Design

In order to assess the overall status of the ecosystem, and to be able to make spatially explicit conclusions about how contaminants vary geographically in the system, a stratified random sampling design was employed. Using this approach, all areas had an equal chance of being selected for contaminant characterization. As a result, no samples were specifically collected to represent background conditions in these areas.

For sediment samples, three geographic strata were initially articulated: inner bay (INR), central bay (CNT), and outer bay (OTR). Within the central bay, a fourth strata (NER) was created, representing the subset of the central bay containing JBNERR. This additional stratum allows the hypothesis that the management of the Reserve might have an impact on the environmental quality of the system to be tested. However, it is acknowledged that, like many reserve boundaries, this does not represent an ecological boundary, and the reserve must be treated as part of the larger ecosystem. In each of these four strata, 10 sites were randomly selected. If a site could not be sampled (e.g., if the site was inaccessible due to shallow water depth) a pre-selected randomly determined alternate site from within that strata was sampled. Sediment strata were constructed from existing benthic habitat maps (Kendall *et al.*, 2001) and included all non-hard bottom sediments.

In addition to the stratified random sediment sites, targeted sediment sample sites (SWP) were co-located with four pre-existing long term water quality monitoring sites operated by the JBNERR as part of the National Estuarine Research Reserve System (NERRS) System-Wide Monitoring Program (SWMP). By chance, one of these sites overlapped with one of the randomly selected sites (CNT16), meaning that there were a total of 41 randomly selected sediment sites, and three additional targeted sediment sites. Sediments were collected from 44 total sites in May 2008 (Figure 4.1).

¹ Center for Coastal Monitoring and Assessment, National Centers for Coastal Ocean Science, National Ocean Service, National Oceanic and Atmospheric Administration

² Jobos Bay National Estuarine Research Reserve

³ University of Arkansas Pine Bluff

⁴ University of Florida

⁵ Corresponding author: dave.whitall@noaa.gov



Figure 4.1. Sediment sampling sites using a stratified random sampling design.

The coral sampling scheme divided the hard bottom habitats of the study area into “nearshore” and “offshore” strata. Within each stratum, eight sites were randomly selected. If a site could not be sampled (e.g., due to a lack of coral, or the site being inaccessible) a pre-selected randomly determined alternate site from within that strata was sampled. Coral tissue was collected from 16 sites in June 2009 (Figure 4.2). *Porites astreoides* was chosen for this study as it is a common species of coral in Florida, the Bahamas and the Caribbean (Humann and DeLoach, 2002), and occurs throughout the study area. Colonies of *P. astreoides* are generally massive but are often found as encrusting forms, particularly in shallow, surging waters (Veron, 2000). Furthermore, previous studies (Pait *et al.*, 2009, 2010) quantified contaminants in *P. astreoides* in other systems in Puerto Rico.



Figure 4.2. Coral sampling sites using a stratified random sampling design.

4.2.2. Field Methods

Sediment samples were collected using standard NOAA National Status and Trends (NS&T) Program protocols (Lauenstein and Cantillo, 1998). Sampling was conducted aboard the vessel *Estuarino* using a GPS programmed with the station coordinates. A modified Van Veen sediment grab was deployed to collect the sediment samples (Figure 4.3). Rocks, large coral or shell fragments or bits of seagrass present in the grab were removed. If an individual grab did not result in 200-300 g of sediment, a second grab was made and composited with material from the first grab. If enough sediment had not been collected after three deployments of the grab, the site was abandoned and the boat moved on to an alternate, randomly preselected site.



Figure 4.3. Project scientists lower modified van Veen grab for sediment collections. Photo: NOAA Center for Coastal Monitoring and Assessment (CCMA).

To avoid contamination of samples by equipment and cross contamination between samples, the grab was scrubbed with a brush, then rinsed with site water, and all of the equipment was rinsed with acetone followed by site water just prior to use. Personnel handling the samples also wore disposable nitrile gloves. The top 3 cm of sediment were collected from the sediment grab using a Kynar-coated sediment scoop. Sediments were placed into a certified clean (IChem[®]) 250 ml labeled jar, capped and then placed on ice in a cooler. Sediments for grain size analysis were placed in a WhirlPack[®] bag, sealed and placed on ice in a cooler. Upon returning to the JBNERR lab, sediment samples were frozen (-15°C). The WhirlPack[®] bags for grain size analysis were refrigerated (4°C), to avoid altering the grain size structure of the sediment that could occur during freezing. A suite of water parameters (dissolved oxygen, temperature, salinity, and conductivity) were measured at each site using a YSI[®] salinity/conductivity/temperature meter. The instrument probe was submerged to a depth of approximately 0.5 m.

For coral tissue samples, a Puerto Rico Department of Natural and Environmental Resources (DNER) Ranger boat was used as the sampling platform. The coral samples were taken by NOAA SCUBA divers in June 2009 using a hammer and a punch made from titanium (not a target trace element for this project). Prior to each use, the punch was rinsed with acetone and site water to minimize cross-contamination.

Divers collecting the coral samples also wore disposable nitrile gloves. The diver hammered the titanium punch into the coral head which produced a coral core with a diameter of approximately 1.5 cm and a core length 1.5 cm. Approximately 20 cores were taken at each site and placed in an IChem[®] certified clean 250 mL jar while underwater. The jar was capped and brought to the surface,

drained of water and placed on ice. At the end of each day, the samples were placed in a freezer (-15°C) at the JBNERR. At the end of the mission, samples were shipped by overnight courier to the laboratory (TDI Brooks, College Station, TX) for analyses.

4.2.3. Chemical Contaminants Analyzed

The list of chemical contaminants analyzed in the sediment and coral samples for this project is shown in Table 4.1. This is the same suite of analytes quantified nationwide as part of NOAA's NS&T Program.

For over 20 years, NS&T has monitored the Nation's estuarine and coastal waters for chemical contaminants in bivalve mollusk tissues and sediments. Work to characterize chemical contaminants as part of the Center for Coastal Monitoring and Assessment's^A (CCMA) ecological characterizations in tropical waters, represents a recent expansion of NS&T activities. NS&T regularly quantifies approximately 150 organic and inorganic contaminants. The compounds analyzed include 58 polycyclic aromatic hydrocarbons (PAHs), 31 organochlorine pesticides, 38 polychlorinated biphenyls (PCBs), four butyltins, and 16 trace and major elements. All samples were analyzed using NS&T analytical protocols.

The analytical protocols for organics (Kimbrough *et al.*, 2006) and trace and major elements (Kimbrough and Lauenstein, 2006) have previously been published. Each of the contaminant classes analyzed for this project are discussed below.

4.2.3.1. Polycyclic aromatic hydrocarbons (PAHs)

Polycyclic aromatic hydrocarbons (PAHs) are associated with the use and combustion of fossil fuels (e.g., oil and gas) and other organic materials (e.g., wood). Natural sources of PAHs include forest fires and volcanoes. The PAHs analyzed are two to six ring aromatic compounds. PAHs were analyzed using gas chromatography/mass spectrometry in the selected ion monitoring (SIM) mode.

Environmental Effects of PAHs

An extensive amount of research on the accumulation and effects of PAHs has been conducted on aquatic organisms; however, very little research has been carried out to address the effects of PAHs on corals. Because of their hydrophobic nature, PAHs readily accumulate in marine organisms through the body surface, gills, or through the diet (Neff, 1985). Exposure to PAHs has been associated with oxidative stress, effects on the immune system and endocrine system, and developmental abnormalities (Hylland, 2006).

In addition, a number of PAHs including benzo[a]pyrene, benz[a]anthracene, chrysene, benzo[b]fluoranthene, benzo[k]fluoranthene, dibenzo[a,h]anthracene, and indeno[1,2,3-c,d]pyrene are likely carcinogens (USDHHS, 1995). The carcinogenic potential of PAHs is associated with their metabolism by Phase I cytochrome P450 enzymes, generating reactive epoxides which can bind to cellular components such as deoxyribonucleic acid (DNA; Neff, 1985; Hylland, 2006). In addition to the living tissues of corals, PAHs can also accumulate in the zooxanthellae, the symbiotic photosynthetic dinoflagellate algae found within coral tissues. Bioaccumulation appears to be related to the lipid content of both (Kennedy *et al.*, 1992). While the simple accumulation of PAHs by corals is not an impact by itself, the accumulation of a chemical contaminant in an organism increases the likelihood of adverse effects. Solbakken *et al.* (1984) showed that both phenanthrene and naphthalene were accumulated by the brain coral *Diploria strigosa* and green cactus coral *Madracis decactis*, and that the lower molecular weight naphthalene was eliminated at a higher rate than phenanthrene (Solbakken *et al.*, 1984). The PAHs fluoranthene and pyrene have been shown to be toxic to adult corals, particularly

^A The Center for Coastal Monitoring and Assessment (CCMA) is a part of National Oceanic and Atmospheric Administration (NOAA), National Ocean Service (NOS), National Centers for Coastal Ocean Science (NCCOS).

in the presence of increased ultraviolet radiation as a result of phototoxicity (Peachey and Crosby, 1996; Guzmán-Martínez *et al.*, 2007).

4.2.3.2. Polychlorinated biphenyls (PCBs)

Polychlorinated biphenyls (PCBs) are a class of synthetic compounds that have been used in numerous applications ranging from electrical transformers and capacitors, to hydraulic and heat transfer fluids, to pesticides and paints. Although no longer manufactured in the United States, environmental contamination by PCBs is widespread due to their environmental persistence and tendency to bioaccumulate. In some cases, use of PCB containing equipment (e.g., railroad locomotive transformers) is still permitted (CFR, 1998). PCBs have a biphenyl ring structure (two benzene rings joined by a carbon to carbon bond) and a varying number of chlorine atoms. There are 209 PCB congeners (structures) possible. PCBs were analyzed using gas chromatography/electron capture detection.

Effects of PCBs

Exposure to PCBs in fish has been linked to reduced growth, reproductive impairment and vertebral abnormalities (USEPA, 1997). Solbakken *et al.* (1984) investigated the bioconcentration of radiolabeled hexaPCB (2,4,5,2',4',5'-hexachlorobiphenyl) in coral. The PCB was rapidly accumulated in *D. strigosa* and *M. decactis*; however, depuration proceeded at a slow rate; after 275 days nearly 33 percent of the original radioactivity from the hexaPCB remained in the coral.

4.2.3.3. Organochlorine Pesticides

A total of 31 organochlorine pesticides and related compounds were analyzed in the sediment and coral samples from Jobos Bay (Table 4.1), using standard NS&T protocols (Kimbrough *et al.*, 2006). Beginning in the 1950s and continuing to the early 1970s, a series of chlorine containing hydrocarbon insecticides were used to control mosquitoes and agricultural pests. One of the best known of the organochlorine pesticides used during this time period was dichloro-diphenyltrichloroethane (DDT). It has been estimated that during the 30 years prior to its cancellation in 1972, 1.35 billion pounds of DDT were applied in the US, with the majority applied to the cotton crop (USEPA, 1975). The use of many of the organochlorine pesticides, including DDT, was banned due to their environmental persistence, potential to bioaccumulate, and toxicity to non-target organisms. Because of their persistence and heavy use in the past, residues of many organochlorine pesticides can be found in the environment, including biota.

Effects of Organochlorine Pesticides

Organochlorine pesticides are typically neurotoxins. Both DDT and PCBs have also been shown to interfere with the endocrine system. DDT and its metabolite dichloro-diphenyldichloroethylene (DDE) were specifically linked to eggshell thinning in birds, particularly raptors. A number of organochlorine pesticides are also known to be toxic to aquatic life including crayfish, shrimp and some species of fish.

4.2.3.4. Butyltins

This class of compounds has a range of uses from biocides to catalysts to glass coatings. In the 1950s, tributyltin or TBT was first shown to have biocidal properties (Bennett, 1996). Beginning in the late 1960s, TBT was incorporated into a very effective antifoulant paint system, quickly becoming one of the most effective paints ever used on boat hulls (Birchenough *et al.*, 2002). TBT was incorporated into a polymer paint system that released the biocide at a constant and minimal rate, to control fouling organisms such as barnacles, mussels, weeds, and algae (Bennett, 1996). In the aquatic environment, TBT is degraded by microorganisms and sunlight (Bennett, 1996). The transformation involves sequential debutylization resulting in dibutyltin, monobutyltin, and finally inorganic tin (Batley,

Table 4.1. List of analytes.

PAHs Low Molecular Weight	PAHs High Molecular Weight	PCBs	Organochlorine Pesticides
Naphthalene	Fluoranthene	PCB8/5	Aldrin
1-Methylnaphthalene	Pyrene	PCB18	Dieldrin
2-Methylnaphthalene	C1-Fluoranthenes/Pyrenes	PCB28	Endrin
2,6-Dimethylnaphthalene	C2-Fluoranthenes/Pyrenes	PCB29	Heptachlor
1,6,7-Trimethylnaphthalene	C3-Fluoranthenes/Pyrenes	PCB31	Heptachlor-Epoxyde
C1-Naphthalenes	Naphthobenzothiophene	PCB44	Oxychlorane
C2-Naphthalenes	C1-Naphthobenzothiophenes	PCB45	Alpha-Chlordane
C3-Naphthalenes	C2-Naphthobenzothiophenes	PCB49	Gamma-Chlordane
C4-Naphthalenes	C3-Naphthobenzothiophenes	PCB52	Trans-Nonachlor
Benzothiophene	Benz(a)anthracene	PCB56/60	Cis-Nonachlor
C1-Benzothiophenes	Chrysene	PCB66	Alpha-HCH
C2-Benzothiophenes	C1-Chrysenes	PCB70	Beta-HCH
C3-Benzothiophenes	C2-Chrysenes	PCB74/61	Delta-HCH
Biphenyl	C3-Chrysenes	PCB87/115	Gamma-HCH
Acenaphthylene	C4-Chrysenes	PCB95	2,4'-DDT
Acenaphthene	Benzo(b)fluoranthene	PCB99	4,4'-DDT
Dibenzofuran	Benzo(k)fluoranthene	PCB101/90	2,4'-DDD
Fluorene	Benzo(e)pyrene	PCB105	4,4'-DDD
C1-Fluorenes	Benzo(a)pyrene	PCB110/77	2,4'-DDE
C2-Fluorenes	Perylene	PCB118	4,4'-DDE
C3-Fluorenes	Indeno(1,2,3-c,d)pyrene	PCB128	DDMU
Anthracene	Dibenzo(a,h)anthracene	PCB138/160	1,2,3,4-Tetrachlorobenzene
Phenanthrene	C1-Dibenzo(a,h)anthracenes	PCB146	1,2,4,5-Tetrachlorobenzene
1-Methylphenanthrene	C2-Dibenzo(a,h)anthracenes	PCB149/123	Hexachlorobenzene
C1-Phenanthrene/Anthracenes	C3-Dibenzo(a,h)anthracenes	PCB151	Pentachloroanisole
C2-Phenanthrene/Anthracenes	Benzo(g,h,i)perylene	PCB153/132	Pentachlorobenzene
C3-Phenanthrene/Anthracenes		PCB156/171/202	Endosulfan II
C4-Phenanthrene/Anthracenes	Trace Elements	PCB158	Endosulfan I
Dibenzothiophene	Aluminum (Al)	PCB170/190	Endosulfan Sulfate
C1-Dibenzothiophenes	Antimony (Sb)	PCB174	Mirex
C2-Dibenzothiophenes	Arsenic (As)	PCB180	Chlorpyrifos
C3-Dibenzothiophenes	Cadmium (Cd)	PCB183	
	Chromium (Cr)	PCB187	Butyltins
	Copper (Cu)	PCB194	Monobutyltin
	Iron (Fe)	PCB195/208	Dibutyltin
	Lead (Pb)	PCB199	Tributyltin
	Manganese (Mn)	PCB201/157/173	Tetrabutyltin
	Mercury (Hg)	PCB206	
	Nickel (Ni)	PCB209	
	Selenium (Se)		
	Silver (Ag)		
	Tin (Sn)		
	Zinc (Zn)		

*PAHs = polycyclic aromatic hydrocarbons; PCBs = polychlorinated biphenyls; DDT = dichloro-diphenyltrichloroethane

1996). Experiments have shown that the half-life of TBT, the amount of time needed to convert half of the TBT to dibutyltin in natural water samples, is on the order of days; degradation to monobutyltin takes approximately a month (Batley, 1996). Experiments with aerobic sediments have shown that the half-life of TBT is similar to that measured in solution. In deeper, anoxic sediments, however, the half-life of TBT is considerably longer, on the order of 2-4 years (Batley, 1996). Butyltins were analyzed using gas chromatography/flame photometric detection.

Effects of TBT

The widespread use of TBT as an antifouling agent was associated with endocrine disruption, specifically an imposex condition in marine gastropod mollusks. Beginning in 1989 in the U.S., the use of TBT as an antifouling agent was banned on vessels smaller than 25 m in length (Gibbs and Bryan, 1996). Negri *et al.* (2002) investigated the effects of TBT in sediments from a shipwreck, on the coral *Acropora microphthalma* from the Great Barrier Reef in Australia. Sediments originally contained approximately 160 µg/g TBT. When diluted to 5 percent of the original concentration, successful settlement of coral larvae in the laboratory was prevented.

4.2.3.5. Major and Trace Elements

A total of 16 trace and major elements were measured in sediments, and 14 in coral tissues for this project (Table 4.1). Most of these elements are metals, however, antimony, arsenic and silicon are metalloids; selenium is a nonmetal. All occur naturally to some extent in the environment. Aluminum, iron, and silicon are major components of the Earth's crust. Some trace and major elements in the appropriate concentrations are biologically essential. As their name implies, trace elements such as chromium, cadmium, lead and nickel occur at lower concentrations in crustal material, however mining and manufacturing processes along with the use and disposal of products containing trace elements result in elevated concentrations in the environment.

Silver, cadmium, copper, lead, antimony, and tin were analyzed using inductively coupled plasma - mass spectrometry. Aluminum, arsenic, chromium, iron, manganese, nickel, silicon and zinc were analyzed using inductively coupled plasma - optical emission spectrometry. Mercury was analyzed using cold vapor - atomic absorption spectrometry. Selenium was analyzed using atomic fluorescence spectrometry. For each element, total elemental concentration (*i.e.*, sum of all oxidation states) was measured. A more detailed description of laboratory methodologies can be found in Kimbrough and Lauenstein (2006).

Effects of Trace Elements

A number of trace elements are toxic at low concentrations. Cadmium, used in metal plating, solders, and batteries has been shown to impair development and reproduction in several invertebrate species, and the ability to osmoregulate in herring larvae (Eisler, 1985; USDHHS, 1999). Mercury is volatile and can enter the atmosphere through processes including mining, manufacturing, combustion of coal, and volcanic eruptions. Effects of mercury on copepods include reduced growth and reproductive rates (Eisler, 1987). Chromium has been shown to reduce survival and fecundity in the cladoceran *Daphnia magna*, and reduced growth in fingerling chinook salmon (*Oncorhynchus tshawytscha*; Eisler, 1986). Copper has a number of uses such as in antifouling paints, wood preservatives, heat exchangers in power plants, electrical wires, coinage, and agriculture. Although an essential element, elevated levels of copper can impact aquatic organisms, including reproduction and development in mysid shrimp (Eisler, 1998). In corals, Reichelt-Brushett and Harrison (2005) found that a copper concentration of 20 µg/L significantly reduced fertilization success in brain coral *Goniastrea aspera*. At copper concentrations at or above 75 µg/L, fertilization success was one percent or less. Fertilization success was also significantly reduced in the coral *Acropora longicyathus* at 24 µg/L, similar to *G. aspera*.

4.2.4. Total Organic Carbon (TOC) and Grain Size

Total organic carbon (TOC) and grain size analyses were also carried out on the sediment samples. These two characterizations are important for assessing the potential for accumulation of contaminants in sediments. Typically, a positive relationship exists between sediment TOC and chemical contaminants, particularly organic contaminants, in freshwater, estuarine and coastal waters (Hassett *et al.*, 1980; Shine and Wallace, 2000). TOC was quantified in the sediments using a sequence of steps that involves combusting the carbon in a sample at a high temperature and then quantifying the CO₂ produced. Grain size is also an important sediment characteristic as many organic contaminants and a number of metals bind to the smaller silt and clay grain size fractions of sediments, due to the larger surface areas of these fractions, and in the case of trace and major elements, the charge characteristics of clays. Grain size analysis was carried out using a series of sieving and settling techniques. Additional information on TOC and grain size analysis can be found in McDonald *et al.* (2006).

4.2.5. Statistical Analyses

All contaminant data were analyzed using JMP® statistical software. The data were first tested for normality using the Shapiro-Wilk test. Most of the data were not normally distributed. If log₁₀ transformations were not effective, nonparametric tests (*e.g.*, Wilcoxon) were run. When a significant Wilcoxon test resulted, the data were then ranked in order to permit an analysis of variance (ANOVA). The Tukey-Kramer HSD (Honestly Significant Difference) test was then used for pairwise comparisons. Correlations were tested using a Spearman's rank correlation coefficient test. Spearman coefficient Rho (ρ) values of 0.707 or higher were discussed as indicative of strong correlation, while values below 0.707 indicate weak correlation. Most of the statistics were calculated on all 44 sites sampled for this project. However, when comparing differences between the strata, the three targeted (SWP) sites were not included, as they were not part of the stratified random sampling design. After data analysis, it was determined that CNT and NER were not statistically different, and because NER is a geographic subset of CNT, these two strata were combined into a singular central stratum.

4.2.6. Providing Context for Results

In addition to comparing contamination results between strata, there are several other ways to evaluate the relative level of contamination of Jobos Bay. First, and most simply, these findings can be compared to the contaminant concentrations in other studies in Puerto Rico, or other tropical systems. Second, the findings can be placed in a national context by comparing the results to a national contaminant monitoring program, such as NS&T, which includes sediment chemistry data from over 300 coastal sites throughout the U.S. Finally, the degree of contamination in Jobos Bay can be assessed using NOAA's numerical sediment quality guidelines (SQG) known as effects range-low (ERL) and effects range-median (ERM) developed by Long and Morgan (1990) and Long *et al.* (1996). The SQG value was not defined for all analytes; existing values are presented in Table 4.2.

Table 4.2. Sediment Quality Guidelines (Long and Morgan, 1990).

Contaminant	ERL	ERM
Total PAHs (ng/g)	4,022	44,792
Total PCBs (ng/g)	22.7	180
Total DDT (ng/g)	1.58	46.1
Ag ($\mu\text{g/g}$)	1	3.7
As ($\mu\text{g/g}$)	8.2	70
Cd ($\mu\text{g/g}$)	1.2	9.6
Cr ($\mu\text{g/g}$)	81	370
Cu ($\mu\text{g/g}$)	34	270
Hg ($\mu\text{g/g}$)	0.15	0.71
Ni ($\mu\text{g/g}$)	20.9	51.6
Pb ($\mu\text{g/g}$)	46.7	NA
Zn ($\mu\text{g/g}$)	150	410
Sediment quality guideline have not been developed for all analytes monitored by the NOAA's National Status and Trends Program (NS&T).		

These guidelines are statistically derived levels of contamination above which toxic effects would be expected to be observed in benthic organisms with at least a 50% frequency (ERM), and below which effects were rarely (<10%) expected (ERL). While these guidelines are neither regulatory, nor confirm that toxicity is present, they can serve as a useful screening tool, *i.e.*, a first step in evaluating the likelihood that contamination at a given site may be at levels of concern. The SQG can be used to identify areas where additional study is needed to further quantify levels of contamination and potential associated toxicity.

It should be noted that there are no guidelines for contaminants in coral tissues, nor is there a national or regional coral tissue contaminant monitoring program. So in the case of corals, contextual comparisons are limited to other studies in similar systems.

4.3. RESULTS – OVERVIEW OF CONTAMINANT PATTERNS

4.3.1. Environmental Parameters

The water depth at the sediment sites sampled was fairly shallow; the mean at the sites was 1.1 ± 0.1 m (n=44). The mean surface salinity was 35.3 practical salinity units (psu), temperature was 29.5°C, and dissolved oxygen was 6.3 mg/L. A Wilcoxon nonparametric test indicated no significant differences in the surface versus bottom measurements for any of these parameters, indicating well mixed waters within the Bay.

The characteristics of the sediments by stratum are shown in Table 4.3. In this study and in NOAA's NS&T Program, the silt and clay fractions are combined and referred to as % fines. The %fines (sum of %silt and %clay fractions) are important as these smaller grain sizes have proportionately higher surface area available for the adsorption of contaminants (Hassett *et al.*, 1980), while the organic carbon content of

Table 4.3. Sediment characteristics by strata.

Stratum*	Map Abbreviation	# of Samples	% Fines	%Total Organic Carbon (TOC)
Inner	INR	10	82.33 ±5.82	2.39 ±0.24
Central	CNT and NER	11	52.17 ±6.14	2.10 ±0.50
Outer	OTR	10	32.54 ±6.39	1.54 ±0.34
SWP	SWP	3	47.05 ±16.70	6.84 ±3.12

* The SWP sites represent targeted, nonrandom sites used by the Jobos Bay National Estuarine Research Reserve (JBNERR) to characterize Jobos Bay; the selection of sites within the other strata were randomized. % Fines is the sum of the % silt and % clay sediment fractions. Abbreviations: SWP, System Wide Monitoring Program (SWMP) for JBNERR.

the silt fraction further increases the adsorption of organic compounds (Shine and Wallace, 2000). From Table 4.3, it can be seen that sediments from the inner stratum had the highest fraction (82%) of fines, followed by the central stratum. A Wilcoxon test indicated a significant (Prob>ChiSq = 0.0003) difference, and a one-way ANOVA and pairwise comparison test on the ranked data confirmed this. Table 4.3 also contains the mean TOC values for the Jobos Bay sediments. Although the inner stratum sediments had numerically higher %TOC values, an ANOVA on the log₁₀ transformed data did not indicate any differences between the strata (p=0.1426). The mean %TOC for the SWP sites (6.84%) was higher than the means for the strata sampled. However, because the SWP sites were not randomly selected, they could not be compared statistically with the inner, central, and outer strata.

4.3.2. Polycyclic Aromatic Hydrocarbons (PAHs)

Total PAHs in the NS&T Program refers to the sum of the 24 PAHs listed in Table 4.1. Concentrations for PAHs in sediments and corals at individual sites can be found in Appendix B (Tables B.1 and B.2).

Sediments

Observed concentrations of total PAHs in the sediments are shown in Figure 4.4. The mean concentration of total PAHs in the sediments sampled in Jobos Bay was 1,062 ng/g; the median was 371 ng/g (Table 4.4). The highest concentration detected was 14,250 ng/g at a site (INR4) in the inner stratum (Figure 4.1), adjacent to a small boat yard. A comparison of the different strata using the \log_{10} transformed data indicated total PAHs were significantly different between strata ($p=0.0004$), and a Tukey-Kramer test indicated that the inner stratum (INR) had significantly higher total PAH concentrations than the central (CNT) and outer (OTR) strata. It is likely that the inner stratum has less flushing to the open ocean than either the central or outer strata, which would tend to accumulate sediments and sediment-bound contaminants (Zitello *et al.*, 2008).

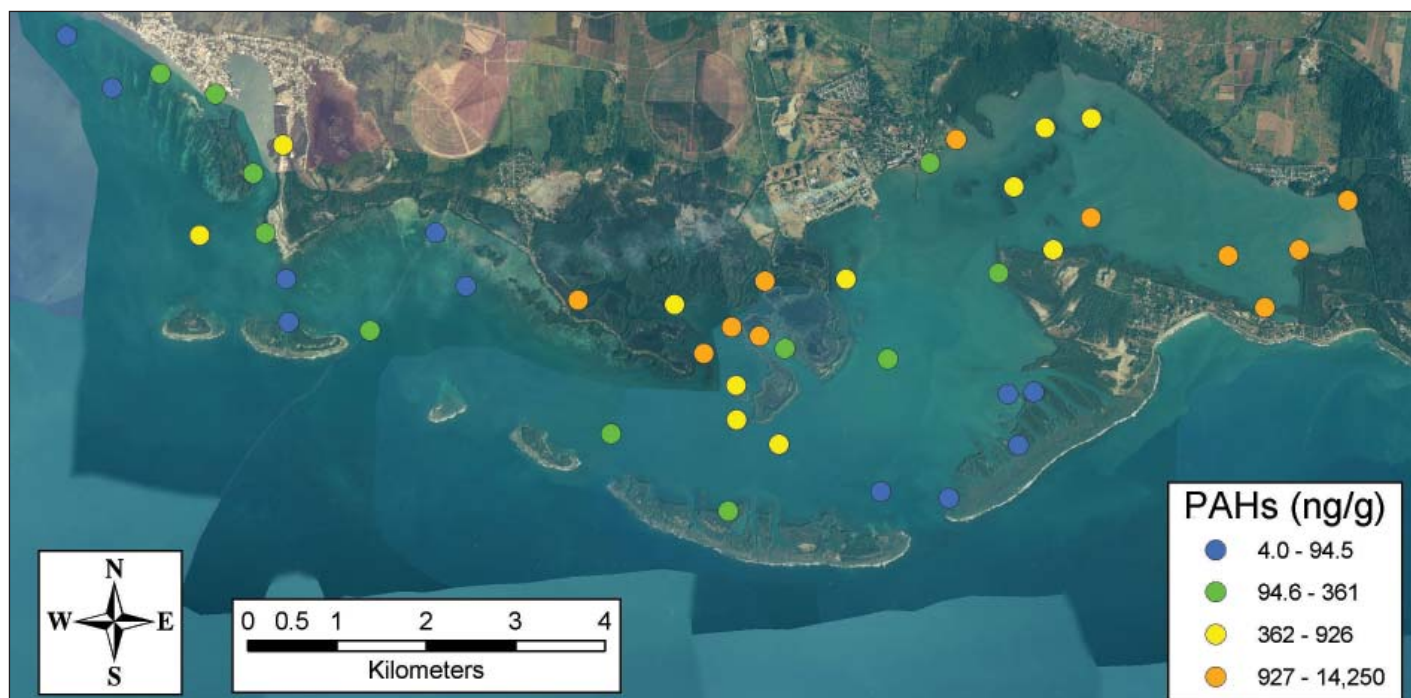


Figure 4.4. Total Polycyclic aromatic hydrocarbons (PAH) concentrations in sediments.

The ERL for total PAHs is 4,022 ng/g. There was only one sediment sample with a total PAH concentration above this value, the sample from INR4 (14,250 ng/g). This value however, is below the ERM (44,792 ng/g) which would have indicated that impacts were more likely from the sum of PAHs. There are also a series of ERLs and ERMs for a number of individual PAHs. None of the individual PAHs exceeded the established ERM values. However, the ERL was exceeded for several individual PAHs (Tables 4.2 and 4.4). Another sediment quality guideline, the PEL or Probable Effects Level, is similar to the ERM except that the PEL is the geometric mean of the 50th percentile of the effects data, and the 85th percentile of the no effects data, and represents a concentration above which McDonald *et al.* (2006) estimate that effects in sediment dwelling organisms are likely to occur. While the PEL was not exceeded for total PAHs, the PEL was exceeded for a number of individual PAHs including phenanthrene, benz(a)anthracene, chrysene, benzo(a)pyrene, and dibenzo(a,h)anthracene at INR4 (Tables 4.2 and 4.4). In addition, while the PEL for naphthalene (391 ng/g) was not exceeded at INR4, it was exceeded at NER24 and SWP43 (Tables 4.2 and 4.4).

The concentrations of PAHs found in the sediments from Jobos Bay can be compared with other assessments. Recently, Aldarondo-Torres *et al.* (2010) published an analysis of trace metals, PAHs, and PCBs in sediments from Jobos Bay. Samples from seven stations were screened for 16 PAHs. The mean PAH concentration in sediments was 593 ng/g, somewhat lower than the mean found in the current study (1,062 ng/g). The higher total PAH concentration found at INR4 in the current study may have been responsible in part for the higher mean; the median for total PAHs in the current study

was 415 ng/g, similar to the median (394 ng/g) calculated from the data presented by Aldarondo-Torres *et al.* (2010). It should also be noted that the calculation of total PAH in the NS&T Program for this study used 58 PAHs; Aldarondo-Torres *et al.* (2010) used 16 PAHs. Interestingly, one of the higher concentrations (940 ng/g) of total PAHs found by Aldarondo-Torres *et al.* (2010) was from a site near (<1 km) INR4 in the current study, and like INR4, may be influenced by activities from the adjacent boat yard. Aldarondo-Torres *et al.* (2010) also noted in general that samples taken from the inner areas of Jobos Bay contained higher levels of total PAHs, similar to the results from the current study. The results for total PAHs found in the sediments can also be compared with work recently completed in southwest Puerto Rico (Pait *et al.*, 2007, 2008) and in Vieques, Puerto Rico (Pait *et al.*, 2010). The mean total PAH concentration found in sediments from southwest Puerto Rico was 80.6 ng/g, and in Vieques, 52.3 ng/g, both substantially below the mean found in Jobos Bay.

Because of the long-term, national-level contaminant monitoring carried out by NS&T, data from Jobos Bay can be compared with the rest of the Nation's coastal waters. The median for total PAHs in Jobos Bay sediments was 370.5 ng/g (Table 4.4), below the NS&T national median of 415 ng/g. However, 19 sites had a total PAH median concentration higher than the NS&T national median, and five sites (INR4, INR3, NER24, SWP43, and SWP44) had total PAH concentrations above the national NS&T 85th percentile of 2,688 ng/g.

Corals

PAH concentrations in coral tissues ranged from 2.90 ng/g to 6.40 ng/g (dry weight), with a mean of 4.58 ng/g and a median of 4.55 ng/g (Table 4.5). There was no statistically significant difference between the inshore and offshore strata (Figure 4.5, Table 4.4). No statistically significant correlations were found between coral tissue PAH concentrations and depth, longitude (*i.e.*, long shore position) or distance from land. Because organic compounds tend to be lipophilic, tissue concentrations can be normalized to lipid content, which can help identify possible sources of contaminants (Lake *et al.*, 1990). Normalizing PAH tissue data to coral lipid content did not change the statistical patterns in the data. Despite high observed PAH concentrations at one sediment site (INR4), coral tissue concentrations of PAHs were low when compared to other studies areas in Puerto Rico (Table 4.5).

Table 4.4. Summary statistics for organic contaminants in sediments, overall and by strata (ng/g dry wt). ERL=effects range-low, ERM= effects range-median).

Stratum*	Total PAHs	Total PCBs	Total DDT	Tributyltin
Inner				
Minimum	610	0.99	0.49	0.07
Maximum	14,250	19.24	3.28	2.27
Median	1,184	3.84	1.00	0.20
Mean	2,711	5.51	1.23	0.43
Central				
Minimum	5.5	0.03	0.01	0.00
Maximum	3,413	5.46	1.81	0.00
Median	306	0.80	0.23	0.00
Mean	515	1.14	0.34	0.00
Outer				
Minimum	4	0.04	0.00	0.00
Maximum	844	0.79	0.74	10.91
Median	148	0.40	0.125	0.30
Mean	231	0.39	0.19	2.03
SWP				
Minimum	80.5	0.07	0.06	0.00
Maximum	3,221	6.06	2.09	0.19
Median	3,157	2.98	0.3	0.00
Mean	2,152	3.04	0.82	0.06
Overall				
Median	370.5	0.81	0.28	0.00
Mean	1,062	2.09	0.54	0.56
NOAA Sediment Guidelines				
ERL	4,022	22.7	1.58	NA
ERM	44,792	180	46.1	NA

* The SWP sites represent targeted, nonrandom sites used by the Jobos Bay National Estuarine Research Reserve (JBNERR) to characterize Jobos Bay; the selection of sites within the other strata were randomized.



Figure 4.5. Total PAH concentrations in corals (*Porites astreoides*). White outline are coral reefs in inner stratum. Red outline are coral reefs in outer stratum.

Table 4.5. Summary statistics for contaminants in coral tissue, including comparison with other studies, Southwest Puerto Rico (SW PR; Pait et al., 2009) and Vieques (Pait et al., 2010).

Contaminant	Minimum	Maximum	Median	Mean	SW PR Mean	Vieques Mean	SW PR Max	Vieques Max
HCH (ng/g)	0.00	0.00	0.00	0.00	0.00	0.00	0.00	0.05
Chlordane (ng/g)	0.00	0.00	0.00	0.00	0.00	0.12	0.00	0.81
Total DDT (ng/g)	0.00	0.60	0.00	0.04	0.08	0.13	0.62	2.26
Total PCBs (ng/g)	2.19	3.56	2.35	2.45	3.81	2.63	10.97	5.76
Total PAHs (ng/g)	2.90	6.40	4.55	4.58	41.91	15.00	154.00	21.50
Ag (µg/g)	100.00	333.00	154.00	177.69	37.80	30.75	82.20	103
Al (µg/g)	0.94	2.44	1.59	1.68	0.00	0.241	0.00	3.42
As (µg/g)	0.21	0.31	0.25	0.25	0.00	0.194	0.00	0.294
Cd (µg/g)	0.00	0.00	0.00	0.00	0.00	0.183	0.00	1.09
Cr (µg/g)	2.37	97.20	68.95	50.30	2.06	0.757	3.54	6.51
Cu (µg/g)	110.00	480.00	176.00	212.13	90.80	51.2	353.00	526
Fe (µg/g)	0.00	0.00	0.00	0.00	0.00	<0.001	0.00	0.0021
Hg (µg/g)	8.33	24.60	11.60	13.33	3.01	2.66	5.36	8.24
Mn (µg/g)	8.33	24.60	11.60	13.33	3.01	2.66	5.36	8.24
Ni (µg/g)	0.80	6.84	2.63	3.13	1.32	0.896	2.70	8.09
Pb (µg/g)	0.08	12.50	0.20	1.43	0.00	0.074	0.07	0.174
Se (µg/g)	0.13	0.26	0.18	0.18	0.05	0.096	0.37	0.338
Sn (µg/g)	0.00	0.10	0.00	0.01	0.02	0.246	0.14	0.396
Zn (µg/g)	2.56	16.90	7.88	8.59	6.09	3.43	18.30	15.2

4.3.3. Polychlorinated Biphenyls (PCBs)

Total PCBs are defined as the sum of the 39 congener and congener combinations listed in Table 4.1. Concentrations for PCBs in sediments and corals at individual sites can be found in the Appendix B (Tables B.1 and B.2).

Sediments

Total PCBs detected in the sediments in Jobos Bay are shown in Figure 4.6. The mean sediment total PCB concentration in the samples collected in Jobos Bay was 2.09 ng/g; the median was 0.81 ng/g (Table 4.4). The highest total PCB concentration was 19.24 ng/g at INR9 in the inner stratum. A comparison of the different strata using the \log_{10} transformed data indicated total PCBs were significantly different between strata ($p < 0.0001$), and a Tukey-Kramer test indicated that the inner strata had a higher total PCB concentration.

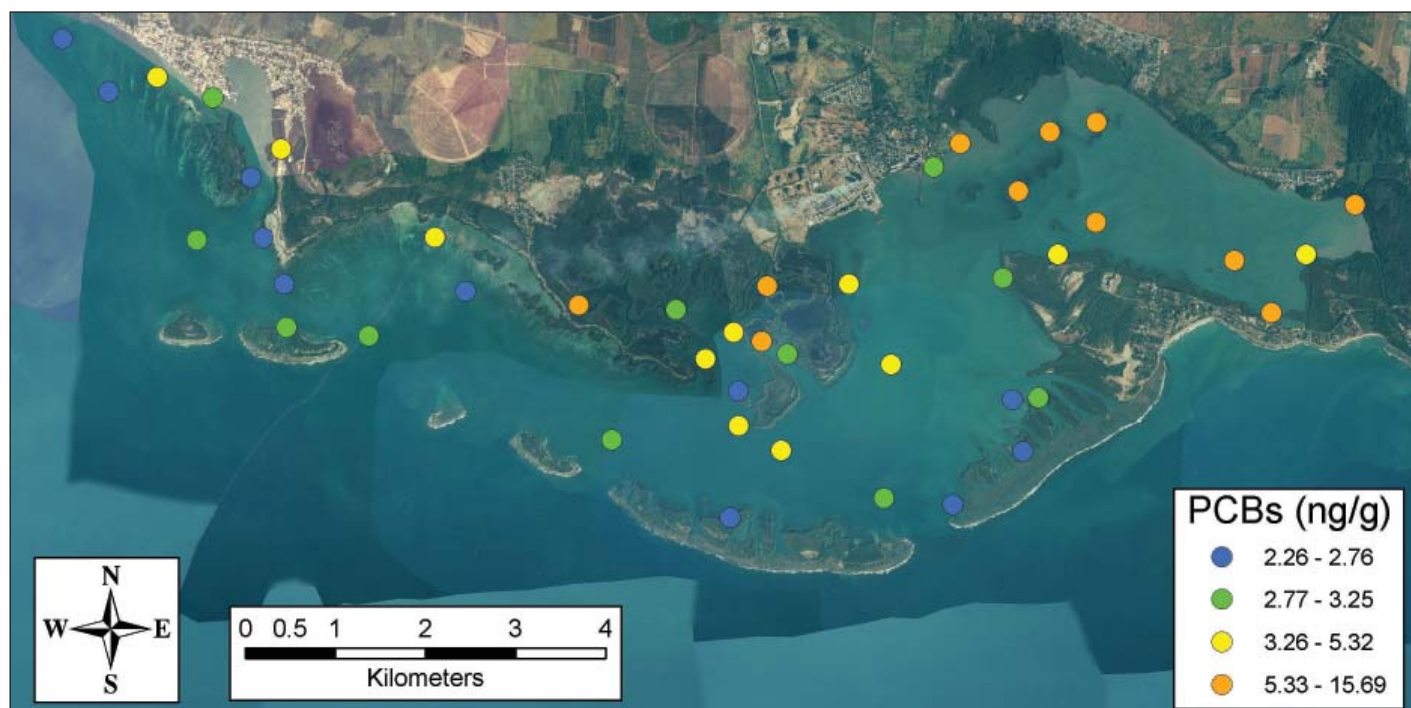


Figure 4.6. Total polychlorinated biphenyl (PCB) concentrations in sediments.

None of the sediments sampled in Jobos Bay had a total PCB concentration near the ERM (180 ng/g) or PEL (189 ng/g) or above the ERL of 22.7 ng/g, although INR9 was close to the ERL. Aldarondo-Torres *et al.* (2010) analyzed PCBs (15 congeners) at six sites from Jobos Bay with a calculated total PCB mean of 2.37 ng/g, similar to the mean detected in the current study. The results for total PCBs can also be compared with work recently completed in southwest Puerto Rico (Pait *et al.*, 2007) and in Vieques, Puerto Rico (Pait *et al.*, 2010). The mean total PCB concentration found in sediments from southwest Puerto Rico was 104.1 ng/g, substantially above the mean found for Jobos Bay. In Vieques, however, the mean total PCB concentration in sediments was 2.86 ng/g, similar to what was found in Jobos Bay. The relatively high PCB concentrations in southwest Puerto Rico are driven by exceptionally high concentrations in a portion of the study area (Guanica Bay), but the source of these PCBs is unknown.

The median for total PCBs in Jobos Bay sediments (0.81 ng/g), is substantially below the NS&T national median of 13.7 ng/g. There was only one site (INR9; 19.24 ng/g) sampled in Jobos Bay that was above the NS&T median for total PCBs.

The statistical relationship between grain size (%fines) and the concentration of total PCBs in the sediment samples indicated a highly significant (Spearman's Rho [ρ] = 0.5462, $p < 0.0001$) correlation between the fines fraction of the sediment and the concentration of total PCBs. A bivariate regression run between \log_{10} total PCBs and \log_{10} TOC indicated a significant ($p < 0.0001$, $r^2 = 0.417$) relationship between TOC and the concentration of total PCBs.

Corals

PCB concentrations in coral tissues ranged from 2.19 ng/g to 3.56 ng/g, with a mean of 2.45 ng/g and a median of 4.35 ng/g (Table 4.5). There was no statistically significant difference between the inshore and offshore strata (Figure 4.7). No statistically significant correlations were found between coral tissue PCB concentrations and depth, longitude (*i.e.*, long shore position) or distance from land. Because organic compounds tend to be lipophilic, tissue concentrations can be normalized to lipid content, which can help identify possible sources of contaminants (Lake *et al.*, 1990). Normalizing PCB tissue data to coral lipid content did not change the statistical patterns in the data. Coral tissue concentrations of PCBs were slightly lower than other published data for *P. astreoides* in Puerto Rico (Table 4.5).



Figure 4.7. Total PCB concentrations in corals (*P. astreoides*). White outline are coral reefs in inner stratum. Red outline are coral reefs in outer stratum.

4.3.4. DDT and Other Chlorinated Pesticides

A series of chlorinated pesticides were analyzed in the sediments as part of this project. The organochlorine insecticide DDT was detected in the sediments and coral tissues in Jobos Bay. Total DDT is defined as the sum of the two parent compounds 2,4'-DDT and 4,4'-DDT, and degradation products 2,4'-DDD, 4,4'-DDD, 2,4'-DDE, 4,4'-DDE and DDMU (Table 4.1). Concentrations for DDTs in sediments and corals at individual sites can be found in the Appendix B (Tables B.1 and B.2).

Sediments

The mean sediment total DDT concentration in the sediment samples collected in Jobos Bay was 0.54 ng/g; the median was 0.28 ng/g (Table 4.4). The highest concentration of total DDT, like total PCBs, was at INR9 in the inner stratum, with a concentration of 3.28 ng/g (Figure 4.8). A comparison of the different strata using the log₁₀ transformed data indicated that total DDT was significantly different between strata ($p=0.0002$), and a Tukey-Kramer test indicated that the inner stratum was significantly different (higher concentration) than the other two strata, similar to what was found for total PAHs and total PCBs.

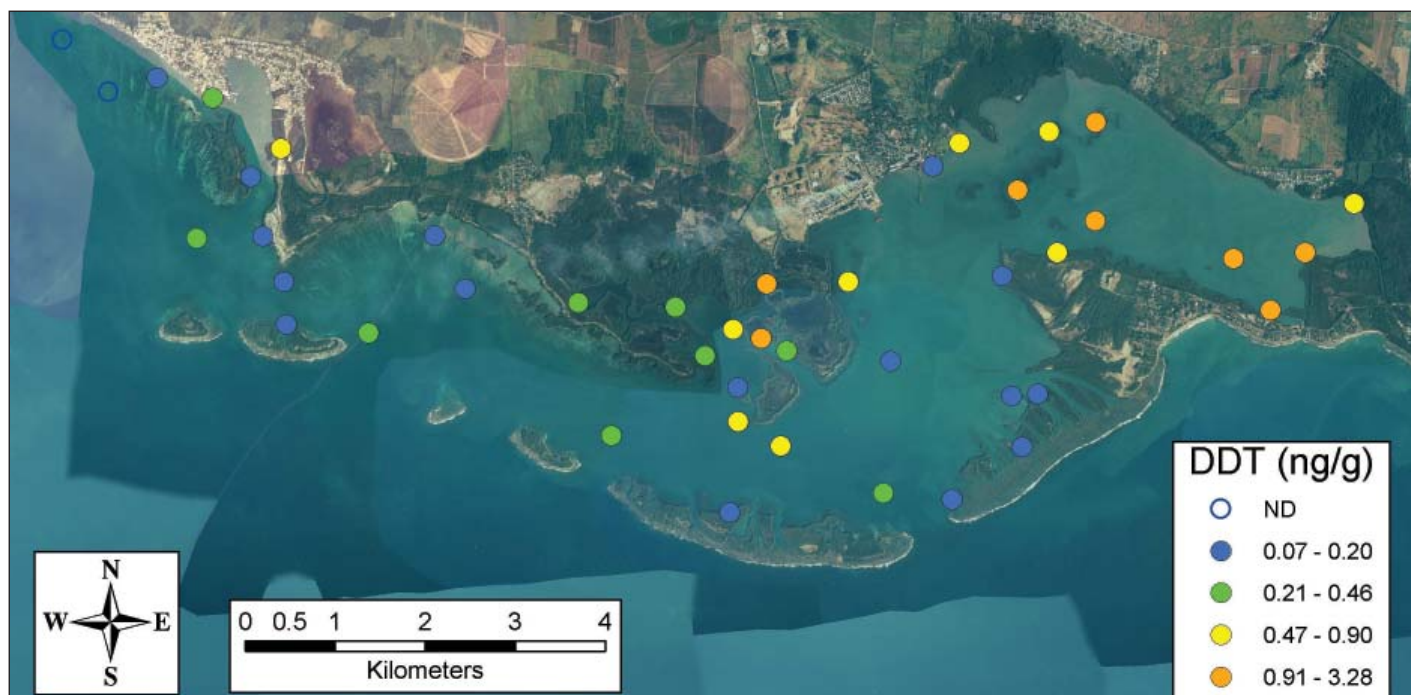


Figure 4.8. Total dichloro-diphenyltrichloroethane (DDT) concentrations in sediments.

Four of the sediments sampled in Jobos Bay (INR9, SWP43, NER24 and INR6) had a total DDT concentration above the ERL of 1.58 ng/g, which may indicate that the more sensitive species or life stages are beginning to experience some degree of toxic effects. However, none of the sediment samples had a total DDT concentration above the ERM (46.1 ng/g) or the PEL (51.7 ng/g) which would have indicated that effects in sediment-inhabiting organisms were likely to occur. A DDT residual spraying program was instituted in Puerto Rico by 1950 for the control of mosquitoes (Fox, 1961) and also DDT was also likely used in agriculture.

The results for total DDT can be compared with work recently completed in southwest Puerto Rico (Pait *et al.*, 2007) and in Vieques, Puerto Rico (Pait *et al.*, 2010). The mean total DDT concentration found in sediments from southwest Puerto Rico (Pait *et al.*, 2008) was 2.10 ng/g, which is above the mean total DDT found for Jobos Bay. In Vieques (Pait *et al.*, 2010), the mean total DDT concentration in sediments was substantially higher (23.6 ng/g), than that found in Jobos Bay. This mean concentration in Vieques is driven by a very high total DDT concentration in a sediment sample from the south shore, and elevated total DDT in the sediments at several locations on the north shore of Vieques.

The median for total DDT in Jobos Bay sediments (0.28 ng/g), is similar to the NS&T national median of 0.40 ng/g. The statistical relationship between grain size and the concentration of total DDT in the sediment samples indicated a highly significant (Spearman's $\rho = 0.7746$, $p < 0.0001$) correlation between the fines fraction of the sediment and the concentration of total DDT. A bivariate regression run between \log_{10} total DDT and \log_{10} TOC indicated a significant ($p < 0.0001$, $r^2 = 0.416$) relationship

between TOC and the concentration of total DDT.

A number of other organochlorine pesticides included in this study were also detected in the sediments from Jobos Bay including dieldrin, heptachlor, endrin, chlordane, chlorpyrifos and endosulfan. The higher concentrations for these chlorinated pesticides tended to occur in the inner stratum, although most concentrations were less than 1 ppb (1 ng/g; data not shown). The highest concentration detected for any of these pesticides was endosulfan at INR4 (2.16 ng/g). Although an ERL and ERM have not been established for endosulfan, they have been established for chlordane and dieldrin. The sediments sampled in Jobos Bay did not exceed the ERMs for either chlordane or dieldrin, however, six sites exceeded the ERL for chlordane (0.5 ng/g) and 13 sites exceeded the ERL (0.02 ng/g) for dieldrin, the majority of which were in the inner stratum.

Corals

DDT concentrations in coral tissues ranged from below levels of detection to 0.6 ng/g, with a mean of 0.04 ng/g and a median of below limits of detection (Table 4.5). There was no statistically significant difference between the inshore and offshore strata (Figure 4.9). No statistically significant correlations were found between coral tissue DDT concentrations and depth, longitude (*i.e.*, long shore position) or distance from land. Because organic compounds tend to be lipophilic, tissue concentrations can be normalized to lipid content, which can help identify possible sources of contaminants (Lake *et al.*, 1990). Normalizing DDT tissue data to coral lipid content did not change the statistical patterns in the data. Coral tissue concentrations of DDT were similar to those observed in Southwest Puerto Rico, but were significant lower than those measured in Vieques, Puerto Rico (Table 4.5).

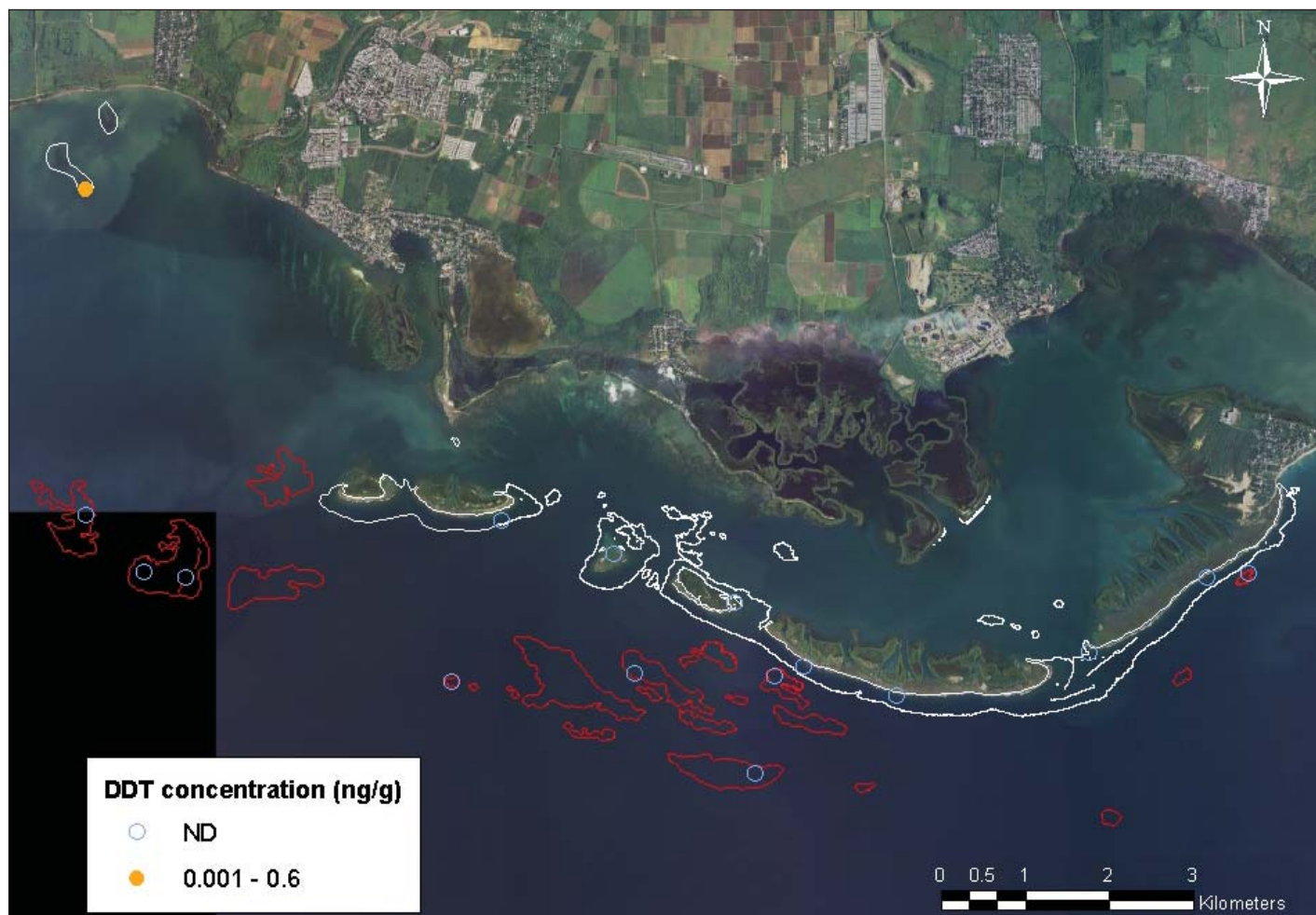


Figure 4.9. Total DDT concentrations in corals (*P. astreoides*). White outline are coral reefs in inner stratum. Red outline are coral reefs in outer stratum. ND = not detect/below limits of detection.

Other chlorinated pesticides were not detected in coral tissues in Jobos Bay.

4.3.5. Butyltins

Mono-, di-, tri-, and tetrabutyltin were also analyzed in the sediment and coral samples as part of this project. Tributyltin or TBT, was used in antifouling paints for boat hulls, and was banned for use in the US on most vessels in 1989 after being associated with endocrine disruption in certain marine gastropod mollusk species. TBT degrades to dibutyltin, monobutyltin, and finally to elemental tin in the environment. Tetrabutyltin is an impurity produced in the manufacture of TBT, and will degrade in the environment to TBT, and eventually elemental tin. Concentrations for TBT in sediments and corals at individual sites can be found in the Appendix B (Tables B.1 and B.2).

Sediments

There were numerous detections of butyltins in Jobos Bay sediments. The mean concentration of TBT in the sediments from Jobos Bay was 0.56 ng/g; the median was 0 ng/g (Table 4.4). The highest TBT values found in the sediments were from OTR31 (10.91 ng/g), OTR37 (4.24 ng/g), and OTR34 (3.64 ng/g; Figures 4.1 and 4.10).

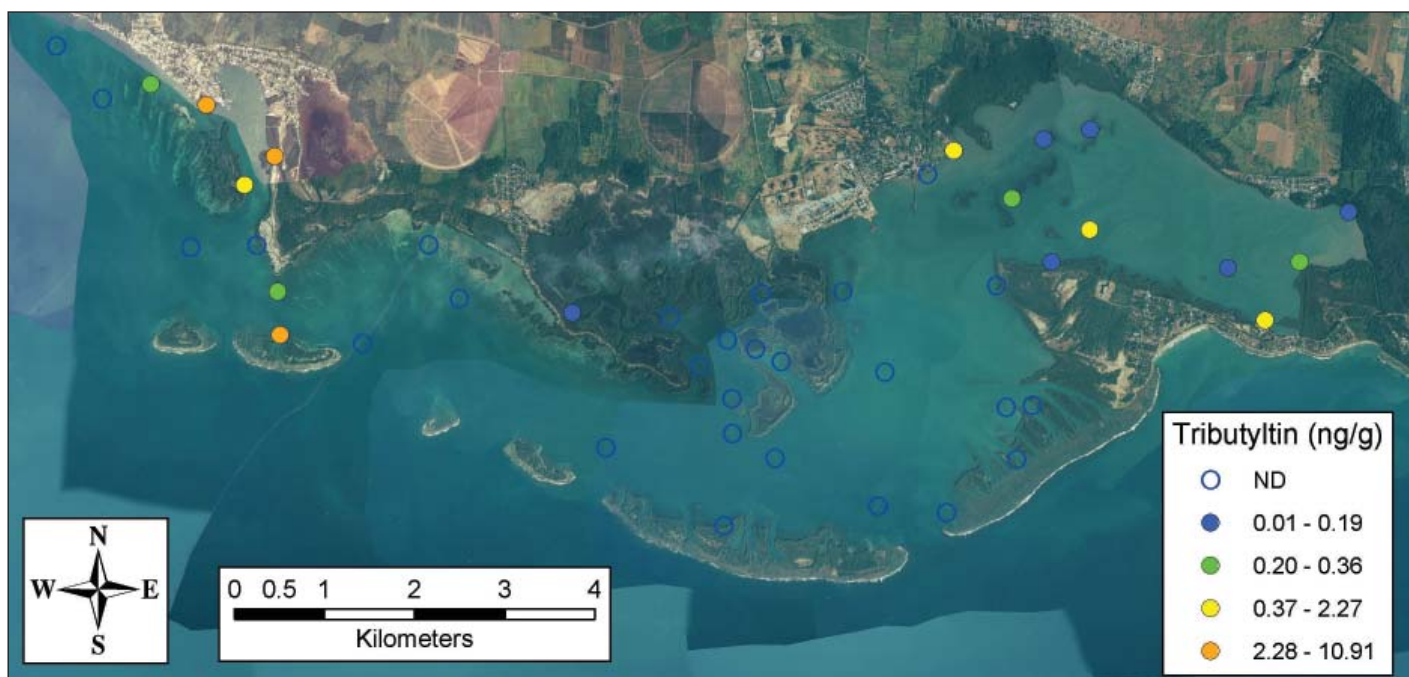


Figure 4.10. Tributyltin (TBT) in sediment.

None of the randomly selected central stratum sites had detectable levels of TBT, and could be related to the restrictions placed on boat traffic in parts of the JBNERR. An ANOVA on the \log^{10} transformed data indicated that the outer stratum was significantly higher than the inner stratum ($p=0.0103$). This is in contrast to a number of the other contaminant classes, in which the inner stratum had statistically higher sediment contaminant values. The outer stratum has what appears to be significant marina-related activity in the area around Playita, which could be associated with the TBT. Four of the top five highest concentrations of TBT were in this area. As noted above, TBT was used in the past as an antifouling on boat hulls. Rankings and ANOVAs on monobutyltin ($p=0.0093$) and dibutyltin ($p<0.0001$) data followed by pairwise comparisons indicated significant differences between the three strata, however, for both monobutyltin and dibutyltin, the inner and outer strata were not significantly different from one another, which might indicate significant use of TBT in these areas of Jobos Bay in the past. The significantly higher levels of TBT in comparison to its degradation products found in the outer stratum could be an indicator of more recent deposition.

The results for TBT can also be compared with work recently completed in southwest Puerto Rico (Pait *et al.*, 2008) and Vieques, Puerto Rico (Pait *et al.*, 2010). In the sediment samples from southwest Puerto Rico, the mean TBT concentration was 0.014 ng/g; whereas, in Vieques sediments, the mean TBT concentration was 0.040 ng/g, both substantially below the mean concentration found in Jobos Bay. The NS&T median for TBT is 0.41 ng/g; higher than the median TBT found in Jobos Bay. There does not appear to be an ERL, ERM or PEL value for TBT.

Corals

Butyltins were not detected in any coral samples. Other studies in Puerto Rico (Pait *et al.*, 2009, 2010) have documented butyltins in *P. astreoides* tissues, so the corals do have the capacity to accumulate these compounds in their tissues. It is not clear why the high (relative to other sites in Puerto Rico) butyltins concentrations in sediments does not result in butyltins ending up in coral tissues in Jobos Bay.

4.3.6. Major and Trace Elements

A summary of concentration ranges and median values for each trace and major element is illustrated in Table 4.6. The results showed a broad variation within the concentration values of each element. In general, concentration differences between the minimum and maximum values of individual element reached two orders of magnitude (Table 4.6). Concentrations for major and trace elements in sediments and corals at individual sites can be found in the Appendix B (Tables B.1 and B.2).

4.3.6.1. Silver (Ag)

Sediments

Silver (Ag) concentrations in sediments ranged from 0.051 µg/g to 0.219 µg/g, with a mean of 0.118 µg/g and a median of 0.105 µg/g (Table 4.6). This is below the NS&T national median of 0.13 µg/g, and similar to other published studies in tropical ecosystems (Table 4.7). Silver did not exceed sediment quality guidelines at any of the sediment sites. Unlike many of the other metals, the highest Ag concentrations were observed in the outer bay stratum at significantly higher concentrations ($p < 0.05$) relative to the other zones of the study area (Figures 4.11 and 4.12).

Table 4.6. Summary statistics for trace elements in sediments (µg/g dry wt).

Element	Minimum	Maximum	Median	Mean
Ag	0.051	0.219	0.105	0.118
Al	629	73700	41850	39138
As	1.79	28.10	12.75	12.59
Cd	0	0.174	0	0.008
Cr	0	29.8	18.5	18.2
Cu	1.37	73.70	29.85	33.83
Fe	1060	50500	26650	26570
Hg	0.0014	0.144	0.0309	0.0432
Mn	33.1	1130	528.5	510.6
Ni	0	31	10.1	11.0
Pb	0.227	16.7	6.02	7.15
Sb	0	0.589	0.2685	0.2170
Se	0	1.56	0.2755	0.3318
Sn	0	2.74	1.17	1.13
Zn	1.57	117	48.5	54.2

Corals

Silver was not detected in any coral samples. Other studies in Puerto Rico (Pait *et al.*, 2009, 2010) have documented silver in *P. astreoides* tissues, so the corals do have the capability to accumulate this metal in their tissues. It is not clear why silver is observed in the sediments but is not accumulating in coral tissues in Jobos Bay.

Table 4.7. Ranges of metal concentration in surficial sediment from Jobos Bay compared to published data from similar habitat environments. Concentration values are in ug/g dry wt. MW= Mussel Watch, JB= Jobos Bay, SW= southwest, VQS= Vieques, PR= Puerto Rico, ERL = Effects Range Low, ERM=Effects Range Median.

Area	Ag	As	Cd	Cr	Cu	Fe	Hg	Mn	Ni	Pb	Sb	Se	Sn	Zn	Reference
This study	0.05 - 0.22	1.79 - 28.1	0.0 - 0.174	29.8	1.37 - 73.7	1060 - 50500	0.001 - 0.144	33.1 - 1130	0 - 31	0.23 - 16.7	0 - 0.59	0 - 1.56	0 - 2.74	1.57 - 117	This study (median)
MW JB	0.0 - 0.08	10.7 - 12.1	0.0 - 0.17	36.9 - 273	10.7 - 155	35700 - 44600	0.03 - 0.051	508 - 990	9.16 - 258	6.74 - 12.3	-	0.24 - 0.29	2.42 - 1.38	74.9 - 139	NOAA (2006)
MW PR	0.1 - 0.3	2.5 - 10	0.1 - 0.3	20 - 80	10 - 40	-	0.05 - 0.2	20 - 100	10 - 20	5 - 20	0.2 - 0.6	0.2 - 0.8	1 - 3	20 - 100	Cantillo et al. (1999)
Jobos 2010	--	17	0.06	--	29	2600	--	--	--	11	--	--	--	64	Aldarondo-Torres et al. (2010)
Tampa Bay	0.05 - 0.20	1 - 5	0.25 - 0.75	20 - 60	10 - 20	-	0.05 - 0.15	20 - 60	5 - 10	20 - 60	-	0.25 - 0.75	0.5 - 1.5	20 - 80	Cantillo et al. (1999)
SW PR	<001	0.01	0.01	31.2	5.21	5210	<0.01	109	26.6	1.93	0.09	0.17	0.21	7.99	Pait et al. (2008)
VQS, PR	0.103	4.37	0.133	22.5	25.9	17610	0.019	301	7.80	5.42	0.2	0.26	0.66	34.3	Pait et al. (2010)
ERL*	1.0	8.2	1.2	81	34	-	0.15	-	20.9	46.7	-	-	-	150	Long et al. (1996)
ERM*	3.7	70	9.6	370	270	-	0.71	-	51.6	-	-	-	-	410	Long et al. (1996)

Values southwest Puerto Rico (Pait et al., 2008), Jobos 2010 (Aldarondo-Torres et al., 2010) and VQS (Pait et al., 2010) are means.

* Sediment quality guideline was not developed for all metals monitored by the NOAA's National Status and Trends Program (NS&T).

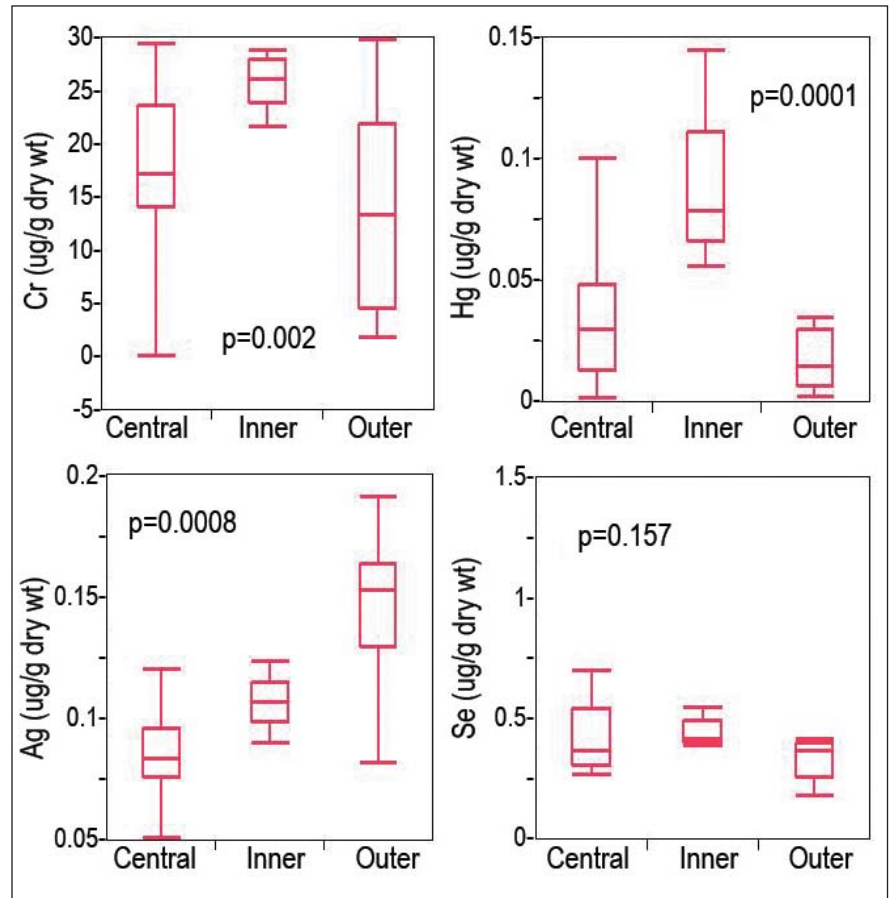


Figure 4.11. Chromium, silver, mercury and selenium concentrations in sediments by strata. Wilcoxon test ($\alpha=0.05$).

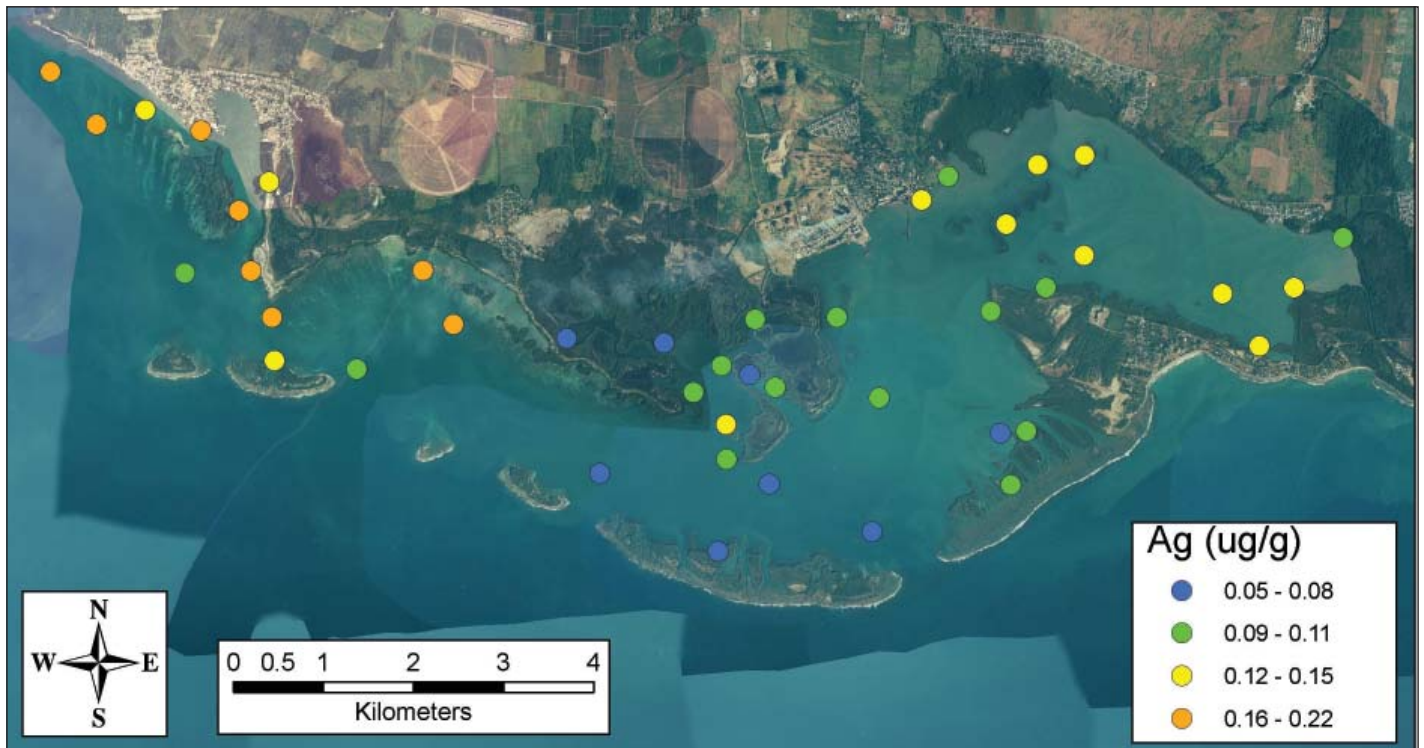


Figure 4.12. Silver (Ag) concentrations in sediments.

4.3.6.2. Aluminum (Al)

Aluminum (Al) is a major crustal element and is generally not considered to be a pollutant. However, examining aluminum distributions can shed light on the origins of other trace elements which have both natural and anthropogenic sources.

Sediments

Aluminum concentrations in sediments ranged from 629 µg/g to 73700 µg/g, with a mean of 39,140 µg/g and a median of 41850 µg/g (Table 4.6). Aluminum concentrations were significantly higher ($p < 0.05$) in the Inner Bay relative to the Central and Outer Bays (Appendix B, Figure B.1). Please see the additional discussion that follows which uses Al as an index of naturally occurring metals.

Corals

Aluminum concentrations in coral tissues ranged from 100 µg/g to 333 µg/g, with a mean of 178 µg/g and a median of 154 µg/g (Table 4.5). There was no statistically significant difference between the inshore and offshore strata (Appendix B, Figure B.2). No statistically significant correlations were found between coral tissue Al concentrations and longitude (*i.e.*, long shore position) or distance from land. However, Al concentrations in coral were weakly negatively correlated with depth ($p = 0.0454$, Spearman's $\rho = -0.5063$). It is possible that this could be explained by location on the reef (or some other confounding factor not measured here), or there could be a difference in coral biology/uptake at lower depths/higher pressures. Coral tissue concentrations of Al were elevated compared to other studies in Puerto Rico. Aluminum is general not considered to be a pollutant, but this could indicate that other observed metals in coral tissues in this area may be naturally occurring. This interpretation of these data should be approached cautiously, however, because differential uptake/incorporation rates between metals in corals are not well understood and ratios of aluminum to other metals in tissues may be altered by biological processes. More research is needed to understand uptake processes of metals in coral species.

4.3.6.3. Arsenic (As)

Sediments

Arsenic (As) concentrations in sediments ranged from 1.79 µg/g to 28.1 µg/g, with a mean of 12.95 µg/g and a median of 12.75 µg/g (Table 4.6). This is higher than the NS&T national median of 8.45 µg/g, and is higher than other studies in tropical systems (Table 4.7) suggesting that As concentrations in Jobos Bay may be elevated compared to the rest of the Nation. Arsenic concentrations were significantly higher ($p < 0.05$) in the Inner Bay relative to the Central and Outer Bays (Appendix B, Figure B.3). Maximum concentrations were observed at sites NER24 and SWP44 in Central Bay for As. Maximum values for As were above their respective ERL values at sites located in the Inner and Central strata (Table 4.7).

Coral

Arsenic concentrations in coral tissues ranged from 0.94 µg/g to 2.44 µg/g, with a mean of 1.68 µg/g and a median of 1.59 µg/g, which is higher than other studies in Puerto Rico (Table 4.5). Arsenic concentrations in corals were higher (Wilcoxon test, $\alpha = 0.05$) in the offshore stratum than inshore (Figure 4.13). This pattern could be a result of atmospherically deposited As from fossil fuel combustion at the nearby power plants (coal and oil fired), *i.e.* the stack height minimizes near shore deposition. No statistically significant correlations were found between coral tissue As concentrations and depth, longitude (*i.e.*, long shore position) or distance from land.

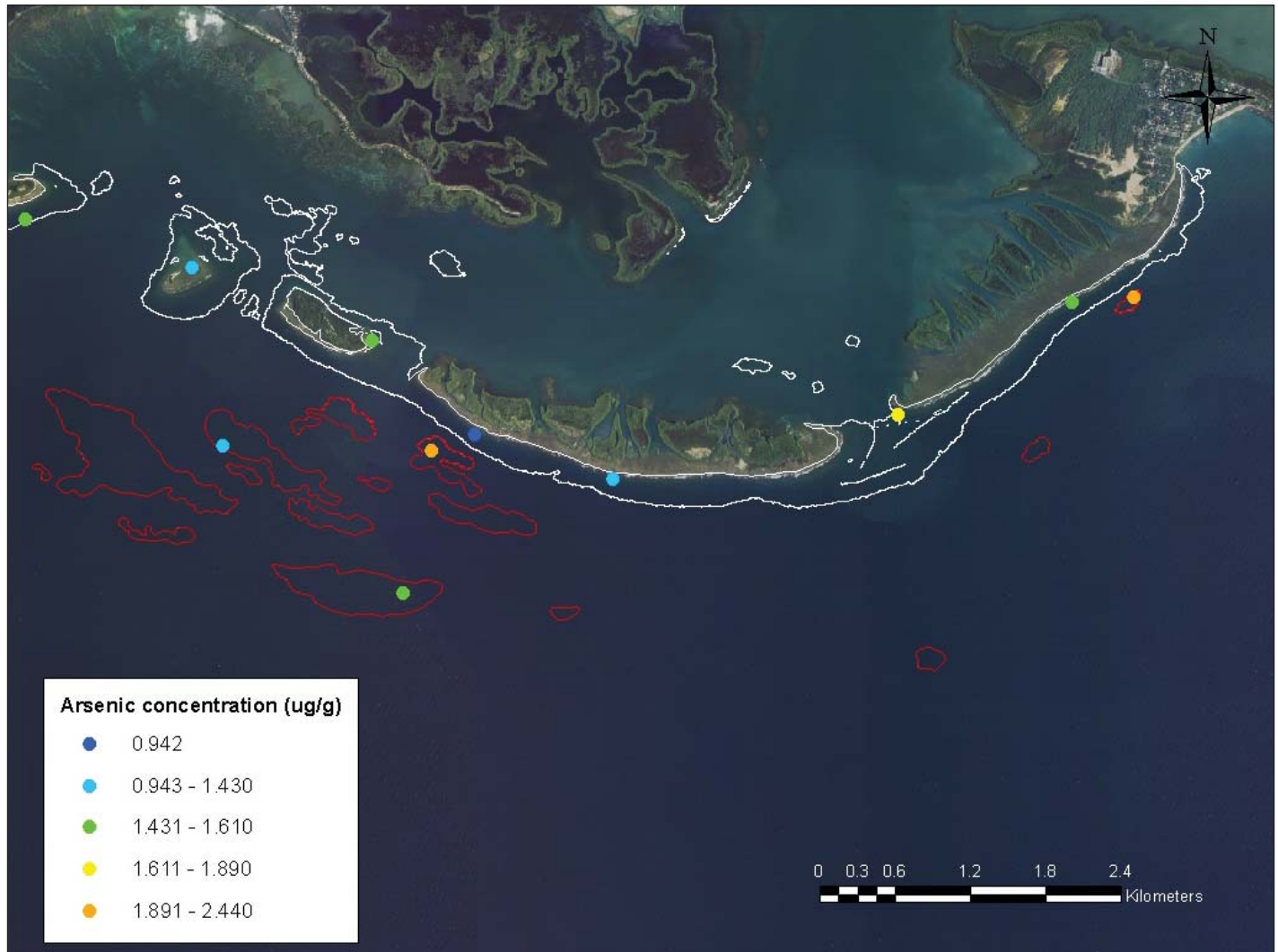


Figure 4.13. Arsenic (As) concentrations in corals (*P. astreoides*). White outline are coral reefs in inner stratum. Red outline are coral reefs in outer stratum.

4.3.6.4. Cadmium (Cd)

Sediments

Cadmium (Cd) concentrations in sediments ranged from 0 $\mu\text{g/g}$ to 0.174 $\mu\text{g/g}$, with a mean of 0.01 $\mu\text{g/g}$ and a median of 0 $\mu\text{g/g}$ (Table 4.6). Cadmium was found to be below the detection limit at all but two sites. This is lower than the NS&T national median of 0.19 $\mu\text{g/g}$, but is similar to other studies in tropical systems (Table 4.7). Neither site with detectable Cd exceeded sediment quality guidelines (Table 4.7). Cadmium concentrations were significantly higher ($p < 0.05$) in the Inner Bay relative to the Central and Outer Bays.

Coral

Cadmium concentrations in coral tissues ranged from 0.21 $\mu\text{g/g}$ to 0.31 $\mu\text{g/g}$, with a mean of 0.25 $\mu\text{g/g}$ and a median of 0.25 $\mu\text{g/g}$ (Table 4.5). This is higher than what was detected in sediments and may indicate that coral are accumulating cadmium in their tissues over time. This is higher than what was observed in southwest Puerto Rico, but similar to what was observed in Vieques, Puerto Rico (Table 4.6). There was no statistically significant difference between the inshore and offshore strata (Appendix B, Figure B.4). No statistically significant correlations were found between coral tissue Cd concentrations and depth, longitude (*i.e.*, long shore position) or distance from land.

4.3.6.5. Chromium (Cr)

Sediment

Chromium (Cr) concentrations in sediments ranged from 0 µg/g to 29.8 µg/g, with a mean of 18.2 µg/g and a median of 18.5 µg/g (Table 4.6). This is lower than the NS&T national median of 66 µg/g and no site exceeded sediment quality guidelines. Cr concentrations were significantly higher ($p < 0.05$) in the Inner Bay relative to the Central and Outer Bays (Figure 4.11 and Appendix B, Figure B.5).

Coral

Chromium was not detected in any coral tissue samples (Table 4.5). Similarly, no Cr was detected in corals in southwest Puerto Rico; however, Cr was detected in coral tissues in Vieques, Puerto Rico (Table 4.5), so corals do have the capacity to accumulate chromium.

4.3.6.6. Copper (Cu)

Sediments

Copper (Cu) concentrations in sediments ranged from 1.37 µg/g to 73.7 µg/g, with a mean of 33.83 µg/g and a median of 29.85 µg/g (Table 4.6). This is higher than the NS&T national median of 15.95 µg/g, and higher than other studies in tropical systems (Figure 4.7), indicating that Jobos Bay has elevated amounts of copper. No site exceeded the ERM guideline but 19 of 43 sites exceeded the ERL, indicating that there is a slight (<10%) chance of toxicity to benthic infaunal organisms. Copper concentrations were significantly higher ($p < 0.05$) in the Inner Bay relative to the Central and Outer Bays (Appendix B, Figure B.6). Potential sources of copper include agricultural fungicides and anti-fouling boat paint.

Coral

Copper concentrations in coral ranged from 2.37 µg/g to 97.20 µg/g, with a mean of 50.30 µg/g and a median of 68.95 µg/g (Table 4.5). This is higher than coral tissues measured in other studies in Puerto Rico (Table 4.5), which mirrors the pattern in sediment Cu and suggests that there may be a copper contamination problem in Jobos Bay. There was no statistically significant difference between the inshore and offshore strata (Appendix B, Figure B.7). No statistically significant correlations were found between coral tissue Cu concentrations and depth, longitude (*i.e.*, long shore position) or distance from land.

4.3.6.7. Iron (Fe)

Sediments

Iron (Fe) concentrations in sediments ranged from 1060 µg/g to 50500 µg/g, with a mean of 26565 µg/g and a median of 26650 µg/g (Table 4.6). Iron is a major crustal element and is generally not considered to be a pollutant. There are no sediment quality guidelines for Fe. Iron concentrations were significantly higher ($p < 0.05$) in the Inner Bay relative to the Central and Outer Bays (Appendix B, Figure B.8).

Coral

Iron concentrations in coral ranged from 110 µg/g to 480 µg/g, with a mean of 212 µg/g and a median of 176 µg/g (Table 4.5). There was no statistically significant difference between the inshore and offshore strata (Appendix B, Figure B.9). No statistically significant correlations were found between coral tissue Fe concentrations and depth, longitude (*i.e.*, long shore position) or distance from land.

4.3.6.8. Mercury (Hg)

Sediments

Mercury (Hg) concentrations in sediments ranged from 0.0014 µg/g to 0.144 µg/g, with a mean of 0.043 µg/g and a median of 0.03085 µg/g (Table 4.6). This is lower than the NS&T national median

of 0.062 $\mu\text{g/g}$ and similar to other studies in tropical systems (Table 4.7). No site exceeded sediment quality guidelines. Mercury concentrations were significantly higher ($p < 0.05$) in the Inner Bay relative to the Central and Outer Bays (Figure 4.11 and Appendix B, Figure B.10).

Coral

Mercury concentrations in coral ranged from 0.001 $\mu\text{g/g}$ to 0.0038 $\mu\text{g/g}$, with a mean of 0.002 $\mu\text{g/g}$ and a median of 0.0019 $\mu\text{g/g}$ (Table 4.5). This is a similar finding to Vieques, Puerto Rico where mercury was detected in six out of 35 samples (Table 4.5). Mercury concentrations were significantly higher ($p < 0.05$) in the offshore stratum than inshore (Appendix B, Figure B.11). This pattern could be a result of atmospherically deposited Hg from fossil fuel combustion at the nearby power plant (Figure 4.14), *i.e.* the stack height minimizes near shore deposition.



Figure 4.14. Power generation facility adjacent to Jobos Bay. Photo: NOAA CCMA

4.3.6.9. Manganese (Mn)

Sediments

Manganese (Mn) concentrations in sediments ranged from 33.1 $\mu\text{g/g}$ to 1130 $\mu\text{g/g}$, with a mean of 510.6 $\mu\text{g/g}$ and a median of 528.5 $\mu\text{g/g}$ (Table 4.6). This is slightly higher than the NS&T national median of 444.5 $\mu\text{g/g}$. Sediment quality guidelines do not exist for Mn. Manganese concentrations were significantly higher ($p < 0.05$) in the Inner Bay relative to the Central and Outer Bays (Appendix B, Figure B.12)

Coral

Manganese concentrations in coral tissues ranged from 8.33 $\mu\text{g/g}$ to 24.60 $\mu\text{g/g}$, with a mean of 13.33 $\mu\text{g/g}$ and a median of 11.60 $\mu\text{g/g}$ (Table 4.5). This is slightly higher than levels measured in other studies in Puerto Rico (Table 4.5). There was no statistically significant difference between the inshore and offshore strata (Appendix B, Figure B.13). No statistically significant correlations were found between coral tissue Mn concentrations and depth, longitude (*i.e.*, long shore position) or distance from land.

4.3.6.10. Nickel (Ni)

Sediments

Nickel (Ni) concentrations in sediments ranged from 0 $\mu\text{g/g}$ to 31 $\mu\text{g/g}$, with a mean of 10.96 $\mu\text{g/g}$ and a median of 10.1 $\mu\text{g/g}$ (Table 4.6). This is below the NS&T national median of 25.05 $\mu\text{g/g}$ and similar to other sites in tropical systems (Table 4.7). No sites exceeded the ERM sediment quality guidelines. Nickel concentrations were significantly higher ($p < 0.05$) in the Inner Bay relative to the Central and Outer Bays (Appendix B, Figure B.14).

Coral

Nickel concentrations in coral tissues ranged from 0.80 $\mu\text{g/g}$ to 6.84 $\mu\text{g/g}$, with a mean of 3.13 $\mu\text{g/g}$ and a median of 2.63 $\mu\text{g/g}$ (Table 4.5). This is similar to what was observed in other studies in Puerto

Rico (Table 4.5). There was no statistically significant difference between the inshore and offshore strata (Appendix B, Figure B.15). No statistically significant correlations were found between coral tissue Ni concentrations and depth, longitude (*i.e.*, long shore position) or distance from land.

4.3.6.11. Lead (Pb)

Sediments

Lead (Pb) concentrations in sediments ranged from 0.227 $\mu\text{g/g}$ to 16.7 $\mu\text{g/g}$, with a mean of 7.15 $\mu\text{g/g}$ and a median of 6.02 $\mu\text{g/g}$ (Table 4.6). This is below the NS&T national median of 22.25 $\mu\text{g/g}$, and similar to other studies in tropical systems (Table 4.7). No sites exceeded sediment quality guidelines. Lead concentrations were significantly higher ($p < 0.05$) in the Inner Bay relative to the Central and Outer Bays (Appendix B, Figure B.16).

Coral

Lead concentrations in coral tissues ranged from 0.08 $\mu\text{g/g}$ to 12.50 $\mu\text{g/g}$, with a mean of 1.43 $\mu\text{g/g}$ and a median of 0.20 $\mu\text{g/g}$ (Table 4.5). The observed concentrations in Jobos Bay are higher than seen in other systems in Puerto Rico (Table 4.5), despite not having high concentrations of Pb in sediments. There was no statistically significant difference between the inshore and offshore strata; however, Pb showed a weak positive correlation with distance from shore ($p = 0.0099$, $\alpha = 0.62$), and a strong negative correlation ($p = 0.001$, $\alpha = -0.7324$) with longitude (Figure 4.15), *i.e.* Pb concentrations were higher to the west. No statistically significant correlation was found between coral tissue Pb concentrations and depth. There are many sources of Pb in the environment and more research is needed to understand these spatial patterns. The positive correlation with distance from shore is similar to what is seen for Hg and As (offshore stratum significantly higher than inshore stratum), and could indicate

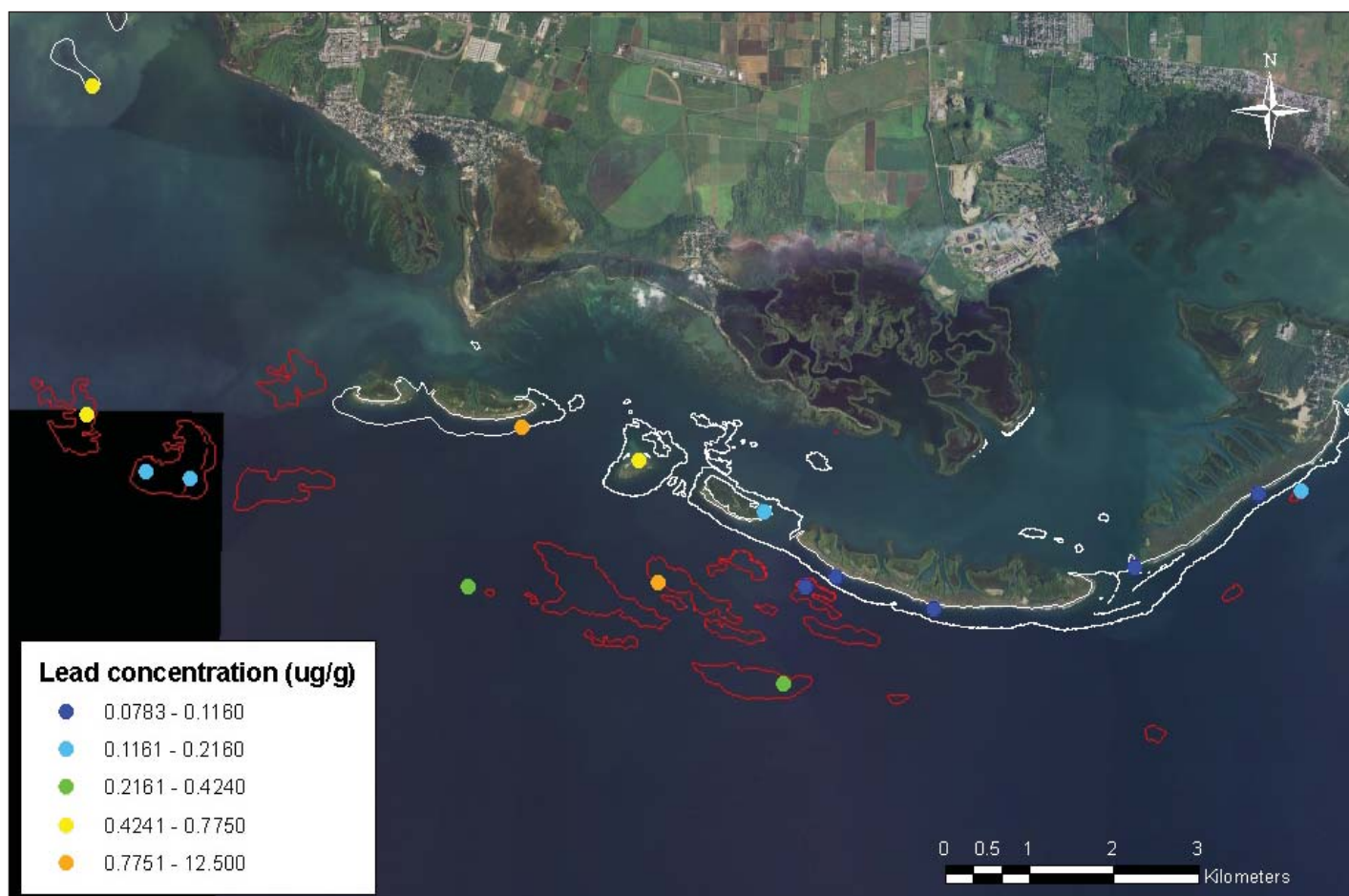


Figure 4.15. Lead (Pb) concentrations in corals (*P. astreoides*). White outline are coral reefs in inner stratum. Red outline are coral reefs in outer stratum.

that the power plant is a source of Pb. Furthermore, satellite imagery of the power plant shows stack plume emissions drifting to the west (Figure 4.16), which could explain the gradient of concentrations from east to west. It is possible that this longitudinal pattern is not observed in the sediment concentration because sediment concentrations are closely tied to sediment TOC and percent fines.



Figure 4.16. Satellite image of Jobos Bay showing plume from power plant.

4.3.6.12. Antimony (Sb)

Sediments

Antimony (Sb) concentrations in sediments ranged from 0 $\mu\text{g/g}$ to 0.589 $\mu\text{g/g}$, with a mean of 0.217 $\mu\text{g/g}$ and a median of 0.2685 $\mu\text{g/g}$ (Table 4.6). This is lower than the NS&T national median of 0.485 $\mu\text{g/g}$ and similar to other studies in Puerto Rico (Table 4.7). There are no sediment quality guidelines for antimony. Antimony concentrations were significantly higher ($p < 0.05$) in the Inner Bay relative to the Central and Outer Bays (Appendix B, Figure B.17)

Coral

Antimony was not measured in coral tissue.

4.3.6.13. Selenium (Se)

Sediments

Selenium (Se) concentrations in sediments ranged from 0 $\mu\text{g/g}$ to 0.156 $\mu\text{g/g}$, with a mean of 0.332 $\mu\text{g/g}$ and a median of 0.2755 $\mu\text{g/g}$ (Table 4.6). This is similar to the NS&T national median of 0.33 $\mu\text{g/g}$, but slightly higher than other studies in Puerto Rico (Table 4.7). There are no sediment quality guidelines for Se. Concentrations of Se showed no statistical difference between the three strata ($p > 0.05$; Appendix B, Figure B.18).

Coral

Selenium concentrations in coral tissues ranged from 0.13 $\mu\text{g/g}$ to 0.26 $\mu\text{g/g}$, with a mean of 0.18 $\mu\text{g/g}$ and a median of 0.18 $\mu\text{g/g}$, which is slightly higher than observed in other locations in Puerto Rico (Table 4.5). There was no statistically significant difference between the inshore and offshore strata (Appendix B, Figure B.19). No statistically significant correlations were found between coral tissue Se concentrations and depth, longitude (*i.e.*, long shore position) or distance from land.

4.3.6.14. Tin (Sn)

Sediments

Tin (Sn) concentrations in sediments ranged from 0 $\mu\text{g/g}$ to 2.74 $\mu\text{g/g}$, with a mean of 1.13 $\mu\text{g/g}$ and a median of 1.17 $\mu\text{g/g}$ (Table 4.6). This is lower than the NS&T national median of 1.75 $\mu\text{g/g}$ and similar to what has been observed in other tropical systems (Table 4.7). There are no sediment quality guidelines for tin. Tin concentrations were significantly higher ($p < 0.05$) in the Inner Bay relative to the Central and Outer Bays (Appendix B, Figure B.20).

Coral

Tin concentrations in coral tissues ranged from 0 µg/g to 0.10 µg/g, with a mean of 0.02 µg/g and a median of 0.01 µg/g; this is similar to what was observed in southwest Puerto Rico, but lower than observed values in Vieques, Puerto Rico (Table 4.5). In Jobos Bay, there was only one site in the study area with measurable Sn (Appendix B, Figure B.21). There was no statistically significant difference between the inshore and offshore strata. No statistically significant correlations were found between coral tissue Sn concentrations and depth, longitude (*i.e.*, long shore position) or distance from land.

4.3.6.15. Zinc (Zn)

Sediments

Zinc (Zn) concentrations in sediments ranged from 1.57 µg/g to 117 µg/g, with a mean of 54.2 µg/g and a median of 48.5 µg/g (Table 4.6). This is lower than the NS&T national median of 74 µg/g, and similar to other studies in tropical systems (Table 4.7). No sites exceeded sediment quality guidelines (Table 4.7). Zinc concentrations were significantly higher ($p < 0.05$) in the Inner Bay relative to the Central and Outer Bays (Appendix B, Figure B.22).

Coral

Zinc concentrations in coral tissues ranged from 2.56 µg/g to 16.90 µg/g, with a mean of 8.59 µg/g and a median of 7.88 µg/g, which was similar to what has been observed in other studies in Puerto Rico (Table 4.5). There was no statistically significant difference between the inshore and offshore strata (Appendix B, Figure B.23). No statistically significant correlations were found between coral tissue Zn concentrations and depth, longitude (*i.e.*, long shore position) or distance from land.

4.4. FURTHER INTERPRETATION OF SEDIMENT RESULTS

The adsorption of organic contaminants onto sediments is strongly influenced by grain size (Hassett *et al.*, 1980). A regression between grain size and the concentration of total PAHs in the sediment samples indicated a highly significant (Spearman's $\rho = 0.6872$, $p < 0.0001$) relationship between the fines fraction of the sediment and the concentration of total PAHs. A bivariate regression run between \log_{10} total PAH and \log_{10} TOC indicated a significant ($p < 0.0001$, $r^2 = 0.515$) relationship between TOC and the concentration of total PAHs, as has been found by others (Hassett *et al.*, 1980; Shine and Wallace, 2000) in aquatic systems.

The distribution of high (≥ 4 rings) molecular weight (HMW) versus low molecular weight (LMW) PAHs (Table 4.1) in sediment samples has been used as an indicator of pyrogenic (combustion-related) versus petrogenic (*e.g.*, petroleum product from fuel or oil spills, or other discharges) sources (Neff *et al.*, 2005). Although the mean concentration of the HMW or pyrogenic PAHs was higher in Jobos Bay sediments, a Wilcoxon test revealed no significant difference in the mix of LMW and HMW PAHs ($\text{Prob} > \text{ChiSq} = 0.0639$). The ratios of phenanthrene to anthracene (P/A), and fluoranthene to pyrene (Fluo/Pyr) have also been used to assess the relative contributions of petrogenic versus pyrogenic sources of PAHs (Budzinski *et al.*, 1997). P/A ratios less than 10 are more indicative of pyrogenic sources, while Fluo/Pyr ratios greater than one are also thought to be associated with pyrogenic sources. Except for SWP43, all the sites sampled had P/A ratios of less than 10, and all the Fluo/Pyr ratios were close to one. These results are similar to those obtained by Aldarondo-Torres *et al.* (2010) who found P/A and Fluo/Pyr ratios in Jobos Bay sediments indicative of pyrogenic sources. There are two dischargers in the watershed with U.S. Environmental Protection Agency (USEPA) National Pollutant Discharge Elimination System (NPDES) permits for oil and grease (see Chapter 1, Table 1.1, Figure 1.1) which are also contributing to PAH levels in the Bay.

Because the measurement of total DDT is made up of both the parent isomers and degradation products, the ratio of parent compounds to degradation products can provide some insight into the relative age or “freshness” of the DDT present. Total DDT concentrations containing higher ratios of the parent compound are more likely to be recently introduced into the environment. The ratio of parent compounds (2,4'-DDT and 4,4'-DDT) to degradation products (2,4'-DDD, 4,4'-DDD, 2,4'-DDE, 4,4'-DDE and DDMU) ranged from zero (no parent compound detected, at 22 sites) to one (parent compound detected, but no degradation products detected, at site OTR31). Five sites (four in the central stratum, plus OTR31) had greater than 50% parent material. This may be indicative of “newer” DDT, although interpretation of these ratios can be problematic when concentration values are close to the detection limit. None of the five sites with greater than 50% parent material had high total DDT concentrations (below the ERL), which does not suggest that the levels of DDT at these sites are of environmental concern.

For the majority of metals, elevated concentrations were observed mostly in sediments collected from the Inner Bay in the eastern stratum. However, spikes of relatively elevated concentrations were observed for some metals throughout the study area. For instance, the highest concentrations were observed at NER24 and SWP44 in Central Bay for As; NER24 and OTR34 in Central and Outer Bays, respectively, for Cr, and the highest concentrations for Ni were found at sites NER24, SWP43 and SWP44 in Central Bay.

4.4.1. Inter-metal and grain size correlation

Spearman rank correlations among all metals, grain size and TOC are shown in Table 4.8. Spearman coefficient Rho (ρ) values of 0.707 or higher were discussed as indicative of strong correlation, while values below 0.707 indicate weak correlation. Strong associations were found among several groups of metals. Among the major elements, Al and Fe showed strong and direct correlations with each other and with virtually all trace metals except Ag. Also, Mn was positively correlated with Al, Fe and all other trace elements except Se ($p > 0.05$). Apart from Ag, which had a poor and inverse correlation; the results indicated that, in general, inter-metal correlations were positive. Other studies have reported significant correlations between major elements, such as Al, Fe, and Mn, and trace metals in similar habitats off the southeastern coast of the United States (Windom *et al.*, 1989; Schropp *et al.*, 1990). These studies suggest that Al and Fe can be used as normalizing factors for metals in natural estuaries and coastal environments to assess anthropogenic metals enrichment.

Grain size and sediment TOC were found to be positively correlated with all major and trace elements, excluding Ag. All metals have a weak correlation with TOC. Relative to TOC, grain size showed stronger correlations ($p > 0.707$) with the major and trace metals. These results confirm that elemental concentrations are elevated in finer sediments because of higher volume to surface ratio (Förstner and Wittmann, 1981). The depositional zone in the Inner bay stratum had metal concentrations greater than the other strata, likely due to fine grained sediments and proximity to metal sources. Total organic carbon ranged from 0.3-4.3% and was only weakly correlated with metals.

The highest percentages of TOC were observed in sediment from the central stratum, while sediments from the eastern and western stratum were relatively low in TOC content. Except for Ni and Se, TOC content was not strongly correlated with metals suggesting that the influence of organic matter on metal distribution may be far less important than that of grain size. This observation corroborates with assertion by Förstner and Wittmann (1981) and Windom *et al.* (1989), which indicated that in natural estuarine and coastal sediments, concentrations of metals are predominantly determined by detrital inorganic material rather than organic and nondetrital materials.

Table 4.8. Spearman rank correlations between metals, grain size (clay + silt) and total organic carbon (TOC) in sediment from Jobos Bay. Bold lettering represents the Rho value (ρ) and standard script represents p values.

Label	%TOC	%Fine	Ag	Al	As	Cr	Cu	Fe	Hg	Mn	Ni	Pb	Sb	Se	Sn
%Fine	0.424														
	0.005														
Ag	-0.111	-0.316													
	0.479	0.039													
Al	0.239	0.911	-0.366												
	0.122	0.000	0.016												
As	0.405	0.720	-0.398	0.740											
	0.007	0.000	0.008	0.000											
Cr	0.520	0.739	-0.075	0.752	0.700										
	0.000	0.000	0.632	0.000	0.000										
Cu	0.619	0.822	-0.133	0.801	0.683	0.892									
	0.000	0.000	0.394	0.000	0.000	0.000									
Fe	0.390	0.911	-0.252	0.965	0.787	0.845	0.873								
	0.010	0.000	0.102	0.000	0.000	0.000	0.000								
Hg	0.693	0.747	-0.169	0.696	0.700	0.815	0.941	0.781							
	0.000	0.000	0.279	0.000	0.000	0.000	0.000	0.000							
Mn	0.039	0.839	-0.402	0.952	0.696	0.615	0.670	0.887	0.582						
	0.801	0.000	0.008	0.000	0.000	0.000	0.000	0.000	0.000						
Ni	0.708	0.573	-0.239	0.555	0.639	0.800	0.814	0.631	0.831	0.373					
	0.000	0.000	0.122	0.000	0.000	0.000	0.000	0.000	0.000	0.014					
Pb	0.689	0.784	-0.233	0.722	0.700	0.798	0.938	0.793	0.975	0.612	0.824				
	0.000	0.000	0.132	0.000	0.000	0.000	0.000	0.000	0.000	0.000	0.000				
Sb	0.368	0.559	-0.286	0.633	0.790	0.725	0.648	0.665	0.622	0.539	0.697	0.642			
	0.015	0.000	0.063	0.000	0.000	0.000	0.000	0.000	0.000	0.000	0.000	0.000			
Se	0.918	0.510	-0.156	0.353	0.521	0.639	0.687	0.482	0.721	0.137	0.789	0.709	0.497		
	0.000	0.000	0.318	0.020	0.000	0.000	0.000	0.001	0.000	0.380	0.000	0.000	0.001		
Sn	0.560	0.842	-0.253	0.747	0.626	0.823	0.887	0.798	0.852	0.635	0.686	0.868	0.607	0.650	
	0.000	0.000	0.102	0.000	0.000	0.000	0.000	0.000	0.000	0.000	0.000	0.000	0.000	0.000	
Zn	0.541	0.900	-0.200	0.893	0.720	0.891	0.964	0.945	0.891	0.777	0.735	0.906	0.654	0.627	0.914
	0.000	0.000	0.199	0.000	0.000	0.000	0.000	0.000	0.000	0.000	0.000	0.000	0.000	0.000	0.000

In Jobos Bay, the distribution of inorganic material (grain size) demonstrated a distinctive general pattern. Fine grained material showed a decreasing gradient from the eastern to the western zone of the study area (Figure 4.17). These findings are in agreement with previous results reported by the Puerto Rico Nuclear Center (PRNC, 1972), which characterized the eastern area (Inner Bay) stratum as having silty bottom sediment relative to areas of the bay where sediments are more or less sandy.

The predominantly elevated proportion of fine sediment materials in the Inner bay demonstrates that the area is a low energy depositional zone. Physical conditions and the water circulation in the Inner Bay are suitable for sedimentation of terrigenous fine particles suspended in runoff waters. Sedimentation of these fine particles in the Inner Bay may be favored as a result of surface water input from Quebrada Coquí-Aguas Verdes and Río Seco, the shallowness of the bay and the fact that the Inner Bay is semi-enclosed (PRNC, 1972).

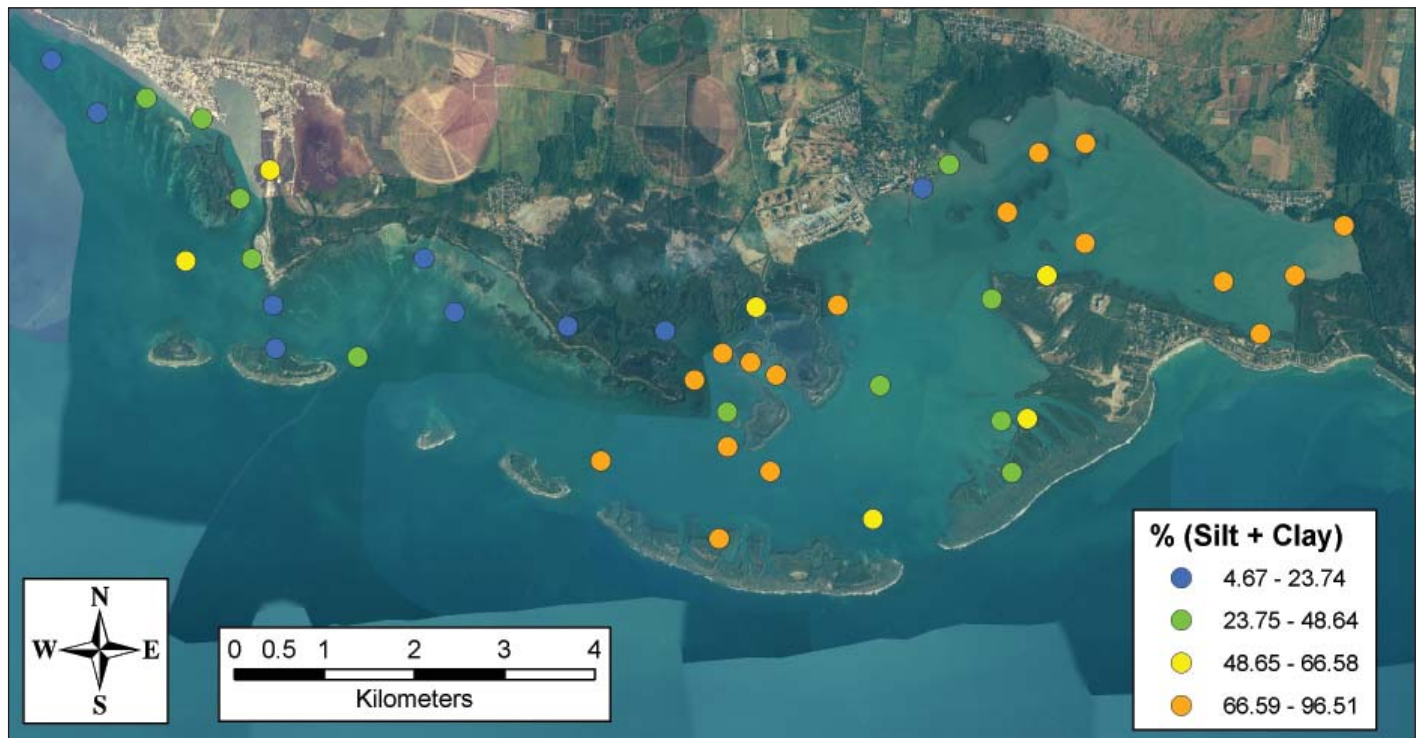


Figure 4.17. Sediment grain size (percent fines).

The concentrations of the majority of metals showed similar distributions as that of grain size. Relative to the Outer and Central Bays, significantly high ($p < 0.05$) metal concentrations are found in the Inner Bay stratum located in the eastern area of the bay. The physiographic characteristic of the stratum and the sediment texture may be the cause of the relatively high metal concentrations in the Inner Bay stratum. The Inner Bay is the receiving basin for Quebrada Coquí-Aguas Verdes and Río Seco, which transport terrigenous detrital materials from the upland. Being physically protected from the scouring of offshore water, the Inner Bay acts like a depositional area characterized by calm waters. As a result, sediment materials transported by Quebrada Coquí-Aguas Verdes and Río Seco are deposited along with pollutants. Furthermore, the presence of metals in elevated concentrations in the Inner Bay may be linked to its characteristically fine grained sediment. It has been shown that because of their high surface to volume ratio, fine sediments like those found in the Inner Bay, tend to sequester higher concentrations of metals (Förstner and Wittmann, 1981; Ujević *et al.*, 2000; Oreščanin *et al.*, 2004). Conversely, the relatively low concentration of metals found in the Outer and Central Bays may be due the presence of a sandier type of sediment and particularly to the fact that these systems are well flushed by offshore water.

Among the trace elements, Cd was measured at very low concentration at virtually all the sites in the study area. Chemically, Cd is strongly affected by diagenetic processes that impact its equilibrium between pore water and the overlying water column (Rosenthal *et al.*, 1995). During this process, Cd migrates into porewater in the top oxidized sediment layer while the inverse occurs in the reduced deeper layers. The diagenetic behavior of Cd is usually linked to its depletion in the upper oxidized layer of sediments (Rosenthal *et al.*, 1995; Apeti *et al.*, 2009). Because of its low concentration in this study, Cd was not included in any subsequent discussion.

The presence of metals at relatively elevated concentration in the eastern area of Jobos Bay may be linked to diffused nonpoint sources of natural and anthropogenic origins. Jobos Bay watershed is host to a variety of residential, commercial and industrial activities, most notably a coal power plant, a petroleum refinery and pharmaceutical facilities (DNER, 2002), that likely contribute pollutants to the bay. In the Jobos Bay watershed, there are three documented point source dischargers of pollutants

relevant to this study (See Chapter 1, Table 1.1, Figure 1.2). These dischargers represent a source of Cr, Cu, Fe, Pb, Mn, Se and Zn, although the amounts of these metals being discharged are fairly low. However, USEPA documented significant non-compliance events for Zn in 2007 and 2008, and Ag, Cu and Fe in 2009. Because sediment sampling for this study was completed in 2008, the 2009 events could not have influenced the data presented here; however, it is noteworthy that these point sources can contribute to the contaminant load of the system.

Coal burning is associated with atmospheric pollution by metals, such as As, Cd, Cu, Hg, Pb, Ni, Zn found in fly ash (Theis *et al.*, 1978; McBride *et al.*, 1978). Atmospheric depositions of metal from industrial emissions in the vicinity of Jobos Bay were assessed (Jiménez-Vélez *et al.*, 2003, 2009; Gioda *et al.*, 2006). Relative to other regions in Puerto Rico, concentrations of metal in airborne particles were higher in the Salinas watershed, which incorporates Jobos Bay (Jiménez-Vélez *et al.*, 2003). Gioda *et al.* (2006) also concluded that the presence of Cd, Cu, Fe, Ni, Hg and Pb in airborne particles in the Jobos Bay may be linked to both long-range atmospheric transport and anthropogenic activities in the bay's watershed. Rather than being from local industrial activities, previous studies indicated that concerns of water quality in Jobos Bay may be linked to land-based sources from agricultural runoff and soil erosion (DNER, 2002).

Preliminary studies (Altieri-Rijos, 2004) revealed that pesticides and fertilizers applied in agricultural fields may also be transported to the JBNERR bay (DNER, 2002). Although metals such as Cd, Cr, Cu, Fe, Hg, Mn, Pb, Ni and Zn are minor constituents of phosphorus fertilizers (Förstner and Wittmann, 1981), they also occur naturally. Copper is also used as an agricultural fungicide, and in anti-fouling boat paint. As a result, it is difficult to distinguish between natural and anthropogenic sources. Metallic contaminants, whether from natural or anthropogenic sources, are supplied in solution or in association with fine-grained suspended solids and colloidal inorganic particles. These particles are usually deposited in areas of low hydrodynamic energy along streams or are transported to lakes, estuaries, or the ocean during times of increased river flow (Loring, 1991; Simpson *et al.*, 2000).

A number of mechanisms, based on geochemical processes that control behavior and fate of metals in coastal waters, have been proposed (Förstner and Wittmann, 1981; Schropp and Windom, 1987). In natural coastal waters, trace metals co-precipitate with the oxide/hydroxides of Al, Fe and Mn usually into the fine-grained fraction (clay or aluminosilicate) of sediments (Schropp and Windom, 1987). Since aluminosilicates are the metal-rich phase of bottom sediment, many approaches to delineate anthropogenic versus natural sources are based on grain size, using Al and Fe for normalization (Förstner and Wittmann, 1981; Windom *et al.*, 1989; MacDonald, 1994). That is, without anthropogenic inputs, metal concentrations are expected to co-vary among each other and with Al, Fe and Mn, given that factors such as precipitation or diagenesis are very small. Deviations from direct metal-Al/Fe or metal-grain size correlations are interpreted as anthropogenic enrichment (Windom *et al.*, 1989; MacDonald, 1994; Carvalho *et al.*, 2002).

In Jobos Bay, most of the metals, except Ag, were found to be positively correlated with grain size (Table 4.8). Correlations of metals versus grain size and Al are exemplified using results for Ag, Fe, Mn and Zn (Figures 4.18 and 4.19). The positive correlations suggest that sediment texture greatly influences the distribution of metals. Additionally, the positive inter-metal correlations, including those between Al, indicate that metal concentrations in Jobos Bay may be of natural origins.

Considering the arid conditions in the watershed and lack of over land flow, other contributions of metals to Jobos Bay may include stormwater runoff, inputs from Quebrada Coquí-Aguas Verdes and Río Seco and atmospheric deposition. Weathering of bedrock and soil erosion produce mineral debris

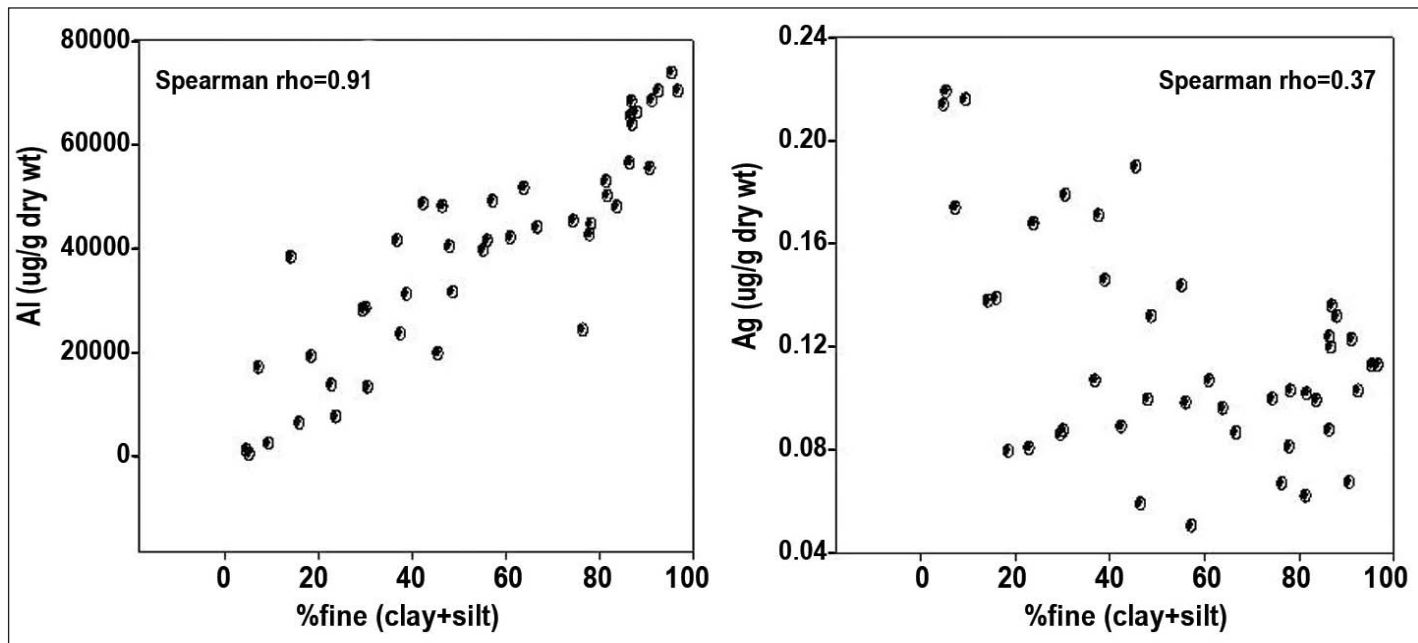


Figure 4.18. Correlation of aluminum and silver with grain size (percent fines).

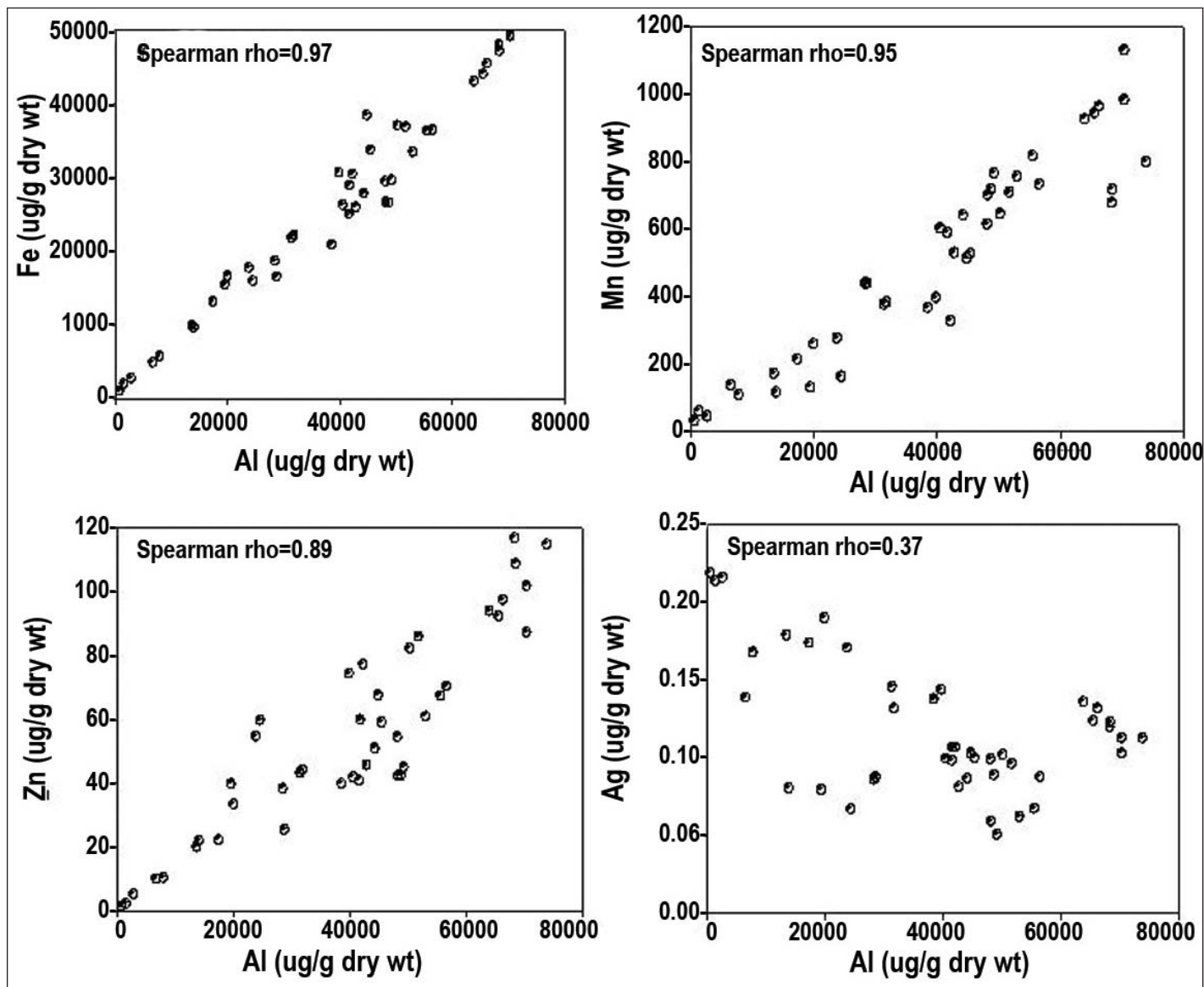


Figure 4.19. Correlation of iron, manganese, zinc and silver with aluminum.

that are natural sources of metal in sediment transported into coastal waters (Förstner and Wittmann, 1981). Transport of detrital materials within watershed by stormwater and runoff, and Quebrada Coquí-Aguas Verdes may constitute the largest source of metals in Jobos Bay. Although Quebrada Río Seco is a seasonal intermittent river, it may also contribute to metal bound sediment transport into the bay especially during wet seasons. However, the characteristic deviations of Ag from direct positive correlation with both Al and grain size may be interpreted as having anthropogenic inputs.

Of the 15 metals, only Ag was found to have a spatial distribution that contrasted with that of the general east-west decreasing pattern (Figure 4.12). Additionally, Ag did not show a direct correlation with Al and grain size. Current levels of Ag concentration in Jobos Bay are lower than the ERL and ERM values, but the fact that it has relatively elevated concentrations in the more sandy western area of the bay (Figure 4.12), suggests enrichment. Possible sources of Ag in the western stratum may include industrial discharges or runoff. It should be noted that there are no NPDES permitted dischargers of silver in the watershed.

4.5. CONCLUSIONS

The concentrations of the contaminants analyzed for this project were generally similar to what has been found in other areas of Puerto Rico. Overall, the levels of chemical contaminants in the sediments in the Jobos Bay study area were below established sediment quality guidelines, suggesting that effects on infaunal biota were unlikely. The ERMs and the PEL were not exceeded for any of the classes of compounds for which these guidelines have been developed. For individual PAHs, however, there were exceedances of the PEL at one site (INR4) in the inner stratum for five PAHs, indicating that infaunal biota at this site could be impacted by the presence of at least these individual PAHs. ERL's were exceeded at some sites for total DDT, total PAHs, chlordane, dieldrin, arsenic and copper.

In general, the concentration of the analyte classes including metals, total PAHs, total PCBs and total DDT were higher in the inner stratum, which is likely a function of land use activities, delivery of the contaminants via surface water runoff and river inputs, and lower water exchange with the open ocean. This pattern was reversed for tributyltin and silver with outer stratum sediments having significantly higher sediment concentrations. The TBT pattern appears to be associated with marina-related activities, but it is unclear what is driving this pattern for silver.

Sediment characteristics, such as grain size and TOC, and baseline metal concentrations have been assessed in Jobos Bay. Overall, the distributions of sediment grain size and TOC content suggested heterogeneous bottom substrates in Jobos Bay. Grain size appears to heavily influence the distribution of all metals except that of Ag. Most metals were found to be significantly higher in the eastern area of the bay relative to central and western areas. However, maximum concentration values were within concentration ranges found in other similar estuarine systems. Sediment normalizing factors, such as Al and grain size, were positively correlated with virtually all metals. This suggests that although the watershed contains several low density population centers and some industrial plants, anthropogenic inputs may be negligible. Likely sources of metals in Jobos Bay may include natural bedrock weathering and transportation of detrital materials by Quebrada Coquí-Aguas Verdes and Río Seco. The more diffuse nonpoint source of atmospheric deposition resulting from local and long range airborne particles are also possible sources, which may be contributing to the overall metal concentration in Jobos Bay. The lack of correlation of Ag with normalizing factors suggested enrichment from anthropogenic sources for this metal. However, the concentrations of Ag as well as those of other metals were well below sediment quality guidelines suggesting that metal toxicity to biota is limited in Jobos Bay. This study is the first comprehensive assessment of metals in Jobos Bay and the associated data serve as baseline information for further assessments and monitoring.

The degradation of coral reef ecosystems worldwide has led to intensive efforts to understand and mitigate the stressors responsible for the declines of these valued and fragile ecosystems. The role of pollution in the degradation of coral reefs is often cited as a major factor, but the degree to which pollution and more specifically chemical contaminants are present in coral reef areas is, in most cases, unknown. Because of this, coral reef managers may be missing an important piece of information needed to effectively manage reef areas. Quantifying the types and concentrations of chemical contaminants present in the sediments in Jobos Bay is an important aspect of the Conservation Effects Assessment Project (CEAP), providing a baseline of conditions in the nearshore waters, and a means for assessing the benefits of Best Management Practices that may be implemented in the Jobos Bay watershed (Figure 4.20).



Figure 4.20. Jobos Bay and the fringing mangrove forest adjacent to the Bay. Photo: NOAA CCMA.

ACKNOWLEDGEMENTS

We would like to thank Captain Claudio Burgos of the *Estuarino* for his skill and patience in getting us to the sampling sites. We also greatly appreciate boat support provided by PRDNER. We would also like to thank the CEAP project partners, JBNERR and the USDA. This chapter was greatly improved thanks to helpful comments from Dr. Gunnar Lauenstein, Dr. Fatin Samara and Dr. Carlos J. Rodríguez-Sierra. Funding for this work was provided by NOAA's Coral Reef Conservation Program and the USDA (CEAP).

REFERENCES

- Aldarondo-Torres, J.X., F. Samara, I. Mansilla-Rivera, D.S. Aga, and C.J. Rodríguez-Sierra. 2010. Trace metals, PAHs, and PCBs in sediments from the Jobos Bay area in Puerto Rico. *Marine Pollution Bulletin* 60: 1350-1358.
- Altieri-Rijos, C. 2004. Determination of pesticides in surface and run-off discharge into the groundwater in the Jobos National Estuarine Research Reserve. Graduate Research Fellow, MS Thesis, University of Puerto Rico/Medical Science Campus.
- Apeti, D.A., G.G. Lauenstein, and G.F. Riedel. 2009. Cadmium distribution in coastal sediments and mollusks of the US. *Marine Pollution Bulletin* 58: 1016-1024.
- Batley, G. 1996. Distribution and fate of tributyltin in the marine environment. pp. 139-165. In: S.J. de Mora (ed.). *Tributyltin: A Case Study of an Environmental Contaminant*, Cambridge Environmental Chemistry Series. Cambridge University Press, Cambridge, England. 301 pp.
- Bennett, R.F. 1996. Industrial manufacture and applications of tributyltin compounds. pp. 21-61. In: S.J. de Mora (ed.). *Tributyltin: A Case Study of an Environmental Contaminant*, Cambridge Environmental Chemistry Series. Cambridge University Press, Cambridge, England. 301 pp.

Birchenough, A.C., N. Barnes, S.M. Evans, H. Hinz, I. Krönke, and C. Moss. 2002. A review and assessment of tributyltin contamination in the North Sea, based on surveys of butyltin tissue burdens and imposex/intersex in four species of neogastropods. *Marine Pollution Bulletin* 44: 534-543.

Budzinski, H., I. Jones, J. Bellocq, C. Piérard, and P. Garrigues. 1997. Evaluation of sediment contamination by polycyclic aromatic hydrocarbons in the Gironde estuary. *Marine Chemistry* 58: 85-97.

Cantillo, A.Y., G.G. Lauenstein, W.E. Johnson, and T.P. and O'Connor. 1999. Status and Trends of contaminant levels in biota and sediments of Tampa Bay. National Oceanic and Atmospheric Administration Regional Report Series 5. Silver Spring, MD. 43 pp.

Carvalho, A., S.J. Schorp, and G.M. Sloane. 2002. Development of an Interpretive Tool for Assessment of Metal Enrichment in Florida Freshwaters Sediment. Florida department of Environmental Protection, C2001-022. Tallahassee, FL. 60 pp.

Code of Federal Regulations (CFR). 1998. PCB allowable uses provisions. 40 CFR 761.80, July 1998. (Online) <http://www.access.gpo.gov/nara/cfr/cfr-table-search.html> (Accessed 13 June 2011).

Department of Natural and Environmental Resources (DNER). 2002. Jobos Bay Estuarine Profile: A National Estuarine Research Reserve. Puerto Rico DNER and National Oceanic and Atmospheric Administration, Office of Ocean and Coastal Resource Management, Estuarine Reserve Division. 107 pp.

Eisler, R. 1985. Cadmium hazards to fish, wildlife, and invertebrates: a synoptic review. U.S. Fish and Wildlife Service Biological Report 85 (1.2). Contaminant Hazard Reviews Report No. 2. 46 pp.

Eisler, R. 1986. Chromium hazards to fish, wildlife, and invertebrates: a synoptic review. U.S. Fish and Wildlife Service Biological Report 85 (1.6). Contaminant Hazard Reviews Report No. 6. 60 pp.

Eisler, R. 1987. Mercury hazards to fish, wildlife, and invertebrates: a synoptic review. U.S. Fish and Wildlife Service Biological Report 85 (1.10). Contaminant Hazards Reviews Report 10. 63 pp.

Eisler, R. 1998. Copper hazards to fish, wildlife, and invertebrates: a synoptic review. Contaminant Hazards Reviews Report 33. U.S. Geological Survey, Biological Resources Division. Biological Sciences Report USGS/BRD/BSR--1997-0002. 98 pp.

Förstner, U. and G.T.W. Wittmann. 1981. Metal pollution in the aquatic environment. Springer-Verlag. Berlin, New York. 486 pp.

Fox, I. 1961. Resistance of *Aedes aegypti* to Certain Chlorinated Hydrocarbon and Organophosphorus Insecticides in Puerto Rico. *Bulletin of the World Health Organization* 24: 489-494.

Gibbs, P.E. and G.W. Bryan. 1996. TBT-induced imposex in neogastropod snails: masculinization to mass extinction. In: S. J. de Mora, editor, Tributyltin: A Case Study of an Environmental Contaminant. Cambridge University Press. Cambridge, England. 301 pp.

Gioda, A., U. Pérez, Z. Rosa, and B.D. Jiménez-Vélez. 2006. Concentration of trace elements in airborne PM₁₀ from Jobos Bay national estuary, Puerto Rico. *Water, Air, and Soil Pollution* 174: 141-159.

Guzmán-Martínez, M.D.C., P. Ramírez-Romero, and A.T. Banaszak. 2007. Photoinduced toxicity of the polycyclic aromatic hydrocarbon, fluoranthene, on the coral, *Porites divaricata*. *Journal of Environmental Science and Health, Part A* 42(10): 1495-1502.

Hassett, J.J., J.C. Means, W.L. Banwart, and S.G. Wood. 1980. Sorption related properties of sediments and energy related pollutants. U.S. Environmental Protection Agency. EPA-600/3-8-041. 133 pp.

Humann, P, and N. DeLoach. 2002. Reef Coral Identification: Florida, Caribbean Bahamas. Second Edition. New World Publications. Jacksonville, Florida. 278pp.

Hylland, K. 2006. Polycyclic aromatic hydrocarbons (PAH) ecotoxicology in marine ecosystems. *Journal of Toxicology and Environmental Health, Part A* 69: 109-123.

Jiménez-Vélez, B.D., Z. Rosa, U. Pérez, and A. Gioda. 2003. Evaluating heavy metal concentrations in airborne PM₁₀ from the Jobos Bay National Estuary, at Salinas, Puerto Rico. Final Report. Center for Environmental and toxicological Research, University of Puerto Rico, Medical Science Campus, School of Medicine.

Jiménez-Vélez, B.D., Y. Detrés, R.A. Armstrong, and A. Gioda. 2009. Characterization of African Dust (PM_{2.5}) across the Atlantic Ocean during AEROSE 2004. *Atmospheric Environment* 43: 2659-2664.

Kendall, M.S., C.R. Kruer, K.R. Buja, J.D. Christensen, M. Finkbeiner, R.A. Warner, and M.E. Monaco. 2001. Methods Used to Map the Benthic Habitats of Puerto Rico and the U.S. Virgin Islands. NOAA Technical Memorandum NOS NCCOS CCMA 152. Silver Spring, MD. 46 pp.

Kennedy, C.J., N.J. Gassman, and P.J. Walsh. 1992. The fate of benzo[a]pyrene in the scleractinian corals *Favia fragum* and *Montastrea annularis*. *Marine Biology* 113: 3131-318.

Kimbrough, K.L. and G.G. Lauenstein (eds). 2006. Major and trace element analytical methods of the National Status and Trends Program: 2000-2006. NOAA Technical Memorandum NOS NCCOS 29. Silver Spring, MD. 19 pp.

Kimbrough, K.L., G.G. Lauenstein, and W.E. Johnson (eds). 2006. Organic contaminant analytical methods of the National Status and Trends Program: Update 2000-2006. NOAA Technical Memorandum NOS NCCOS 30. Silver Spring, MD. 137 pp.

Lake, J.L., N.I. Rubenstein, H. Lee, C.A. Lake, J. Heltshe, and S. Pevigano. 1990. Equilibrium partitioning and bioaccumulation of sediment-associated contaminants by infaunal organisms. *Environmental Toxicology and Chemistry* 9: 1095-1106.

Lauenstein, G.G. and A.Y. Cantillo. 1998. Sampling and Analytical Methods of the National Status and Trends Program Mussel Watch Project: 1993-1996 Update. NOAA Technical Memorandum NOS ORCA 130. Silver Spring, MD. 233 pp.

Long, E.R. and L.G. Morgan. 1990. The Potential for Biological Effects of Sediment-Sorbed Contaminants Tested in the National Status and Trends Program. NOAA Technical Memorandum NOS OMA 52. Seattle, WA. 233 pp.

Long, E.R., A. Robertson, D.A. Wolfe, J. Hameedi, and G.M. Sloane. 1996. Estimates of the spatial extent of sediment toxicity in major U.S. estuaries. *Environmental Science and Technology* 30(12): 3585-3592.

Loring, D.H. 1991. Normalisation of heavy metal data from estuarine and coastal sediments. *ICES Journal of Marine Science* 48(1): 101–115.

MacDonald, D.D. 1994. Approach to the Assessment of Sediment Quality in Florida Coastal Waters. Vol. 2 - Application of the Sediment Quality Assessment Guidelines. Florida Department of Environmental Protection, Office of Water Policy. Tallahassee, FL. 139 pp.

McDonald, S.J., D.S. Frank, J.A. Ramirez, B. Wang, and J.M. Brooks. 2006. Ancillary methods of the National Status and Trends Program: 2000-2006 Update. Silver Springs, MD. NOAA Technical Memorandums NOS NCCOS 28. 17 pp.

McBride, J.P., R.E. Moore, J.P. Witherspoon, and R.E. Blanco. 1978. Radiological Impact of Airborne Effluents of Coal and Nuclear Plants. *Science* 202(4372): 1045-1050.

National Oceanic and Atmospheric Administration (NOAA). 2006. National Status and Trends Data Portal: Mussel Watch Jobos Bay. (Online) <http://egisws02.nos.noaa.gov/nsandt/index.html#> (Accessed 13 June 2011).

Neff, J.M. 1985. Polycyclic aromatic hydrocarbons. pp. 416-454. In: G.M. Rand and S.R. Petrocelli (eds.). *Fundamentals of Aquatic Toxicology*. Hemisphere Publishing Corporation, Washington, D.C. 666 pp.

Neff, J.M., S.A. Stout, and D.G. Gunster. 2005. Ecological risk assessment of polycyclic aromatic hydrocarbons in sediments: identifying sources and ecological hazard. *Integrated Environmental Assessment and Management* 1(1): 22-33.

Negri, A.P., L.D. Smith, N.S. Webster, and A.J. Heyward. 2002. Understanding ship-grounding impacts on a coral reef: potential effects of anti-foulant paint contamination on coral recruitment. *Marine Pollution Bulletin* 44: 111-117.

Oreščanin, V., Lulić, S., Pavlović, G. and Mikelic, L. 2004. Granulometric and chemical composition of the Sava River sediments upstream and downstream of the Krško nuclear power plant. *Environmental Geology* 46: 605-613.

Pait, A.S., D.R. Whitall, C.F.G. Jeffrey, C. Caldow, A.L. Mason, J.D. Christensen, M.E. Monaco, and J. Ramirez. 2007. An assessment of chemical contaminants in the marine sediments of southwest Puerto Rico. NOAA Technical Memorandum NOS NCCOS 52. Silver Spring, MD. 116 pp. (Online) <http://www.ccma.nos.noaa.gov/publications/southwestpuertorico.pdf> (Accessed 13 June 2011).

Pait, A.S., D.R. Whitall, C.F.G. Jeffrey, C. Caldow, A.L. Mason, G.G Lauenstein, and J.D. Christensen. 2008. Chemical contamination in southwest Puerto Rico: an assessment of organic contaminants in nearshore sediments. *Marine Pollution Bulletin* 56: 580-606.

Pait, A.S., C.F.G. Jeffrey, C. Caldow, D.R. Whitall, S.I. Hartwell, A.L. Mason, and J.D. Christensen. 2009. Chemical contaminants in the coral *Porites astreoides* from Southwest Puerto Rico. NOAA Technical Memorandum NOS NCCOS 91. Silver Spring, MD. 32 pp.

Pait, A.S., A.L. Mason, D.R. Whitall, J.D. Christensen, and S.I. Hartwell. 2010. Assessment of Chemical Contaminants in Sediments and Corals in Vieques. pp. 101-150. In: L.J. Bauer and M.S. Kendall (eds.). An Ecological Characterization of the Marine Resources of Vieques, Puerto Rico Part II: Field Studies of Habitats, Nutrients, Contaminants, Fish, and Benthic Communities. NOAA Technical Memorandum NOS NCCOS 110. Silver Spring, MD. 174 pp.

Peachey, R.L. and D.G. Crosby. 1996. Phototoxicity in tropical reef animals. *Marine Environmental Research* 42(1-4): 359-362.

Puerto Rico Nuclear Center (PRNC). 1972. Aguirre Power Project Environmental Studies 1972 Annual Report. PRNC-162. 464 pp.

Reichelt-Brushett, A.J. and P.L. Harrison. 2005. The effect of selected trace elements on the fertilization success of several scleractinian coral species. *Coral Reefs* 24: 524-534.

Rosenthal, Y., P. Lam, E.A. Boyle, and J. Thomson. 1995. Authigenic cadmium enrichment in suboxic sediments: Precipitation and postdepositional mobility. *Earth and Planetary Science Letters* 132: 99-111.

Schropp, S.J. and H.L. Windom. 1987. A guide to the interpretation of metal concentrations in estuarine sediments. Florida Department of Environmental Regulation, Coastal Zone Management Section. Tallahassee, FL. 73 pp.

Schropp, S.J., F.G. Lewis, H.L. Windom, J.D. Ryan, F.D. Calder, and L.C. Burney. 1990. Interpretation of metal concentrations estuarine sediments of Florida using aluminum as a reference element. *Estuaries* 13(3): 227-235

Shine, J. and G. Wallace. 2000. Chemical aspects of organic carbon and ecosystem stress in benthic ecosystems. pp. 40-44. In: Ad Hoc Benthic Indicator Group - results of initial planning meeting. IOC Technical Series No 57. UNESCO Intergovernmental Oceanographic Commission (IOC), Paris, France. 65 pp.

Simpson, S.J., J.D. Fett, D.T. Long, and L.C. Patino. 2000. Understanding Processes Influencing Patterns of Chemical Loadings to the Environment: Sources, Pathways And Environmental Regulations. In: I. Nriagu (ed.). 11th Annual International Conference on Heavy Metals in the Environment, Contribution #1171. University of Michigan, School of Public Health, Ann Arbor, MI (CD-ROM).

Solbakken, J.E., A.H. Knap, T.D. Sleeter, C.E. Searle, and K.H. Palmork. 1984. Investigation into the fate of ¹⁴C-labeled xenobiotics (naphthalene, phenanthrene, 2,4,5,2',4',5'-hexachlorobiphenyl, octachlorostyrene) in Bermudian corals. *Marine Ecology Progress Series* 16: 149-154.

Theis, T.L., J.D. Westrick, C.L. Hsu, and J.J. Marley. 1978. Field Investigation of Trace Metals in Groundwater from Fly Ash Disposal. *Water Pollution Control Federation* 50 (11): 2457-2469.

Ujević, I., N. Odžak, and A. Barić. 2000. Trace metal accumulation in different grain size fractions of the sediment from a semi-enclosed bay heavily contaminated by urban and industrial wastewaters. *Water Research* 34(11): 3055-3061.

U.S. Environmental Protection Agency (USEPA). 1975. DDT Regulatory History: A Brief Survey (to 1975). (Online) <http://www.epa.gov/aboutepa/history/topics/ddt/02.html> (Accessed 13 June 2011).

U.S. Environmental Protection Agency (USEPA). 1997. Management of polychlorinated biphenyls in the United States. Environmental Protection Agency, Office of Pollution Prevention and Toxics, U.S. Environmental Protection Agency. 6 pp. (Online) <http://www.chem.unep.ch/pops> (Accessed 13 June 2011).

U.S. Department of Human Health and Services (USDHHS). 1995. Toxicological Profile for Polycyclic Aromatic Hydrocarbons. Agency for Toxic Substance and Disease Registry (ATSDR). Atlanta, GA. 487 pp.

U.S. Department of Human Health and Services (USDHHS). 1999. Toxicological Profile for Cadmium. Agency for Toxic Substance and Disease Registry (ATSDR). Atlanta, GA. 439 pp.

Veron, J.E.N. (ed.). 2000. Corals of the World, Volume 3. Australian Institute of Marine Science. Townsville, Australia. 490 pp.

Windom, H.L., S.J. Schropp, F.D. Calder, J.D. Ryan, R.G. Smith Jr., L.C. Burney, F.G. Lewis, and C.H. Rawlinson. 1989. Natural trace metal concentrations in estuarine and coastal marine sediments of the southeastern United States. *Environmental Science and Technology* 23: 314-320.

Zitello, A.G., D.R. Whitall, A. Dieppa, J.D. Christensen, M.E. Monaco, and S.O. Rohmann. 2008. Characterizing Jobos Bay, Puerto Rico: A Watershed Modeling Analysis and Monitoring Plan. NOAA Technical Memorandum NOS NCCOS 76. Silver Spring, MD. 81 pp.

Chapter 5



Spatial and Temporal Variability in the Water Column Nutrients and Pesticides of Jobos Bay

David Whitall^{1,4}, Angel Dieppa² and Thomas L. Potter³

5.1. INTRODUCTION

The objectives of this portion of the ecological characterization project of Jobos Bay were to:

1. Quantify magnitude and spatiotemporal variability of surface water nutrients and pesticides within the Jobos Bay National Estuarine Research Reserve (JBNERR or Reserve);
2. Establish a baseline of nutrient and pesticide conditions against which to measure changes in the future;
3. Link observed concentrations of nutrients and pesticides to hydrological forcing factors.

5.1.1. Nutrients

Primary productivity in marine systems is most often limited by nitrogen (N), but phosphorus (P) can be co-limiting under certain circumstances, and systems can alternate from N limitation to P limitation through space and time. In estuarine systems, nutrient enrichment can result in algal blooms, changes in algal community composition (including harmful algal blooms) and increases in hypoxia/anoxia (Bricker *et al.*, 2007). In tropical systems, excess nutrient loads can cause increases in macroalgal growth and can have deleterious effects on corals, such as macroalgae outcompeting and overgrowing corals. Finally, nitrogen and phosphorus can impact corals directly by lowering fertilization success (Harrison and Ward, 2001), and reducing both photosynthesis and calcification rates (Marubini and Davies, 1996).

In Jobos Bay, the primary producers within the submerged environment consist of microbial mats, nearly 90 species of algae (Almodóvar, 1964) and the dominant seagrasses that include the climax species *Thalassia testudinum*, *Syringodium filiforme*, *Halodule wrightii*^A, and *Halophila decipiens*. Diatoms and dinoflagellates dominate the phytoplankton community.

Land based contributions of nutrients come from a variety of sources. Phosphorus and reactive nitrogen can enter the environment from chemical fertilizer (agriculture, lawns, golf courses), industrial sources, animal waste, and human waste (Galloway *et al.*, 2003). Additionally, nitrogen can be contributed from biological nitrogen fixation and atmospheric nitrogen deposition (originating from fossil fuel combustion and ammonia volatilization from agriculture; Mathews *et al.*, 2002).

Although a comprehensive watershed nutrient budget is beyond the scope of this study, it seems likely, based on watershed land use, that agriculture is a significant contributor of nutrients to the near coastal environment (Figure 5.1). Modeling of potential nutrient fluxes from the watershed was previously published (Zitello *et al.*, 2008). Results indicated that agricultural practices, like the use of chicken manure and commercial fertilizers, may be affecting water and air quality.

^A The taxonomic name for *Halodule wrightii* has been recently changed to *Halodule beaudettei* (<http://www.itis.gov/index.html>); however, the original name will be used in this document as it is more widely known.

¹ Center for Coastal Monitoring and Assessment, National Centers for Coastal Ocean Science, National Ocean Service, National Oceanic and Atmospheric Administration

² Jobos Bay National Estuarine Research Reserve

³ Southeast Watershed Research Laboratory, Agricultural Research Service, United States Department of Agriculture

⁴ Corresponding author: dave.whitall@noaa.gov

An extensive groundwater study (Rodríguez, 2006) found nitrate concentrations above the U.S. Environmental Protection Agency (USEPA) maximum contaminant level for drinking water (10 mg/L) in three wells in the watershed, although these wells are used for agricultural irrigation rather than drinking water. The JBNERR Monitoring Program studied several freshwater wells in the Jobos Bay watershed. This program detected high levels of nitrates (90 mg/L) in some wells, exceeding the drinking water standard (10 mg/L) of the Puerto Rico Environmental Quality Board (PREQB). Several groundwater wells studied by JBNERR's Water



Figure 5.1. Center pivot irrigation on silage farm adjacent to Jobos Bay National Estuarine Research Reserve (JBNERR). Photo: NOAA CCMA.

Quality Program cannot be used due to high nitrate levels. As a result, more stringent management practices regarding the use of chicken manure on farmland have been imposed by the PREQB. Near-shore water quality in the Bay is also being affected by increased surface run-off. Urban growth along the coast is affecting estuarine habitat and increasing the direct discharge of untreated wastewater from local communities that have no water treatment facilities such as Aguirre. It should be noted that the regional waste water treatment plant does not discharge into the Bay. Untreated waters reach directly into the Bay from an old sewage system in Aguirre community and leakage from septic tanks in Las Mareas Community and Pozuelo. A new sewage system is being constructed in Aguirre and Pozuelo that will take untreated waters to the regional plant.

Other communities such Pozuelo and Las Mareas may be sources of waste water from septic tanks seepage due a shallow water table affected by tides; Coquí, Mosquito, San Felipe, Puerto de Jobos have sewage systems that overflows during storms events.

5.1.2. Pesticides

Jobos Bay watershed has been used as agricultural lands since Spanish Colonial times and has changed from a landscape dominated by heavy sugar cane production (Figure 5.2) to silage, seed production, and minor fruits and vegetables comprising 11% of the watershed land cover (Zitello *et al.*, 2005). Agricultural and non-agricultural pesticide use in the watershed also has the potential to impact near-shore waters in the estuary. For example, investigations conducted on the silage farm adjacent to the JBNERR found that a variety of herbicides, insecticides and

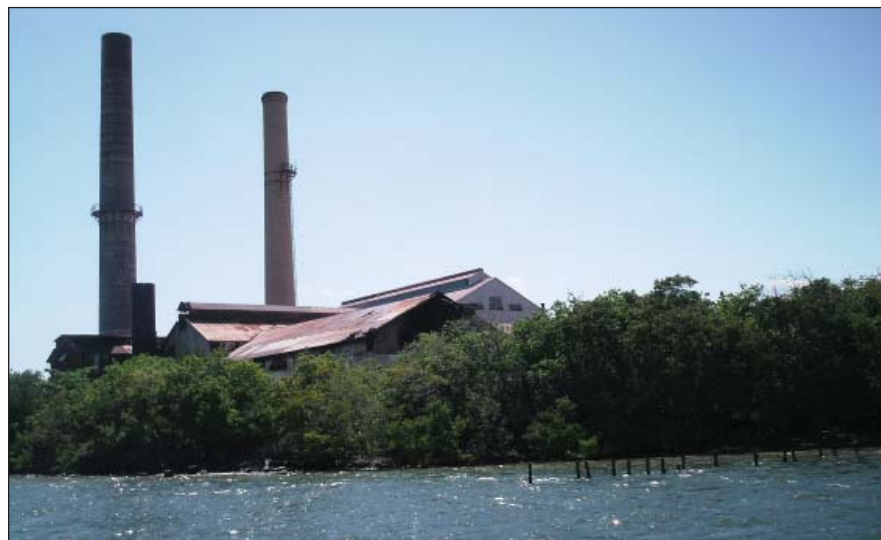


Figure 5.2. Abandoned sugar mill adjacent to Jobos Bay. Photo: NOAA CCMA.

fungicides are used. The most common (by weight, 2008-2010; Table 5.1) were atrazine, pendimethalin, glyphosate, paraquat (herbicides) and chlorpyrifos (insecticide). Pesticides and their degradation products can have adverse effects on aquatic organisms (Humberg *et al.*, 1989; Ahrens, 1994; USEPA, 1995, 2006) and can enter coastal waters via surface runoff or groundwater flux, drift, and wet and dry deposition. It should be noted that due to problems with the irrigation system, farming on the silage farm adjacent to the Reserve was stopped in late 2009. It is anticipated that farming will resume when the center pivot system is replaced by 2011.

Table 5.1. On farm pesticide use 2008 to 2010.

Pesticide	Use	Mass applied (kg)	Annual rate (kg/ha/yr)
atrazine	herbicide	361	2.8
pendimethalin	herbicide	188	1.4
glyphosate	herbicide	173	1.3
paraquat	herbicide	106	0.8
fluazifop-P-buty	herbicide	5	0.04
Total herbicide		831 (76%)	6.4
chlorpyrifos	insecticide	109	0.8
methomyl	insecticide	49	0.4
malathion	insecticide	44	0.3
thiodicarb	insecticide	33	0.3
spinosad	insecticide	7	0.1
esfenvalerate	insecticide	5	0.04
permethrin	insecticide	5	0.04
Total Insecticide		252 (23%)	1.9
azoxystrobin	fungicide	2	0.01
propiconazole	fungicide	2	0.01
Total Fungicide		4 (<1%)	0.03

5.2. METHODS

5.2.1. Nutrients, Pesticides and Chlorophyll a Sampling and Analysis

Nutrients and chlorophyll a were sampled monthly at the four active JBNERR System-Wide Monitoring Program (SWMP) sites, which are targeted sampling sites (Figure 5.3). Pesticides were also sampled at the four active JBNERR sites, plus a fifth site (site 11; Figure 5.3). Station number nine (09; Figure 5.3) is considered to be an impacted site. Water quality data collected at this site is associated with runoff from littoral and basin mangrove areas. This lagoon has an average depth of 1.5 m and water regime is subject to high concentrations of tannin pigments associated with red mangroves. Station 09 is characterized by a low water exchange due to a restricted circulation pattern. This sampling station is located in the most inland lagoon northeast of Mar Negro, closest to the thermoelectric power plant. It is subjected to runoff, which may include agrochemicals from agricultural activities within the northern boundary of JBNERR. Information compiled from historical environmental documents indicate that station nine (09) was used as a disposal site for residues of

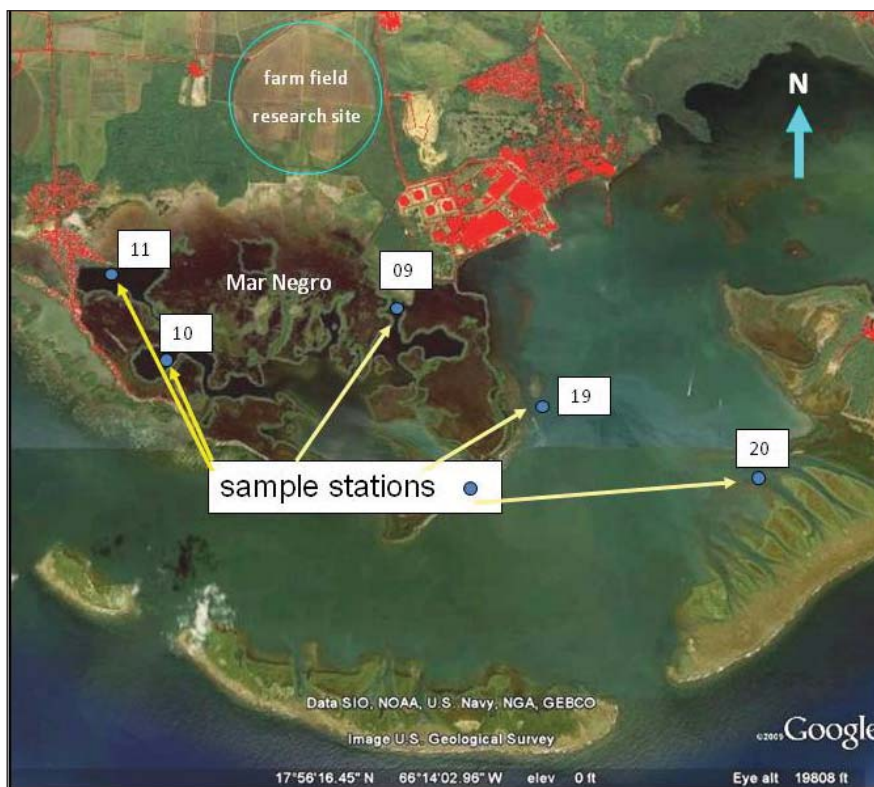


Figure 5.3. Map of Jobos Bay National Estuarine Research Reserve System-Wide Monitoring Program (JBNERR SWMP) sites. Nutrients were sampled monthly at sites 09, 10, 19 and 20. Pesticides were sampled monthly at all five sites.

the previously operating sugar mill operation, and therefore might have high organic input into the sediments. Among the four water quality monitoring stations, this station has the lowest dissolved oxygen values during the year. Benthic vegetation is scarce (NERRS, 2011).

Station number ten (10; Figure 5.3), located in a mangrove lagoon area towards the southwestern section of Mar Negro, is considered the reference or non-impacted site. This station is characterized by a low water exchange due to a restricted circulation pattern. This lagoon has an average depth of 2 m and the water regime is subject to high concentrations of tannin pigments associated with red mangroves. Benthic vegetation is scarce.

Station number eleven (11) may also be impacted by land based sources of pollution, specifically, untreated sewage and septic systems from near coastal residences and runoff from agriculture (NERRS, 2011).

Station number nineteen (19; Figure 5.3) is located in Jobos Bay surrounded by sea grass beds composed of *T. testudinum*. This station is close to the power plant navigation channel (Figure 5.4), used by barges to bring oil and gas into the power plant pier. This area is exposed to barge strandings and sediment re-suspension. Oil spills are always a threat (NERRS, 2011).



Figure 5.4. Aguirre Power Plant adjacent to Jobos Bay. Photo: NOAA CCMA.

Station number twenty (20; Figure 5.3) is located adjacent to Cayos Caribe reef system. Water streams coming from the reef platform may mean that this station is representative of water conditions behind the coral reef. These waters are part of the main marine current coming from the eastern side of Jobos Bay that runs along the coast, coming into contact with potential sources such as agricultural fields, a coal power plant, a Phillips Core oil refinery (closed in 2005) and other industries (NERRS, 2011).

5.2.2. Nutrient and Chlorophyll a Sample Collection Methods

Monthly grab samples for nutrients and chlorophyll a were taken at the four SWMP stations (site 09, 10, 19 and 20; Figure 5.3). Grab samples were taken from the four sites on the same day at or as near as possible to slack low-tide conditions. Efforts were made to collect samples at approximately monthly (30 days) intervals. Sample dates were selected so as to not be influenced by previous storm events; an antecedent dry period of 72 hours was desirable but was not always practical throughout the year (e.g., during the rainy season). Because the sites are shallow and well-mixed, two surface grab samples were collected that are representative of the sampling area. Replicate (N=2) samples were collected by hand at an approximate depth of 30 cm.

Nutrient and chlorophyll a grab samples were taken in duplicate (two separate samples collected in different bottles), resulting in a total of eight samples. All samples were collected in amber, Nalgene™ sample bottles that were previously acid washed (10%) rinsed (3x) with distilled-deionized water, dried and followed by rinsing (3x) of ambient water prior to collection of the sample.

5.2.3. Diel Sampling Program of Nutrients and Chlorophyll a

Diel nutrient samples were taken at station 09. Samples were collected over a full lunar cycle (24 hr : 48 min) at 2 hour intervals using an ISCO brand auto-sampler model 6712. The suction intake line was set to sample at a depth of 0.5 m, and was covered with a mesh to avoid clogging the line with organic debris. The ISCO sampler was programmed to automatically sample 1000 mL of water every 2 hours and contained a one frozen plastic gallon to keep samples cold. A field blank consisting of deionized (DI) water was placed in the bottle rack and left open during the diel sampling. All samples were pumped into polyethylene sample bottles that were previously acid washed (10%), rinsed (3x) with distilled-deionized water and dried. At the end of the 24 hr period, the 12 samples were kept in the dark and returned to the laboratory for immediate processing.

5.2.4. Nutrient and Chlorophyll a Analysis

All samples, monthly grab and diel, were pre-processed at JBNERR laboratory. Samples were filtered immediately after collection; the filtrate was placed in 250 mL Nalgene™ bottles. The filtered chlorophyll-a samples were placed in amber (empty) vials, stored in a cooler (dark) on ice packs and sent via overnight delivery to Virginia Institute of Marine Sciences (VIMS) laboratory for analysis. VIMS serves as the analytical lab for SWMP sample analysis for several NERRS sites. Nutrients were determined colorimetrically and chlorophyll a was determined fluourometrically following extraction in 90% acetone. Method detection limits and methods for nutrients and chlorophyll a are shown in Table 5.2. In addition to oxidized nitrogen, reduced nitrogen (ammonium) is also routinely measured by the JBNERR SWMP. However, at the time of publication of this document, these ammonium data were still being reviewed for quality assurance purposes and are not included here.

Table 5.2. Methods and method detection limits for nutrient and chlorophyll analyses.

Parameter	Method Detection Limit	Method
Ammonium	0.0054 mg/L	Methods for Chemical Analysis of Water and Wastes - USEPA (1974)
Nitrate plus Nitrite	0.0010 mg/L	USEPA Method 353.4 - Zhang <i>et al.</i> (1997)
Orthophosphate	0.0015 mg/L	USEPA Method 365.5 - Zimmermann and Keefe (1997)
Chlorophyll a	0.50 ug/L	USEPA Method 445.0 - Arar and Collins (1997)

5.2.5. Pesticide Sample Collection Methods

Water samples for pesticide analysis were collected from the Bay on a monthly basis between April 2008 and November 2010 at the five JBNERR reference sites that were established in 1995 (Figure 5.3). Each sample was collected by submerging a 1-L pre-cleaned amber glass bottle by hand from the boat used to reach sampling sites. After sealing with Teflon® lined screw caps, bottles were placed in an on-board ice-chest and upon return to the laboratory transferred to refrigerated storage.

5.2.6. Pesticide Sample Handling and Preparation

Within 3 days of collection, project staff prepared the pesticide samples for analysis by drawing each sample through solid-phase extraction (SPE) cartridges (Oasis® HLB; Waters Inc., Milford, MA) using a vacuum manifold. Procedure performance, in terms of percent recovery of numerous current use pesticides active ingredients, has been previously published (Potter *et al.*, 2007). After SPE was complete, cartridges were flushed with four 5-mL aliquots of high-performance liquid chromatography (HPLC) grade water, dried by vacuum reapplication, wrapped in aluminum foil, placed in ziplock bags, and stored in a refrigerator. The following day they were shipped to the analytical laboratory using an overnight delivery service. Upon receipt cartridges were eluted sequentially with methanol and methylene chloride. Combined eluents were concentrated to about 1 mL by evaporation under a stream of nitrogen (N₂) gas followed by solvent exchange to toluene using a Turbovap® concentrator (Caliper Life Sciences, Hopkinton, MA, USA) and N₂ gas. Concentrated extracts were fortified with

2-chlorolepidine and octafluoronaphthalene, internal standards for the positive ion electron impact and negative chemical ionization gas chromatography-mass spectrometry (GC-MS) analyses, respectively. Extracts were stored in the dark at -20°C.

Pesticide Analysis via GC-MS

All extracts were analyzed using a ThermoQuest Finnegan DSQII GC-MS system (ThermoFisher, San Jose, CA, USA) while scanning for positive ions generated by electron impact at 70 eV and for negative ions produced during methane chemical ionization (methane 1.5 mL min⁻¹; source temperature 200°C). Prior to use in each ionization mode the instrument was autotuned to meet manufacturer specifications. For enhanced sensitivity data acquisitions were in the selected ion monitoring (SIM) mode. Target compounds, SIM methods, and the limits of quantification are shown in Table 5.3. Compounds were selected based on a review of crops produced in the region (USDA-NASS, 2009) and their pest management profiles (USDA-IPMCENTERS, 2011). Suitability for GC analysis was also a requirement. Ions monitored were base peaks (primary) and the second most abundant ion (confirmatory) obtained during full-scan (m/z=50 to 450 daltons) data acquisitions of standards. Chromatographic separations were on a 30 m DB5[®] column, 0.25 mm i.d., 0.25 µ film (Agilent, San Jose, CA, USA). Helium carrier gas flow was 2 mL min⁻¹ with automated compensation for oven temperature programming and vacuum in the ion source. Automated 1-µL injections were splitless. At the injection column head pressure was surged to 250 kPa for 1 minute. Quantitation limits were based on extraction of 1-L samples, concentration to 1 mL, and the lowest concentration standard used for calibration. Compounds detected were considered confirmed if the ratio between the two ions monitored was within ±20% of the diagnostic ratio obtained for standards.

Table 5.3. Target analytes, methods and limit of quantification (LOQ).

Compounds	Method †	LOQ (ug L ⁻¹)
acetochlor	GC-MS-EI-POS-SIM	0.006
alachlor	GC-MS-EI-POS-SIM	0.006
ametryn	GC-MS-EI-POS-SIM	0.006
atrazine	GC-MS-EI-POS-SIM	0.006
desethylatrazine	GC-MS-EI-POS-SIM	0.006
desisopropylatrazine	GC-MS-EI-POS-SIM	0.006
α-BHC	GC-NCI-MS-SIM	0.004
carbaryl	GC-MS-EI-POS-SIM	0.006
chlorothalonil	GC-NCI-MS-SIM	0.004
chlorpyrifos	GC-NCI-MS-SIM	0.004
dacthal	GC-NCI-MS-SIM	0.004
diazinon	GC-NCI-MS-SIM	0.004
dicofol	GC-MS-EI-POS-SIM	0.006
α-endosulfan	GC-NCI-MS-SIM	0.004
β-endosulfan	GC-NCI-MS-SIM	0.004
endosulfan sulfate	GC-NCI-MS-SIM	0.004
ethalfuralin	GC-NCI-MS-SIM	0.004
ethoprop	GC-MS-EI-POS-SIM	0.006
lindane	GC-NCI-MS-SIM	0.004
malathion	GC-NCI-MS-SIM	0.004
metalaxyl	GC-MS-EI-POS-SIM	0.006
metolachlor	GC-MS-EI-POS-SIM	0.006
metribuzin	GC-NCI-MS-SIM	0.004
oxadiazon	GC-NCI-MS-SIM	0.004
pendimethalin	GC-NCI-MS-SIM	0.004
prometon	GC-MS-EI-POS-SIM	0.006
prometryne	GC-MS-EI-POS-SIM	0.006
propiconazole	GC-MS-EI-POS-SIM	0.006
simazine	GC-MS-EI-POS-SIM	0.006
tebuconazole	GC-MS-EI-POS-SIM	0.006
tribufos	GC-NCI-MS-SIM	0.004
trifluralin	GC-NCI-MS-SIM	0.004

† GC-MS-EI-POS-SIM = Gas chromatography-mass spectrometry (GC-MS) with positive ion electron impact ionization; GC/MS with methane negative chemical ionization.

Pesticide Analysis Quality Control

A laboratory blank was prepared during SPE of each sample set. One liter of HPLC grade water was used. None of the target analytes were detected in blanks indicating a low potential for false-positive results in Bay samples. To assess the potential for false-negatives a matrix spike was prepared and analyzed for each of the 40 samples. Spikes were prepared using a duplicate sample of water from station 20 and addition of 1 mL of 1 $\mu\text{g mL}^{-1}$ methanol solution of 11 of the target analytes (Table 5.3). Among the five spikes prepared and analyzed recoveries ranged from 54 and 108% and relative standard deviations from 6 to 35%. Results were comparable to prior investigations using the same analytical techniques (Potter *et al.*, 2007). The relatively high recoveries and low variability are indicative of data with low false-negative potential. No corrections were made for recovery in reported results.

5.2.7. Statistical Analysis of Data

Data were analyzed using JMP® statistical software. The data were first tested for normality using the Shapiro-Wilk test. Because the data were not normally distributed, non-parametric statistical tests were used; a Wilcoxon test was used to examine differences between sites and seasons, and a Spearman's rank correlation coefficient test was used to test for relationships between nutrients, chlorophyll and precipitation (Figure 5.5).

The temperature in Jobos Bay is relatively constant throughout the year, with relatively more precipitation occurring during hurricane season (June to November). Therefore, seasonal nutrient patterns were examined between hurricane and non-hurricane seasons.



Figure 5.5. Weather station at silage farm. Photo: NOAA CCMA.

5.3. RESULTS AND DISCUSSION

5.3.1. Orthophosphate

Orthophosphate concentrations ranged from below the method detection limit to 0.17 mg phosphate (P)/L, with a mean of 0.015 mg P/L and a median of 0.011 mg P/L (Table 5.4). This is similar to what was observed in near shore waters in Vieques, Puerto Rico (Whitall *et al.*, 2010). Standard deviations were much higher at site 09 because of the diel sampling at that site, *i.e.* sampling over a 24 hour cycle will capture a much wider range of values than a single grab sample (Figure 5.6) due to diel variations in photosynthesis/respiration and the tidal cycle. Concentrations were significantly higher ($p < 0.05$) at site 09 compared with the other three sites (Figure 5.6). Site 09 is the closest to shore, so this pattern may reflect the input of phosphorus reaching the system via overland flow. Based on watershed land use and previous modeling estimates (Zitello *et al.*, 2008) agricultural fertilizer is likely to be a very important source of phosphorus to this system. Phosphorus concentrations were not correlated with precipitation. This may be because the NERRS SWMP sampling protocols dictate not sampling after a rainfall event. However, at site 09 phosphorus concentrations were significantly higher during the wet season (December through May) than during the rainy season (June through November; hurricane season) as shown in Figure 5.7. This further supports the theory that surface runoff is driving the observed phosphorus concentrations at the site closest to shore. The other three sites did not exhibit seasonal patterns for phosphorus.

5.3.2. Oxidized Nitrogen

Oxidized nitrogen (nitrate plus nitrite) concentrations ranged from below the method detection limit to 0.12 mg nitrogen (N)/L, with a mean of 0.013 mg N/L and a median of 0.007 mg N/L (Table 5.4). This is similar to what was observed in near shore waters in Vieques, Puerto Rico (Whitall *et al.*, 2010). Standard deviations were much higher at site 09 because of the diel sampling at that site, *i.e.*

Table 5.4. Summary statistics for nutrients and chlorophyll a. MDL= Method Detection Limit.

Analyte	Units	Min	Max	Mean	Median
Nitrate plus nitrite	mg N/L	MDL	0.1177	0.01252	0.0072
Orthophosphate	mg P/L	MDL	0.1705	0.014835	0.01115
Chlorophyll a	ug/L	MDL	142.56	4.386596	1.34

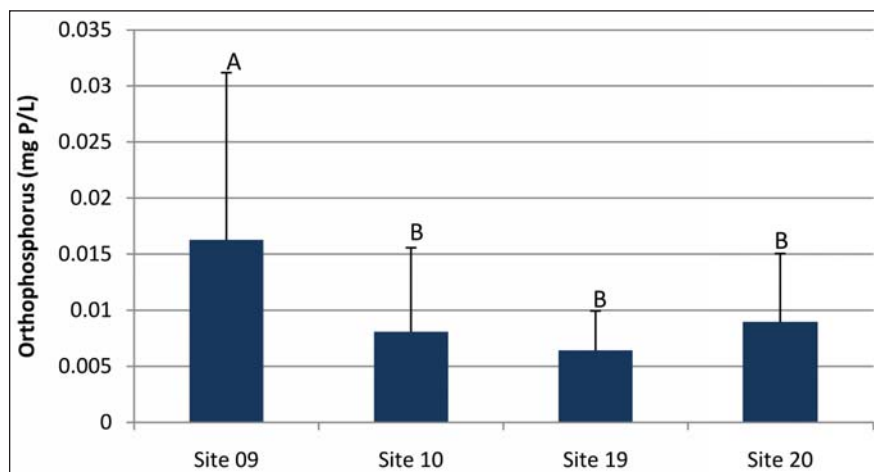


Figure 5.6. Mean orthophosphorus concentrations from 2008 to 2010. Letters indicate statistical groupings (Wilcoxon test, $P < 0.05$). Error bars represent standard deviation.

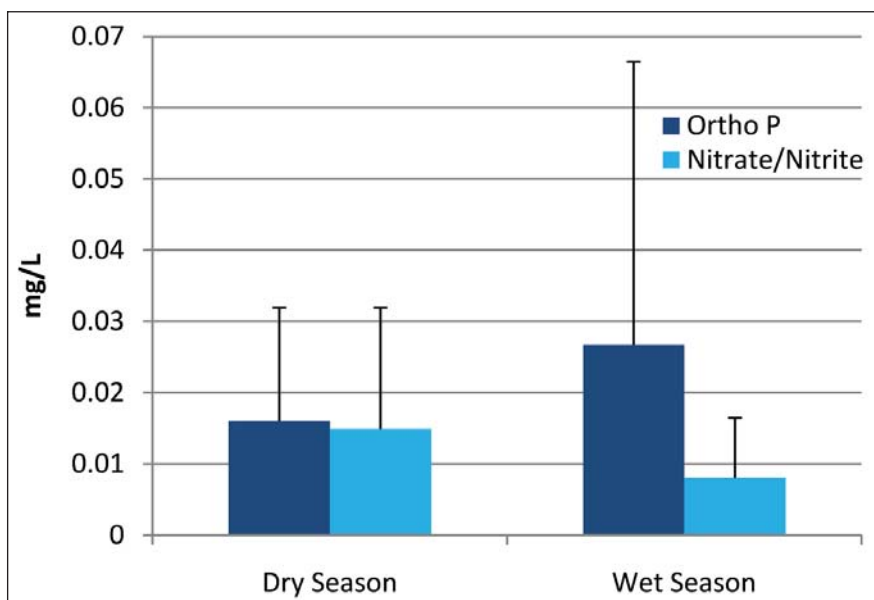


Figure 5.7. Seasonal variability in orthophosphorus and nitrate/nitrite between wet (hurricane) and dry seasons at site 09 from 2008 to 2010. For both analytes, there were statistical differences between seasons (Wilcoxon test, $P < 0.05$).

sampling over a 24 hour cycle will capture a much wider range of values than a singular grab sample (Figure 5.8) due to diel variations in photosynthesis/respiration and the tidal cycle. Concentrations were significantly lower ($p < 0.05$) at site 20, compared to the other three sites (Figure 5.8). Site 20 is the farthest site from shore indicating a relatively low potential for impact from runoff from the land. Oxidized nitrogen concentrations were not correlated with precipitation. This may be because the NERRS SWMP sampling protocols dictate not sampling after a rainfall event, although nitrate concentrations may be disconnected from rainfall because groundwater transport of oxidized nitrogen is often a primary mechanism for nitrogen flux to coastal systems. This is not the case with phosphorous. The different spatial patterns in nitrogen versus phosphorus patterns may reflect groundwater versus runoff flux pathways. Seasonally, at sites 09 and 20 oxidized nitrogen concentrations were significantly higher during the dry season (December to May) than the wet season (June to November, hurricane season) as shown in Figure 5.9. Since it is hypothesized that nitrogen is reaching the estuary through groundwater, this pattern may represent dilution of ambient nitrogen by freshwater flows during the rainy season. There was no statistically significant difference between seasons at sites 10 and 19.

5.3.3. Chlorophyll a

Chlorophyll a concentrations ranged from below the method detection limit to 142.6 $\mu\text{g/L}$, with a mean of 4.39 $\mu\text{g/L}$ and a median of 1.34 $\mu\text{g/L}$ (Table 5.4). Concentrations varied significantly between all sites (Figure 5.10), which likely reflected multiple forcing factors controlling phytoplankton populations including nutrient concentrations, zooplankton grazing, and circulation patterns. Chlorophyll a was not correlated with nutrients or precipitation. Seasonally,

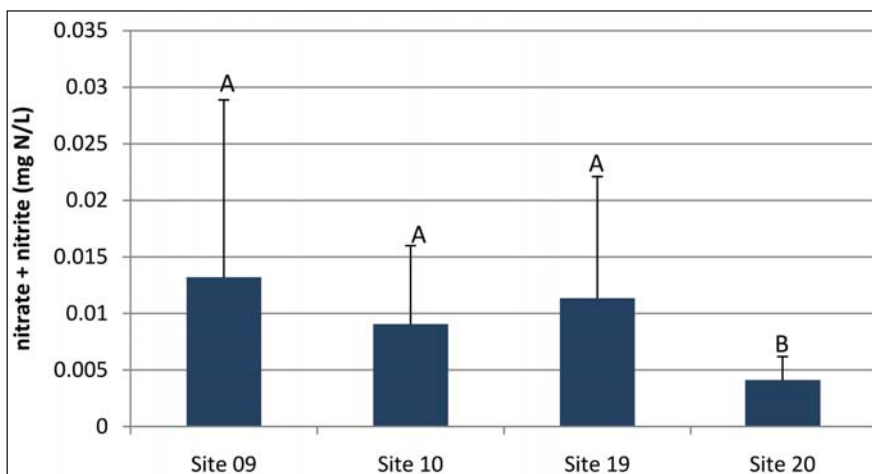


Figure 5.8. Mean nitrate plus nitrite concentrations from 2008-2010. Letters indicate statistical groupings (Wilcoxon test, $P < 0.05$). Error bars represent standard deviation.

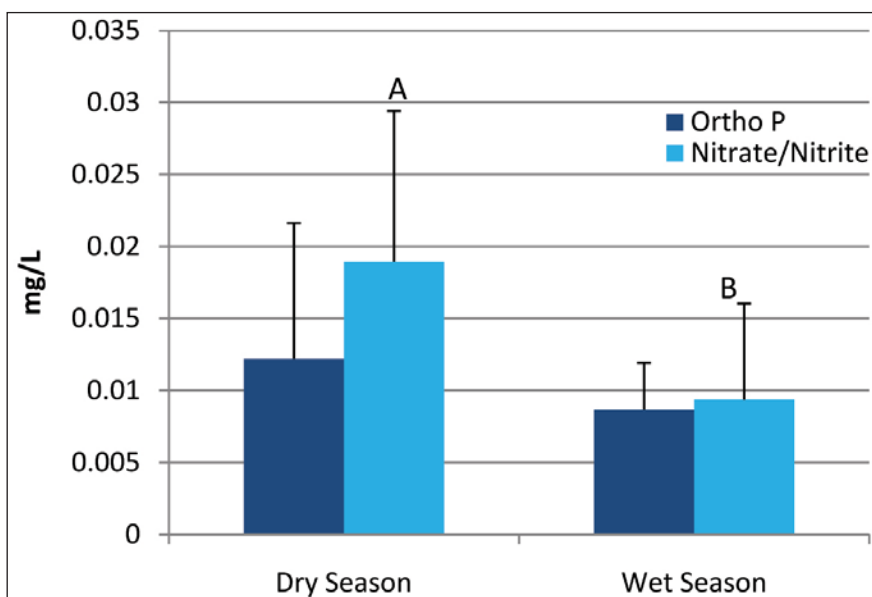


Figure 5.9. Seasonal variability in orthophosphorus and nitrate/nitrite between wet (hurricane) and dry seasons at site 20 from 2008-2010. There was a statistical difference between seasons for nitrate/nitrite (Wilcoxon test, $P < 0.05$).

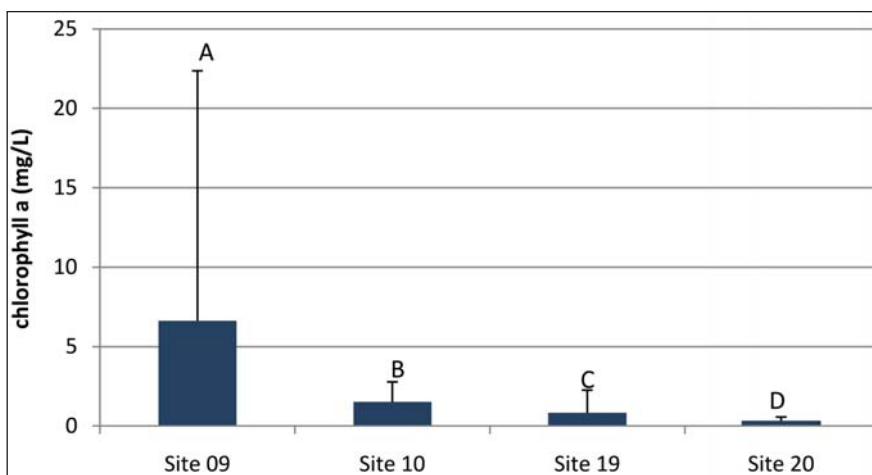


Figure 5.10. Mean chlorophyll a concentrations. Letters indicate statistical groupings (Wilcoxon test, $P < 0.05$). Error bars represent standard deviation.

chlorophyll a was significantly higher at site 09 during the wet season (Figure 5.11). This could be due to changes in nutrient dynamics (see above) with freshwater inputs. It is also possible that changes in salinity could directly or indirectly affect phytoplankton communities.

5.3.4. Pesticide Results

Among the thirty two pesticides and degradates tested for in each sample only two were detected, atrazine and its degradation product desethylatrazine (DEA). Their detection

was limited to the near shore stations (sites 09, 10 and 11; Figure 5.12) during the rainy season in 2008. The highest concentrations were observed in a sample collected at station 9. The sample was collected four days after a large rainfall-runoff event. Comparison with management records from the silage farm adjacent to Mar Negro indicated that the herbicide was applied to farm field three days prior to the event (Figure 5.13). The short period of time between pesticide application and rainfall created conditions that resulted in relatively high atrazine discharge to the Bay. The south shore of Puerto Rico is typically subjected to multiple tropical storms/depressions every year. Figure 5.14 shows the passing of two tropical storms (Faye, Kyle) in 2008 which impacted salinity and pesticide concentrations in the estuary. Results indicate these storms contribute to high pesticide runoff risk and care should be taken to avoid application of pesticides immediately prior to approaching tropical storms.

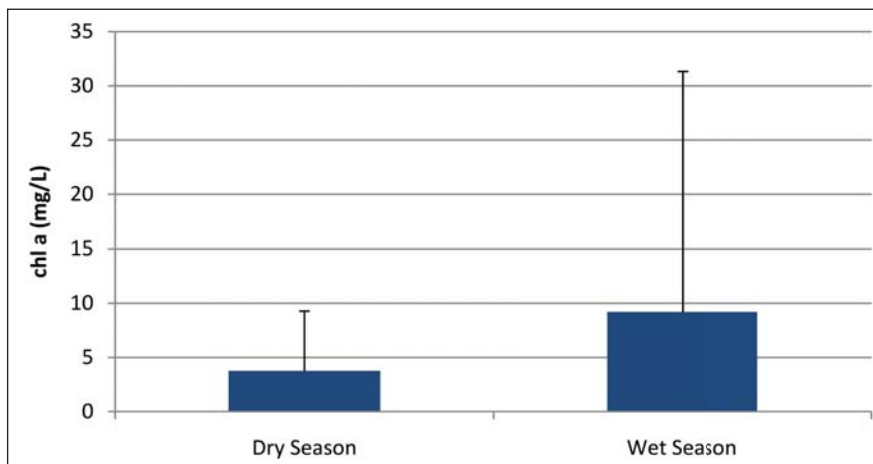


Figure 5.11. Seasonal variability in chlorophyll a between wet (hurricane) and dry seasons at site 09 from 2008-2010. There was a statistical difference between seasons (Wilcoxon test, $P < 0.05$).

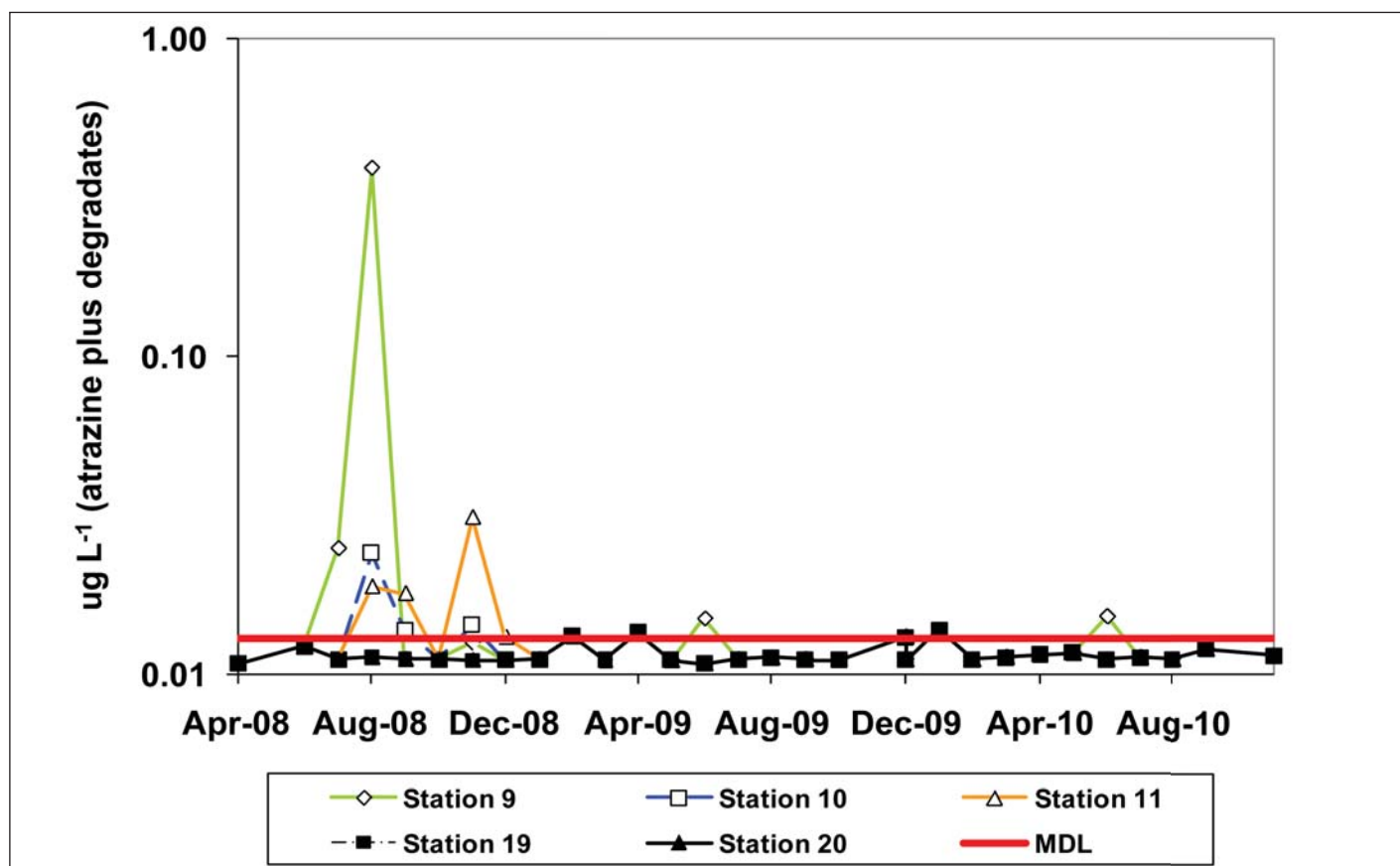


Figure 5.12. Atrazine and atrazine degradate concentrations in Jobos Bay. Red line represents method detection limit.

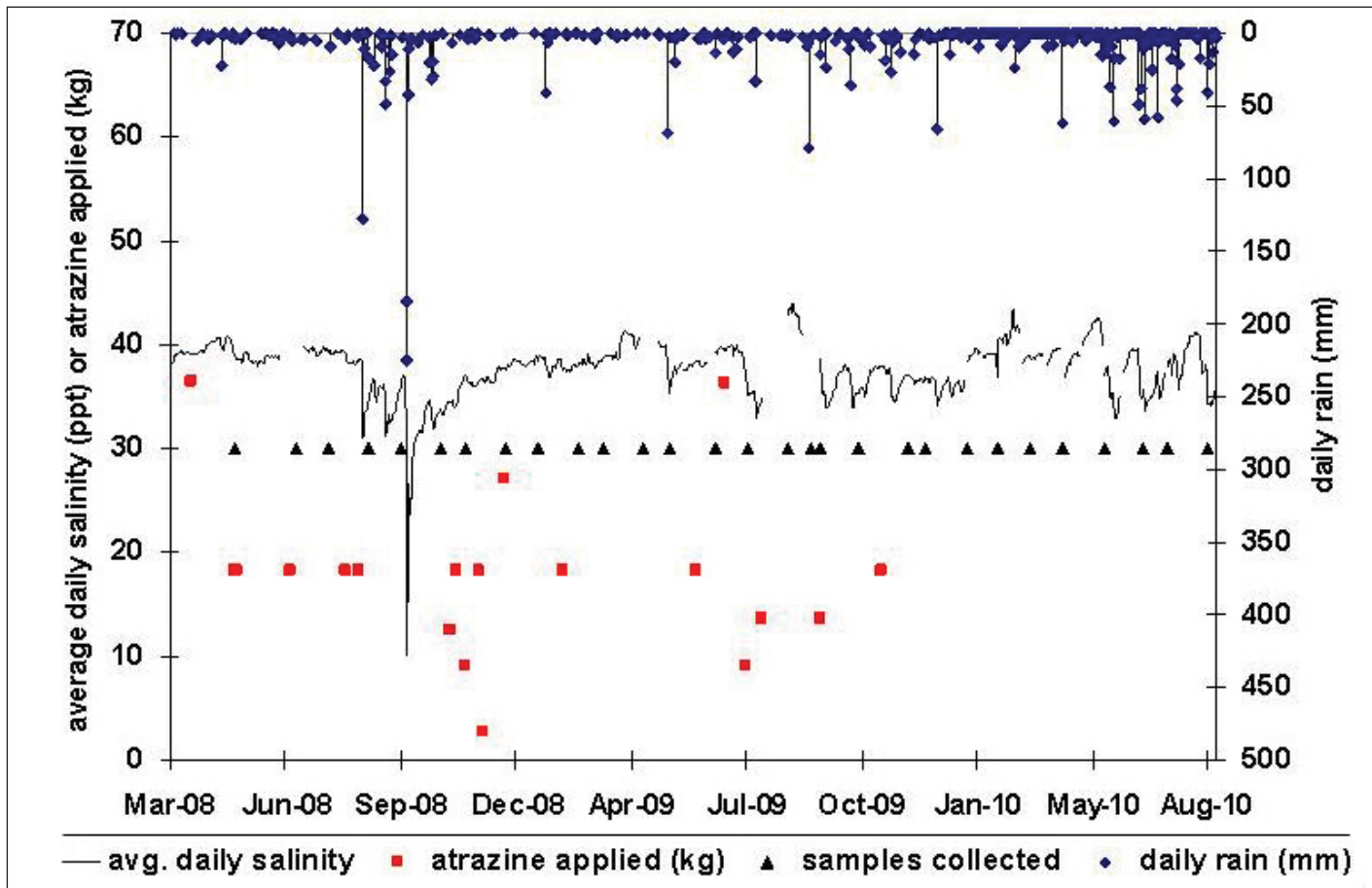


Figure 5.13. Atrazine application rates on the farm and precipitation and salinity at SWMP site 09.

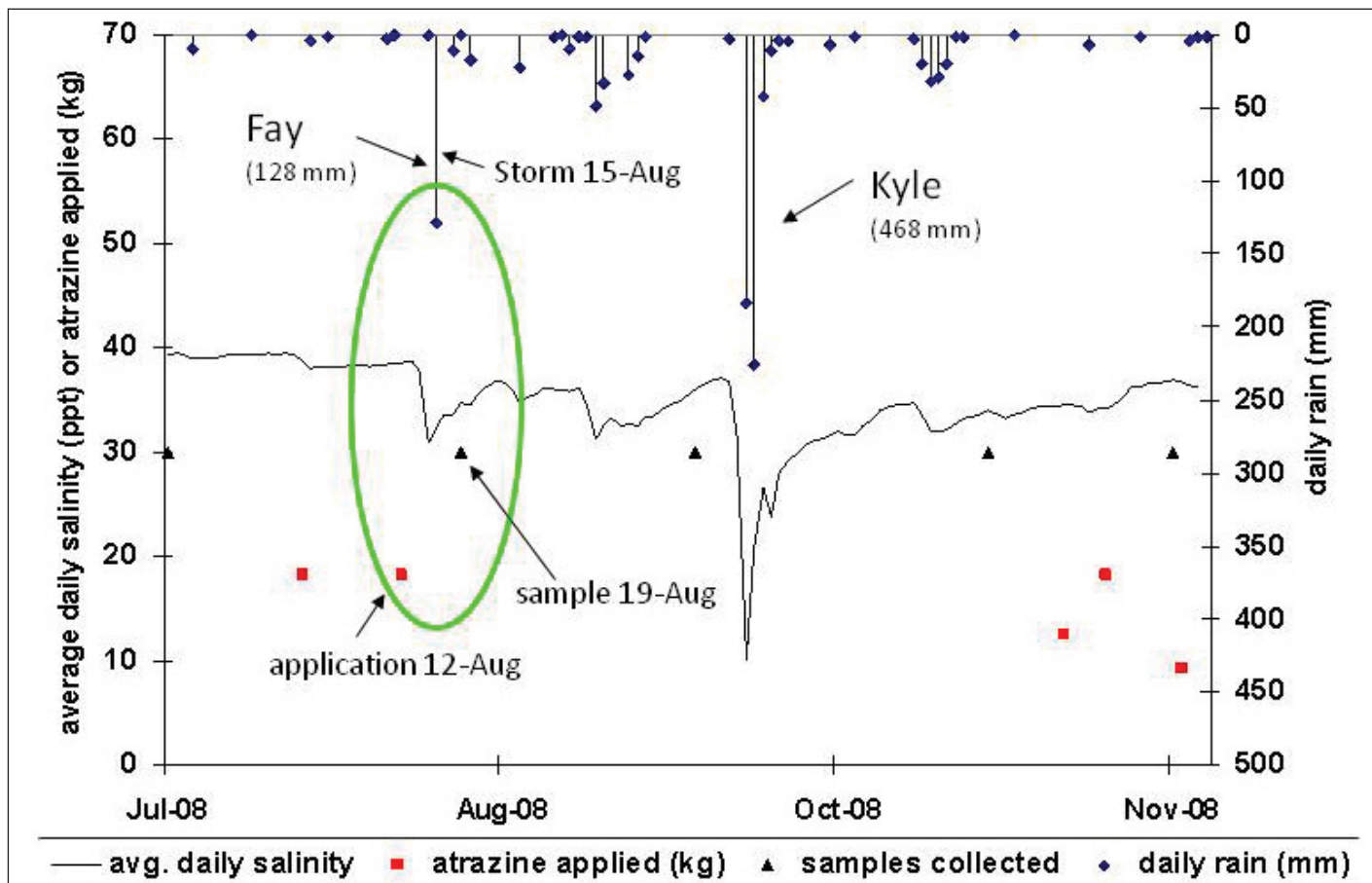


Figure 5.14. Timing of atrazine application in relation to tropical storms in Jobos Bay.

5.4. CONCLUSIONS

These data demonstrate that land based sources of pollution (pesticides and nutrients) are reaching Jobos Bay via surface runoff and/or groundwater discharge. These pathways of transport may be of concern to the mangrove ecosystem in Mar Negro and sensitive offshore coral reef ecosystems (Figure 5.15). The pesticide data presented here demonstrate the relationship between pesticide application and rainfall driven runoff in contributing pesticide residues to the Bay.

These data make up part of a larger baseline assessment of this system which will be used to evaluate the efficacy of and planning for implementation of watershed best management practices. The water quality parameters discussed here will likely respond very quickly to changes in the watershed, making them especially useful for documenting short term changes to the system.



Figure 5.15. Mangrove forest lining Jobos Bay.

ACKNOWLEDGMENTS

Funding for this research was provided the U.S. Department of Agriculture, Natural Resource Conservation Program (Conservation Effects Assessment Project), and NOAA's Coral Reef Conservation Program. Additionally, the authors would like to thank Dr. Michael Piehler, Dr. Suzanne Bricker and Dr. Edward Johnson for their helpful editorial comments which greatly improved this chapter.

REFERENCES

- Ahrens, W.H. (ed.). 1994. *Herbicide Handbook of the Weed Science Society of America*, 7th ed. Weed Science Society of America. Champaign, IL. 352 pp.
- Almodóvar, L.R. 1964. The marine algae of Bahía de Jobos, Puerto Rico. *Nova Hedwigia* VII(1/2): 33-52.
- Arar, E.J. and G.B. Collins. 1997. Method 445.0 - *In Vitro* Determination of Chlorophyll *a* and Pheophytin *a* in Marine and Freshwater Algae by Fluorescence. pp. 132-153. In: *Methods for the Determination of Chemical Substances in Marine and Estuarine Environmental Matrices- 2nd Edition*. USEPA 600/R--97/072. National Exposure Research Laboratory, Office of Research and Development, U.S. Environmental Protection Agency. 199 pp. (Online) http://archive.chesapeakebay.net/pubs/quality_assurance/EPA_Marine_Methods_2nd_ed.pdf (Accessed 13 June 2011).
- Bricker, S., B. Longstaff, W. Dennison, A. Jones, K. Boicourt, C. Wicks, and J. Woerner. 2007. *Effects of Nutrient Enrichment in the Nation's Estuaries: A Decade of Change*, National Estuarine Eutrophication Assessment Update. NOAA Coastal Ocean Program Decision Analysis Series No. 26. National Centers for Coastal Ocean Science, Silver Spring, MD. 322 pp.

Galloway J.N., J.D. Aber, J.W. Erisman, S.P. Seitzinger, R.H. Howarth, E.B. Cowling, and B.J. Cosby. 2003. The nitrogen cascade. *BioScience* 53: 341-356.

Harrison, P.L. and S. Ward. 2001. Elevated levels of nitrogen and phosphorus reduce fertilisation success of gametes from scleractinian reef corals. *Marine Biology* 139: 1057-1068.

Humburg, N.E., S.R. Colby, E.R. Hill, L.M. Kitchen, R.G. Lym, W.J. McAvoy, and R. Prasad (eds.). 1989. *Herbicide Handbook of the Weed Science Society of America*, 6th ed. Weed Science Society of America. Champaign, IL. 301 pp.

Marubini, F. and P.S. Davies. 1996. Nitrate increases zooxanthellae population density and reduces skeletogenesis in corals. *Marine Biology* 127: 319-328.

Mathews, L.G, F.R. Homans, and K.W. Easter. 2002. Estimating the benefits of phosphorus pollution reductions: An application in the Minnesota River. *Journal of the American Water Resources Association* 38: 1217-1223.

National Estuarine Research Reserve System (NERRS). 2011. Data Export System: Jobos Bay Nutrient Metadata. Centralized Data Management Office, National Estuarine Research Reserve System. (Online) <http://cdmo.baruch.sc.edu/> (Accessed 13 June 2011).

Potter, T.L., M. Mohamed, and H. Ali. 2007. Solid-Phase Extraction Combined with High-Performance Liquid Chromatography–Atmospheric Pressure Chemical Ionization–Mass Spectrometry Analysis of Pesticides in Water: Method Performance and Application in a Reconnaissance Survey of Residues in Drinking Water in Greater Cairo, Egypt. *Journal of Agricultural Food Chemistry* 55(2): 204-210.

Rodríguez, J.M. 2006. Evaluation of hydrologic conditions and nitrate concentrations in the Río Nigua de Salinas alluvial fan aquifer, Salinas, Puerto Rico, 2002-03. U.S. Geological Survey Scientific Investigations Report 2006-5062. 38 pp.

U.S. Department of Agriculture- Integrated Pest Management Centers (USDA-IPMCENTERS). 2011. National Information System for the Regional Integrated Pest Management Centers: USDA Crop Profiles. National Science Foundation Center for Integrated Pest Management and National Institute of Food and Agriculture, U.S. Department of Agriculture. Raleigh, NC. (Online) http://www.ipmcenters.org/cropprofiles/cp_form.cfm (Accessed 13 June 2011).

U.S. Department of Agriculture- National Agricultural Statistics Service (USDA-NASS). 2009. 2007 Census of Agriculture. National Agricultural Statistics Service, U.S. Department of Agriculture. Washington, D.C. (Online) http://www.agcensus.usda.gov/Publications/2007/Full_Report/index.asp (Accessed 13 June 2011).

U.S. Environmental Protection Agency (USEPA). 1974. Nitrogen, Ammonia (Automated Colorimetric Phenate Method). pp. 168-174. In: *Methods for chemical analysis of water and wastes*. Methods Development and Quality Assurance Research Laboratory, National Environmental Research Center, U.S. Environmental Protection Agency. Cincinnati, OH. 298 pp.

U.S. Environmental Protection Agency (USEPA). 1995. Metolachlor: Reregistration Eligibility Decision (RED). Office of Pesticide Programs, U.S. Environmental Protection Agency. (Online) <http://www.epa.gov/oppsrrd1/REDs/0001.pdf> (Accessed 13 June 2011).

U.S. Environmental Protection Agency (USEPA). 2006. Atrazine: Interim Reregistration Eligibility Decision (IREED). (Online) http://www.epa.gov/oppsrrd1/REDs/atrazine_combined_docs.pdf (Accessed 13 June 2011).

Whitall, D.R., A.L. Mason, A.S. Pait, V. Ransibrahmanakul, and J.D. Christensen. 2010. Characterization of Spatial and Temporal Nutrient Dynamics. pp. 151-168. In: L.J. Bauer and M.S. Kendall (eds.). An Ecological Characterization of the Marine Resources of Vieques, Puerto Rico Part II: Field Studies of Habitats, Nutrients, Contaminants, Fish, and Benthic Communities. NOAA Technical Memorandum NOS NCCOS 110. Silver Spring, MD. 174 pp.

Zhang, J.Z., P.B. Ortner, and C.J. Fischer. 1997. Method 353.4 - Determination of Nitrate and Nitrite in Estuarine and Coastal Waters by Gas Segmented Continuous Flow Colorimetric Analysis. pp. 80-99. In: Methods for the Determination of Chemical Substances in Marine and Estuarine Environmental Matrices- 2nd Edition. USEPA 600/R--97/072. National Exposure Research Laboratory, Office of Research and Development, U.S. Environmental Protection Agency. 199 pp. (Online) http://archive.chesapeakebay.net/pubs/quality_assurance/EPA_Marine_Methods_2nd_ed.pdf (Accessed 13 June 2011).

Zimmermann, C.F. and C.W. Keefe. 1997. Method 365.5 - Determination of Orthophosphate in Estuarine and Coastal Waters by Automated Colorimetric Analysis. pp. 100-108. In: Methods for the Determination of Chemical Substances in Marine and Estuarine Environmental Matrices- 2nd Edition. USEPA 600/R--97/072. National Exposure Research Laboratory, Office of Research and Development, U.S. Environmental Protection Agency. 199 pp. (Online) http://archive.chesapeakebay.net/pubs/quality_assurance/EPA_Marine_Methods_2nd_ed.pdf (Accessed 13 June 2011).

Zitello, A.G., D.R. Whitall, A. Dieppa, J.D. Christensen, M.E. Monaco, and S.O. Rohmann. 2008. Characterizing Jobos Bay, Puerto Rico: A Watershed Modeling Analysis and Monitoring Plan. NOAA Technical Memorandum NOS NCCOS 76. Silver Spring, MD. 81 pp.

Chapter 6



Conclusions

This report presents a suite of studies investigating fish fauna, benthic communities, nutrient levels, and chemical contaminants in the marine environment in Jobos Bay (Figure 6.1) and the surrounding coral reef ecosystem. The overarching goal of these studies was to establish an environmental baseline of Jobos Bay. Now that this baseline has been established, environmental change in the system can be measured in future years. The ability to detect change is especially important to coastal managers as a variety of watershed changes, ranging from development to changes in best management practices, occur over time. Best management practices that have already been applied to the silage farm adjacent to the Bay include: improved water management and the use of cover crops. Pest management improvement may also be of some benefit, including the importance of the timing of pesticide applications during hurricane season to avoid major rainfall events immediately after application (see Chapter 5).



Figure 6.1. Mangroves in Jobos Bay. Photo: NOAA Center for Coastal Monitoring and Assessment (CCMA).

By design, components of the studies in this assessment shared many sampling sites, sampling periods, strata, and methods with those used to monitor nearby islands. Results can therefore be easily combined and compared for more integrated analyses. We intentionally did not examine all variables from all studies simultaneously for correlations. Doing so would have yielded a high chance of spurious or random correlations due to the large number of variables involved. Instead, in this chapter we highlight some key observations and point out findings that merit further assessment.

Key findings from this report include:

The new benthic habitat map represents an improvement on the previous NOAA map due to newly acquired acoustic and optical imagery, a more detailed classification scheme, and a smaller minimum mapping unit. In particular, use of acoustic imagery enabled the delineation of features within areas of the Bay too turbid to be identified in optical imagery. Compared to the 2001 map, an additional 22 km² was able to be mapped in the new effort (Chapter 2).

The biota, nutrients, and chemical contaminant levels in Jobos Bay and the surrounding coral reef ecosystem are generally similar to those for other coral reef ecosystems in the Puerto Rico and U.S. Virgin Islands region and are likely to have been shaped primarily by regional-scale processes rather than local factors (see Chapters 3, 4 and 5). Locations with the highest observed live coral cover were located on reef seaward of the cays. Sites along these reefs, as well as with the adjacent mangrove complex, were also characterized by the highest observed fish species richness, abundance, and biomass in the study.

Distribution of sediment contaminants were generally driven by grain size, and magnitudes were, for the most part, below levels which might indicated environmental concern, based on the established sediment quality guidelines that are currently available (see Chapter 4).

Future Work

A major knowledge gap is the direct causal effect between pollution stressors and coral ecosystem health. While this study definitively establishes that a variety of pollutants exist in the water column (e.g., pesticides) and sediments (e.g., heavy metals, pesticides, polycyclic aromatic hydrocarbons [PAHs]) of Jobos Bay, and that many of these contaminants are being incorporated in offshore coral tissues, it is not understood what ramifications this might have for coral health. Additional biological field data might allow for correlative explorations via kriging (see Pait *et al.*, 2007), but even finding a correlation between contaminants and indices of ecological health (e.g., coral species richness) does not indicate a causal effect. It would be extremely valuable to have laboratory (mesocosm) experiments to test the dose-response relationship between contaminants (both as individual pollutants and suites of contaminants) and individual coral health. Establishing the relationship between specific pollutant stressors and coral biomarkers (Downs *et al.*, 2000) would also be extremely useful, although to this point biomarkers have not been linked to specific pollutants.

This interdisciplinary data set provides a valuable baseline assessment of the system which will be useful from a variety of perspectives, including the most comprehensive study to date of the Jobos Bay National Estuarine Research Reserve (JBNERR). This study will be of excellent use to coastal managers as a starting point against which to measure change. In order to track these changes, future assessment efforts will be required. The authors recommend that future assessment activities utilize the same methodologies described here so that the new results are directly comparable with this baseline assessment.

It should be noted that different environmental parameters will change more quickly than others. These differing time scales of change need to be considered when planning future assessments. For example, water quality parameters (nutrients, chlorophyll a, pesticides) change on daily, if not hourly, time scales, and therefore will respond very quickly as land-based sources of pollution change. On the other end of the spectrum, biological indices of ecosystem health are likely to respond more slowly, on the time scales of years to decades, especially when considering slow growing species such as corals (Figure 6.2).



Figure 6.2. Hardbottom habitat of Jobos Bay. Photo: NOAA CCMA.

It is also important to realize that the environmental status of the near coastal environment can respond in different ways to watershed management actions. Ideally, the environment will improve in response to management actions and the “before” and “after” assessments will allow coastal managers to track how well the management actions have worked. However, it is possible that environmental conditions could remain the same or even get worse. For example, if other environmental stressors are more detrimental to the ecology of the system than the stressors targeted for management, or if the watershed is changing very quickly (e.g., rapid coastal development), the system could actually

degrade (Figure 6.3). Further, the coral reef community is affected by regional and global factors beyond the realm of the watershed (e.g., disease, overfishing, climate change, etc.). From a scientific perspective, all of these outcomes provide important information that will be useful to managers by providing critical information that will lead to better, more effective management decisions in the future.



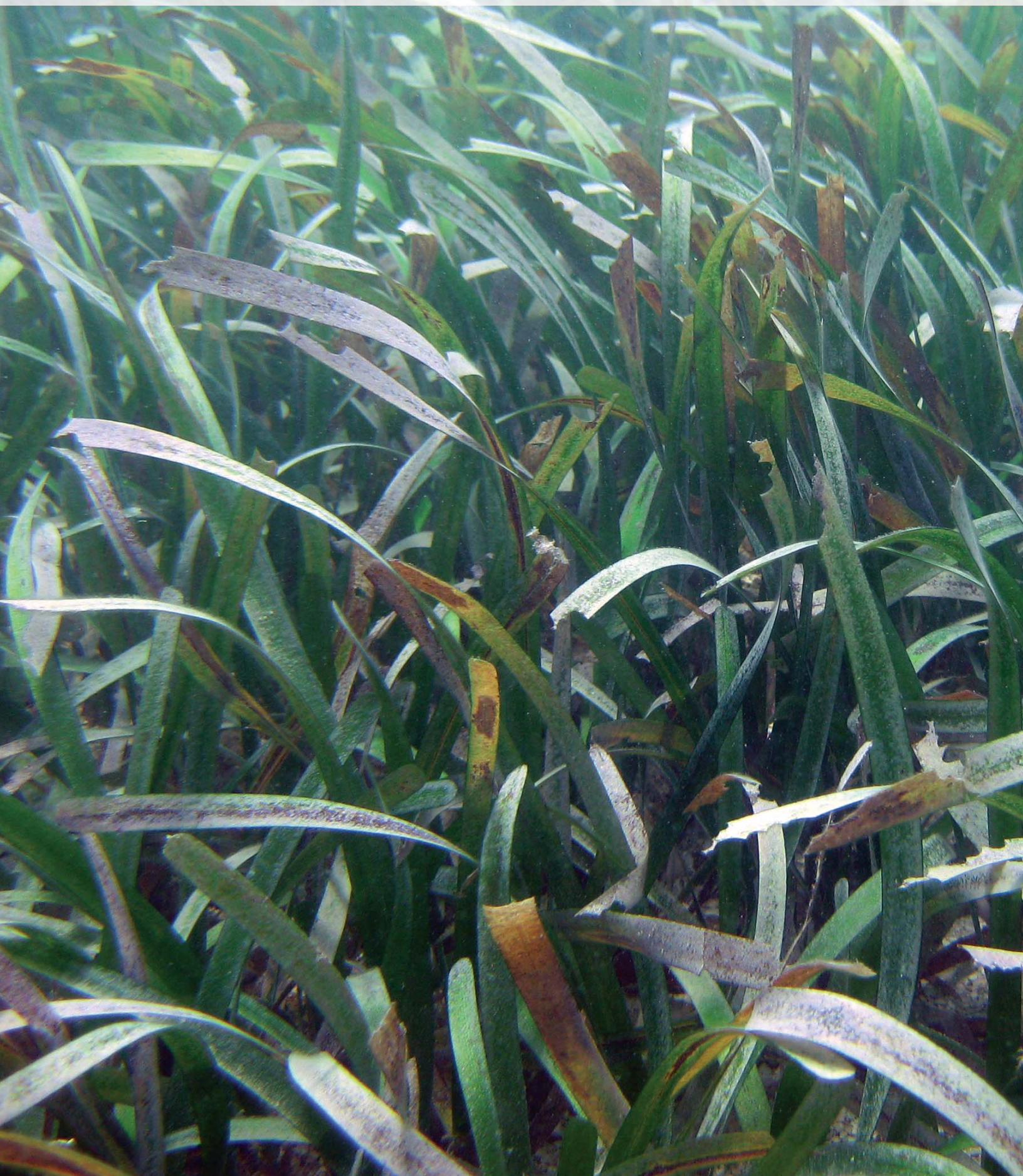
Figure 6.3. Industrialized shoreline of Jobos Bay. Photo: NOAA CCMA.

REFERENCES

Downs, C.A., E. Mueller, S. Phillips, J.E. Fauth, and C.M. Woodley. 2000. A Molecular Biomarker System for Assessing the Health of Coral (*Montastraea faveolata*) during Heat Stress. *Journal of Marine Biotechnology* 2: 533-544.

Pait, A.S., D.R. Whitall, C.F.G. Jeffrey, C. Caldow, A.L. Mason, J.D. Christensen, M.E. Monaco, and J. Ramirez. 2007. An assessment of chemical contaminants in the marine sediments of southwest Puerto Rico. NOAA Technical Memorandum NOS NCCOS 52. Silver Spring, MD. 116 pp. (Online) <http://www.ccma.nos.noaa.gov/publications/southwestpuertorico.pdf> (Accessed 13 June 2011).

Appendices



Appendix A

Table A.1. Mean species frequency, density, and biomass for fish species observed at Jobos Bay in the June 2009 survey.

Species	Common name	Family	Trophic Group	% of Surveys	Mean Density (SE)	Mean Biomass (SE)
<i>Abudefduf saxatilis</i>	sergeant major	Pomacentridae	I	22%	0.65 (0.52)	1.35 (0.59)
<i>Acanthurus bahianus</i>	ocean surgeonfish	Acanthuridae	H	42%	2.40 (0.58)	73.81 (30.09)
<i>Acanthurus chirurgus</i>	doctorfish	Acanthuridae	H	40%	1.44 (0.70)	194.56 (141.63)
<i>Acanthurus coeruleus</i>	blue tang	Acanthuridae	H	24%	0.73 (0.41)	28.20 (20.41)
<i>Anisotremus virginicus</i>	porkfish	Haemulidae	I	18%	0.17 (0.07)	16.76 (8.02)
<i>Apogon</i> sp.	cardinalfish species	Apogonidae	I	2%	0.11 (0.11)	0.05 (0.05)
<i>Archosargus rhomboidalis</i>	sea bream	Sparidae	H	2%	0.00 (0.00)	0.02 (0.02)
<i>Balistes vetula</i>	queen triggerfish	Balistidae	I	2%	0.01 (0.01)	5.28 (5.28)
<i>Bodianus rufus</i>	spanish hogfish	Labridae	I	9%	0.08 (0.05)	1.99 (1.16)
<i>Calamus calamus</i>	saucereye porgy	Sparidae	I	4%	0.02 (0.01)	9.11 (7.79)
<i>Cantherhines macrocerus</i>	whitespotted filefish	Monacanthidae	I	2%	0.01 (0.01)	0.12 (0.12)
<i>Cantherhines pullus</i>	orangespotted filefish	Monacanthidae	I	7%	0.05 (0.03)	1.99 (1.44)
<i>Canthigaster rostrata</i>	sharpnose puffer	Tetraodontidae	I	24%	0.39 (0.17)	0.40 (0.18)
<i>Carangoides ruber</i>	bar jack	Carangidae	P	4%	0.05 (0.04)	1.01 (0.81)
<i>Caranx crysos</i>	blue runner	Carangidae	P	2%	0.05 (0.05)	11.95 (11.95)
<i>Centropomus undecimalis</i>	common snook	Centropomidae	P	2%	0.00 (0.00)	0.03 (0.03)
<i>Cephalopholis cruentata</i>	graysby	Serranidae	P	7%	0.07 (0.05)	1.48 (0.95)
<i>Cephalopholis fulva</i>	coney	Serranidae	I	2%	0.03 (0.03)	2.94 (2.94)
<i>Chaetodon capistratus</i>	foureye butterflyfish	Chaetodontidae	I	20%	0.14 (0.06)	1.62 (0.90)
<i>Chaetodon sedentarius</i>	reef butterflyfish	Chaetodontidae	I	9%	0.29 (0.21)	3.39 (2.67)
<i>Chaetodon striatus</i>	banded butterflyfish	Chaetodontidae	I	4%	0.05 (0.04)	0.53 (0.41)
<i>Chromis cyanea</i>	blue chromis	Pomacentridae	PL	2%	0.02 (0.02)	0.01 (0.01)
<i>Coryphopterus glaucofraenum</i>	bridled goby	Gobiidae	I	18%	0.70 (0.40)	0.46 (0.26)
<i>Coryphopterus personatus/hyalinus</i>	masked/glass goby	Gobiidae	I	7%	0.12 (0.07)	0.08 (0.05)
<i>Cryptotomus roseus</i>	bluelip parrotfish	Scaridae	H	11%	0.49 (0.26)	0.81 (0.44)
<i>Ctenogobius saepepallens</i>	dash goby	Gobiidae	I	2%	0.16 (0.16)	0.10 (0.10)
<i>Dasyatis americana</i>	southern stingray	Dasyatidae	I	2%	0.00 (0.00)	1.34 (1.34)
<i>Elacatinus evelynae</i>	sharknose goby	Gobiidae	I	11%	0.11 (0.06)	0.03 (0.01)
<i>Epinephelus guttatus</i>	red hind	Serranidae	I	2%	0.01 (0.01)	2.61 (2.61)
<i>Eucinostomus melanopterus</i>	flagfin mojarra	Gerreidae	I	2%	0.01 (0.01)	0.21 (0.21)
<i>Gerres cinereus</i>	yellowfin mojarra	Gerreidae	I	24%	0.65 (0.53)	2.01 (1.56)
<i>Gnatholepis thompsoni</i>	goldspot goby	Gobiidae	H	7%	0.33 (0.26)	0.07 (0.06)
<i>Grama loreto</i>	fairly basslet	Grammatidae	I	4%	0.06 (0.05)	0.02 (0.02)
<i>Gymnothorax moringa</i>	spotted moray	Muraenidae	P	2%	0.05 (0.05)	3.13 (3.13)
<i>Haemulon aurolineatum</i>	tomtate	Haemulidae	I	9%	0.09 (0.05)	3.19 (1.85)
<i>Haemulon carbonarium</i>	caesar grunt	Haemulidae	I	2%	0.04 (0.04)	0.42 (0.42)
<i>Haemulon flavolineatum</i>	French grunt	Haemulidae	I	24%	0.55 (0.43)	20.82 (17.32)
<i>Haemulon macrostomum</i>	spanish grunt	Haemulidae	I	2%	0.01 (0.01)	0.42 (0.42)
<i>Haemulon plumieri</i>	white grunt	Haemulidae	I	4%	0.02 (0.01)	2.92 (2.01)
<i>Haemulon sciurus</i>	bluestriped grunt	Haemulidae	I	9%	0.02 (0.01)	1.75 (1.29)

Table A.1. Continued...

Species	Common name	Family	Trophic Group	% of Surveys	Mean Density (SE)	Mean Biomass (SE)
<i>Haemulon</i> sp.	grunt species	Haemulidae	I	16%	1.66 (1.17)	2.54 (1.89)
<i>Halichoeres bivittatus</i>	slippery dick	Labridae	I	24%	2.08 (0.79)	8.12 (3.18)
<i>Halichoeres garnoti</i>	yellowhead wrasse	Labridae	I	16%	0.40 (0.17)	0.91 (0.48)
<i>Halichoeres maculipinna</i>	clown wrasse	Labridae	I	22%	0.63 (0.19)	1.74 (0.55)
<i>Halichoeres pictus</i>	rainbow wrasse	Labridae	I	2%	0.18 (0.18)	0.13 (0.13)
<i>Halichoeres poeyi</i>	blackear wrasse	Labridae	I	33%	2.28 (0.74)	18.94 (11.49)
<i>Halichoeres radiatus</i>	puddingwife	Labridae	I	16%	0.09 (0.04)	0.21 (0.14)
<i>Heteropriacanthus cruentatus</i>	glasseye snapper	Priacanthidae	PL	2%	0.05 (0.05)	0.03 (0.03)
<i>Holocentrus adscensionis</i>	squirrelfish	Holocentridae	I	16%	0.14 (0.06)	4.60 (1.98)
<i>Holocentrus rufus</i>	longspine squirrelfish	Holocentridae	I	20%	0.15 (0.06)	3.68 (1.47)
<i>Holacanthus tricolor</i>	rock beauty	Pomacanthidae	I	2%	0.03 (0.03)	1.37 (1.37)
<i>Hypoplectrus chlorurus</i>	yellowtail hamlet	Serranidae	I	2%	0.01 (0.01)	0.20 (0.20)
<i>Hypoplectrus indigo</i>	indigo hamlet	Serranidae	I	2%	0.01 (0.01)	0.04 (0.04)
<i>Hypoplectrus</i> sp.	hamlet species	Serranidae	I	11%	0.07 (0.04)	0.66 (0.61)
<i>Hypoplectrus puella</i>	barred hamlet	Serranidae	I	11%	0.12 (0.06)	0.92 (0.50)
<i>Hypoplectrus unicolor</i>	butter hamlet	Serranidae	I	2%	0.01 (0.01)	0.07 (0.07)
<i>Jenkinsia</i> sp.	herring species	Clupeidae	PL	11%	0.32 (0.29)	0.03 (0.02)
<i>Kyphosus sectator/incisor</i>	chub (Bermuda/ yellow)	Kyphosidae	H	2%	0.01 (0.01)	1.23 (1.23)
<i>Lachnolaimus maximus</i>	hogfish	Labridae	I	4%	0.03 (0.02)	2.89 (2.40)
<i>Lophogobius cyprinoides</i>	crested goby	Gobiidae	H	2%	0.00 (0.00)	0.00 (0.00)
<i>Lutjanus analis</i>	mutton snapper	Lutjanidae	I	7%	0.00 (0.00)	0.02 (0.02)
<i>Lutjanus apodus</i>	schoolmaster	Lutjanidae	P	33%	0.39 (0.28)	18.84 (13.90)
<i>Lutjanus griseus</i>	gray snapper	Lutjanidae	I	16%	0.08 (0.07)	0.84 (0.53)
<i>Lutjanus jocu</i>	dog snapper	Lutjanidae	P	4%	0.02 (0.01)	13.86 (12.01)
<i>Lutjanus mahogoni</i>	mahogany snapper	Lutjanidae	P	4%	0.01 (0.01)	0.12 (0.11)
<i>Lutjanus synagris</i>	lane snapper	Lutjanidae	I	4%	0.00 (0.00)	0.01 (0.01)
<i>Lutjanus</i> sp.	snapper species	Lutjanidae	P	2%	0.05 (0.05)	0.36 (0.36)
<i>Malacoctenus macropus</i>	rosy blenny	Labrisomidae	I	2%	0.00 (0.00)	0.00 (0.00)
<i>Malacoctenus triangulatus</i>	saddled blenny	Labrisomidae	I	9%	0.11 (0.07)	0.10 (0.09)
<i>Microspathodon chrysurus</i>	yellowtail damselfish	Pomacentridae	H	16%	0.19 (0.07)	5.01 (2.01)
<i>Microgobius</i> sp.	goby species	Gobiidae	H	2%	0.05 (0.05)	0.01 (0.01)
<i>Mulloidichthys martinicus</i>	yellow goatfish	Mullidae	I	2%	0.04 (0.04)	0.37 (0.37)
<i>Myripristis jacobus</i>	blackbar soldierfish	Holocentridae	I	2%	0.05 (0.05)	0.12 (0.12)
<i>Nes longus</i>	orangespotted goby	Gobiidae	H	7%	0.42 (0.23)	2.20 (1.48)
<i>Ocyurus chrysurus</i>	yellowtail snapper	Lutjanidae	PL	27%	1.29 (0.59)	32.59 (16.04)
<i>Opistognathus aurifrons</i>	yellowhead jawfish	Opistognathidae	PL	2%	0.05 (0.05)	0.01 (0.01)
<i>Ophioblennius macclurei</i>	redlip blenny	Blenniidae	H	11%	0.13 (0.06)	0.46 (0.22)
<i>Oxyurichthys stigmalocephus</i>	spotfin goby	Gobiidae	H	2%	0.05 (0.05)	0.02 (0.02)
<i>Pomacanthus arcuatus</i>	gray angelfish	Pomacanthidae	I	11%	0.09 (0.06)	34.03 (21.79)
<i>Pomacanthus paru</i>	French angelfish	Pomacanthidae	I	4%	0.07 (0.06)	28.33 (22.28)
<i>Pseudupeneus maculatus</i>	spotted goatfish	Mullidae	I	27%	0.90 (0.74)	33.07 (29.62)

Table A.1. Continued...

Species	Common name	Family	Trophic Group	% of Surveys	Mean Density (SE)	Mean Biomass (SE)
<i>Ptereleotris helenae</i>	hovering goby	Microdesmidae	PL	9%	0.42 (0.23)	0.48 (0.30)
<i>Sargocentron coruscum</i>	reef squirrelfish	Holocentridae	I	2%	0.11 (0.11)	0.05 (0.05)
<i>Scarus iseri</i>	striped parrotfish	Scaridae	H	44%	1.39 (0.37)	16.78 (5.05)
<i>Scorpaena plumieri</i>	spotted scorpionfish	Scorpaenidae	I	7%	0.12 (0.07)	18.50 (13.42)
<i>Scomberomorus regalis</i>	cero	Scombridae	P	2%	0.05 (0.05)	28.14 (28.14)
<i>Scarus taeniopterus</i>	princess parrotfish	Scaridae	H	4%	0.03 (0.02)	2.07 (1.43)
<i>Serranus baldwini</i>	lantern bass	Serranidae	P	4%	0.32 (0.26)	0.11 (0.10)
<i>Serranus flaviventris</i>	twinspot bass	Serranidae	P	4%	0.06 (0.05)	0.54 (0.46)
<i>Serranus</i> sp.	seabass species	Serranidae	P	2%	0.05 (0.05)	0.31 (0.31)
<i>Serranus tabacarius</i>	tobaccofish	Serranidae	P	4%	0.16 (0.11)	0.06 (0.04)
<i>Serranus tigrinus</i>	harlequin bass	Serranidae	I	13%	0.22 (0.12)	1.42 (0.63)
<i>Serranus tortugarum</i>	chalk bass	Serranidae	PL	9%	3.21 (1.82)	1.15 (0.65)
<i>Sparisoma</i> sp.	parrotfish species	Scaridae	H	2%	0.00 (0.00)	0.00 (0.00)
<i>Sparisoma atomarium</i>	greenblotch parrotfish	Scaridae	H	9%	0.29 (0.17)	0.10 (0.06)
<i>Sparisoma aurofrenatum</i>	redband parrotfish	Scaridae	H	36%	1.23 (0.28)	27.60 (8.25)
<i>Sphyraena barracuda</i>	great barracuda	Sphyraenidae	P	11%	0.02 (0.01)	122.73 (114.31)
<i>Sparisoma radians</i>	bucktooth parrotfish	Scaridae	H	9%	0.16 (0.11)	0.06 (0.04)
<i>Sparisoma rubripinne</i>	yellowtail parrotfish	Scaridae	H	11%	0.08 (0.04)	11.03 (7.15)
<i>Sphoeroides spengleri</i>	bandtail puffer	Tetraodontidae	I	2%	0.00 (0.00)	0.01 (0.01)
<i>Sphoeroides testudineus</i>	checkered puffer	Tetraodontidae	I	4%	0.12 (0.11)	0.06 (0.05)
<i>Sparisoma viride</i>	stoplight parrotfish	Scaridae	H	27%	0.30 (0.08)	13.29 (4.63)
<i>Stegastes adustus</i>	dusky damselfish	Pomacentridae	H	18%	0.83 (0.48)	3.41 (2.33)
<i>Stegastes diencaeus</i>	longfin damselfish	Pomacentridae	H	38%	2.36 (0.83)	6.40 (2.10)
<i>Stegastes leucostictus</i>	beaugregory	Pomacentridae	I	42%	1.13 (0.25)	6.03 (1.50)
<i>Stegastes partitus</i>	bicolor damselfish	Pomacentridae	H	31%	1.39 (0.44)	0.91 (0.29)
<i>Stegastes planifrons</i>	threespot damselfish	Pomacentridae	I	13%	0.48 (0.32)	4.53 (3.02)
<i>Stegastes variabilis</i>	cocoa damselfish	Pomacentridae	H	2%	0.00 (0.00)	0.00 (0.00)
<i>Synodus intermedius</i>	sand diver	Synodontidae	P	4%	0.06 (0.05)	0.26 (0.22)
<i>Thalassoma bifasciatum</i>	bluehead	Labridae	I	42%	4.55 (1.21)	6.53 (2.21)
<i>Xyrichtys martinicensis</i>	rosy razorfish	Labridae	I	2%	0.58 (0.58)	2.44 (2.44)
<i>Xyrichtys splendens</i>	green razorfish	Labridae	I	7%	0.32 (0.21)	0.50 (0.30)

Appendix B

Table B.1. Sediment contaminant data by site.

Site Name	Strata	Total HCH ng/g	Total Chlor- dane ng/g	Total DDT ng/g	Total PCB ng/g	Total PAHs ng/g	TBT ng/g	Ag ug/L	As ug/L	Cd ug/L	Pb ug/L	Sb ug/L
INR2	Inner Bay	0.00	0.06	0.90	5.46	1246	0.19	0.103	23.1	0	11.4	0.279
INR3	Inner Bay	0.00	0.07	1.06	4.95	3935	0.23	0.113	22.4	0	14.3	0.318
INR4	Inner Bay	0.00	2.21	1.19	9.25	14250	0.64	0.136	18.5	0	14.5	0.341
INR5	Inner Bay	0.13	0.77	1.28	6.66	1897	0.13	0.124	18	0	15.3	0.336
INR6	Inner Bay	0.00	0.19	1.80	7.13	1732	0.40	0.132	18.7	0	16.7	0.346
INR7	Inner Bay	0.00	0.67	0.94	6.64	768	0.08	0.113	15.5	0	12.1	0.254
INR8	Inner Bay	0.00	0.21	0.51	5.53	610	0.1	0.123	13.2	0	11.3	0.274
INR9	Inner Bay	0.70	1.95	3.28	15.69	631	0.21	0.12	12.9	0	12.3	0.395
INR10	Inner Bay	0.00	0.11	0.87	5.36	1122	2.27	0.107	11.4	0.173	12.8	0.304
AIN55	Inner Bay	0.00	0.02	0.49	4.09	926	0.00	0.0963	11.3	0	11.4	0.265
CNT11	Central Bay	0.00	0.00	0.16	3.22	221	0.00	0.0862	6.92	0	5.06	0
CNT12	Central Bay	0.00	0.03	0.20	2.81	306	0.00	0.138	9.34	0	4.63	0.351
CNT14	Central Bay	0.02	0.01	0.10	3.54	98.5	0.00	0.0892	12.3	0	3.78	0.252
CNT15	Central Bay	0.00	0.03	0.25	3.22	79.6	0.00	0.0508	18	0	4.45	0.298
CNT16	Central Bay	0.00	0.10	0.76	5.32	517	0.00	0.102	17.5	0	10.9	0.319
CNT17	Central Bay	0.00	0.02	0.36	2.95	361	0.00	0.0623	15.4	0	7.09	0.323
CNT18	Central Bay	0.00	0.03	0.01	2.69	12.3	0.00	0.216	2.22	0	0.786	0
CNT19	Central Bay	0.00	0.00	0.03	3.26	5.5	0.00	0.219	1.79	0	0.227	0
CNT20	Central Bay	0.00	0.01	0.23	2.90	207	0.00	0.0997	17	0	4.72	0.27
ACT45	Central Bay	0.00	0.01	0.03	2.26	25.0	0.00	0.0891	7.87	0	1.98	0
ACT46	Central Bay	0.00	0.01	0.59	3.36	395	0.00	0.0676	17	0	7.38	0.305
NER21	Central Bay (Reserve)	0.00	0.01	0.05	2.81	94.5	0.00	0.0985	10.9	0	4.2	0.253
NER22	Central Bay (Reserve)	0.00	0.00	0.07	2.59	59.3	0.00	0.0877	9.95	0	2.78	0
NER23	Central Bay (Reserve)	0.00	0.07	0.28	3.23	336	0.00	0.0994	14.9	0	7.23	0.306
NER24	Central Bay (Reserve)	0.00	0.26	1.81	9.83	3413	0.00	0.107	28.1	0.174	14	0.562
NER25	Central Bay (Reserve)	0.00	0.07	0.66	4.47	1706	0.0	0.103	20	0	8.25	0.338
NER26	Central Bay (Reserve)	0.00	0.00	0.10	2.69	380	0.00	0.132	10.2	0	5.66	0.231
NER27	Central Bay (Reserve)	0.00	0.06	0.53	4.93	750	0.00	0.0878	15.7	0	8.43	0.377
NER28	Central Bay (Reserve)	0.00	0.08	0.18	2.76	199	10.91	0.0814	14.6	0	5.07	0.347
NER29	Central Bay (Reserve)	0.00	0.10	0.46	4.53	1283	0.23	0.1	17.7	0	7.06	0.225
NER30	Central Bay (Reserve)	0.00	0.31	0.28	3.13	381	0.00	0.0807	7.07	0	4.41	0
OTR31	Outer Bay	0.24	0.02	0.13	3.04	23.9	3.64	0.139	3.06	0	1.4	0
OTR32	Outer Bay	0.02	0.03	0.07	2.51	58.9	0.93	0.168	3.15	0	1.27	0
OTR33	Outer Bay	0.00	0.02	0.10	2.74	140	0.00	0.179	3.69	0	2.49	0
OTR34	Outer Bay	0.00	0.14	0.74	3.73	844	4.24	0.144	16	0	8.27	0.35
OTR35	Outer Bay	0.30	0.01	0.16	2.74	301.9	0.36	0.19	9.6	0	4.72	0
OTR36	Outer Bay	0.00	0.01	0.34	3.25	449	0.00	0.0868	14	0	6.15	0.268
OTR37	Outer Bay	0.00	0.05	0.21	3.05	317	0.00	0.171	7.47	0	5.89	0
OTR38	Outer Bay	0.00	0.02	0.12	3.28	156	0.00	0.146	7.83	0	3.91	0.202
OTR39	Outer Bay	0.00	0.00	0.00	2.28	4	0.00	0.214	2.84	0	1.5	0
OTR40	Outer Bay	0.04	0.00	0.00	2.30	17	0.19	0.174	4.63	0	1.65	0
SWP41	Target Site (NERR SWMP)	0.00	0.00	0.06	2.30	80.5	0.00	0.0593	12.6	0	3.7	0.269
SWP43	Target Site (NERR SWMP)	0.00	0.91	2.09	7.87	3221	0.00	0.0672	6.54	0	15.9	0
SWP44	Target Site (NERR SWMP)	0.61	0.68	0.30	6.57	3157	0.07	0.0797	23.3	0	7.53	0.589

Table B.1 continued... Sediment contaminant data by site.

Site Name	Strata	Sn ug/L	Al ug/L	Cr ug/L	Cu ug/L	Fe ug/L	Mn ug/L	Ni ug/L	Si ug/L	Zn ug/L	Hg ug/L	Se ug/L
INR2	Inner Bay	1.24	70200	24.1	66.5	49200	982	13.1	198000	87.5	0.0782	0.279
INR3	Inner Bay	1.64	70200	27.6	73.7	49300	1130	15.4	183000	102	0.102	0.283
INR4	Inner Bay	1.78	63800	25.9	65.4	43100	925	13.8	172000	94.2	0.109	0.317
INR5	Inner Bay	1.73	65400	25.8	63.6	44100	943	14.5	175000	92.6	0.118	0.267
INR6	Inner Bay	1.91	66100	27.7	68.1	45500	963	16	178000	97.7	0.144	0.31
INR7	Inner Bay	1.91	73700	28.3	72.8	50500	799	16.7	161000	115	0.0758	0.389
INR8	Inner Bay	1.73	68300	26.2	68.5	47200	717	16.1	154000	109	0.0651	0.479
INR9	Inner Bay	2.02	68200	28.9	69	48100	678	18.6	151000	117	0.0659	0.468
INR10	Inner Bay	1.12	41600	22.7	44.4	29000	589	12.7	151000	60.1	0.056	0.284
AIN55	Inner Bay	1.65	51600	21.7	50.4	36900	709	13	128000	86.2	0.0787	0.291
CNT11	Central Bay	0.787	28300	11.7	21.6	18700	440	6.11	120000	38.5	0.0312	0.157
CNT12	Central Bay	0.568	38400	23.8	32.1	20900	368	22	235000	40.1	0.0303	0.167
CNT14	Central Bay	1.01	48600	15.6	18.9	26600	718	6.04	229000	42.6	0.0147	0.119
CNT15	Central Bay	1.02	49100	17.1	22.3	29700	765	7	209000	45.2	0.0136	0.134
CNT16	Central Bay	1.89	50100	23.6	44.2	37100	645	13.4	137000	82.5	0.067	0.402
CNT17	Central Bay	1.63	52900	21	33.5	33500	756	9.59	185000	61.1	0.0305	0.235
CNT18	Central Bay	0	2690	1.33	3.09	2780	45.9	0	13600	5.43	0.0046	0.114
CNT19	Central Bay	0	629	0	1.37	1060	33.1	0	7370	1.57	0.0014	0.106
CNT20	Central Bay	0.909	40400	16.7	20.2	26300	602	10.1	158000	42.1	0.0182	0.158
ACT45	Central Bay	0.476	24400	8.69	9.33	15500	413	4.01	124000	22.3	0.0098	0.104
ACT46	Central Bay	1.82	55400	21.4	37.2	36400	816	9.88	193000	67.6	0.0319	0.241
NER21	Central Bay (Reserve)	1.19	41500	14	24.3	25100	590	6.81	160000	41	0.0132	0.179
NER22	Central Bay (Reserve)	0.642	28600	9.43	13.1	16600	440	4.39	133000	25.7	0.0079	0.113
NER23	Central Bay (Reserve)	1.35	48000	20.6	33	29500	615	9.8	166000	54.7	0.0354	0.388
NER24	Central Bay (Reserve)	2.1	42100	29.4	58	30500	329	26.6	107000	77.5	0.1	1.56
NER25	Central Bay (Reserve)	1.23	44700	27.2	36.9	38500	514	15	135000	67.7	0.0554	0.684
NER26	Central Bay (Reserve)	0.979	31700	16	24.3	22200	383	8.53	92900	44.4	0.0259	0.345
NER27	Central Bay (Reserve)	1.68	56400	24.8	39	36500	733	14	176000	70.6	0.0442	0.318
NER28	Central Bay (Reserve)	1.23	42700	17.5	25.5	26000	530	7.76	152000	45.9	0.0217	0.29
NER29	Central Bay (Reserve)	1.16	45300	23.5	35.3	33800	527	12.2	131000	59.3	0.0481	0.55
NER30	Central Bay (Reserve)	0	13900	9.07	16.3	9700	117	14.1	44100	22.2	0.0132	0.476
OTR31	Outer Bay	0	6570	4.4	7.12	4930	139	0	22700	10.2	0.005	0
OTR32	Outer Bay	0	7790	4.51	7.14	5810	110	2.07	27400	10.6	0.0074	0.18
OTR33	Outer Bay	0.427	13500	8.85	12.4	9980	173	4.86	39300	20.2	0.0109	0.255
OTR34	Outer Bay	2.35	39700	29.8	52.3	30700	397	14.6	129000	74.6	0.0672	0.687
OTR35	Outer Bay	0.726	19900	12.8	20.8	16700	260	6.68	63400	33.6	0.0259	0.271
OTR36	Outer Bay	1.18	44100	19.3	26.2	27900	641	10.1	158000	51.1	0.0285	0.215
OTR37	Outer Bay	1.26	23700	16.7	40.4	17800	278	7.46	78900	54.9	0.035	0.311
OTR38	Outer Bay	1.1	31300	29.1	26.3	21800	378	10.9	112000	43.4	0.0195	0.272
OTR39	Outer Bay	0	1400	1.82	1.84	2020	60.5	0	10100	2.42	0.0026	0
OTR40	Outer Bay	0	17300	13.7	12.3	13200	216	5.62	65400	22.4	0.009	0.128
SWP41	Target Site (NERR SWMP)	0.922	48100	15.1	20.3	26700	701	7.51	217000	42.5	0.0114	0.161
SWP43	Target Site (NERR SWMP)	2.74	24400	17.7	42	16000	164	24.4	79500	60	0.107	0.631
SWP44	Target Site (NERR SWMP)	0.702	19400	15.5	27.6	15500	132	31	63700	40	0.0609	1.28

Table B.2 Coral tissue contaminant data by site.

Site ID	Strata	Chlor-											PAHs ng/g	TBT ng/g	Ag ug/L	As ug/L	Pb ug/L	Se ug/L	Sn ug/L	Al ug/L	Cd ug/L	Cr ug/L	Cu ug/L	Fe ug/L	Mn ug/L	Ni ug/L	Zn ug/L	Hg ug/L
		HCH ng/g	dane ng/g	DDT ng/g	PCB ng/g																							
IN20	Inner	0	0	0	2.38	4.6	0	0	0	1.35	0.527	0.134	0	132	0.236	0	69.9	152	8.33	2.44	7.64	0.001						
IN21	Inner	0	0	0	2.92	5.9	0	0	0.942	0.0796	0.178	0	146	0.235	0	9.57	164	11.9	1.51	3.11	0.0016							
IN22	Inner	0	0	0	2.34	5.8	0	0	1.31	0.0876	0.152	0	125	0.273	0	3.62	148	10.6	1.08	2.89	0.0014							
IN23	Inner	0	0	0	2.19	3.8	0	0	1.89	0.116	0.17	0	178	0.309	0	97.2	274	18	6.84	16.4	0.0016							
IN25	Inner	0	0	0	2.19	3.5	0	0	1.6	12.5	0.152	0	123	0.208	0	4.17	128	10.4	0.796	3.51	0.002							
IN26	Inner	0	0	0.60	3.56	4.6	0	0	1.43	0.775	0.169	0.1	330	0.279	0	91.7	396	19.6	5.42	16.9	0.0019							
IN27	Inner	0	0	0	2.39	4.4	0	0	1.56	0.0783	0.172	0	105	0.216	0	70.5	118	10.5	3.69	11.5	0.0015							
IN33a	Inner	0	0	0	2.19	4.5	0	0	1.58	0.17	0.192	0	120	0.286	0	74.4	133	11.4	4.38	14.2	0.0016							
OF01	Outer	0	0	0	2.24	4.8	0	0	2.44	0.216	0.185	0	125	0.294	0	9.27	146	11	2.15	4.36	0.0038							
OF02	Outer	0	0	0	2.58	5.7	0	0	1.33	6.64	0.194	0	174	0.227	0	68	188	11.4	2.65	7.16	0.0021							
OF03	Outer	0	0	0	2.36	4.2	0	0	1.78	0.424	0.257	0	237	0.248	0	85.8	285	15	6.6	13	0.0032							
OF04	Outer	0	0	0	2.19	2.9	0	0	1.54	0.298	0.159	0	282	0.217	0	2.37	289	14.3	0.817	2.56	0.0022							
OF05	Outer	0	0	0	2.19	3.5	0	0	1.61	0.561	0.192	0	162	0.268	0	70.2	193	10.5	3.43	7.09	0.0016							
OF06	Outer	0	0	0	2.19	6.4	0	0	2.08	0.188	0.229	0	100	0.283	0	6.49	110	13.9	2.52	8.12	0.0018							
OF07	Outer	0	0	0	2.93	4.9	0	0	2.33	0.0934	0.196	0	171	0.242	0	73.8	190	11.8	3.22	9.11	0.0025							
OF08	Outer	0	0	0	2.43	3.7	0	0	2.1	0.151	0.136	0	333	0.25	0	67.8	480	24.6	2.61	9.92	0.0019							

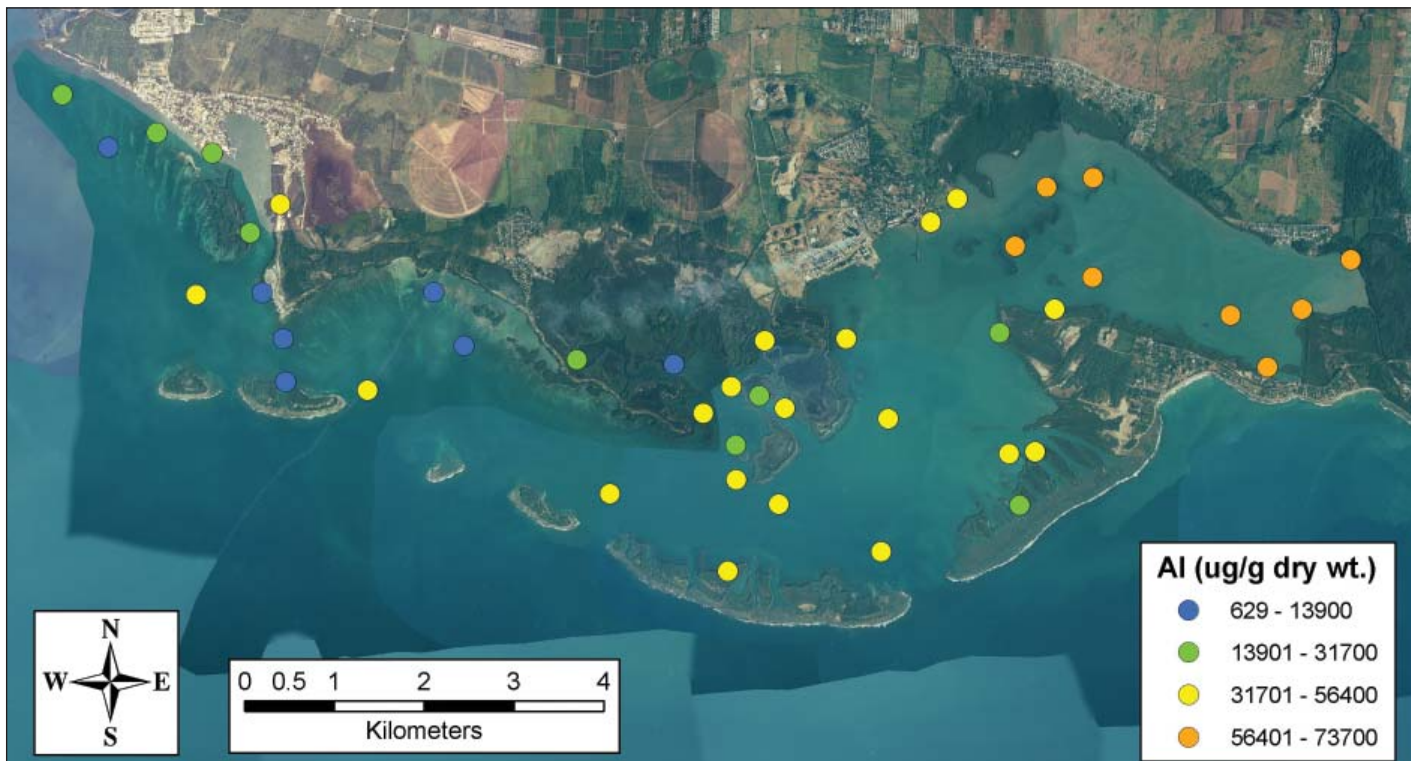


Figure B.1. Aluminum concentrations in sediments.

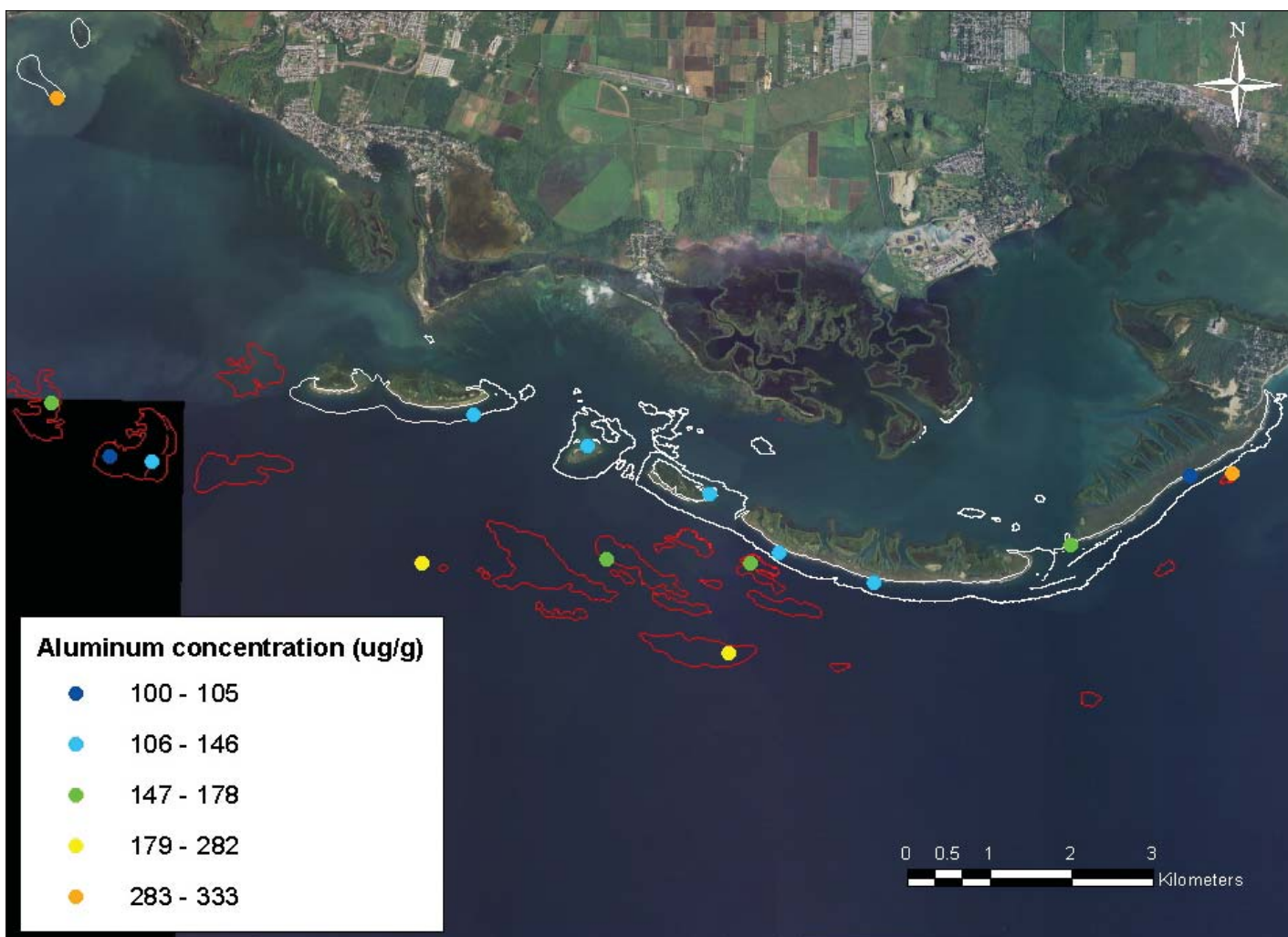


Figure B.2. Aluminum concentrations in corals (*Porites astreoides*). White outline are coral reefs in inner stratum. Red outline are coral reefs in outer stratum.

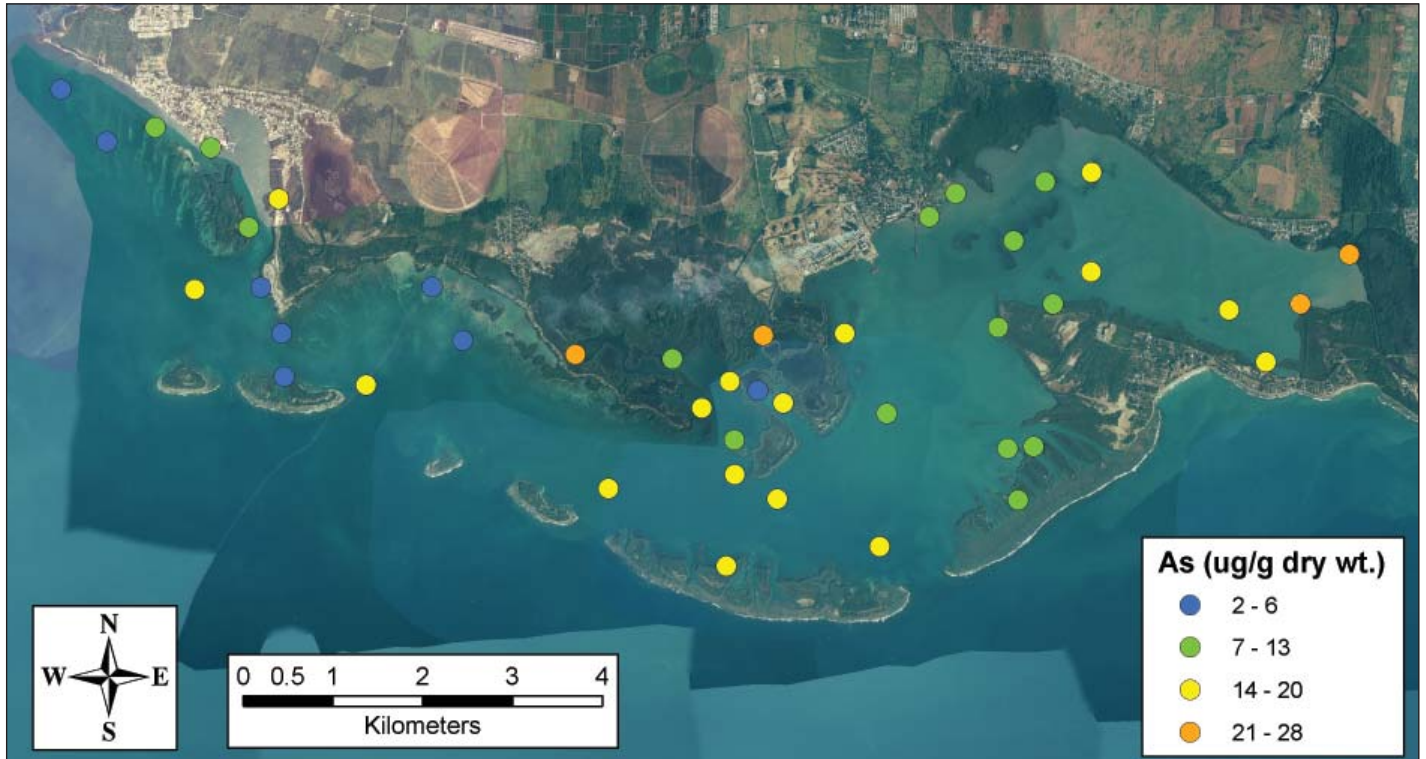


Figure B.3. Arsenic (As) concentrations in sediments.

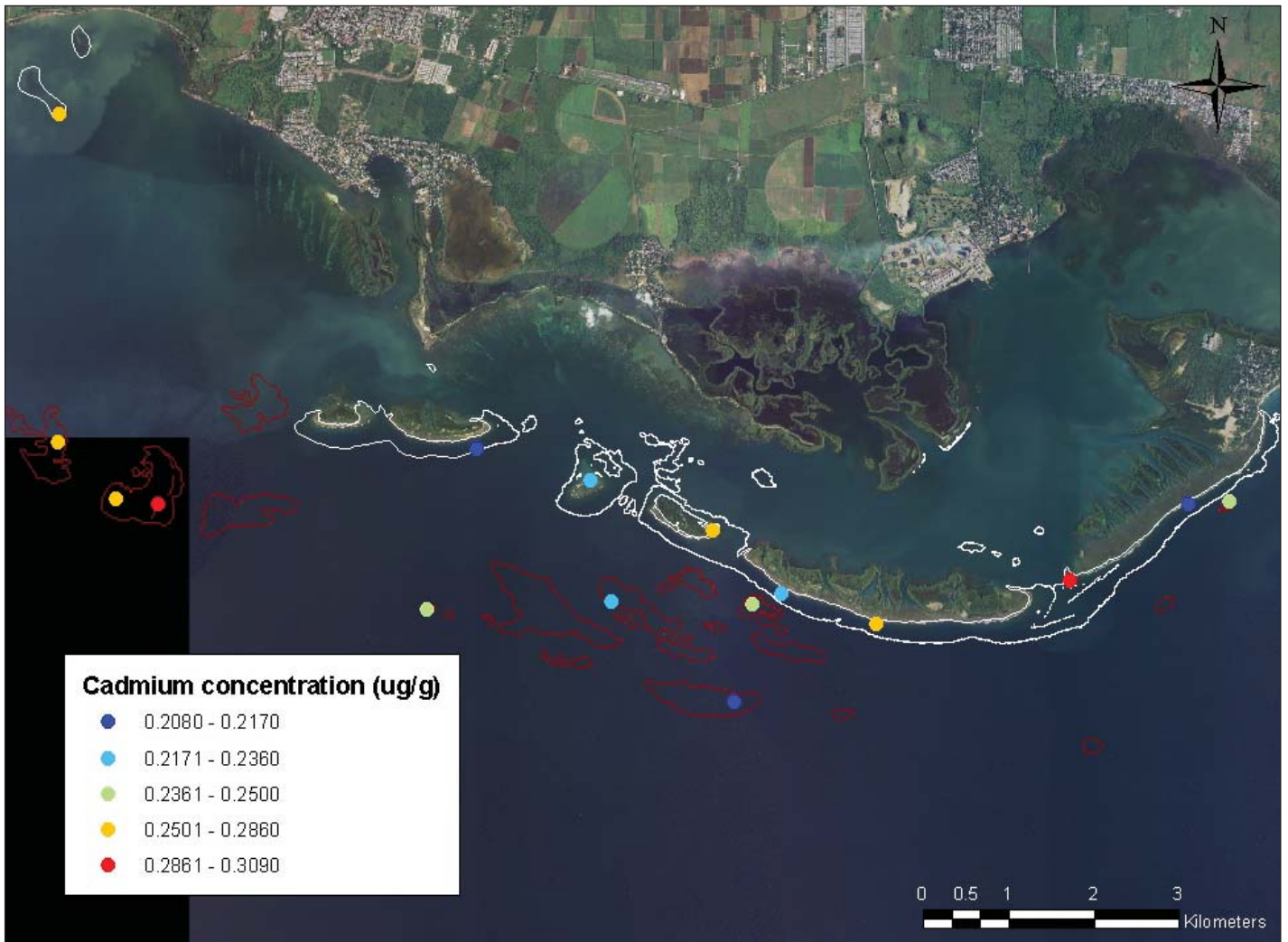


Figure B.4. Cadmium (Cd) concentrations in coral (*P. astreoides*). White outline are coral reefs in inner stratum. Red outline are coral reefs in outer stratum.

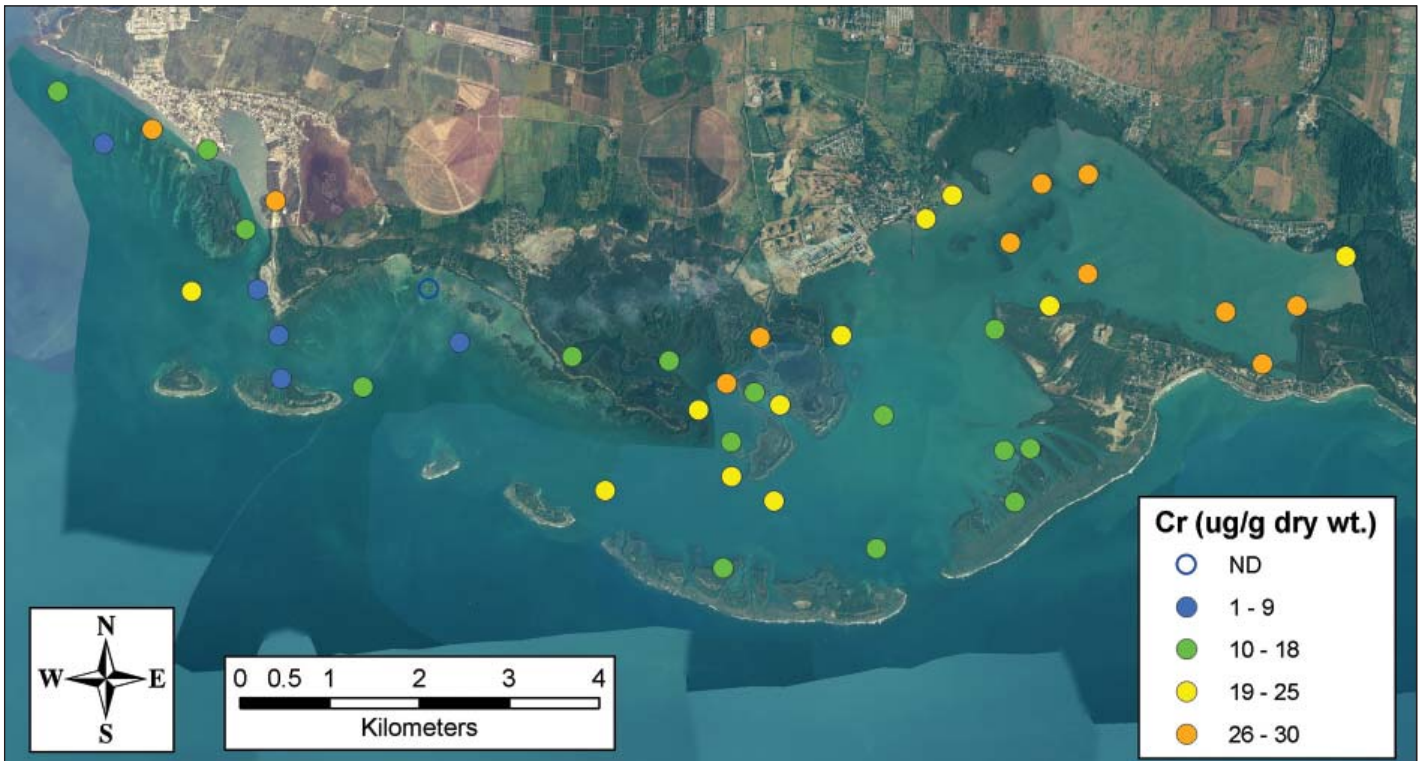


Figure B.5. Chromium (Cr) concentrations in sediments.

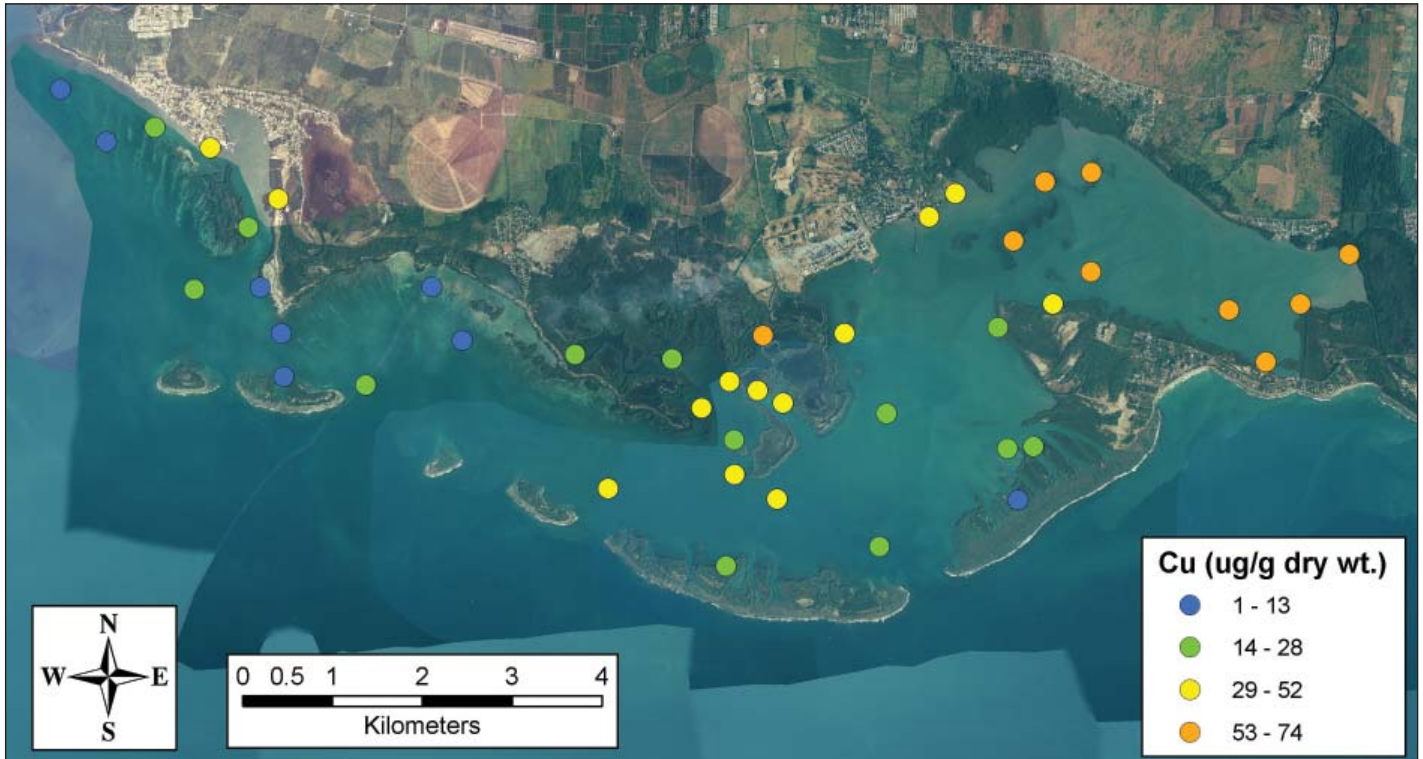


Figure B.6. Copper (Cu) concentrations in sediments.

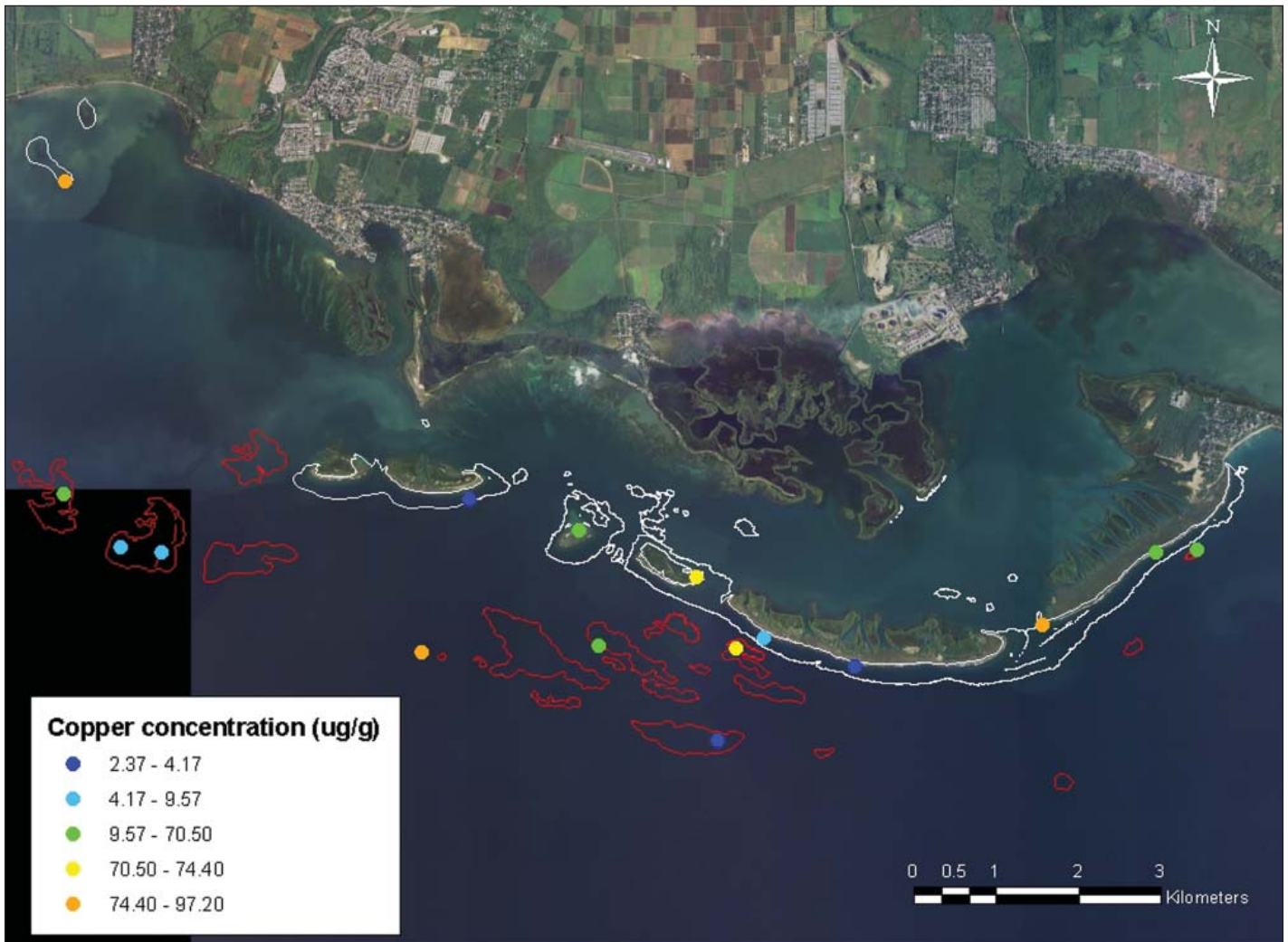


Figure B.7. Copper concentrations in coral (*P. astreoides*). White outline are coral reefs in inner stratum. Red outline are coral reefs in outer stratum.

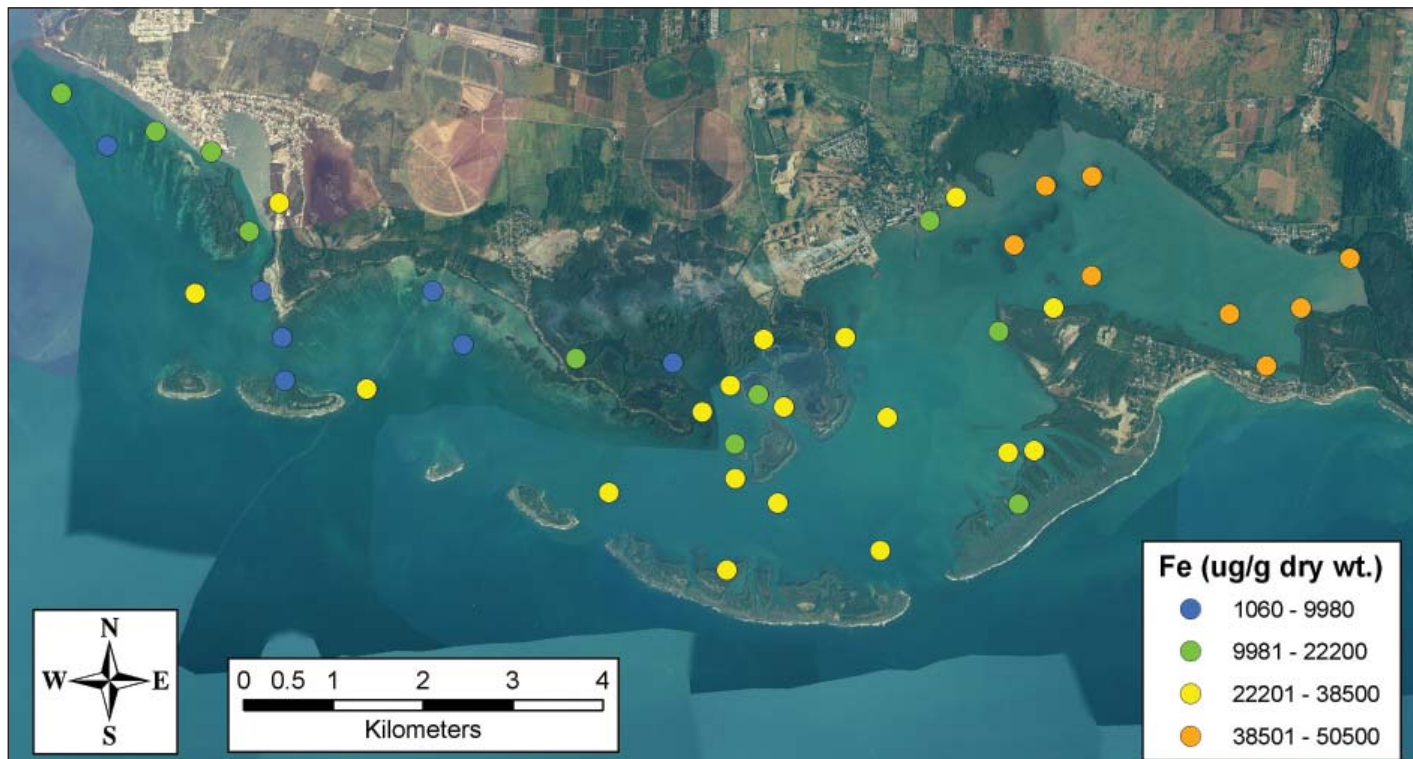


Figure B.8. Iron (Fe) concentrations in sediments.



Figure B.9. Iron concentrations in coral (*P. astreoides*). White outline are coral reefs in inner stratum. Red outline are coral reefs in outer stratum.

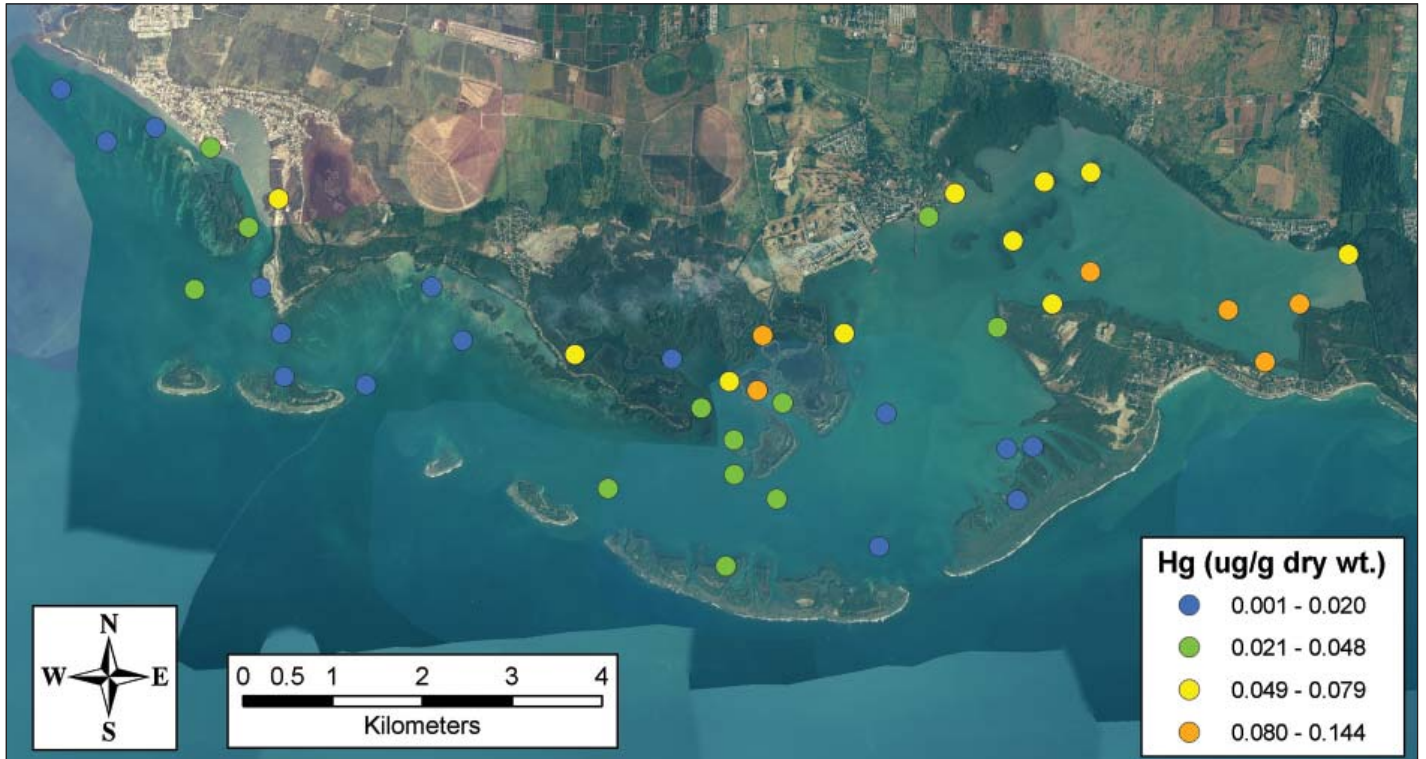


Figure B.10. Mercury (Hg) concentrations in sediments.

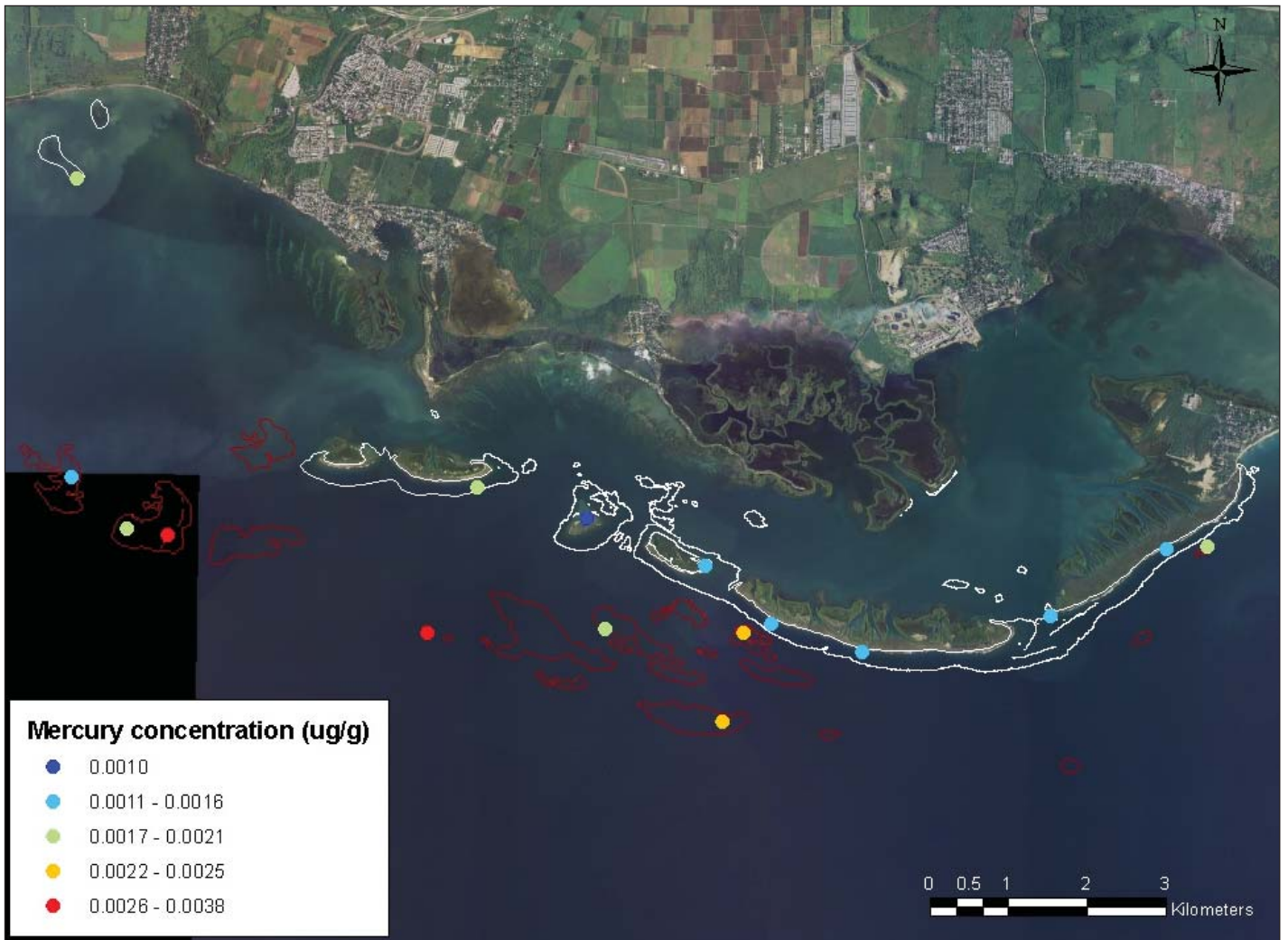


Figure B.11. Mercury concentrations in coral (*P. astreoides*). White outline are coral reefs in inner stratum. Red outline are coral reefs in outer stratum.

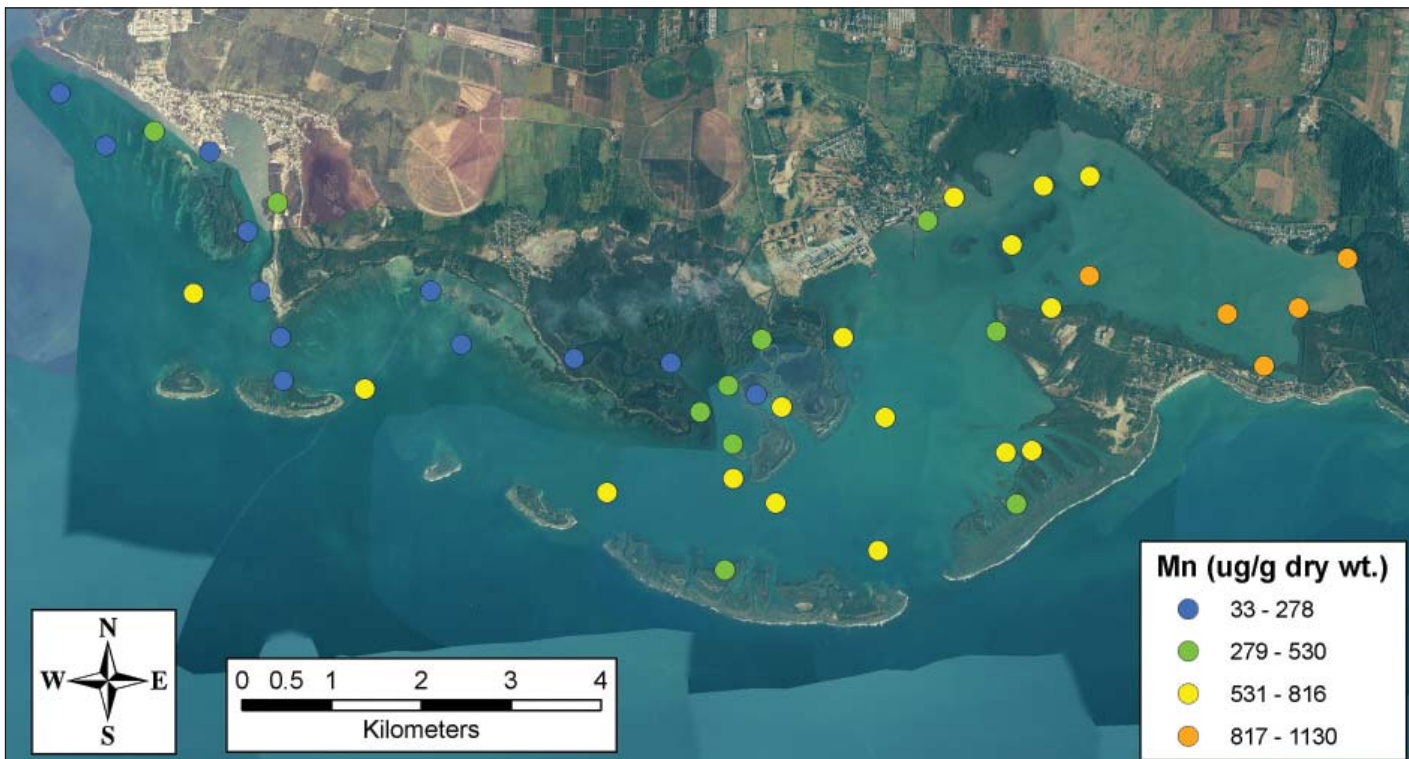


Figure B.12. Manganese (Mn) concentrations in sediments.

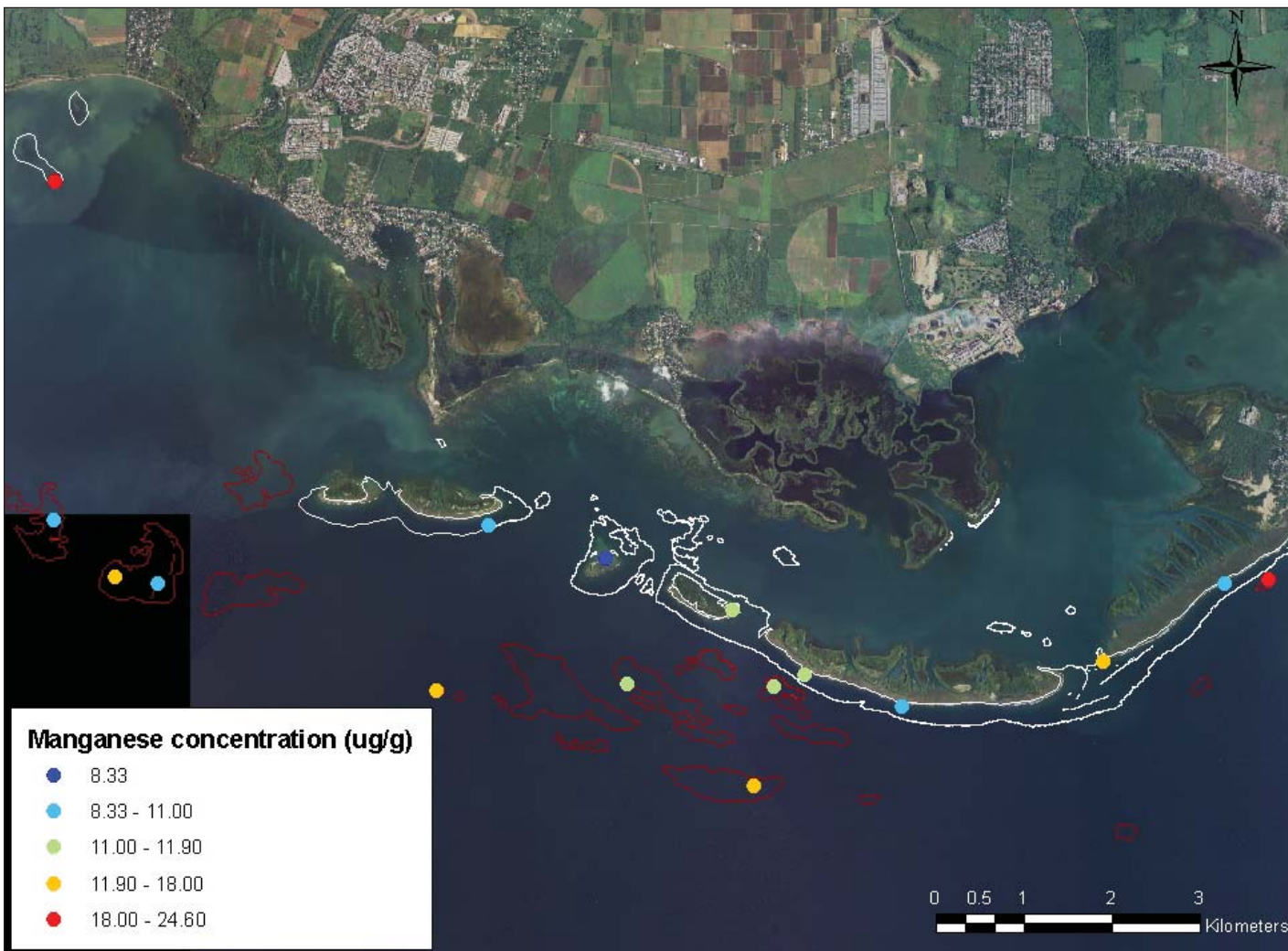


Figure B.13. Manganese concentrations in coral (*P. astreoides*). White outline are coral reefs in inner stratum. Red outline are coral reefs in outer stratum.

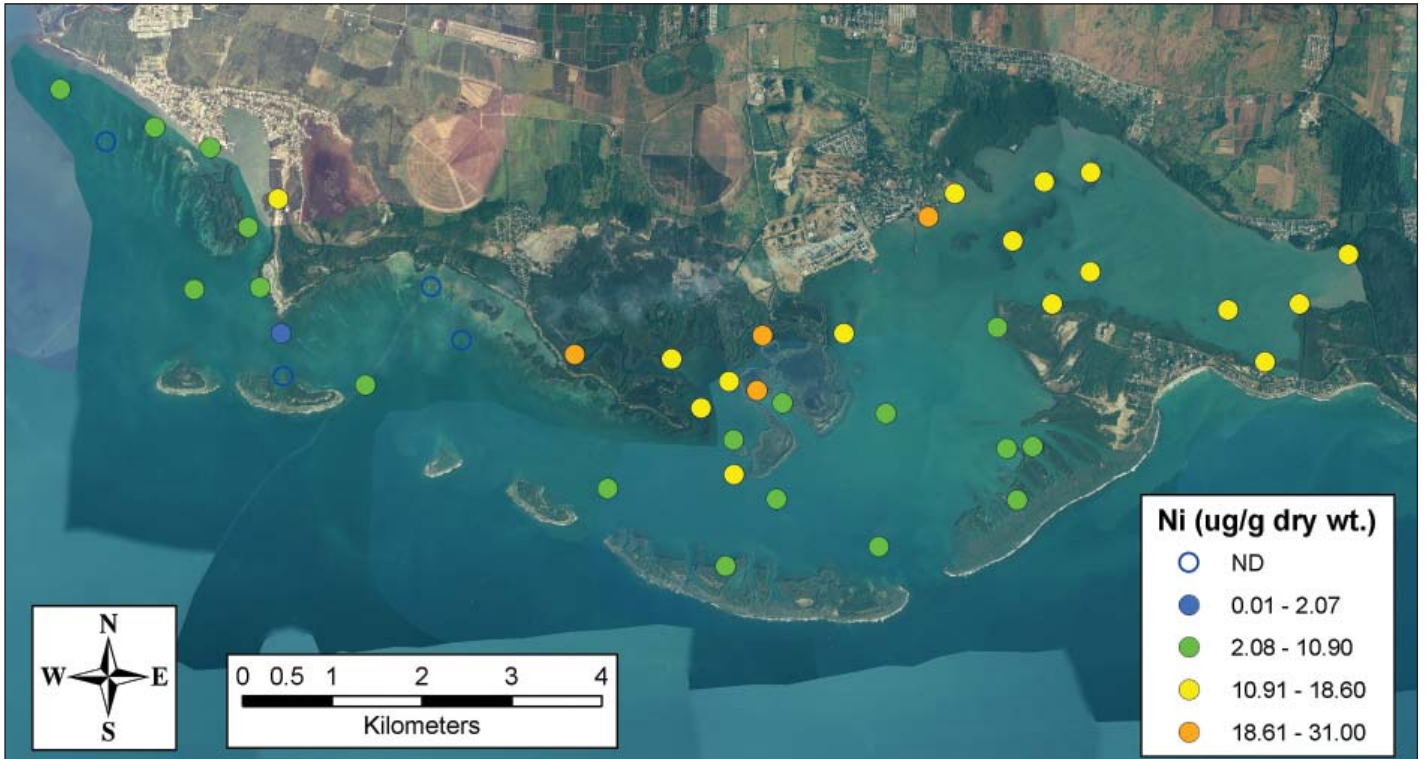


Figure B.14. Nickel (Ni) concentrations in sediments.



Figure B.15. Nickel concentrations in coral (*P. astreoides*). White outline are coral reefs in inner stratum. Red outline are coral reefs in outer stratum.

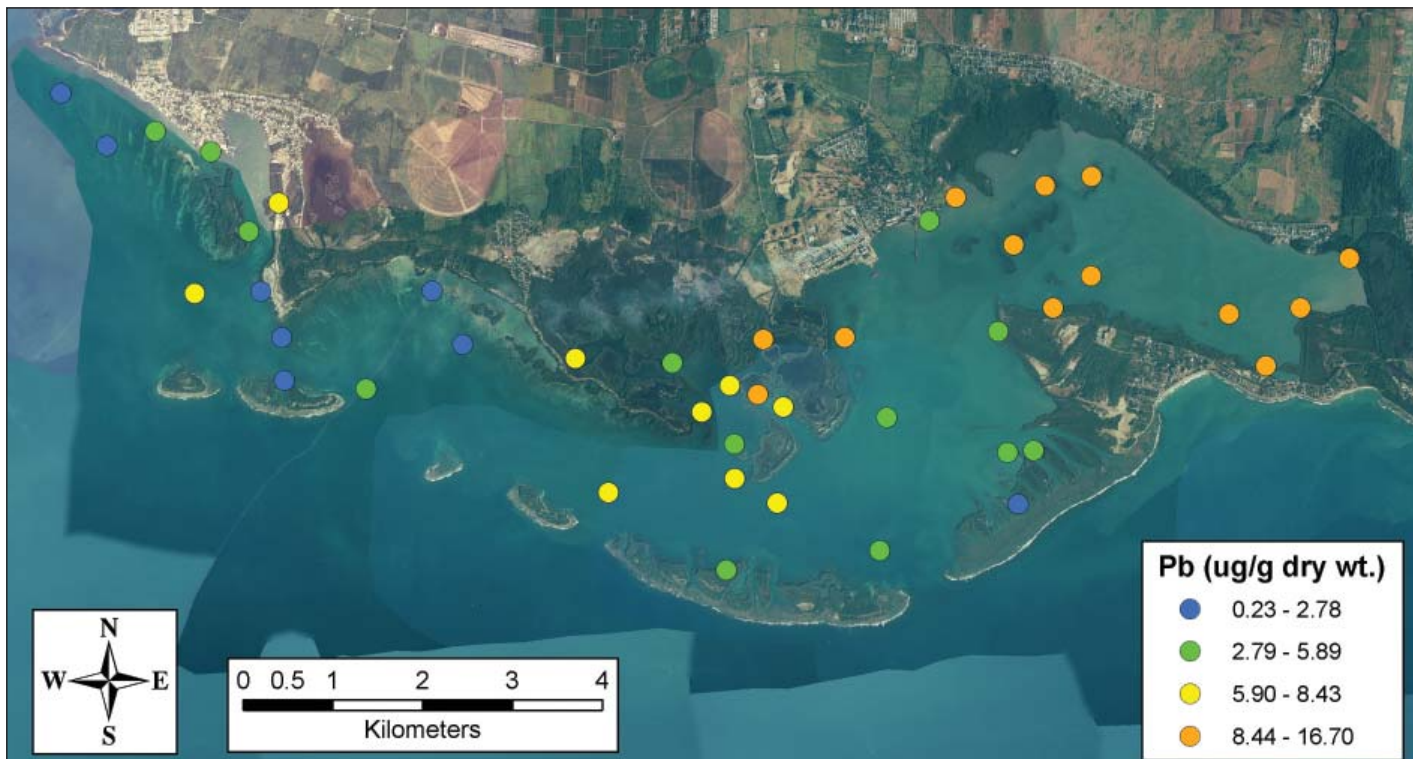


Figure B.16. Lead (Pb) concentrations in sediments.

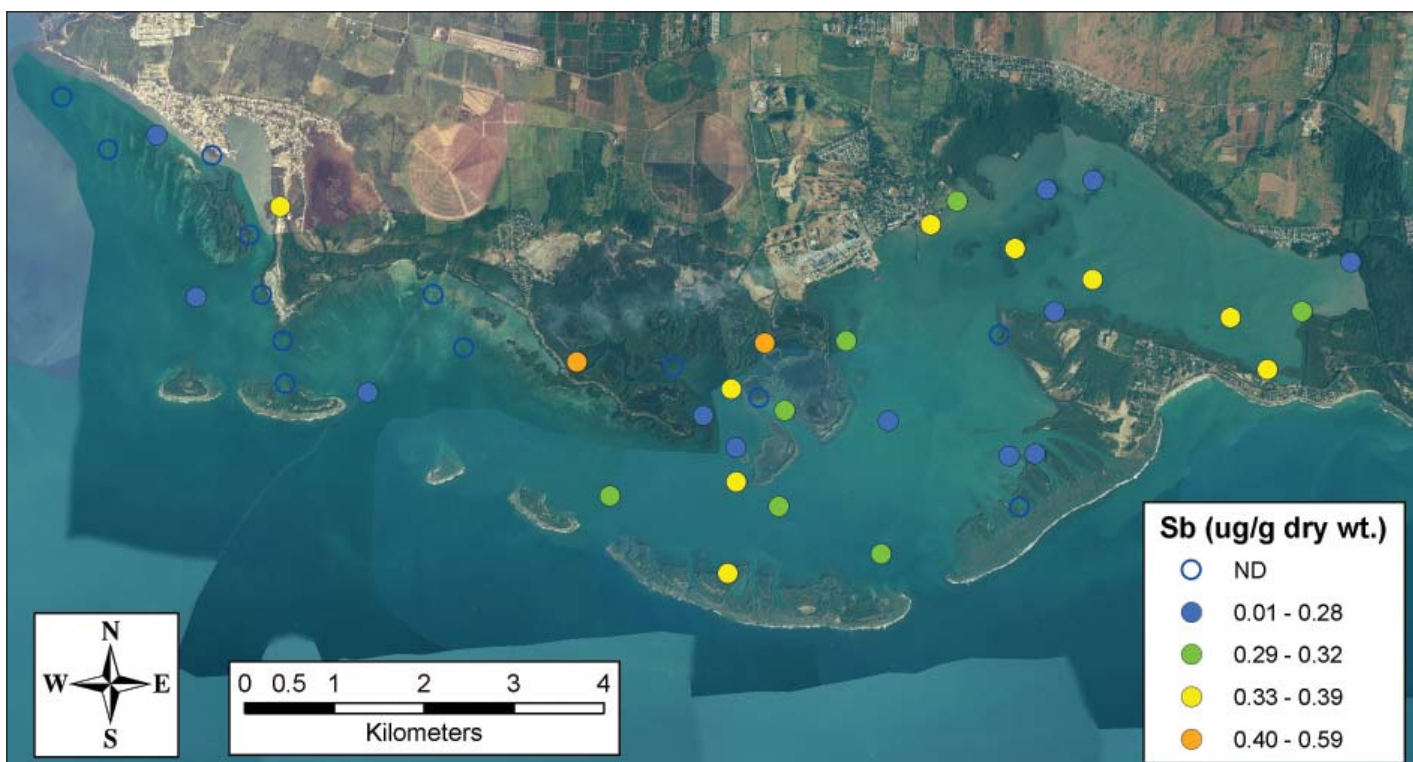


Figure B.17. Antimony (Sb) concentrations in sediments.

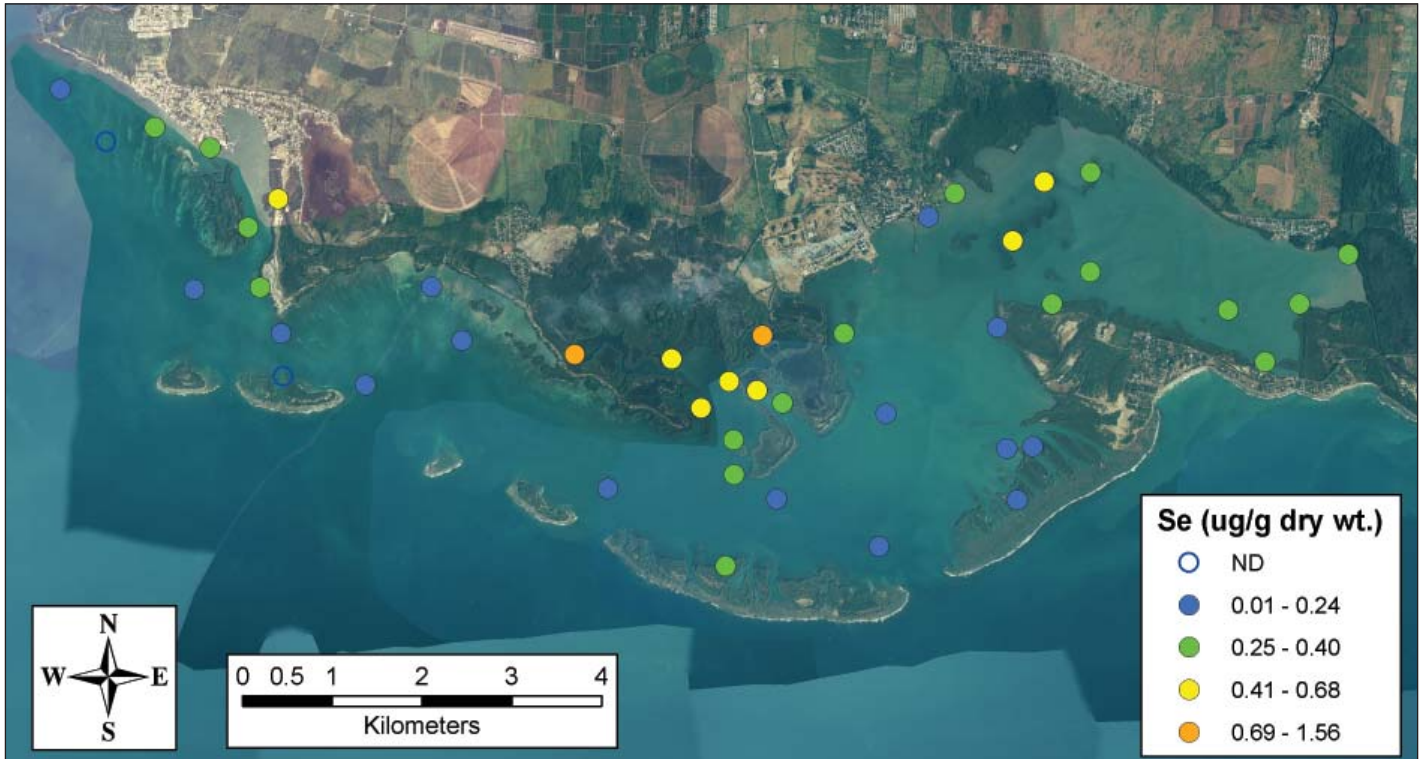


Figure B.18. Selenium (Se) concentrations in sediments.

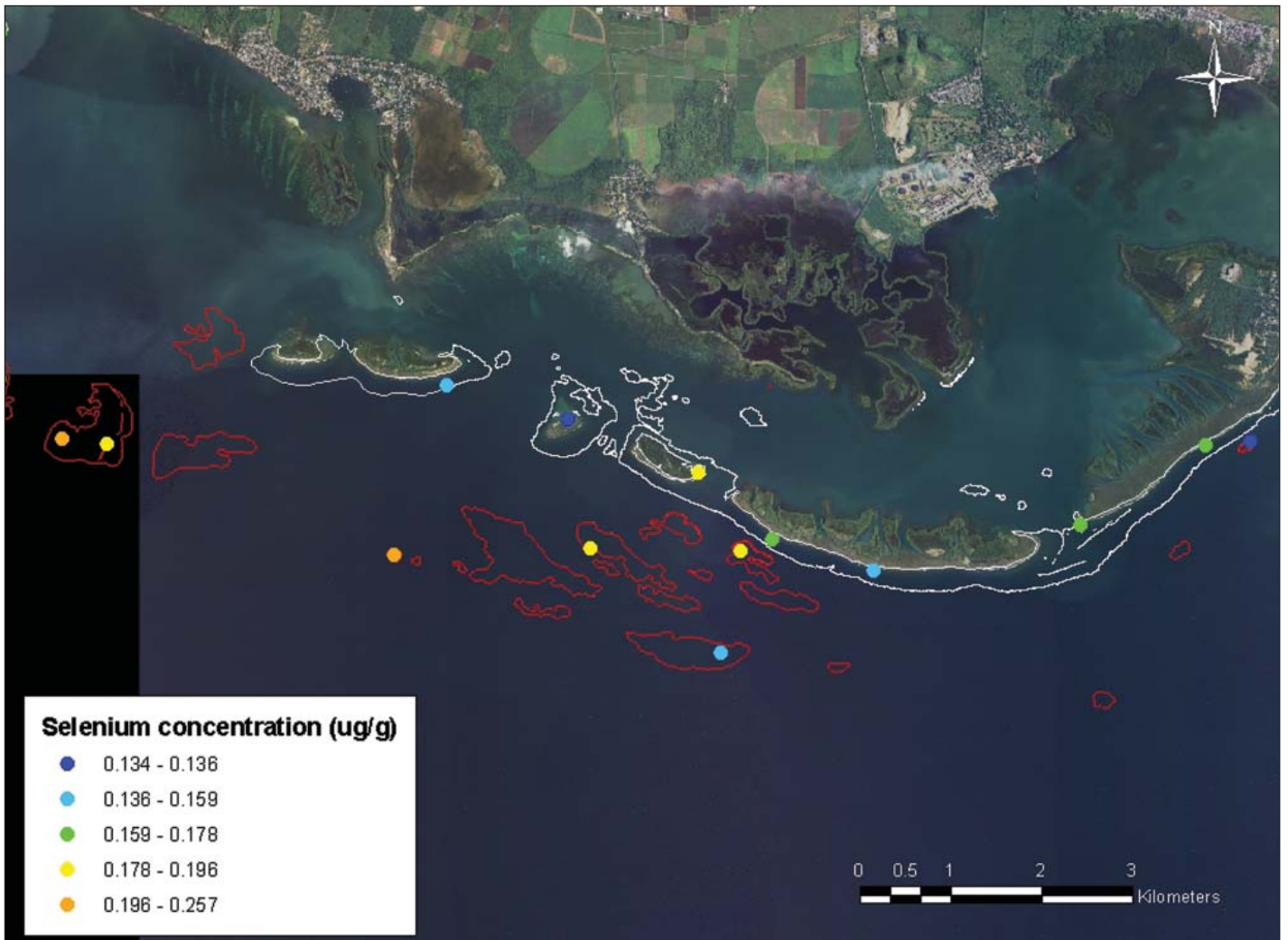


Figure B.19. Selenium concentrations in coral (*P. astreoides*). White outline are coral reefs in inner stratum. Red outline are coral reefs in outer stratum.

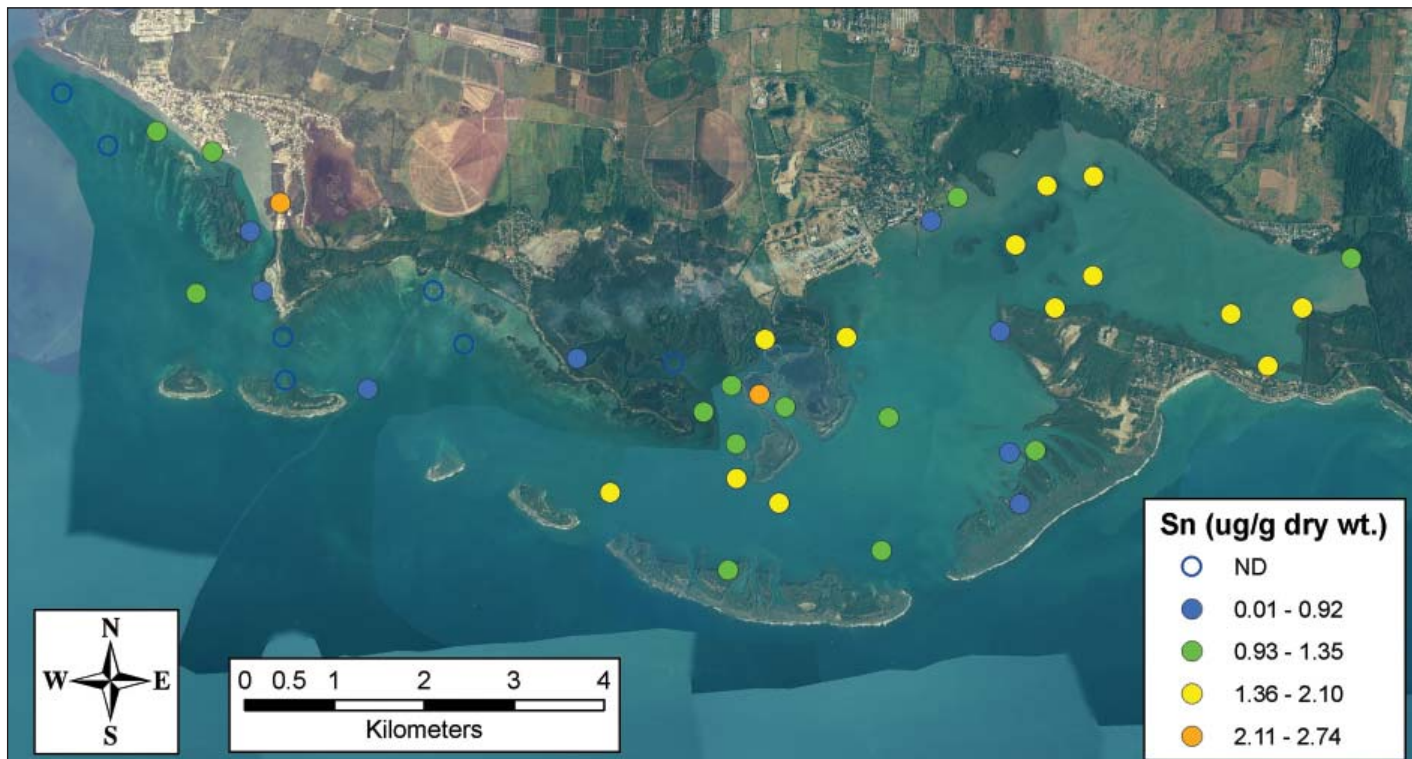


Figure B.20. Tin (Sn) concentrations in sediments.

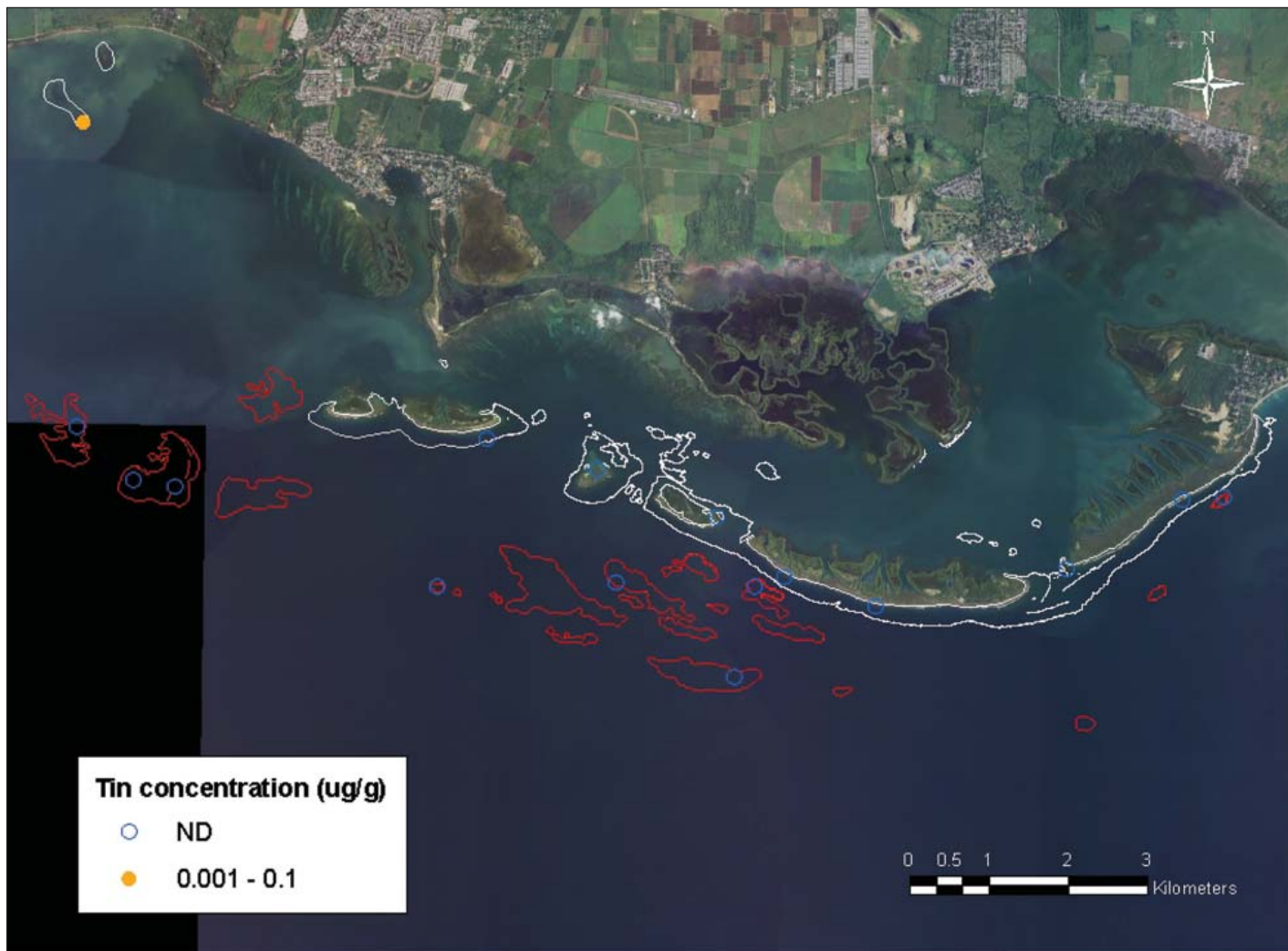


Figure B.21. Tin concentrations in coral (*P. astreoides*). White outline are coral reefs in inner stratum. Red outline are coral reefs in outer stratum.

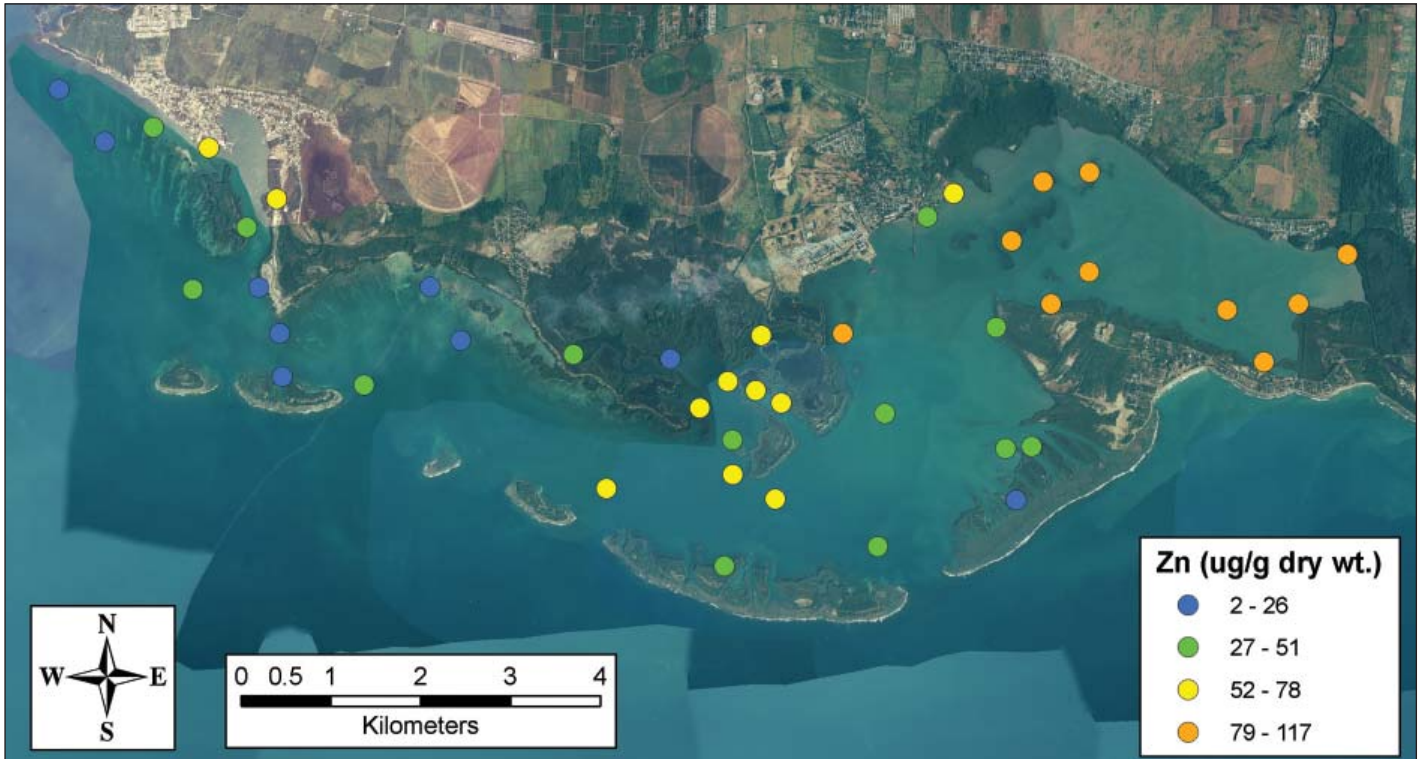


Figure B.22. Zinc (Zn) concentrations in sediments.



Figure B.23. Zinc concentrations in coral (*P. astreoides*). White outline are coral reefs in inner stratum. Red outline are coral reefs in outer stratum.



U.S. Department of Commerce

Gary Locke
Secretary

National Oceanic and Atmospheric Administration

Jane Lubchenco, Ph.D.
Under Secretary for Oceans and Atmosphere

National Ocean Service

David Kennedy
Assistant Administrator for Ocean Service and Coastal Zone Management

